





# Unraveling the regulation of plant vascular identity

Margot Evelien Smit

## **Thesis committee**

### **Promotor**

Prof. Dr D. Weijers  
Professor of Biochemistry  
Wageningen University & Research

### **Other members**

Prof. Dr C. Testerink, Wageningen University & Research  
Prof. Dr K.H.W.J. ten Tusscher, Utrecht University  
Prof. Dr E. Scarpella, University of Alberta, Canada  
Dr A.P. Mähönen, University of Helsinki, Finland

This research was conducted under the auspices of the Graduate School of Experimental Plant Sciences.

# Unraveling the regulation of plant vascular identity

Margot Evelien Smit

## **Thesis**

submitted in fulfilment of the requirements for the degree of doctor  
at Wageningen University  
by the authority of the Rector Magnificus  
Prof. Dr A.P.J. Mol,  
in the presence of the  
Thesis Committee appointed by the Academic Board  
to be defended in public  
on Wednesday 19 June 2019  
at 1.30 p.m. in the Aula.

Margot Evelien Smit  
Unraveling the regulation of plant vascular identity,  
206 pages.

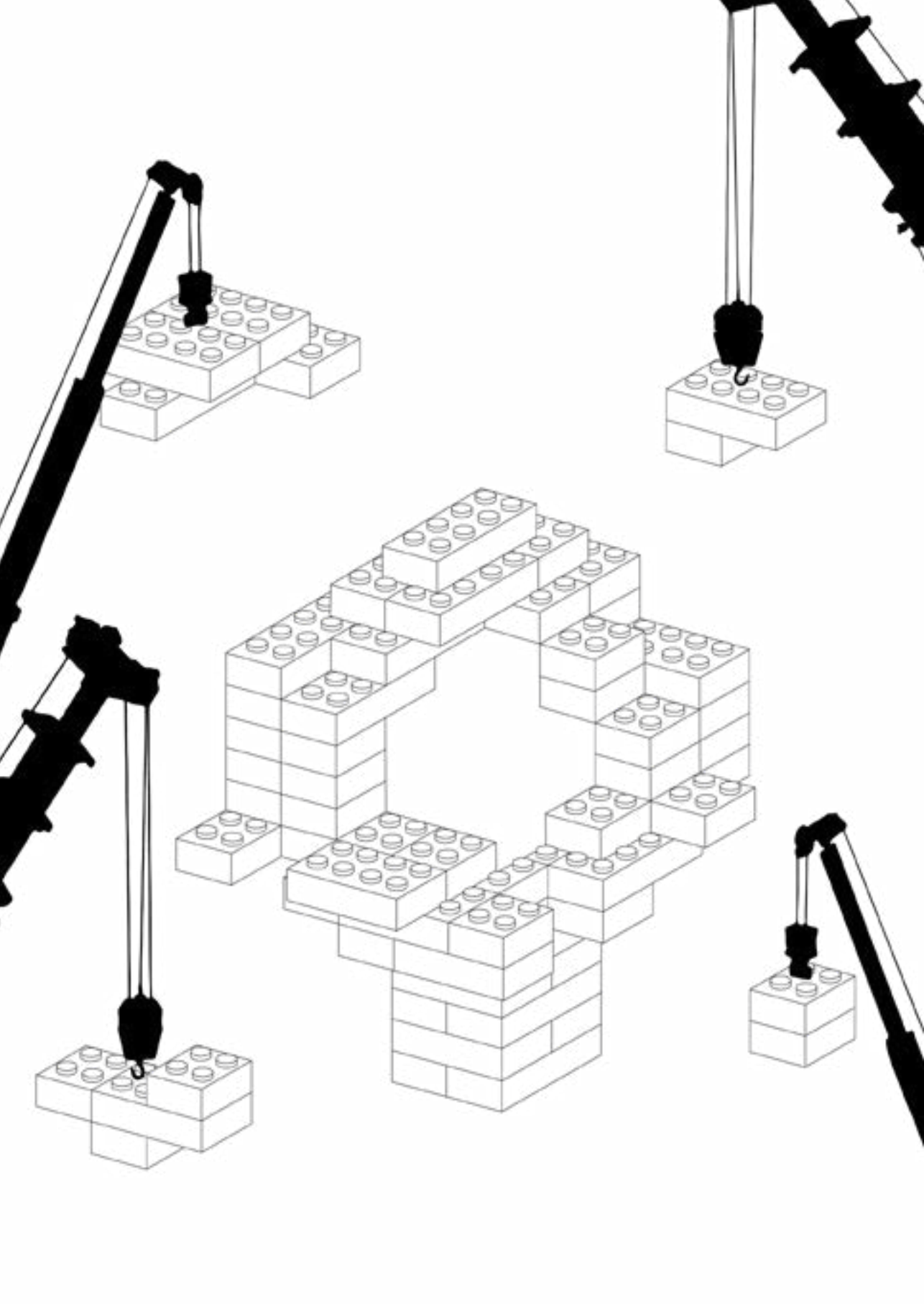
PhD thesis, Wageningen University, Wageningen, the Netherlands (2019)  
With references, with summary in English

ISBN: 978-94-6343-957-2

DOI: <https://doi.org/10.18174/476094>

# Table of Contents

<b>Chapter 1</b>	7
Introduction	
<b>Chapter 2</b>	17
The role of auxin signaling in early embryo pattern formation	
<b>Chapter 3</b>	29
Molecular characterization of vascular tissue ontogeny in the Arabidopsis embryo	
<b>Chapter 4</b>	57
Auxin signaling is necessary but not sufficient in establishing vascular identity	
<b>Chapter 5</b>	75
A Yeast One Hybrid screen for candidate regulators of vascular identity	
<b>Chapter 6</b>	117
Candidate regulators of vascular identity modulate auxin-dependent expression of vascular genes	
<b>Chapter 7</b>	151
Parallels in vascular tissue specification across tissues and species	
<b>Chapter 8</b>	173
General Discussion	
<b>References</b>	183
<b>Summary</b>	198
<b>Acknowledgements</b>	200
<b>Curriculum Vitae</b>	202
<b>Publications</b>	203
<b>Education statement</b>	204





# Chapter 1

## **Introduction**



### Cell identities are laid down during plant embryogenesis

Plants are complex, multi-cellular organisms that continuously adapt to their environment. While they look extremely different from animals, on a molecular level they undergo similar developmental processes, such as organogenesis, and use similar tools to control these transitions, such as cell-cell communication (Wolpert 2011). All land plants reproduce sexually and subsequently use embryogenesis to lay down a basic body plan. While after embryogenesis most, though not all, animals stick to the same body plan without major changes, plants continuously develop new organs and tissue types, some as a part of regular development, some in response to the environment (Raven et al. 2005). They retain the ability to regenerate and have groups of cells that have stem cell properties (Heidstra & Sabatini 2014). The mechanisms plants use to build and develop their body plan are in some ways similar to those used by animals. Plant cells communicate with hormones and other signaling compounds and they use intricate signaling pathways to control development and response to external stimuli (Beck 2010).

During animal embryogenesis the body plan is laid down in great detail: signaling gradients are interpreted and inform on cell position and identity (Rossant & Tam 2009, Stathopoulos & Levine 2002). Cells that previously were naive transition to a specific identity with an attached future function and developmental trajectory. Similarly, during plant embryogenesis cells start as naive before adopting a specific identity. Because plant cells are immobilized by their rigid cell walls, in the *Arabidopsis* embryo their division patterns are highly reproducible (Scheres et al. 1994). As a result researchers were able to trace back the origins of the three major plant cell identities in the embryo: vascular, ground tissue and epidermal cell identities are first separated when the embryo contains 32 cells, at early globular stage. In this thesis we focus on the vascular cells that are specified during embryogenesis: what defines their identity and how is this identity initiated? We will look at vascular genes, hormone signaling, regulatory proteins and the interactions between these components.

### The development of a vascular bundle employs a series of regulatory modules

The innovation of lignified vascular tissues around 425 million years ago resulted in increases in plant body size and complexity (Beck 2010, Raven et al. 2005). The woody vascular tissues transport liquids through the plant, redistributing water and the solutes within: minerals, sugars, signaling compounds and so forth. With these transport abilities plant size was able to increase and dedicated tissues such as roots developed. The woody nature

of vascular cells provided plants with rigidity, further enabling increases in plant size and complexity. Today plant species that lack differentiated vascular tissues - mosses, liverworts, hornworts - remain small. In contrast, vascular plants can grow to greater heights than any other organism and their body structures can develop into large, intricate 3D shapes. The vascular tissues themselves are similarly complex: after initiation vascular cells proliferate, develop into different types of transport cells and differentiate to develop thick secondary cell walls. Each of these steps needs to be initiated multiple times during a plant's life and is controlled by multiple signals.

The size of vascular bundles influences its transport and support capabilities, therefore it is under strict control. Cell proliferation in the vascular bundle is regulated by a series of developmental modules. Different sets of transcription factors and associated gene products have been identified that control the width of vascular bundles across plant species and tissues. TARGET OF MONOPTEROS 5 (TMO5) is a basic helix-loop-helix (bHLH) transcription factor that together with its partner, the bHLH LONESOME HIGHWAY (LHW), forms dimers in the centrally located xylem and induces the expression of genes that control cytokinin production (De Rybel et al. 2013, 2014; Ohashi-Ito et al. 2014). Cytokinin signaling then promotes periclinal cell division in the neighboring cambium cells, acting in part through action of the DOF2.1 transcription factor (Mähönen et al. 2006, Smet et al. 2019). In addition, a separate regulatory module acts in the phloem: PHLOEM EARLY DOFs (PEARs) and their homologs regulate proliferation of phloem-adjacent cells and their activity is balanced by xylem-expressed Class III Homeodomain leucine zipper (HD-ZIP III) transcription factors (Miyashima et al. 2019). A final module, in the stem cambium, was shown to depend on the phloem-derived tracheary element differentiation inhibitory factor (TDIF) peptide which controls PHLOEM INTERCALATED WITH XYLEM (PXY) signaling. Downstream of PXY signaling, Wuschel-like homeobox 4 and 14 (WOX4/14) activity initiates cambial divisions that separate xylem and phloem (Etchells et al. 2013, Fisher & Turner 2007, Hirakawa et al. 2010). These modules are likely tightly connected and they are specifically activated in the vascular cells.

In concert with proliferation, cells in the vascular bundle develop a pattern of distinct sub-identities. In most tissues a centrally located xylem domain is surrounded by phloem with (pro)cambial cells in between (Raven et al. 2005). The meristem-like, dividing (pro) cambium contributes to both the xylem and the phloem cell populations (Smetana et al. 2019). Xylem development is associated with high auxin and its further development into proto- and metaxylem depends on a combination of cytokinin response and the activity of HD-ZIP III transcription factors (Baima et al. 2001, Bishopp et al. 2011, Carlsbecker et al.

2010, Mähönen et al. 2006, McConnell et al. 2001). In normal development, cytokinin response is blocked in the outer xylem cells by Arabidopsis Histidine Phosphotransfer Protein 6 (AHP6) but general reduction of cytokinin response results in diminished proliferation and increased differentiation into protoxylem (Mähönen et al. 2006). In addition, HD-ZIP III levels are regulated by a gradient of microRNA 165/166 (miR165/6) originating from the endodermis (Carlsbecker et al. 2010, Di Laurenzio et al. 1996). The interplay of these pathways allocates proto- and metaxylem cell identity. Conversely phloem development is generally associated with high cytokinin activity and the presence of ALTERED PHLOEM DEVELOPMENT (APL): without either phloem development is impaired (Bonke et al. 2003). The further subspecification of phloem cell types depends on both a set of membrane localized polar proteins and on a peptide receptor module: membrane localized OCTOPUS (OPS) and BREVIX RADIX (BRX) proteins promote protophloem development (Bauby et al. 2007, Mouchel et al. 2006) and the binding of peptide CLAVATA 3/EMBRYO SURROUNDING REGION 45 (CLE45) to the BARELY ANY MERISTEM 3 (BAM3) receptor inhibits protophloem development (Depuydt et al. 2013). All in all, vascular development relies on a series of regulatory modules, many of which can be individually switched on or off. It is the regulation of these modules that develops and patterns the vascular bundle.

### Auxin is the key to vascular development

The development of vascular tissues depends on and can be initiated by auxin. Mutants in auxin production, transport or signaling have vascular defects and application of exogenous auxin can induce new vascular bundles. Early experiments with auxin have shown that auxin can induce the formation of new vascular bundles and affects the formation of vascular connections upon wounding (Jacobs 1952; Sachs 1969, 1975). This strong link between auxin and vascular development was further underlined by mutants in auxin production, transport and signaling that each displayed vascular defects. The production of auxin requiring YUCCA (YUC) proteins (Cheng et al. 2006), subsequent polar transport mediated by PIN-FORMED (PIN) (Gallagher et al. 1998) and final translation to transcriptional output by AUXIN RESPONSE FACTORS (ARFs) such as MONOPTEROS (MP) were each described with mutants that had strong vascular defects (Guilfoyle & Hagen 2007, Hardtke & Berleth 1998). Lack of MP activity results in aberrant vascular development during the embryo which leads to a rootless seedling (Mayer et al. 1991) and MP was found to control a variety of vascular specific genes and pathways (De Rybel et al. 2013, Donner et al. 2009, Möller et al. 2017, Schlereth et al. 2010, Yoshida et al. 2019). However, disruption of auxin

production, transport and signaling output did never affect only the vascular tissues: the outputs of auxin signaling are diverse and ubiquitous, ranging from floral development to gravitropism (Bennett et al. 1996, Cheng et al. 2006, Marchant 1999, van den Berg & ten Tusscher 2017). This variety of outputs can only in part be explained by the different expression patterns of the 23 ARF proteins (Rademacher et al. 2011). Specificity could come from cell specific ARF composition and function, but it appears that ARF proteins do not bind distinct motifs (Boer et al. 2014, O'Malley et al. 2016, Ulmasov 1997), instead it could be their protein interactions that set them apart (as reviewed in Roosjen et al. 2018). This suggests that the response to auxin depends on developmental context. However, vascular development appears to be the dominant response to an auxin maximum. Application of exogenous auxin induces vascular bundles and auxin maxima are often associated with vascular development (Miyashima et al. 2019, Sachs 1969, Scarpella et al. 2006, Wabnik et al. 2013). In this thesis we investigate the role that auxin signaling plays in the initiation of vascular identity.

### Specification of vascular identity is best studied during Arabidopsis embryogenesis

The initiation of vascular identity occurs many times during plant development. New vascular connections need to be formed as old tissues are damaged or new tissues are formed. However, it is challenging to focus on the initiation of vascular identity during wounding, grafting or organ development as these each employ a variety of developmental programs (León et al. 2001, Melnyk et al. 2015, Yin et al. 2012). During embryogenesis, the developmental context is relatively simple with only several cells participating in limited developmental pathways (Palovaara et al. 2016). In addition, the Arabidopsis embryo has a predictable division pattern where vascular development can be traced back to early globular stage (Scheres et al. 1994). Recent transcriptomic work has suggested we can find the first vascular cells one cell division earlier, at dermatogen stage (Palovaara et al. 2017). Modeling and auxin reporters have indeed suggested that the inner cells at dermatogen stage already accumulate auxin which is then correlated with emergence of vascular identity (Wabnik et al. 2013). Auxin has been compared to the morphogens that have been described in animal embryogenesis (Bhalerao & Bennett 2003), gradients of such morphogens provide positional information that informs cell fate (Ashe 2006, Lawrence & Struhl 1996, Turing 1952). One major difference between Arabidopsis and animal embryogenesis is the size of the embryo at the moment gradients are employed to instruct distinct cell identities. While morphogen gradients during animal embryogenesis usually cover more than a dozen of cells or nuclei, an auxin gradient in the early Arabidopsis embryo would form a peak over only a few cells (Lawrence & Struhl 1996, Möller et al. 2017, Scheres et al. 1994, Stathopoulos &

Levine 2002). It is difficult to imagine such a short gradient as being informative, irrespective of whether it is the absolute or relative amount of signal that is interpreted.

### Scope of this thesis

Early on during *Arabidopsis* embryogenesis, the three major cell identities are laid down. The centrally located vascular cells will subsequently divide and pattern to form a vascular bundle that provides the plant with transport capabilities and structural integrity. While vascular development has been a popular field of study, it remains unclear how vascular identity is initiated. In this thesis we focus on the specification of the first vascular cells during embryogenesis.

**Chapter 2** outlines the role auxin plays during embryogenesis. In the early embryo local auxin production and directional transport result in auxin maxima that are interpreted. We describe how auxin then controls division orientation and cell-type specific expression of target genes. Both MP and its targets control the shape and development of the embryo. Despite recent advances it remains unclear how auxin signaling specifically triggers vascular identity in the inner cells in the early embryo.

Our goals of tracking vascular identity and determining factors that control it can not be accomplished without first describing vascular identity in detail. In **Chapter 3** we first determine the expression patterns of previously described vascular marker genes in the early embryo. Next we use the embryo transcriptome atlas to identify novel marker genes to track vascular identity. This unbiased approach allowed for the identification of new vascular genes independent of MP. The expression of many vascular genes starts in the inner cells of dermatogen stage, indicating that vascular identity is initiated as soon as there is an inner and outer cell layer. One division later it becomes clear that many vascular genes are not restricted to the vascular cells in the globular stage embryo.

These tools to track vascular identity then help in **Chapter 4** with identifying the role that auxin signaling plays in the initiation of vascular identity. In the root, auxin treatment can increase expression of vascular genes but cannot expand their expression domain. In the embryo, we demonstrate that auxin signaling is needed for vascular identity but that MP activity is not sufficient for expanding the expression domains of vascular marker genes. In addition, auxin signaling reporters indicate there is no difference in auxin signaling between inner and outer cells at dermatogen stage. This suggests that additional factors are needed to

create new vascular cells.

In **Chapter 5** we try to find such additional factors that might control vascular identity. Using a Yeast One Hybrid approach we identify DNA-binding proteins that interact with vascular specific promoter sequences. Next we apply an unbiased selection algorithm to select 23 candidate regulators of vascular identity. 10 of these candidates are expressed at the time and location of vascular initiation during embryogenesis and as such could play a role. All of these are expressed broadly at the moment of specification, indicating that it is not their presence but their local activation that might provide cell type specificity.

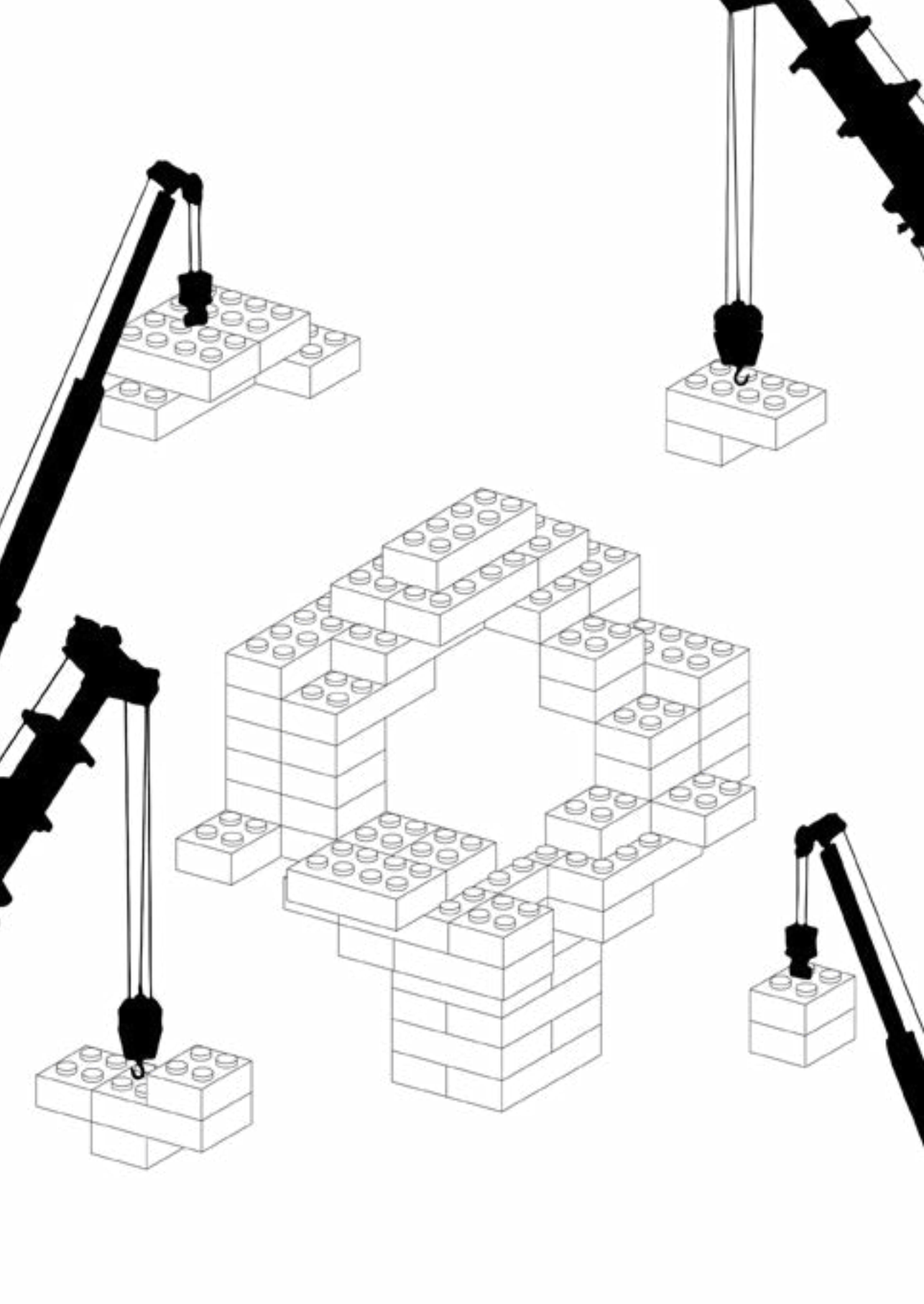
The ability to bind vascular promoters and the localization of these 10 candidate regulators indicates a potential function in vascular development. When overexpression at the start of **Chapter 6** does not result in strong developmental defects we hypothesize that these factors act in parallel with auxin signaling in controlling vascular identity. Indeed misexpression of several candidate regulators alters root growth and gene expression in response to auxin. In addition, we describe the interaction between MP and G-BOX BINDING FACTOR (GBF) proteins and hypothesize that they could cooperate in the control of vascular gene expression. Indeed AuxREs and Gboxes often co-occur and in vascular promoters their presence contributes to both the amplitude and expression pattern of vascular promoters.

**Chapter 7** aims to connect the mechanisms of vascular development found in the Arabidopsis embryo to Cucumber grafts. After finding that early vascular genes are similarly induced in Arabidopsis embryos and grafts, we want to use the graft as an additional model for following vascular specification. After testing compatible and incompatible Cucumber grafting combinations, an RNAseq experiment comparing the two reveals that upon grafting, compatible grafts express additional genes in their rootstock. Among the Arabidopsis homologs of these Cucumber genes are targets of auxin signaling and regulators of development, confirming the parallels between both processes.

Finally in **Chapter 8** the findings of this thesis are discussed and the newly gained insights are placed in a broader perspective. This chapter also suggests approaches for further research into the mechanisms that specify vascular cell identity.







# Chapter 2

## The role of auxin signaling in early embryo pattern formation

Margot E. Smit and Dolf Weijers

A version of this chapter has been published as:

**Smit, M.E., and Weijers D. 2015.** The Role of Auxin Signaling in Early Embryo Pattern Formation. *Current Opinion in Plant Biology* 28: 99–105

Laboratory of Biochemistry, Wageningen University, Stippeneng 4, 6708WE Wageningen, the Netherlands

### **Abstract**

Pattern formation of the early *Arabidopsis* embryo generates precursors to all major cell types, and is profoundly controlled by the signaling molecule auxin. Here we discuss recent milestones in our understanding of auxin-dependent embryo patterning. Auxin biosynthesis, transport and response mechanisms interact to generate local auxin accumulation in the early embryo. New auxin-dependent reporters help identifying these sites, while atomic structures of transcriptional response mediators help explain the diverse outputs of auxin signaling. Key auxin outputs are control of cell identity and cell division orientation, and progress has been made towards understanding the cellular basis of each. Importantly, a number of studies have combined computational modeling and experiments to analyze the developmental role, genetic circuitry and molecular mechanisms of auxin-dependent cell division control.

## Introduction

Elucidating the mechanisms that underlie the control of pattern formation and the establishment of cell identity remains a key challenge in plant development. Most plant organs are composed of multiple, functionally distinct cell types, which are each genetically instructed. Because plant development is continuous and iterative, the study of pattern formation and cell identity is served by simple, predictable model systems. Here, we will focus on the *Arabidopsis* embryo in which, during less than 10 cell division cycles, the zygote generates an embryo that carries dedicated precursors to all major cell types in the seedling (Scheres et al. 1994, ten Hove et al. 2015; Figure 1). A great deal has been learnt about early embryo patterning (Dolan et al. 1994, Mayer et al. 1991, Wendrich & Weijers 2013), and perhaps unsurprisingly, the plant signaling molecule auxin has repeatedly surfaced as a key regulator (Friml et al. 2003, Hamann et al. 2002, Möller & Weijers 2009). We will review recent insights into how this molecule controls different aspects of embryo development, with an emphasis on vascular tissue development, a well-known auxin-dependent process (De Rybel et al. 2014b, Hardtke & Berleth 1998). First however, we will discuss new findings that lead to a better understanding of the molecular basis for cellular auxin response.

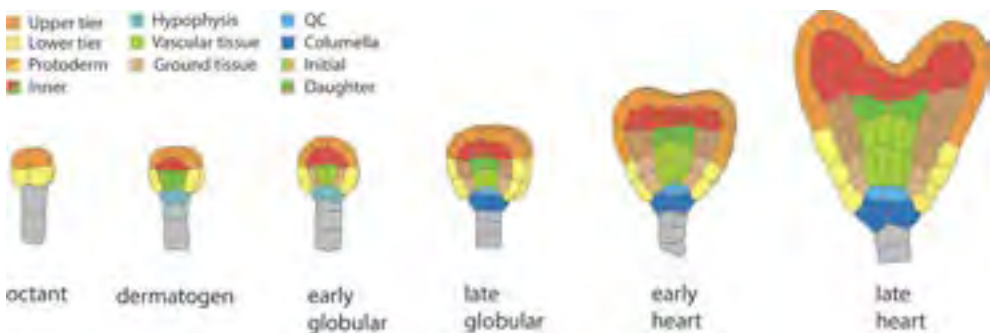


**Figure 1: Stages of *Arabidopsis* embryogenesis**

Cross-sections of a developing *Arabidopsis* embryo during the stages where major patterning events occur. Cells are colored according to cell identity/lineage as specified in key.

## Strategic auxin production and relocation

Auxin production and perception mutants often have severe, sometimes lethal phenotypes, indicating the critical role auxin plays in development (Mayer et al. 1991, Zhao et al. 2001). Auxin signaling output depends on the combination of biosynthesis, inactivation, transport, perception and transcriptional response. In addition to transcriptional auxin response, the ABP1 (AUXIN BINDING PROTEIN 1) protein likely perceives extracellular auxin, and feeds into a non-transcriptional response (Chen et al. 2014, Grones & Friml 2015, Grones

et al. 2015, Tromas et al. 2013, Xu et al. 2014). However, while earlier reports showed dramatic phenotypes upon ABP1 downregulation, recent work suggested that ABP1 is not required for normal development, as the *abp1-5* mutant contains many additional SNPs (Enders et al. 2015) and new pair of knockout mutants does not show any of the previously described phenotypes (Gao, Y., Zhang, Y., Zhang, D., Dai, X., Estelle 2015). As these conflicting reports have not yet been reconciled, we will focus only on the well-established nuclear auxin response.

Recently, a combined modeling/experimentation effort revealed how auxin biosynthesis and transport interact to promote local auxin accumulation in the early embryo (Robert et al. 2013, 2015; Wabnik et al. 2013). The most abundant auxin, IAA (Indole-3-Acetic Acid), is produced using the amino acid tryptophan as a substrate (Zhao et al. 2001), predominantly via the IPyA (indole-3-pyruvic acid) pathway in two enzymatic steps that are mediated by the TAA1 (TRYPTOPHAN AMINOTRANSFERASE OF ARABIDOPSIS 1) and YUC (YUCCA) enzymes (Mashiguchi et al. 2011, Stepanova et al. 2011), respectively. By systematically determining YUC gene expression patterns, Robert et al. showed that auxin is initially synthesized in suspensor cells, and transported into the embryo through the efflux regulator PIN7 (PIN-FORMED 7) (Robert et al. 2013). Once the embryo reaches about 32 cells, a new auxin source is created at its apex, mediated by TAA1 and later YUC gene expression. This new auxin source is required for establishing polar localization of PIN1 in the provascular cells and thus directed auxin transport towards the future root tip (Robert et al. 2013, Wabnik et al. 2013). Importantly, simulation of these auxin sources and transport routes on embryo templates showed that a biosynthesis-transport connection could account for the dynamic properties of auxin accumulation in the embryo (Wabnik et al. 2013). How auxin biosynthesis and PIN protein polarization are mechanistically linked remains an open question.

Furthermore, while efflux proteins have been shown to play a dominant role in directional auxin transport during embryogenesis (Friml et al. 2003), it was recently shown that also auxin influx proteins are required for normal embryo development. Without AUX/LAX (AUXIN/LIKE AUX1) auxin influx proteins embryos show developmental defects in shoot and root pole (Robert et al. 2015), similar to those observed in mutants with reduced efflux activity (Friml et al. 2003). The same study also showed that auxin signaling influences auxin transport, as the expression of influx and efflux proteins is altered in response to auxin signaling (Robert et al. 2015).

### Tuning auxin regulatory output

Auxin promotes the degradation of the Aux/IAA (AUXIN/INDOLE-3-ACETIC ACID) transcriptional repressor proteins (Ulmasov et al. 2007), which otherwise bind to and inhibit DNA-binding AUXIN RESPONSE FACTORS (ARFs) (Figure 2). ARFs bind Auxin Response Elements (AuxREs) in promoters and promote or inhibit target gene transcription (Boer et al. 2014, Ulmasov et al. 2007). Auxin facilitates the binding of Aux/IAs to an SCF (SKP1-CUL1-F box) complex which results in ubiquitination and subsequent degradation of the Aux/IAA proteins (Kepinski & Leyser 2005). The auxin ‘receptor’ in this scenario is a TIR1/AFB (TRANSPORT INHIBITOR RESPONSE 1/AUXIN-BINDING F-BOX) protein that is the part of the SCF complex that can bind to Aux/IAA via auxin. This complex perception mechanism allows for many levels of signal modification, as there are 6 TIR1/AFB proteins, 29 different Aux/IAA proteins and 23 ARF proteins (Peer 2013). The dazzling complexity that arises from combinations of components likely contributes to generating diverse auxin responses. Differential TIR/AFB-Aux/IAA interactions were shown (Calderón Villalobos et al. 2012), while Aux/IAA-ARF interactions may also have some specificity (Nanao et al. 2014, Stewart et al. 2014) and ARFs are expressed in discrete patterns, especially in the embryo (Rademacher et al. 2011).

Molecular and biochemical properties of the auxin signaling pathway have been described in detail (Calderón Villalobos et al. 2012, Lau et al. 2008), but until very recently, the structural basis of Aux/IAA and ARF function were not known. Several recent papers

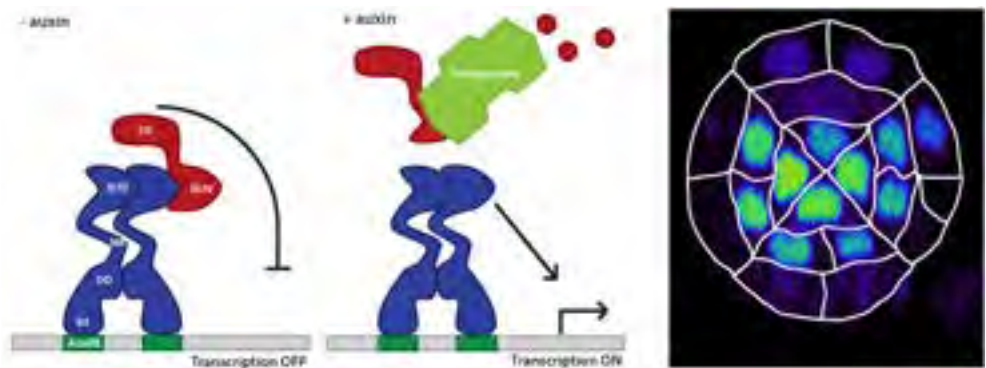


**Figure 2: Auxin signaling in the early embryo.**

(left) Aux/IAA (red) and ARF (blue) simplified protein structures and interactions as described in main text. ARF proteins bind to AuxRE inverted repeats as dimers, interacting via both their DNA Binding Domain and Domain III/IV. In the absence of auxin, Aux/IAA oligomers inhibit ARF's effect on transcription. In the presence of auxin, Aux/IAA proteins are degraded and ARFs can influence transcription. (right) Cross section showing DR5v2 reporter activity in the lower tier of the early globular embryo. DR5v2 signal is displayed on a false color scale and indicates higher levels of auxin signaling in the inner four cells.

have now revealed protein structures that illuminate the atomic basis of protein-protein and protein-DNA interactions within this network, and these can help explain interaction specificity. It was long recognized that ARFs and Aux/IAA proteins share homologous C-terminal domains, which mediate both homotypic and heterotypic interactions (Lau et al. 2008, Ulmasov et al. 2007)(Figure 2). Crystal and NMR structures now reveal that this domain adopts a PB1 fold, and can form head-to-tail oligomers in vitro (Han et al. 2014, Korasick et al. 2014, Nanao et al. 2014). Interactions depend on oppositely charged residues, and mutagenesis suggests that these residues are indeed required for interactions in vivo (Korasick et al. 2014, Nanao et al. 2014). Importantly, kinetic interaction analysis showed that Aux/IAA-ARF interactions have higher affinity than the homotypic interactions, which explains the efficiency of auxin response inhibition by Aux/IAA proteins.

Finally, structural analysis of ARF DNA-binding domains (DBD) provided a structural basis for the recognition of DNA elements (Boer et al. 2014). Investigated ARF proteins (ARF1 and ARF5) have very similar intrinsic DNA specificity; yet have different in vivo functions (Boer et al. 2014, Rademacher et al. 2011) which suggests distinct sets of target genes. Interestingly, ARF DBD's dimerize to bind complex sites with an inverted repeat of the AuxRE (Figure 2). Different ARF homodimers were shown to allow for different spacing between AuxRE's, likely due to variation in ARF structure flexibility (Boer et al. 2014). With the added potential for heterodimerization this suggests a new level of target gene specificity, and a key future question will be if and how this mechanism selects target sites in vivo.

### Auxin building blocks defining the embryo pattern

Genetic interference with auxin action in embryogenesis has two clear effects: changes in cell division plane and defects in cell identity (Hamann et al. 2002, Hardtke & Berleth 1998, Yoshida et al. 2014). Clearly, these two processes are connected as different cell types have unique cell division planes. Yet auxin action on each might also be direct and independent.

Auxin-dependent reporters such as DR5 (Ulmasov et al. 2007), DR5v2 (Liao et al. 2015), DII-Venus (Brunoud et al. 2012) or R2D2 (Liao et al. 2015) indicate sites of accumulation and/or action in the embryo, while the biological significance is known only for some of these. Particularly the earliest auxin “maxima” have long remained unconnected to cellular responses. By generating a complete 4D reconstruction of Arabidopsis embryogenesis, including cell segmentation, it was suggested that the majority of the cell divisions



in the embryo occur according to a simple rule that is approximated by the shortest wall going through the center of the cell (Besson & Dumais 2011, Errera 1888, Yoshida et al. 2014). However, some cells, most notably the hypophysis, deviate from this rule and divide asymmetrically (Yoshida et al. 2014). Strikingly, expression of the mutant *iaa12/bdl* protein, which cannot be degraded and constitutively inhibits ARF proteins (Hamann et al. 1999), caused a marked change to the 3D cell division pattern (Yoshida et al. 2014). Upon ARF inhibition, all cells divided according to the simple, shortest wall rule. Importantly, this auxin-dependent control of cell division plane appears independent of cell identity regulation as differential cell specification only occurs after the normally asymmetric division (Scheres et al. 1994, Yoshida et al. 2014). Thus, through as yet unknown mechanisms, auxin influences cell division orientation away from a default rule.

Differential establishment of cell identity is essential in plant shape and function and is a fundamental principle in pattern formation. The three major tissue identities; vascular, ground and epidermal identity; are established during early embryogenesis with each identity following distinct cell division patterns and differentiation during subsequent development (Figure 1) (Scheres et al. 1994). Likewise, precursors to the root stem cells and quiescent center (QC; its precursor is called hypophysis) are established early during embryogenesis (Dolan et al. 1993, Schlereth et al. 2010, Weijers et al. 2006). At least some of these early patterning events depend strongly on auxin activity, notably involving the ARF5/MONOPTEROS (MP) transcription factor (Hardtke & Berleth 1998, Schlereth et al. 2010). Mutations in ARF5/MP impair vascular tissue and hypophysis development, and cause a rootless phenotype (Berleth & Jürgens 1993, Hardtke & Berleth 1998). In recent years, several direct transcriptional targets of ARF5/MP have been identified (De Rybel et al. 2013, Konishi et al. 2015, Schlereth et al. 2010), and these appear to mediate specific ARF5/MP functions. These can be loosely divided into genes affecting hypophysis division/

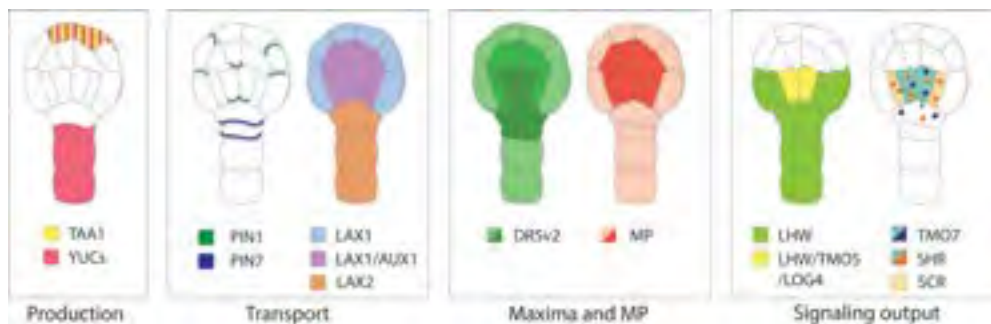


**Figure 3: Auxin production, transport, reporter and output components in the early globular embryo.** Colors indicate expression domains or localization of components according to accompanying keys.

stem cell niche establishment and genes affecting vascular patterning.

Hypophysis division and subsequent distal stem cell fate involves the basic helix-loop-helix protein (bHLH) TMO7 (Schlereth et al. 2010) and the recently described NTT transcription factor (Crawford et al. 2015). TMO7 is directly activated by ARF5/MP in provascular cells, but the protein moves to the hypophysis, where it contributes to the highly asymmetric division that generates the QC (Schlereth et al. 2010)(Figure 3). An analysis of the NO TRANSMITTING TRACT (NTT) protein and its two close homologs identified these as important mediators of auxin-dependent root formation (Crawford et al. 2015). Triple mutants of NTT and its two closest homologs (*nww; ntt wip4 wip5*) have hypophysis division defects and rootless seedlings, resembling the *mp* phenotype (Crawford et al. 2015). Furthermore, NTT expression in the hypophysis is absent in the *mp* mutant, indicating NTT functions downstream of MP. Given that ARF5/MP activity in the proembryo itself is sufficient for normal function (Schlereth et al. 2010, Weijers et al. 2006), it remains to be seen if NTT regulation by ARF5/MP is direct, or involves auxin action in the hypophysis itself. An interesting question is how the multiple ARF5/MP-dependent outputs converge upon hypophysis specification and division.

Vascular patterning is regulated early on during embryogenesis by another MP target, TMO5 (De Rybel et al. 2013, Ohashi-Ito et al. 2013). This bHLH transcription factor is active in the (pro)vasculature, where together with its interaction partner LONESOME HIGHWAY (LHW) it induces periclinal cell divisions (De Rybel et al. 2013, 2014a; Schlereth et al. 2010)(Figure 3). While the dimer has the ability to induce these divisions in other cell types, its function is restricted to the provascular by the combined expression patterns of TMO5 and LHW (De Rybel et al. 2013). Recent analysis showed that these divisions are induced through increased cytokinin signaling. Several of the dimer's target genes, LONELY GUY 3 and 4 (LOG3 and LOG4), catalyze the final step of cytokinin biosynthesis resulting in a cytokinin maximum in the future xylem cells with diffusion to surrounding cells. Cytokinin signaling is however inhibited in these xylem cells by another direct target of the dimer: AHP6 (ARABIDOPSIS HISTIDINE PHOSPHOTRANSFER PROTEIN 6) (Mähönen et al. 2006, Ohashi-Ito et al. 2014), resulting in maximal cytokinin signaling in the cells directly adjacent. In this way auxin and cytokinin signaling closely interact to control which cells divide and at what rate, shaping the vascular bundle.

This was confirmed in silico: a model containing only these genetic components and basic information on auxin and cytokinin dynamics was able to reproduce vascular pattern formation in the early embryo (De Rybel et al. 2014a). One additional component

was needed in the process: unequal distribution of auxin in the four provascular cells at the early globular stage. This underlines that seemingly minor differences in auxin signaling can have large developmental consequences. The results of this work indicate that only a small number of components is indispensable to create a complex pattern (De Rybel et al. 2014a).

### The more the better, or enough is enough?

Auxin directs cell division orientation, vascular tissue formation and hypophysis establishment, and likely several other developmental processes in the embryo. A key question is what the principal mode of action is. Conceptually, auxin could act similar to animal morphogens, eliciting unique responses at discrete concentrations (Lawrence & Struhl 1996). Alternatively, auxin may trigger cellular responses above a certain concentration threshold, and cellular context defines the exact output. We here discuss this problem taking the specification of vascular tissue as an example. Can differences in auxin signaling between cells in the embryo alone control local establishment of vascular identity?

Throughout plant development, auxin levels strongly correlate with vascular identity (Bennett et al. 2014, Ohashi-Ito & Fukuda 2010). Classical experiments by Sachs showed that application of auxin results in the formation of new vascular bundles in competent tissues (Sachs 1969). In leaves auxin signaling was repeatedly shown to precede the expression of vascular marker genes (Lee et al. 2014, Scarpella et al. 2010). Furthermore, a recent paper on graft formation showed that auxin signaling is necessary for and precedes the formation of new vascular bundles (Melnik et al. 2015). Nonetheless, it is unknown whether a sufficiently steep gradient of auxin signaling can be formed to allow only central cells of the embryo to become specified (Figure 1). Improved versions of auxin reporters now allow to semi-quantitatively assess the auxin signaling output on a single cell level (Liao et al. 2015). The DR5v2 reporter shows that the provascular, innermost cells indeed have slightly higher levels of auxin signaling (Figure 2B; Liao et al. 2015). However, while the provascular cells contain more auxin than the ground tissue cells, this difference is small. The question is thus how the auxin signal is read and processed such that only the four inner cells become provascular. At this point it is not known whether also ground tissue specification depends on auxin input, and if this represents a quantitatively different output.

If an auxin signaling gradient indeed directly leads to different identities based on direct readout with identity-specific thresholds, then cells should be able to detect small differences in auxin signaling. This appears possible, as slightly higher auxin levels in two out

of four provascular cells contribute to the formation of a xylem axis (De Rybel et al. 2014a). The molecular underpinnings of auxin signaling also suggest that small differences in auxin levels may be non-linearly processed. TIR1/AFB-Aux/IAA interactions depend on auxin level (Calderón Villalobos et al. 2012), ARF DBD dimerization allows high-affinity co-operative DNA binding, and Aux/IAA-ARF interactions generate complex concentration-dependent dynamics (Boer et al. 2014, Farcot et al. 2015, Korasick et al. 2014, Nanao et al. 2014). A difficulty in this model is that auxin signaling levels may only vary very little. While developmental control is generally strict and redundant, slight variation between embryos should be expected.

Alternative to a purely concentration-based mode of action, a single threshold level might result in vascular specification. Part of the response may then include cell-cell signaling to either prevent neighboring cells from adopting vascular identity or promote ground tissue fate. Provascular cells engage in several cell-cell communication pathways. Transport of auxin and the TMO7 protein to the hypophysis both contribute to correct division of the hypophysis and are both induced by auxin-ARF5/MP signaling (Schlereth et al. 2010). Similarly, SHR is produced in the provascular cells and is translocated to the ground tissue (Nakajima et al. 2001).

It will be interesting to determine which model best explains auxin action in embryo pattern formation. Key to our understanding will be the identification of more ARF target genes, as well as a detailed characterization of the auxin/ARF-dependent activation of such targets.

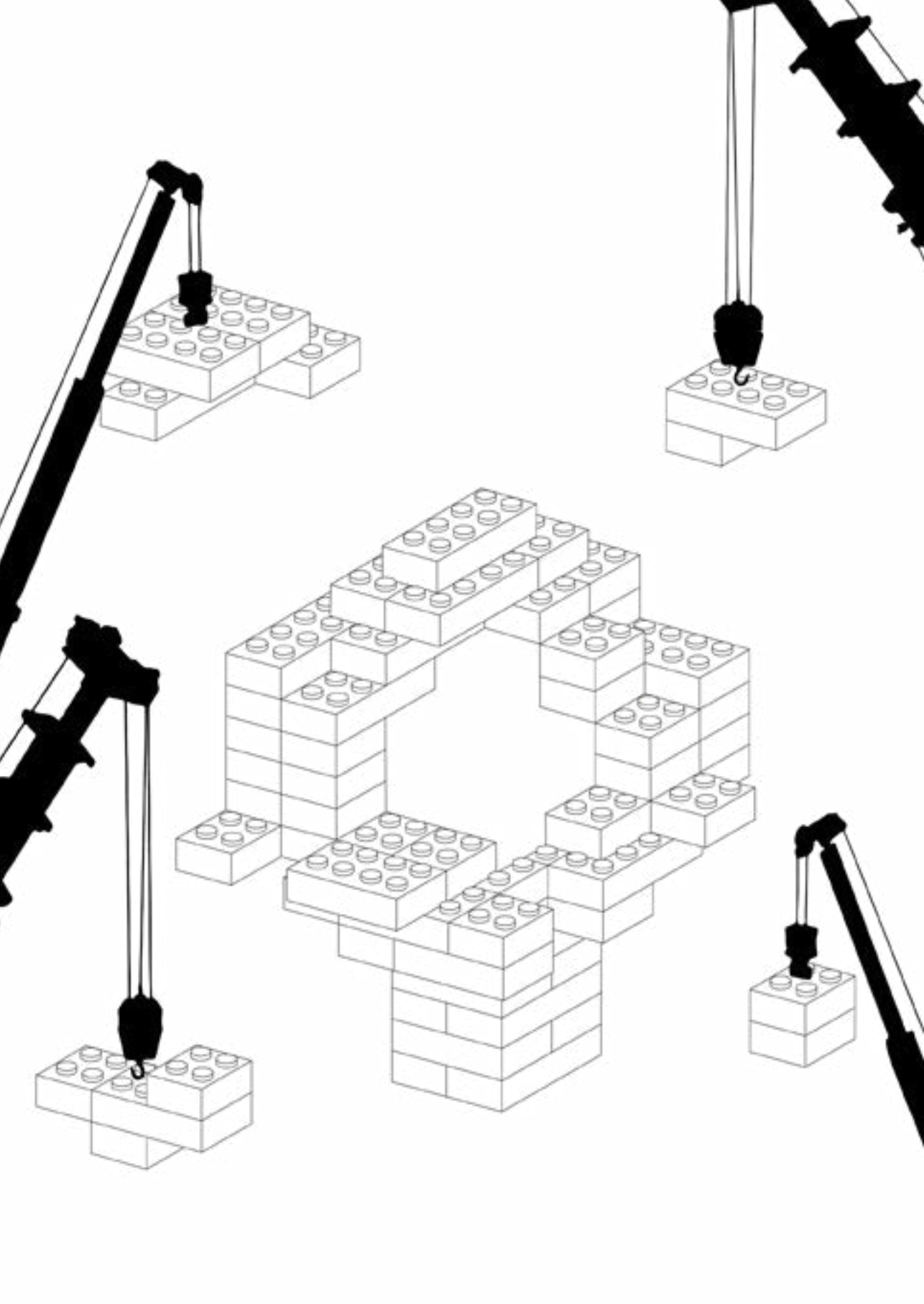
## Conclusions

The past few years have seen several important milestones in our understanding of pattern formation in the embryo, in particular in the action of auxin through controlling cell divisions and cell identity. Auxin is produced at specific locations in the early embryo (Robert et al. 2013, Wabnick et al. 2013), with both efflux and influx proteins playing a crucial role in auxin distribution (Robert et al. 2015). Detailed insight in transcriptional auxin response was gained through identification of protein-protein and protein-DNA interactions and the unraveling of ARF and Aux/IAA protein structures (Boer et al. 2014, Dinesh et al. 2015, Korasick et al. 2014, Nanao et al. 2014). Downstream of auxin signaling new factors were described that link auxin to vascular and stem cell niche development (Crawford et al. 2015) and to cell division via cytokinin signaling (De Rybel et al. 2014a), while factors controlling cell division plane remain elusive (Yoshida et al. 2014). Important questions

remain, particularly pertaining to whether auxin acts in controlling multiple cell fates in a concentration-dependent manner. Together with new tools for visualizing auxin and auxin signaling (Liao et al. 2015), these studies pave the way to understanding the diverse functions auxin has in early development.

### Acknowledgements

We apologize to authors whose valuable contributions we could not include due to space constraints. Work on vascular identity in the embryo in the authors' lab is supported by the Netherlands Organization for Scientific Research (NWO-ALW; Grant ALW 831.14.003 to M.E.S.) and the European Research Council (Starting Grant 'CELLPATTERN', contract no. 281573 to D.W.).



# Chapter 3

## **Molecular characterization of vascular tissue ontogeny in the *Arabidopsis* embryo**

Margot E. Smit, Branimir Velinov, Koyan Bruggeling, Dolf Weijers

**Abstract**

Vascular tissues perform essential functions in plant development; they are required for fluid transport and structural support. The study of vascular development has previously focused on cell proliferation, patterning and differentiation with less attention for the initiation of vascular bundles. In this chapter we use vascular marker genes to describe the specification of vascular identity in the early *Arabidopsis* embryo. Previously described vascular marker genes and new vascular marker genes reveal that vascular identity is initiated at dermatogen stage and that the initially diffuse identity becomes restricted to the vascular cells around transition stage. The initial vascular cells have unique identity characteristics that are not found in the adult plant; they co-express phloem and xylem markers and are surrounded by the expression of vascular inverse markers. The differences between root and embryo are not restricted to the vascular cells: genes expressed in other cell types also show discrepancies between embryo and root. All in all, vascular identity is initiated during embryogenesis at dermatogen stage and while this identity is largely conserved post-embryonically, gene expression patterns reveal that certain traits are lost after early embryogenesis.



## Introduction

Vascular cells play a central role in land plant development. Land plants rely on the fluid transport by these cells for their growth, and the erect nature of plant structures is facilitated by the mechanical support provided by vascular bundles, which are located in the center of all plant tissues. Because of their key role in plant growth, the vascular tissues have been a popular field of study. Vascular research has focused on vascular differentiation (Kondo et al. 2014, Rodriguez-Villalon et al. 2014, Yamaguchi et al. 2010), cell proliferation (De Rybel et al. 2014, Ohashi-Ito et al. 2014), patterning (Mähönen et al. 2000, 2006; Rodriguez-Villalon et al. 2014) and the initiation of new vascular bundles (Donner et al. 2009, Kondo et al. 2016, Mattsson et al. 2003, Sachs 1969). During a plant's life new vascular bundles are initiated with the formation of new tissues, such as lateral roots or leaves. However, new vascular bundles can also be induced independently of organogenesis in the event of grafting or application of exogenous auxin (Mattsson et al. 2003, Melnyk et al. 2015, Sachs 1969). Thus, there are several developmental paths to establishing vascular tissue, either during regular development or as part of a response to injury. No matter the origin of the vascular tissue induction, it must start with the reprogramming of an undifferentiated or differentiated cell type towards vascular identity. Strikingly, while later steps in vascular tissue establishment have been studied in some detail and key regulators have been identified, this first step of commitment towards vascular identity has remained elusive. One difficulty with defining vascular tissue specification and identifying its regulators is the often complex tissue context in which the specification occurs, and the lack of predictability of which cells will form vascular tissue (e.g. in grafts). Here, we use the early Arabidopsis embryo as a model to describe the molecular ontogeny of vascular tissue specification. The embryo is a relatively simple model in which identity specification is not accompanied by wound response or organogenesis. Through both lineage tracing (Scheres et al. 1994), and 3D reconstruction of embryo cells (Yoshida et al. 2014), it has become clear that 4 dedicated vascular precursors can be identified in the early globular embryo. Their identification however, has been principally by their position, and a molecular characterization of the vascular lineage has been lacking. Cell identities are essentially a product of the genes that are expressed, and differences between cell types are reflected in unique expression patterns of lineage-specific genes. As such, cell identity can be described by the expression of a set of marker genes, unique to that cell type. Conversely, cell lineage ontogeny can be inferred from the dynamic expression of a set of such marker genes. Here, we aimed to describe the specification of vascular tissue identity in the early Arabidopsis embryo using a set of marker genes.

A number of marker genes has been shown to follow vascular development in root

and leaf. The expression patterns of these marker genes at the time of vascular specification during embryogenesis is only known for a few. When we started this study, the expression patterns during early embryogenesis were reported for *IQ-DOMAIN15* (*IQD15*; Möller et al. 2017), *SOSEK11* (*SOK1*; Yoshida et al. 2019), *TARGET OF MONOPTEROS5* (*TMO5*; Schlereth et al. 2010), *TMO6* (Schlereth et al. 2010), *SHORT-ROOT* (*SHR*; Möller et al. 2017), *WRKY17* (Möller et al. 2017), *ZWILLE* (*ZLL*; Moussian et al. 1998) and *PHLOEM EARLY DOF1* (*PEAR1*)/*DOF6* (Miyashima et al. 2019). Because most of these genes were initially identified due to their regulation by auxin (Schlereth et al. 2010), we additionally used the Arabidopsis embryo transcriptome atlas (Palovaara et al. 2017) to select potential vascular markers in an auxin-independent manner. Here, we describe the dynamic expression patterns of this panel of vascular-specific or vascular-enriched genes, and draw conclusions on the process of vascular specification during embryogenesis, on its timing, its specificity and its parallels to root development.

## Results

### Vascular identity is a diffuse trait in the early Arabidopsis embryo

Several vascular-specific genes have been used to track vascular identity in tissues such as root and leaf (Gardiner et al. 2010, Melnyk et al. 2015). To determine whether these genes also mark vascular tissue in the early embryo, we re-examined their expression patterns in detail. If these genes mark all vascular cells, expression is expected to start in the vascular initials at early globular stage. Surprisingly, we found that expression of many of these vascular marker genes was not tightly restricted to the vascular cells. Here we show their root and embryo expression patterns according to their transcriptional reporters (except for *SHR* and *TMO6* for which translational fusions were used). The vascular genes examined here are described starting with those least restricted to the first vascular cells in the embryo and ending with those whose expression is most specific.

Least strict in their expression, timing-wise, were *TMO5-LIKE1* (*T5L1*) and *TMO6*; their expression was not found in the early globular (EG) embryo. *T5L1* is a homolog of the basic helix-loop-helix (bHLH) transcription factor *TMO5* and contributes to vascular proliferation by stimulating cytokinin biosynthesis through the transcriptional activation of *LONELY GUY 3* and *4* (*LOG3/4*) genes (De Rybel et al. 2014, Ohashi-Ito et al. 2014). *TMO6* is a Dof transcription factor that also contributes to regulation of vascular proliferation (Miyashima et al. 2019). Both genes were identified as targets of auxin signaling through the AUXIN RESPONSE FACTOR (ARF) MONOPTEROS (MP; Schlereth et al. 2010) during embryogenesis but we did not detect their expression in the vascular

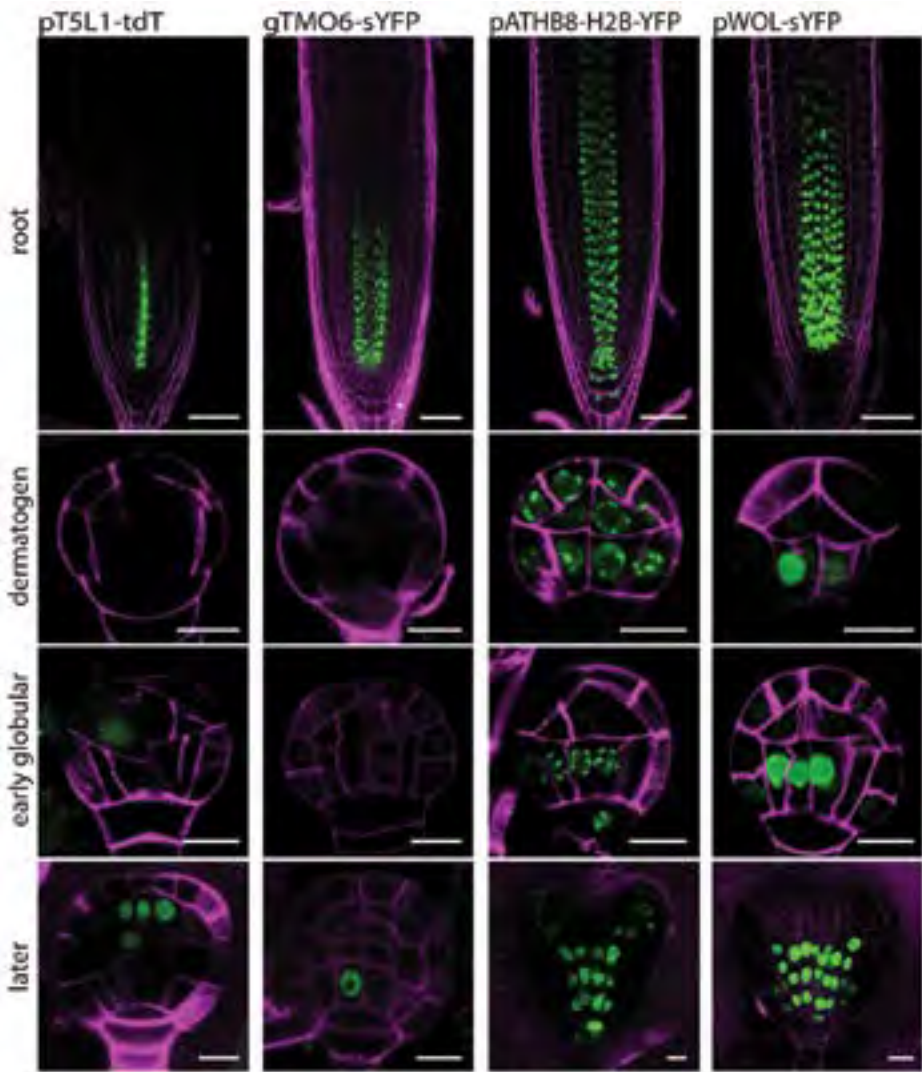


**Figure 1-1: Expression of established early vascular genes in root and early embryo.**

Genes are organized roughly from least (left) to most (right) specific in the embryo. For genes not yet vascular-specific at early globular stage, the first stage where expression is vascular-specific is included: late globular stage (EPM, PED1, T5L1, TMO6), transition stage (ZLL) or early heart stage (ATHB8, WOL). Transcriptional reporters are shown where available, translational reporters are shown for gSHR and gTMO6. Gene expression is in green regardless of fluorophore, magenta counterstaining is Propidium Iodide for root or Renaissance for embryo. Root scale bars represent 50 micrometer, embryo scale bars represent 10 micrometer.

cells of the EG stage embryo (Figure 1-1). *T5L1* and *TMO6* expression was first seen in the vascular cells of the late globular stage embryo.

In contrast, *ARABIDOPSIS THALIANA HOMEODOMAIN LEUCINE ZIPPER CLASS III (ATHB8)* expression did commence earlier but showed a diffuse expression pattern at these early stages. *ATHB8* is a procambial gene that is often used to track vascular identity in the leaf (Gardiner et al. 2010, 2011). It is a member of the Homeodomain Leucine Zipper Class III (HD-ZIP III) transcription factor family and plays a role in vascular proliferation and differentiation (Baima et al. 2001). *ATHB8* was also identified as a target of MONOPTEROS (MP) (Donner et al. 2009, Mattsson et al. 2003). We first observed *ATHB8* expression at 8-cell stage in all cells of the proembryo (data not shown). At early globular stage expression shifted to the lower tier of the proembryo and the upper cell of the suspensor (Figure 1-1). Afterwards, it took several more divisions before, around heart stage, *ATHB8* expression was confined to vascular cells.

Vascular specificity during embryogenesis was reached earlier by *WOODEN-LEG (WOL)*, *ZLL*, *PEAR1* and *DOF6*. *WOL* encodes for a histidine kinase receptor for cytokinin in vascular cells, and thereby controls the size and composition of the vascular bundle (Mähönen et al. 2000, Scheres et al. 1995). The *ZLL* protein is known to sequester MicroRNA156/166 (miR165/166) and thereby plays a key role in shoot apical meristem development (Roodbarkelari et al. 2015, Zhou et al. 2015, Zhu et al. 2011). In addition, we know the *ZLL* expression domain since the Q0990 GAL4/UAS enhancer trap line, which confers vascular expression of GAL4 and the GAL4-responsive GFP, was found to carry its insert upstream of the *ZLL* gene (Radoeva et al. 2016). PHLOEM EARLY DOF 1 (*PEAR1*) and *DOF6* were identified as regulators of vascular bundle size (Miyashima et al. 2019). Together with other Dof transcription factors they were shown to promote cambial divisions from the phloem poles. *WOL*, *ZLL*, *PEAR1* and *DOF6* were all four previously seen to play roles in vascular development and are expected to show vascular specific expression patterns. In the root and later embryonic stages these four genes were present exclusively in the vascular cells (Figure 1-1; Figure 1-2). However, at early globular stage all four were expressed at similar levels in the vascular and ground tissue precursors (Figure 1-1; Figure 1-2). One stage earlier, in the dermatogen embryo, we found that all 4 were expressed in the inner lower tier cells but not, or with lower expression levels, in the outer cells. Summarizing, these four genes already exhibit cell type specific expression at dermatogen stage but this specificity is not confined to the vascular cells until later stages.

*IQD15* and *SOK1* are both enriched in the vascular cells at early globular stage. These genes were identified as targets of MP signaling in the embryo (Schlereth et al. 2010). Recent work indicates that *SOK1* plays a role in cell polarity while *IQD15* appears to play a role in auxin and calcium signaling (Wendrich 2016, Yoshida et al. 2019). At dermatogen

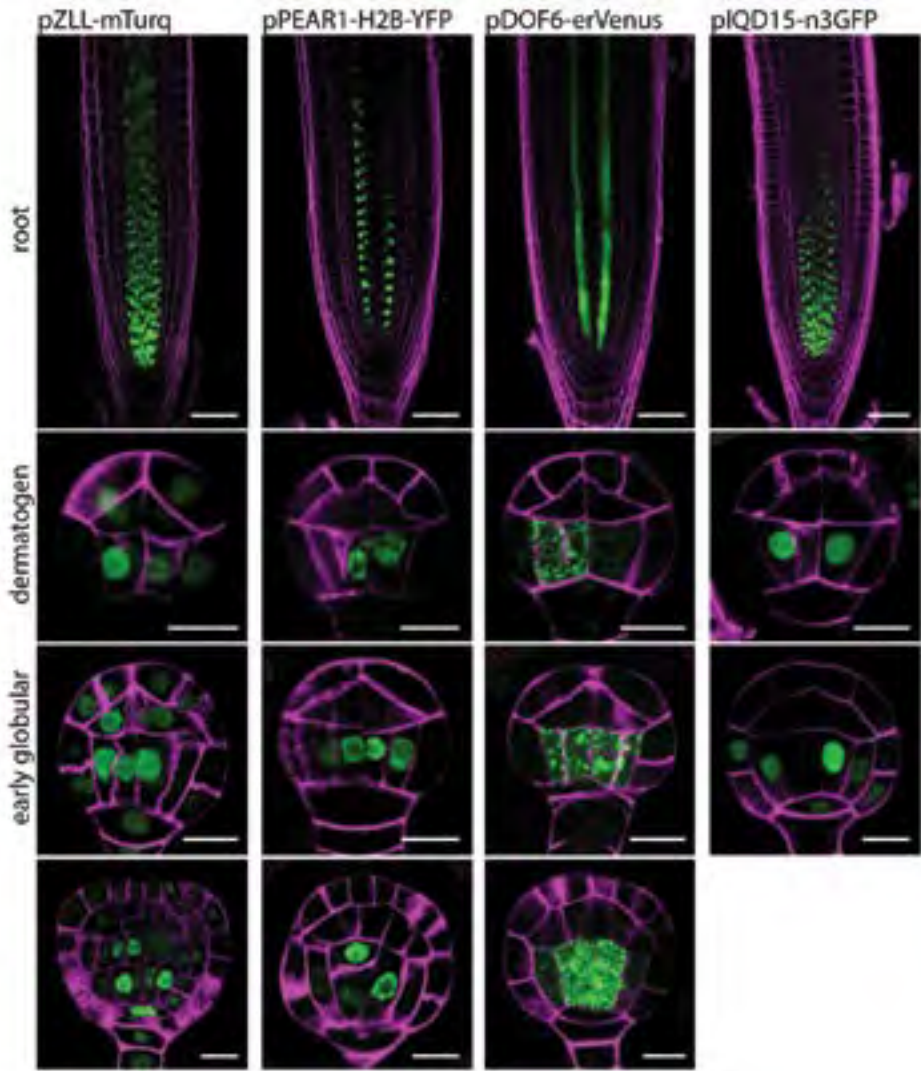


**Figure 1-2: Expression of established early vascular genes in root and early embryo.** Full description at Figure 1-1.

stage both *IQD15* and *SOK1* are expressed in the inner lower tier cells (Figure 1-2; Figure 1-3). After the periclinal division of these cells, the inner daughter cells show the highest expression levels, but fluorescence can also be found in the surrounding ground tissue cells. As such, these genes mark the vascular cells with their peak expression but are not exclusively present in the vascular cells until later in development.



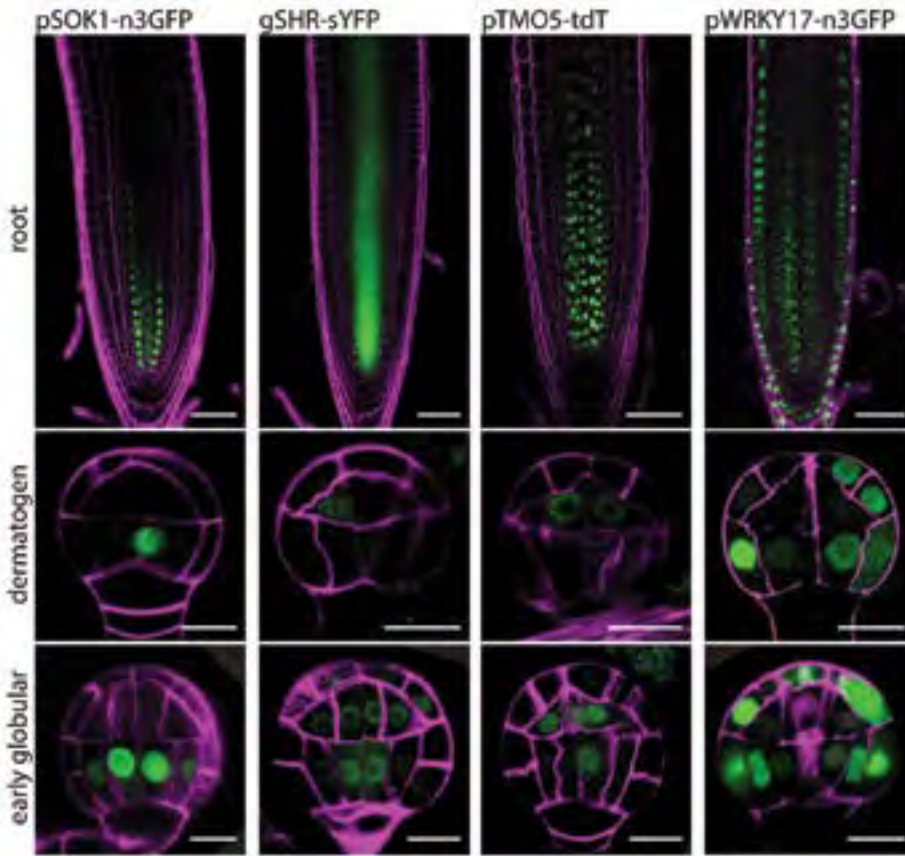


**Figure 1-3: Expression of established early vascular genes in root and early embryo.** Full description at Figure 1-1.

The distinction between ground tissue and vascular cells was most clear in the expression domains of *SHR* and *TMO5*. *SHR* encodes a GRAS-type transcription factor which is transported to the neighboring ground tissue cells where it triggers division to form the endodermis and cortex layers (Nakajima et al. 2001). *TMO5* encodes a basic Helix-Loop-Helix (bHLH) type transcription factor that together with LONESOME HIGHWAY (LHW) coordinates cytokinin accumulation in the vascular cells, causing them to undergo periclinal divisions (De Rybel et al. 2014, Ohashi-Ito et al. 2014). We found that both genes were always expressed in a strictly vascular specific manner in the lower tier, showing no signal in surrounding cells (Figure 1-3). *SHR* and *TMO5* were both expressed in the vascular cells at early globular stage. However, *SHR* expression started before that of *TMO5*: all EG embryos showed *TMO5* expression in the upper inner cells but a large amount of these embryos did not show *TMO5* promoter activity in the lower vascular cells. This indicates that its activity in the vascular cells starts later during early globular stage and thus follows after

*SHR*, which is active in the vascular cells and in the upper inner cells in all EG embryos. At dermatogen stage, *SHR* and *TMO5* are expressed but in the inner upper tier cells. This sets them apart from the other markers which all show expression in the inner lower tier cells.

A unique expression pattern was seen for *WRKY17*. This transcription factor was found as a target of MP in the embryo but its function during embryogenesis remains unknown (Möller et al. 2017). In the adult plant *WRKY17* was shown to play a role in basal resistance to *Pseudomonas* (Journot-Catalino et al. 2006). *WRKY17* was expressed broadly in the root meristem but in the embryo its expression was seen in all cells except for the vascular cells (Figure 1-3). We decided to coin this an inverse marker of vascular identity. Expression of *WRKY17* is highest in the protoderm cells and absent from the vascular cells and the upper inner cells. This pattern was already found at dermatogen stage where *WRKY17* expression was lower in the inner cells compared to the protoderm.

In summary, from this panel of established vascular marker genes, it appears that vascular genes are often first expressed in the inner cells of the dermatogen stage embryo. Subsequently, in the early globular stage embryo, most markers are not restricted to vascular cells. Expression then becomes restricted to the vascular cells within the next few cell divisions. In addition, the first vascular cells co-express marker genes that later in development are strictly separated. In the root, *DOF6* and *PEAR1* are expressed exclusively in the phloem and *TMO5* and *T5L1* are only present in the xylem (De Rybel et al. 2013, Miyashima et al. 2019), but in the embryo their expression patterns overlap. This unique identity is further underlined by the inverse marker *WRKY17*, whose pattern shows that some aspects of vascular identity might change or be lost during subsequent development as its exclusion from the vascular cells is embryo-specific. In conclusion, this set of genes marks diverse aspects of vascular identity during embryogenesis.

#### Novel vascular-enriched marker genes corroborate vascular origin and diffuseness

While the previously described vascular genes help us track vascular identity, this set of genes has several shortcomings. In addition to not only marking the vascular cells during embryogenesis, most vascular marker genes are known targets of auxin signaling through MONOPTEROS (MP). IQD15, SOK1, TMO5, T5L1 and TMO6 were all first investigated because they are direct targets of MP. This leads to a biased view of vascular identity. More vascular genes are therefore necessary to describe vascular identity in a more precise and unbiased manner.

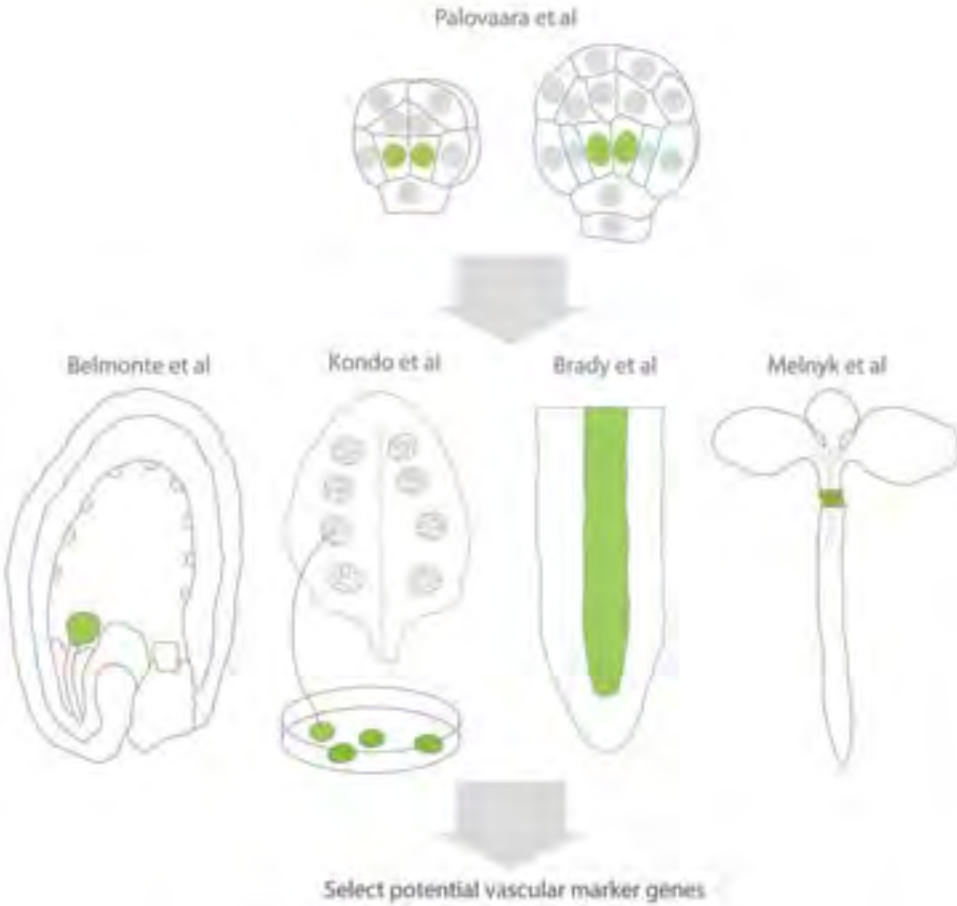


**Figure 2: Schematic overview of transcriptomic data sources used in the selection pipeline for potential vascular marker genes.**

We used the cell type-specific embryo transcriptome atlas to select potential vascular marker genes (Palovaara et al. 2017). This atlas was generated by Isolation of Nuclei TAgged in specific Cell Types (INTACT), followed by a comparison of transcripts from these tissue-specific nuclei to transcripts from all nuclei of the early embryo (Palovaara et al. 2017). By comparing transcripts isolated from *IQD15*-expressing nuclei to those from either the entire embryo, or to those from other cell types, we selected genes whose transcripts were enriched in the first vascular cells. We then added transcriptomics data from embryo (Belmonte et al. 2013), root (Brady et al. 2007), leaf disk (Kondo et al. 2015), and graft junction (Melnik et al. 2018) to select genes that were likely expressed during embryogenesis and during vascular development (Figure 2).



**Table 1: Expression pattern overview of potential vascular marker genes in root and embryo.**

Schematic overview of the expression pattern analysis of 36 potential vascular marker genes. For simplicity only presence and vascular specificity of expression are indicated (O = no, X = yes).

Locus	Gene name	Expression in root		Expression in embryo					
		Vascular		Before globular stage		At Globular stage		After globular stage	
		Present	specific/enr	Present	specific/enr	Present	specific/enr	Present	specific/enr
AT2G26320	AGL33	O	O	O	O	O	O	O	O
AT1G69180	CRC	O	O	O	O	O	O	O	O
AT5G47000	PERO	O	O	O	O	O	O	O	O
AT4G31800	WRKY18	O	O	O	O	O	O	O	O
AT1G80840	WRKY40	O	O	O	O	O	O	O	O
AT3G24650	ABI3	O	O	X	O	X	O	X	O
AT1G14440	ATHB31	O	O	X	O	X	O	X	O
AT3G22100	bHLH117	O	O	X	O	X	O	X	O
AT3G24500	MBF1C	O	O	X	O	X	O	X	O
AT1G32640	MYC2	X	O	O	O	O	O	O	O
AT2G05810	ARM	X	O	O	O	O	O	O	O
AT5G09330	ANAC082	X	O	O	O	O	O	O	O
AT5G44570	UNKN1	X	O	O	O	O	O	O	O
AT5G54480	DUF632	X	O	O	O	O	O	O	O
AT2G22500	PUMP5	X	X	O	O	O	O	O	O
AT2G42960	PK1	X	X	O	O	O	O	O	O
AT5G05340	PRX52	X	X	O	O	O	O	O	O
AT5G35960	PK2	X	X	O	O	O	O	O	O
AT4G00050	UNE10	X	X	O	O	O	O	X	O
AT4G16560	HSP20	X	X	O	O	?	O	X	O
AT2G27580	A20AN1	X	O	X	O	X	O	X	O
AT5G05410	DREB2A	X	O	X	O	X	O	X	O
AT2G27500	GH17	X	O	X	O	X	O	X	O
AT3G12580	HSP70	X	O	X	O	X	O	X	O
AT5G67300	MYB44	X	O	X	O	X	O	X	O
AT1G07350	SR45A	X	O	X	O	X	O	X	O
AT2G43290	MSS3	X	O	X	X	X	X	X	X
AT5G24590	ANAC091	X	X	X	O	X	O	X	O
AT4G11460	CRK30	X	X	X	O	X	O	X	O
AT2G26150	HSFA2	X	X	X	O	X	O	X	O
AT1G48000	MYB112	X	X	X	O	X	O	X	O
AT3G15210	ERF4	X	X	X	O	X	O	X	X
AT4G03170	AP2B3	X	X	X	O	X	X	?	?
AT4G00260	MEE45	X	X	X	O	X	X	X	X
AT2G18380	GATA20	X	X	X	X	X	X	X	X
AT1G11735	MIR1718	X	X	X	X	X	X	X	X

These datasets were used in two steps. The first step was to select genes enriched in the vascular cells at dermatogen, early globular or late globular stage using the cell type-specific transcriptome atlas. For selection, a gene should be either enriched in the vascular cells compared to the whole embryo or enriched in the vascular cells compared to the ground tissue cells. The second step was to add the additional four datasets. In this step a gene should be enriched in the target tissue of at least one of the four datasets. This method yielded 36 potential marker genes for which we generated transcriptional reporters by fusing 1.5-3.3 kb of promoter sequence upstream of the start codon to a sensitive nuclear 3xGFP, and checked their expression in root and embryo (Table 1; Supplementary Table 4).

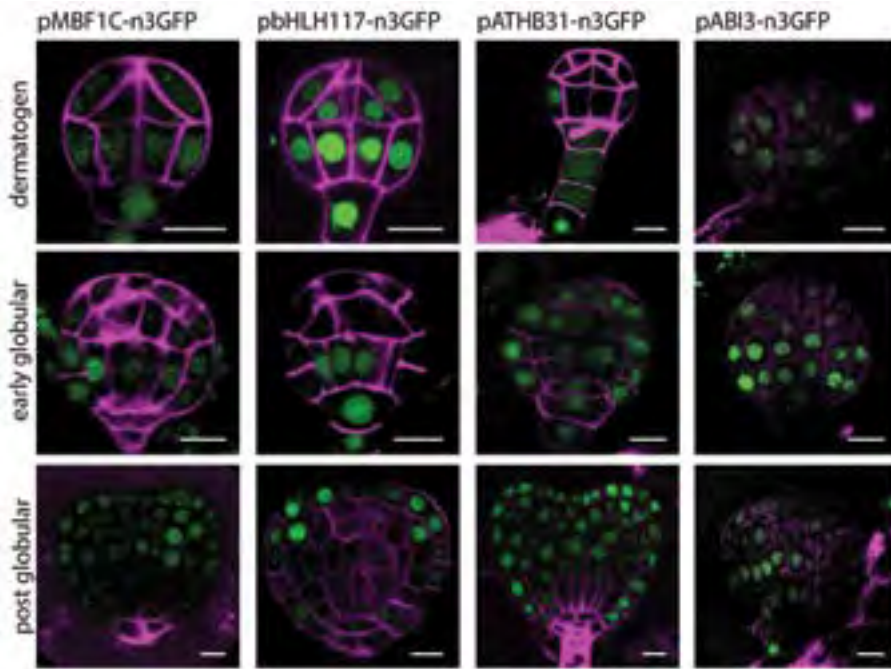


**Figure 3-1: Expression of embryo expressed potential vascular marker genes in root and early embryo.** Genes are organized as described in the main text, based on expression pattern: roughly from least (left) to most (right) vascular specific in the embryo. Expression of the transcriptional reporter is shown in green, magenta counterstaining is Propidium Iodide for root or Renaissance for embryo. Root scale bars represent 50 micrometer, embryo scale bars represent 10 micrometer.

Of the 36 genes that were examined, no signal could be found in root or embryo for 5 transcriptional reporters (Table 1). In addition, for 9 genes expression was seen in the root but not in the embryo (Supplementary Figure 1). For the remaining 22 genes, promoters were active during embryogenesis and were further examined to determine their expression pattern during vascular tissue specification.

Expression of *ABI3*, *ATHB31*, *bHLH117* and *MBF1C* was absent in the root but could be found in the embryo. All 4 were expressed as early as early globular stage, but none were vascular specific at that stage or later in embryo development (Figure 3-1)(Table 1).

18 other genes were expressed in both root and embryo. Of these, expression for 7 was not vascular-enriched in the root. *A20AN1*, *MYB44* and *SR45A* were expressed in all cell types of the root and this pattern was conserved in the embryo (Figure 3-2; Figure 3-3). In contrast, the genes *DREB2A*, *GH17*, *HSP70* and *MSS3* each showed cell type specificity in the root, but this specificity was not vascular. These four were expressed in the outer tissues of the root: the columella and/or lateral root cap (LRC). For *DREB2A* and *HSP70* this

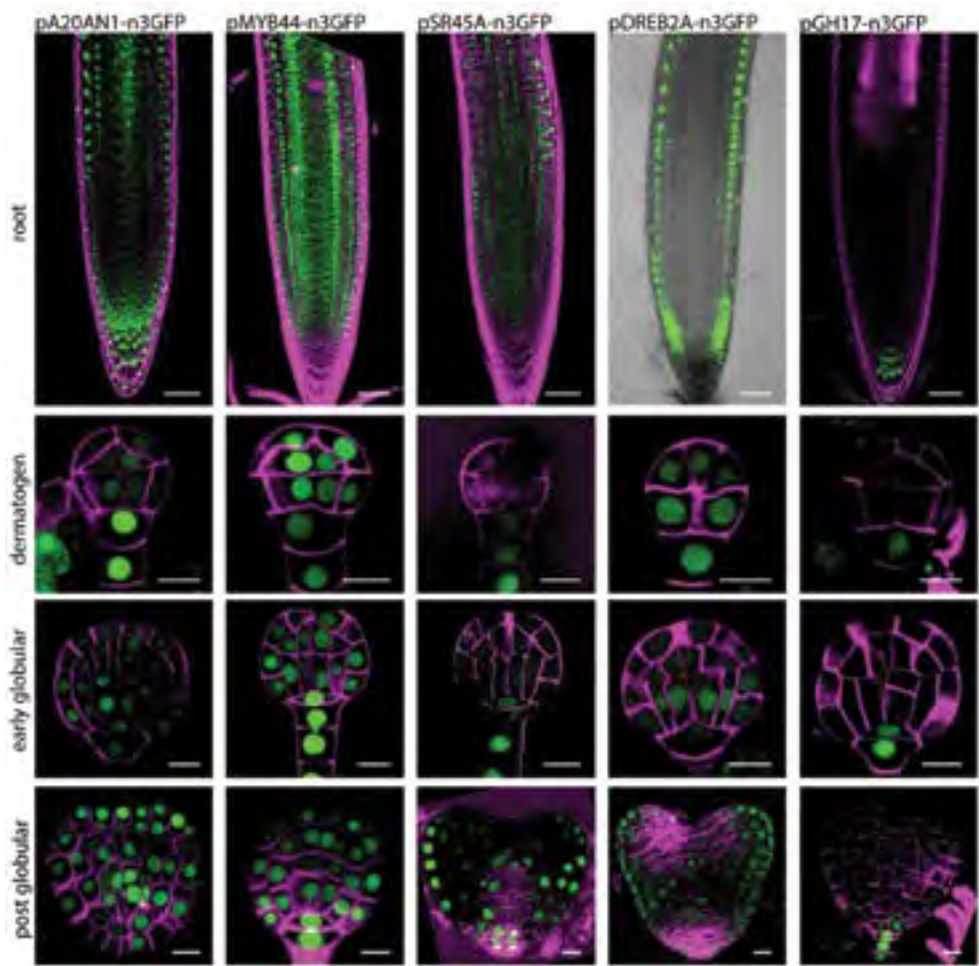


**Figure 3-2: Expression of embryo expressed potential vascular marker genes in root and early embryo.**  
Full description at Figure 3-1.

specificity was not replicated in the embryo where we saw either random or broad expression (Figure 3-2; Figure 3-3). *GH17* and *MSS3* did also show cell type specific expression in the embryo. *GH17* was present in the columella in the root and in the embryo was seen in the columella precursors. *MSS3* was found in the columella and LRC of the root and in the embryo was similarly expressed in the outer cell layer. However, two aspects of *MSS3* expression stand out. Firstly, in the root *MSS3* is also expressed in two vascular cell files away from the stem cell niche (SCN) (Figure 3-3). Secondly, *MSS3* expression in the embryo is also present in the ground tissue. This means that during embryogenesis the *MSS3* promoter is active in all cell types but the vascular cells, which means that *MSS3* can be used as an inverse marker

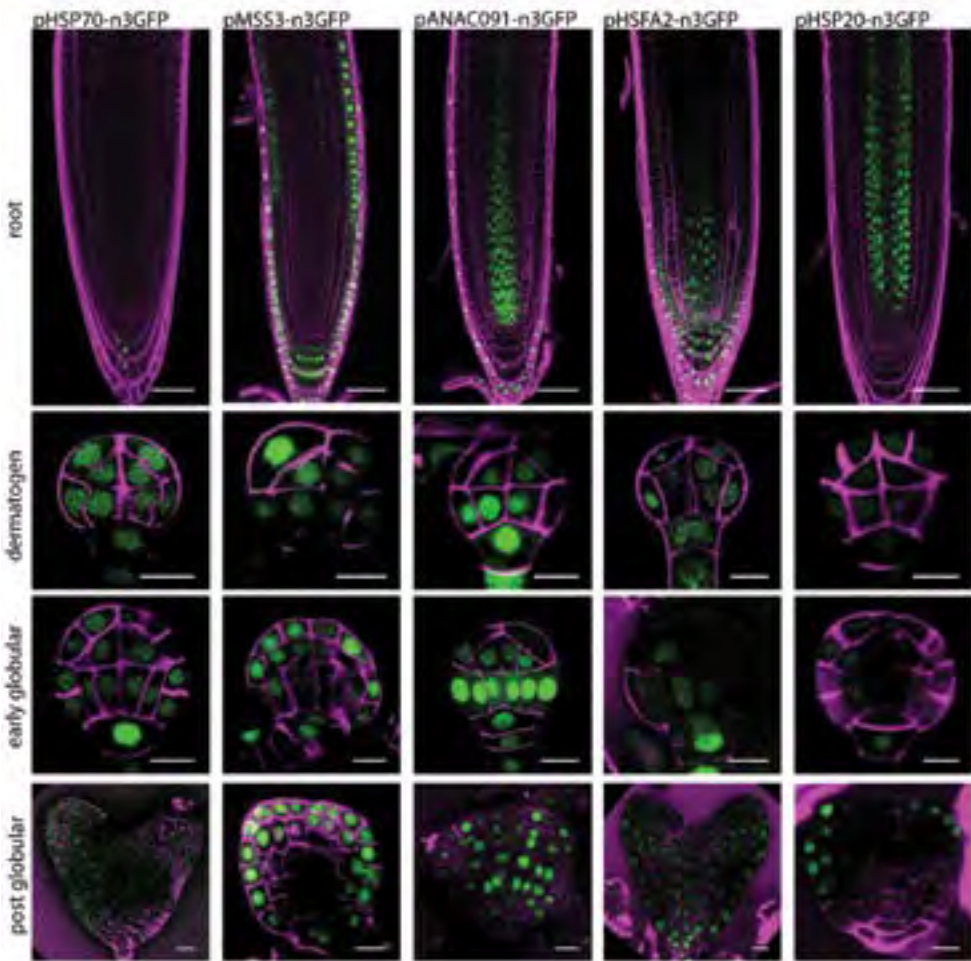


**Figure 3-3: Expression of embryo expressed potential vascular marker genes in root and early embryo.**  
Full description at Figure 3-1.

of vascular identity during embryogenesis.

Of the potential vascular markers selected, 11 genes showed vascular expression in the root. However, their embryo expression patterns were highly diverse. *ANAC091* and *HSA2* are present in the root within the vascular cells and in some cells of the lateral root cap and columella (Figure 3-3). However, in the early embryo these genes displayed broad expression, indicating that the expression of these genes is not regulated in a vascular-specific manner in early development. The next two genes, *ERF4* and *CRK30* were expressed in the vascular cells and some surrounding cells in the root and a similar pattern was seen in the embryo where promoters of both were active in the future root stem cell niche, showing



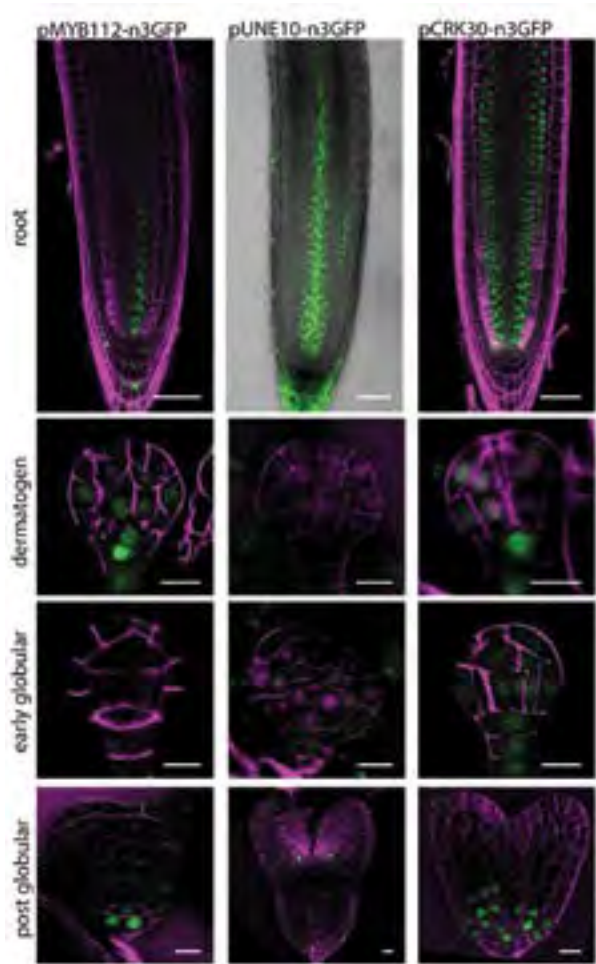


**Figure 3-4: Expression of embryo expressed potential vascular marker genes in root and early embryo.**  
*Full description at Figure 3-1.*

broader but similar expression (Figure 3-4; Figure 3-5). In contrast, the three other genes in this group showed clear differences in expression between root and embryo. In the root, *HSP20* was expressed in the vascular bundle, starting at approximately the 4th cell from the QC (Figure 3-3). In the embryo, no vascular specificity was seen, expression started in seemingly random cells around globular stage before becoming restricted to the future cotyledon regions. *MYB112* and *UNE10* displayed the most dissimilar patterns of expression between root and embryo (Figure 3-4). In the root these genes were expressed in the vascular cells but in the embryo they were expressed in different cell types: *MYB112* in and below the hypophysis and *UNE10* late in embryogenesis at the SAM-cotyledon boundary.

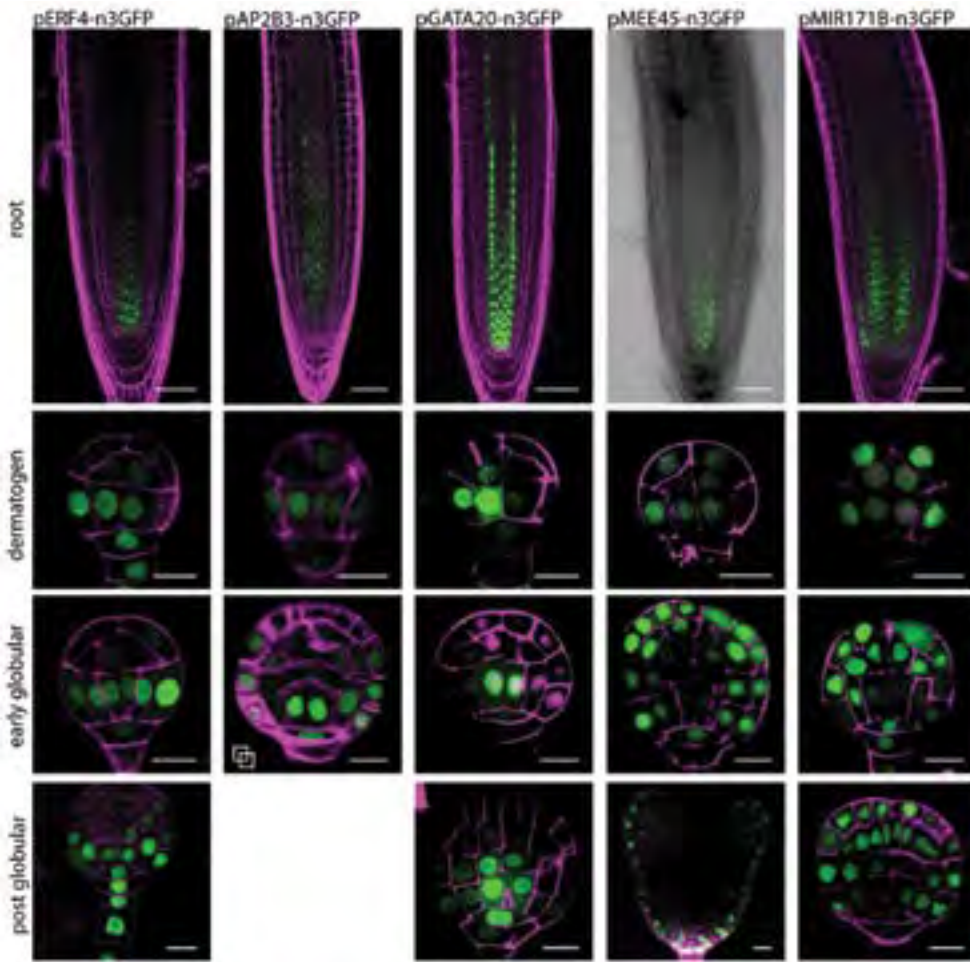


**Figure 3-5: Expression of embryo expressed potential vascular marker genes in root and early embryo.** Full description at Figure 3-1.

The final four genes were the most specific to the vascular cells. *AP2B3* and *GATA20* were both expressed exclusively in the vascular cells in the root and in the embryo they were strongly enriched in the vascular cells (Figure 3-5). However, *AP2B3* expression was not vascular-enriched until late globular stage. Thus, while it specifically marks vascular cells later, its expression is broad at the initiation of vascular identity. In contrast, *GATA20* expression, which started at dermatogen stage, was at each stage specifically marking the vascular cells.

In addition to these conventional vascular marker genes, two more inverse vascular markers were identified. *MEE45* and *MIR171B* were expressed in the vascular cells of the root but in the embryo showed the opposite expression pattern (Figure 3-5). Expression

of both genes was present in all cells except for the vascular cells and was strongest in the protoderm. As a result, *MEE45* and *MIR171B* can be used as vascular marker genes during embryogenesis despite showing the opposite of what was expected based on the embryo transcriptome atlas and root expression.

This set of reporter lines shows a variety of expression patterns in root and embryo from which we can infer general patterns. In general, gene expression patterns in the root seem to be poor predictor of the expression in the early embryo. If a gene is also expressed during embryogenesis, it often shows a broader expression pattern in the early embryo and some even show different cell type specificity. These new vascular genes also affirm that at dermatogen stage the inner cells have vascular identity. From the potential marker genes we selected 6 genes that can help describe vascular identity: *MSS3*, *ERF4*, *AP2B3*, *GATA20*, *MEE45* and *MIR171B*. Not all vascular genes become restricted to the vascular cells at the same point in development and this set of genes reflects those findings.

## Discussion

In this chapter, we set out to better describe vascular identity in the Arabidopsis embryo using transcriptional reporters of both previously identified and novel vascular genes. We found that expression of most genes was not limited to the vascular cells at the early stages of embryogenesis. In this chapter we use these findings to describe the development of vascular identity over time. It should be noted however, that this broad pattern could also be the result of technical artefacts. We have examined the expression patterns of transcriptional reporters. While a promoter of 3 kb is generally more than sufficient to report genuine gene activity (Maher et al. 2018, Medford et al. 2007, Yu et al. 2016), additional factors including regulation sites within or downstream of the gene and post-transcriptional modification can contribute to the localization of the transcript. However this is difficult to check as for most vascular markers no in situ hybridization data is present for the embryo, and when it is available this data closely corroborates the transcriptional reporter (Schlereth et al. 2010) or does not provide information on the earliest stages of embryogenesis (Baima et al. 1995). In addition, fluorophore stability could result in signal being present in daughter cells that themselves no longer have promoter activity. This could potentially explain low levels of fluorescence in the ground tissue cells for *IQD15* and *SOK1* after the periclinal division in the 16-cell stage, but is unlikely the cause for the level of fluorescence found in ground tissue cells for genes such as *ZLL* and *PEAR1* (Figure 1). To circumvent this problem, it is possible to decrease fluorophore stability: adding destruction boxes can decrease GFP half-life

3 in mammalian cells from about 26 hours to about 5,5 hours (Corish & Tyler-Smith 1999). This would eliminate nonrelevant signal, but it would also reduce the reporter signal such that imaging in the embryo would likely become challenging. Finally, the broad embryo expression patterns seen for many of the new reporter genes could be caused by the method of selection. The embryo transcriptome atlas we based our selection on uses enrichment of transcripts in vascular nuclei compared to nuclei of the entire embryo (Palovaara et al. 2017). Given that enrichment does not mean exclusive expression in vascular cells, selecting for vascular-enriched transcripts using this dataset therefore does not exclude genes which are present in more cell types in the embryo. The additional datasets we used to add vascular specificity did result in many reporters that were vascular-specific in the root, but this specificity was evidently often not shared in the embryo (Figure 3; Supplementary Figure 1). Lastly, the embryo transcriptome atlas used for selection of new marker genes is constructed using nuclear extraction (Palovaara et al. 2017). Recent work has highlighted the differences between nuclear and cytosolic transcripts, most notably the distribution of transcripts with different half-lives between the two compartments, with nuclear transcripts having on average shorter half-lives (Palovaara & Weijers 2018). As a result, genes with vascular specific transcripts in the cytosol were missed in our selection. Altogether, keeping in mind the limitations of transcriptomics data and transcriptional reporters, we believe that the genes we selected provide a good tool for tracking and understanding the development of vascular identity.

Many of the vascular genes we looked at in this chapter start cell type-specific expression at dermatogen stage. At dermatogen stage these genes are expressed in the inner cells, most of them in the inner lower tier but several (*SHR* and *TMO5*) in the inner upper tier. The inverse markers for their part have reduced expression in the inner cells compared to the protoderm (Figure 1 and 3). This observation indicates that the gene expression program that marks future vascular cells is first present one stage earlier than was previously reported based on lineage tracing (Scheres et al. 1994). This matches the results of Palovaara et al 2017 who performed GO term analysis on their embryo transcriptome atlas (Palovaara et al. 2017). This analysis showed that the inner lower tier cells at dermatogen stage closely resemble the vascular cells one stage later, but that the ground tissue cells have undergone significant changes, making them distinct from the inner lower tier and vascular cells. These findings suggest that the most central cells at any stage of *Arabidopsis* embryogenesis have (pro)vascular identity and that during embryogenesis ground tissue identity arises from vascular identity. The presence of a large number vascular genes in surrounding cells at globular stage could reflect that after the initiation of vascular identity, further development and re-



striction takes place until several divisions later, when vascular genes are no longer observed in ground tissue cells. These findings indicate that during embryogenesis, vascular identity is initiated at dermatogen stage after which vascular genes step by step become excluded from surrounding cells until identities are completely separated around transition stage. From a biological perspective it is plausible that one or several gradients first select the first vascular cells in a quantitative fashion but that feedback through gene regulatory networks is then needed to convert identity into a qualitative trait (Ashe 2006, Briscoe & Small 2015, Lawrence & Struhl 1996, Turing 1952).

The broad expression in the embryo of many genes that are vascular specific in the root could reflect the likely continuous process of vascular development in the embryo. It appears that identity is not laid down in one step but takes several steps before being strict and complete. However, the differences in expression patterns between root and embryo are larger than could be explained this way. While many vascular genes are simply expressed in additional cells early on, a large number of genes that are vascular-specific in the root are expressed in all cells of the embryo, showing no specificity (Figure 3). In addition, we now have four inverse vascular markers (*WRKY17*, *MIR171B*, *MEE45*, *MSS3*). Each of these is excluded from the vascular cells in the embryo but show unrelated patterns in the root. *MIR171B* and *MEE45* are even present in what seem to be the opposite cell types in the root as compared to the embryo (Figure 3). It appears that the embryo is not simply a miniature version of the root. This is further underlined by several non-vascular markers that show different cell type specificity between root and embryo (*SR45A*, *DREB2A*, *HSP20*). In addition to these findings, the first vascular cells seem to have an identity that is unique to the embryo. These cells express both xylem (*TMO5*, *T5L1*) and phloem (*DOF6*, *PEAR1*) marker genes and thus have a mixed identity that is unique to the embryo. The differences between root and embryo we describe here do make it more difficult to extrapolate findings from one to the other but do better explain the development of vascular identity during embryogenesis.

In conclusion we have added to the collection of genes that can be used to identify and track vascular cells. In addition, we show that vascular identity is first initiated at dermatogen stage and that the specification process is not complete until about transition stage. The development of vascular identity is likely started through signaling gradients at dermatogen stage but then likely takes several steps to become a specific trait, likely through feedback and feedforward regulation. With this increased understanding of the development of vascular identity we can now take steps to better understand its regulation.

## Material and methods

### Plant material and growth conditions

Arabidopsis seeds were surface-sterilized and plated on ½ MS plates with or without antibiotic. After 2 days of stratification they were grown at 21 °C under standard long-day (16:8h light:dark) conditions. If antibiotics selection was used seedlings were transferred to plates without antibiotics after 7 days of growth. After the appearance of the first true leaves the seedlings were transferred to soil and grown under the same conditions.

Reporter lines for *DOF6*, *PEAR1* and *TMO6* were previously published in (Miyashima et al. 2019). Transcriptional reporters for targets of MP: *IQD15*, *SOK1*, *T5L1*, *TMO5* and *WRKY17* were previously published (De Rybel et al. 2013, Möller et al. 2017, Schlereth et al. 2010). The reporters for *ATHB8* and *SHR* were previously published (Donner et al. 2009, Nakajima et al. 2001). Reporters generated for *WOL* and *ZLL* using primers documented in Supplementary Table 4 reproduce previously described expression patterns (Mähönen et al. 2000, Radoeva et al. 2016).

### Cloning and plant transformation

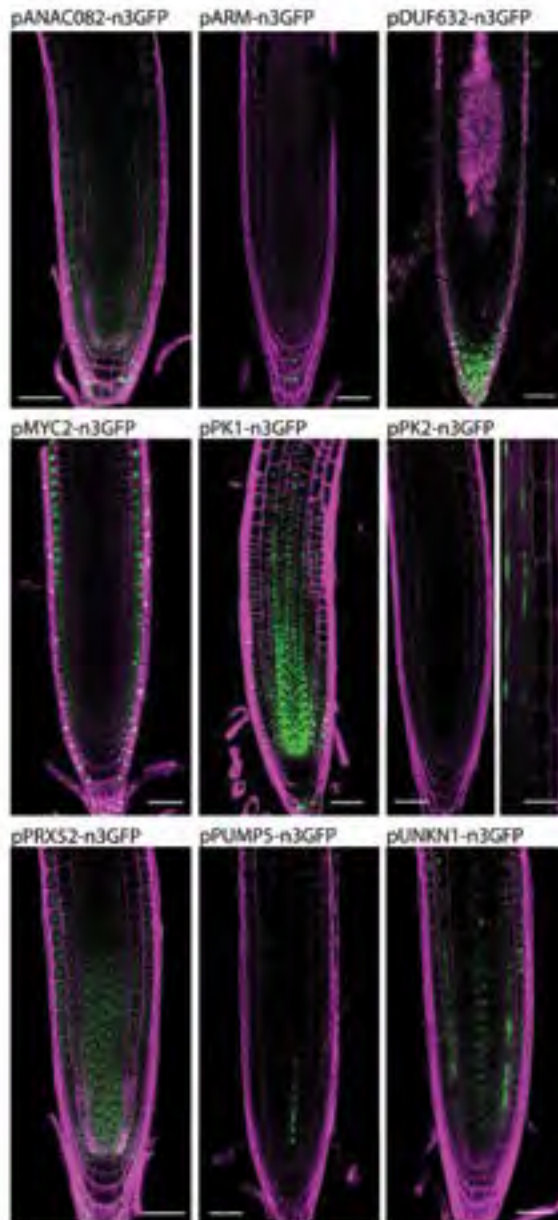
Transcriptional fusion constructs were created by first amplifying 1.5-3.3 kb upstream of the start codon using Phusion Flash DNA polymerase (Phusion Flash PCR Master Mix; Thermo Scientific) and the primers listed in Supplementary Table 4. Promoter fragments were cloned into the pPLV04\_v2 vector (De Rybel et al. 2011, Wendrich et al. 2015) using the Seamless Ligation Cloning Extract (SliCE) method (Zhang et al. 2014b). All constructs were confirmed by sequencing before transformation into Col-0 wildtype Arabidopsis plants by simplified floral dipping (De Rybel et al. 2011).

### Microscopy, selection and sample preparation

Sample preparation for imaging of roots consisted of a brief incubation of roots from 5-10 day old seedlings in a solution containing 10 µg/ml propidium iodide (PI) for counterstaining. For embryo imaging, ovules were isolated and embryos were squeezed out by applying slight pressure on the coverslip. Ovules and embryos were imaged in a solution containing 10% glucose and 0,01% SCRI Renaissance Stain 2200 (R2200; Renaissance Chemicals, UK) for counterstaining. Expression patterns were deemed reliable if roots of more than 3 transformants showed the same expression pattern after which embryo expression was checked for 2 lines with similar root expression.

Confocal imaging was performed on a Leica SP5 II system equipped with Hybrid Detectors (embryos, roots) or on a Leica SP8 X SMD confocal microscope equipped with a hybrid (HyD) detectors and a pulsed white-light laser (roots). Both systems were used for the detection of GFP and PI which were excited at 488 and 514 nm, and detected between 500-535 nm and 630-700 nm, respectively. On the SP5 system R2200 was visualized by excitation at 405 nm and detection between 430-470 nm.

## Supplementary figures and tables



**Supplementary figure 1: Root expression patterns for potential vascular markers not expressed in the embryo.**

Expression of the transcriptional reporter is shown in green, magenta counterstaining is Propidium Iodide and scale bars represent 50 micrometer. Second picture of pPK2-n3GFP is higher up in the root.

**Supplementary table 1: Expression values of potential vascular markers in the first iteration of INTACT.** Two version of these data are shown: as normalized using LOESS (left) or RMA (right). Samples were limited to vascular cells compared to the entire embryo (IQD15-RPS5a) at late and early globular stage (LG and EG). Q-values and genes selected based on this dataset are highlighted.

Gene Name	Locus	LOESS norm FC IQD15_LG- RPS5a_LG	q-value IQD15_LG- RPS5a_LG	LOESS norm FC IQD15_EG- RPS5a_EG	q-value IQD15_EG- RPS5a_EG	RMA norm FC IQD15_LG- RPS5a_LG	q-value IQD15_LG- RPS5a_LG	RMA norm FC IQD15_EG- RPS5a_EG	q-value IQD15_EG- RPS5a_EG
SP4SA	AT1G07350	2.532	0.002	1.847	0.070	7.111	0.003	6.125	0.009
MR1718	AT1G13735	1.047	0.353	1.012	0.895	1.850	0.012	1.018	0.804
ATH831	AT1G14440	1.165	0.066	1.014	0.908	2.578	0.013	1.041	0.798
MYC2	AT1G12640	1.127	0.389	1.136	0.804	1.131	0.452	1.837	0.467
MYB112	AT1G48000	1.166	0.024	1.086	0.483	2.705	0.006	1.563	0.343
CRC	AT1G69180	1.020	0.627	1.039	0.781	1.414	0.183	1.326	0.500
WRX140	AT1G08040	1.184	0.421	1.271	0.556	1.290	0.412	2.263	0.453
ARM	AT2G05810	1.244	0.356	1.002	0.928	1.106	0.462	1.185	0.751
GATA20	AT2G18380	1.095	0.083	1.015	0.882	1.757	0.031	1.111	0.715
PUMPS	AT2G27500	1.558	0.100	1.150	0.811	1.632	0.284	1.013	0.816
H5FA2	AT2G26150	3.420	0.001	1.314	0.721	23.595	0.002	3.240	0.359
AGL33	AT2G26320	1.111	0.259	1.073	0.713	2.324	0.046	1.483	0.510
GH17	AT2G27500	1.256	0.017	1.021	0.898	1.872	0.060	1.145	0.718
A20AN1	AT2G27580	2.295	0.004	1.076	0.889	5.554	0.012	1.142	0.775
PK1	AT2G42960	1.085	0.287	1.003	0.934	1.055	0.456	1.018	0.807
MY33	AT2G41290	1.127	0.370	1.081	0.790	1.538	0.225	1.165	0.759
HSP70	AT3G12580	13.399	0.000	2.910	0.250	39.313	0.001	18.444	0.008
ERF4	AT3G15210	5.516	0.000	2.538	0.032	7.818	0.005	4.768	0.060
SHU117	AT3G22100	1.159	0.041	1.013	0.905	2.629	0.014	1.303	0.761
MBF1C	AT3G24500	4.091	0.001	1.715	0.418	8.553	0.006	2.985	0.265
ARE3	AT3G24650	1.087	0.153	1.003	0.923	1.928	0.029	1.132	0.713
UNE10	AT4G00050	1.086	0.196	1.058	0.641	1.998	0.021	1.239	0.585
MYE45	AT4G00260	1.092	0.192	1.021	0.886	2.287	0.023	1.012	0.813
AP2B3	AT4G03170	1.094	0.154	1.056	0.657	1.857	0.027	1.482	0.305
CRC30	AT4G11460	1.067	0.209	1.068	0.443	1.660	0.013	1.602	0.043
HSP70	AT4G16560	1.085	0.134	1.116	0.098	2.070	0.013	2.192	0.016
WRKY18	AT4G31800	1.013	0.652	1.132	0.615	1.127	0.432	1.589	0.461
PRXS2	AT5G05340	1.056	0.391	1.155	0.063	1.513	0.111	2.381	0.010
DHER2A	AT5G05410	1.442	0.064	1.096	0.830	3.204	0.039	1.266	0.710
ANAC082	AT5G09330	1.781	0.041	1.139	0.833	1.449	0.323	1.289	0.714
ANAC091	AT5G24590	2.153	0.009	1.510	0.365	2.768	0.122	3.162	0.261
PK2	AT5G35960	1.041	0.376	1.010	0.900	1.011	0.499	1.095	0.707
UNON1	AT5G44570	1.063	0.469	1.022	0.895	1.325	0.286	1.105	0.762
PERO	AT5G47000	1.037	0.491	1.034	0.852	1.015	0.498	1.175	0.622
DUF632	AT5G54480	1.080	0.094	1.010	0.899	1.888	0.004	1.091	0.702
MYB44	AT5G67300	1.423	0.003	1.091	0.800	3.015	0.019	1.419	0.571

**Supplementary table 2: Expression values of potential vascular markers in the final iteration of INTACT.** Data was available for three developmental stages (16cell, EG, LG). For 16cell stage nuclear transcripts from inner lower tier cells could be compared to the entire embryo (nLT vs nEMB). At early and late globular stages three comparisons could be made to select for vascular enrichment: vascular cells against the entire embryo (nVSC vs nEMB); vascular cells against ground tissue cells (nVSC vs nGSC); and vascular cells against suspensor cells (nVSC vs nSUS). Q-values and genes selected based on this dataset are highlighted.

Name	AGI	FC		Q-value		FC		Q-value		FC		Q-value		FC		Q-value		FC		Q-value	
		nLT	16cell	vs	nEMB	nLT	16cell	vs	nEMB	nLT	16cell	vs	nEMB	nLT	16cell	vs	nEMB	nLT	16cell	vs	nEMB
SRFSA	AT1G07750	-1.066	0.863	-1.239	0.604	-2.543	0.158	-3.089	0.176	2.601	0.235	-1.404	0.387	2.178	0.656	0.656	0.656	0.656	0.656	0.656	0.656
MIR1718	AT1G11735	-2.658	0.317	1.117	0.654	1.078	0.748	-1.131	0.783	-1.018	0.857	1.203	0.476	1.109	0.925	0.925	0.925	0.925	0.925	0.925	0.925
ATHB31	AT1G14440	-1.532	0.384	1.083	0.632	1.297	0.404	-1.467	0.360	-1.160	0.735	1.087	0.484	1.154	0.875	0.875	0.875	0.875	0.875	0.875	0.875
MYC2	AT1G32840	2.027	0.341	2.642	0.026	-1.171	0.665	1.443	0.539	3.110	0.221	1.179	0.453	1.356	0.842	0.842	0.842	0.842	0.842	0.842	0.842
MYB112	AT1G48000	-1.327	0.725	1.053	0.682	1.120	0.696	1.031	0.818	1.492	0.523	1.763	0.143	1.035	0.935	0.935	0.935	0.935	0.935	0.935	0.935
CRC	AT1G69180	-1.031	0.865	2.168	0.019	3.826	0.000	2.448	0.045	1.131	0.779	1.773	0.257	1.446	0.692	0.692	0.692	0.692	0.692	0.692	0.692
WRR40	AT1G69840	3.250	0.285	10.511	0.001	-1.062	0.759	2.140	0.449	5.431	0.025	-1.041	0.560	1.183	0.915	0.915	0.915	0.915	0.915	0.915	0.915
ARM	AT2G05810	5.112	0.047	3.604	0.030	-1.014	0.775	1.854	0.476	4.265	0.032	-1.141	0.508	-1.133	0.920	0.920	0.920	0.920	0.920	0.920	0.920
GATA20	AT2G18180	-1.932	0.213	1.132	0.598	1.798	0.106	1.213	0.681	1.094	0.810	1.091	0.496	-1.186	0.875	0.875	0.875	0.875	0.875	0.875	0.875
PUMPS	AT2G22500	2.979	0.154	3.495	0.013	-1.196	0.666	1.761	0.453	4.130	0.013	-1.067	0.538	-2.345	0.476	0.476	0.476	0.476	0.476	0.476	0.476
H5FA2	AT2G26150	1.048	0.856	1.680	0.358	-6.108	0.004	-4.582	0.048	3.994	0.033	-1.199	0.476	3.128	0.357	0.357	0.357	0.357	0.357	0.357	0.357
AGL33	AT2G26120	-1.130	0.818	-1.190	0.530	1.002	0.778	1.044	0.799	1.061	0.828	1.522	0.177	1.276	0.823	0.823	0.823	0.823	0.823	0.823	0.823
GH17	AT2G27500	2.238	0.259	2.459	0.039	1.136	0.694	2.484	0.137	2.419	0.095	1.071	0.531	-1.287	0.863	0.863	0.863	0.863	0.863	0.863	0.863
A20AN1	AT2G27580	-1.915	0.560	1.187	0.628	-2.183	0.231	1.313	0.715	2.284	0.311	1.762	0.256	1.953	0.687	0.687	0.687	0.687	0.687	0.687	0.687
PK1	AT2G42960	1.010	0.873	2.210	0.021	2.125	0.040	2.983	0.021	1.015	0.855	-1.489	0.203	-1.869	0.429	0.429	0.429	0.429	0.429	0.429	0.429
M553	AT2G41290	3.297	0.194	3.554	0.015	-1.059	0.754	1.139	0.773	2.133	0.290	1.124	0.508	1.013	0.939	0.939	0.939	0.939	0.939	0.939	0.939
H5P70	AT3G12580	2.351	0.426	-1.171	0.641	-12.096	0.000	-19.219	0.000	6.129	0.008	1.676	0.291	7.594	0.040	0.040	0.040	0.040	0.040	0.040	0.040
F894	AT3G15210	1.620	0.629	1.399	0.468	1.116	0.720	1.646	0.517	1.701	0.500	1.351	0.377	-1.533	0.793	0.793	0.793	0.793	0.793	0.793	0.793
BHLH117	AT3G22100	-1.480	0.648	-1.313	0.482	1.094	0.722	-3.465	0.558	1.036	0.846	1.311	0.364	1.059	0.930	0.930	0.930	0.930	0.930	0.930	0.930
MIR31C	AT3G24500	2.346	0.462	2.560	0.150	-3.672	0.060	-3.822	0.136	6.933	0.008	1.508	0.361	2.858	0.531	0.531	0.531	0.531	0.531	0.531	0.531
AB3	AT3G24650	-1.982	0.496	-1.219	0.598	-1.379	0.558	1.025	0.819	-1.378	0.707	-3.071	0.051	1.354	0.866	0.866	0.866	0.866	0.866	0.866	0.866
LINE10	AT4G00050	1.010	0.873	1.566	0.176	-1.015	0.771	1.050	0.795	1.013	0.855	1.262	0.334	-1.004	0.939	0.939	0.939	0.939	0.939	0.939	0.939
MIE45	AT4G02060	-1.124	0.831	1.205	0.542	1.169	0.641	-1.221	0.692	-1.216	0.735	1.063	0.528	1.299	0.834	0.834	0.834	0.834	0.834	0.834	0.834
AP7B3	AT4G03110	-1.697	0.427	1.907	0.091	2.089	0.070	-1.483	0.406	-1.483	0.502	1.275	0.359	1.009	0.939	0.939	0.939	0.939	0.939	0.939	0.939
CRC80	AT4G11460	1.039	0.856	1.003	0.715	1.064	0.707	-1.242	0.540	1.304	0.484	1.666	0.052	1.330	0.680	0.680	0.680	0.680	0.680	0.680	0.680
H5P20	AT4G16160	-1.020	0.874	1.381	0.419	1.873	0.481	1.102	0.777	-1.090	0.821	1.308	0.358	1.365	0.820	0.820	0.820	0.820	0.820	0.820	0.820
WRR18	AT4G31860	5.262	0.020	3.141	0.026	-1.482	0.481	1.046	0.806	5.007	0.006	1.947	0.172	1.686	0.737	0.737	0.737	0.737	0.737	0.737	0.737
PRX52	AT5G05340	-1.268	0.691	1.059	0.662	-1.106	0.671	-1.237	0.622	1.098	0.729	1.548	0.285	1.796	0.938	0.938	0.938	0.938	0.938	0.938	0.938
DRI82A	AT5G05410	4.025	0.118	1.804	0.319	-1.825	0.357	1.735	0.540	3.940	0.046	1.064	0.546	-1.046	0.937	0.937	0.937	0.937	0.937	0.937	0.937
ANAC082	AT5G09110	-1.038	0.869	-2.207	0.216	-2.781	0.154	-1.694	0.594	-1.224	0.801	-2.583	0.138	-1.718	0.799	0.799	0.799	0.799	0.799	0.799	0.799
ANAC091	AT5G24590	1.614	0.672	2.196	0.165	-1.095	0.757	1.230	0.742	2.807	0.140	1.015	0.570	-1.545	0.811	0.811	0.811	0.811	0.811	0.811	0.811
PK2	AT5G15960	-1.352	0.692	1.657	0.183	2.274	0.039	1.567	0.421	1.356	0.616	2.215	0.048	1.101	0.914	0.914	0.914	0.914	0.914	0.914	0.914
UNON1	AT5G44570	-1.370	0.703	1.332	0.448	2.483	0.036	1.265	0.680	-1.257	0.719	2.371	0.048	-1.078	0.924	0.924	0.924	0.924	0.924	0.924	0.924
PERO	AT5G47000	1.184	0.834	1.486	0.458	-1.390	0.584	-1.890	0.464	4.642	0.018	5.029	0.014	4.478	0.163	0.163	0.163	0.163	0.163	0.163	0.163
DUF632	AT5G54480	-1.091	0.850	3.751	0.004	4.268	0.004	4.075	0.021	-1.096	0.821	1.327	0.363	1.087	0.924	0.924	0.924	0.924	0.924	0.924	0.924
MYB44	AT5G56700	1.160	0.875	1.279	0.511	-2.096	0.116	-1.354	0.635	1.709	0.399	1.326	0.357	1.142	0.910	0.910	0.910	0.910	0.910	0.910	0.910



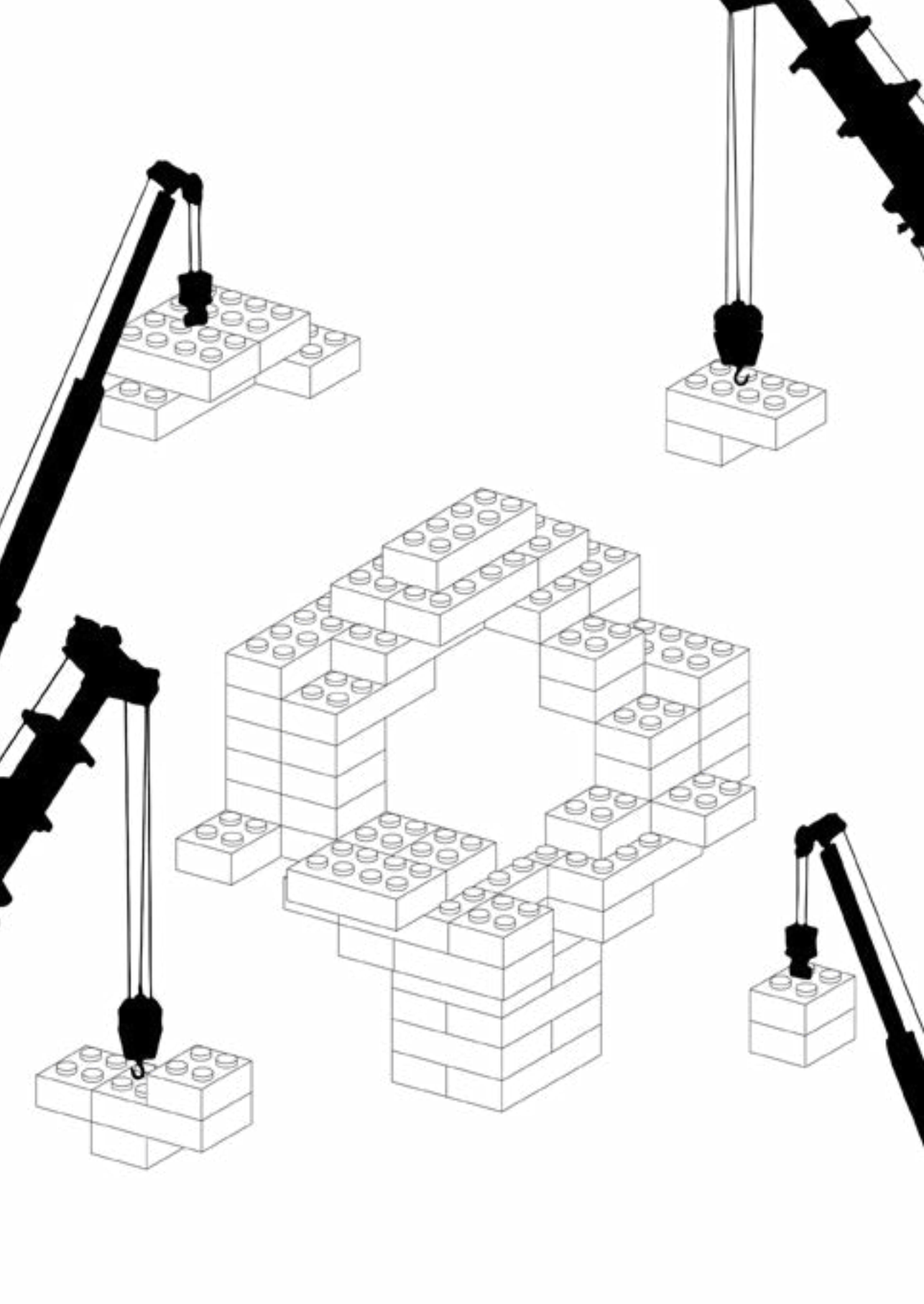


Supplementary table 4: Primers used for cloning promoter fragments.

Gene Name	Locus		Sequence	Promoter size (kb)
SR45A	AT1G07350	sense antisense	TAGTTGGAATGGGTTCCGAACAGAACTGAGAGATCATGAAGC TTATGGAGTTGGGTTCCGAAGatggtgggaatataatgtagag	2.7
MIR171B	AT1G11735	sense antisense	TAGTTGGAATGGGTTCCGAACCGGCAAAAGACGTCACC TTATGGAGTTGGGTTCCGAAGaaacacactgtgtgac	2.0
ATHB31	AT1G14440	sense antisense	TAGTTGGAATGGGTTCCGAAGaaacacactgtgtgac TTATGGAGTTGGGTTCCGAACttttaaagggtg	3.0
MYC2	AT1G32640	sense antisense	TAGTTGGAATGGGTTCCGAACtctactactactacag TTATGGAGTTGGGTTCCGAAGtccaaacacgggtgac	3.0
MYB112	AT1G48000	sense antisense	TAGTTGGAATGGGTTCCGAAGtctagataggttaaatgtgtgac TTATGGAGTTGGGTTCCGAAGcttgagatctgagaacactgtgag	2.9
CRC	AT1G69180	sense antisense	TAGTTGGAATGGGTTCCGAACaatataaglogactaacg TTATGGAGTTGGGTTCCGAAGgtctctaggaatgagtg	3.1
WRKY40	AT1G80840	sense antisense	TAGTTGGAATGGGTTCCGAAGaatatgaaacagtaaatgg TTATGGAGTTGGGTTCCGAAGtaaatatgtaggtgagtg	3.0
ARM	AT2G05810	sense antisense	TAGTTGGAATGGGTTCCGAAGattgtgtatgtgtgtgtg TTATGGAGTTGGGTTCCGAAGGAGGAGTGGTCACATAAGAG	3.0
GATA20	AT2G18380	sense antisense	TAGTTGGAATGGGTTCCGAAGtccatccactgtgtgtg TTATGGAGTTGGGTTCCGAAGaaatgagactacagtagag	3.0
PUMP5	AT2G22500	sense antisense	TAGTTGGAATGGGTTCCGAAGtctagatctatgtaactgtg TTATGGAGTTGGGTTCCGAAGtgaatgtgtgtgtgtgtgtg	3.0
HSFA2	AT2G26150	sense antisense	TAGTTGGAATGGGTTCCGAATCATTAATTCGACATCTTCAGC TTATGGAGTTGGGTTCCGAAGtctgtgtatctcaacttc	3.0
AGL33	AT2G26320	sense antisense	TAGTTGGAATGGGTTCCGAATCTCTGTCTATGACTATTGG TTATGGAGTTGGGTTCCGAAGtctataaatgaagtttagag	3.0
GH17	AT2G27500	sense antisense	TAGTTGGAATGGGTTCCGAAGtctgtgtgtgtgtgtgtg TTATGGAGTTGGGTTCCGAAGgaggaactgtgtgtgtg	2.9
A20AN1	AT2G27580	sense antisense	TAGTTGGAATGGGTTCCGAAGGTTGAATTCGAATGATGC TTATGGAGTTGGGTTCCGAAGacagatgtgtgtgtgtgtgtg	2.6
PK1	AT2G42960	sense antisense	TAGTTGGAATGGGTTCCGAAGtctgtgtgtgtgtgtgtg TTATGGAGTTGGGTTCCGAAGtctgtgtgtgtgtgtgtg	2.9
MSS3	AT2G43290	sense antisense	TAGTTGGAATGGGTTCCGAAGtctgtgtgtgtgtgtgtg TTATGGAGTTGGGTTCCGAAGtctgtgtgtgtgtgtgtg	3.0
HSP70	AT3G12580	sense antisense	TAGTTGGAATGGGTTCCGAATagagaggttctttagcaccac TTATGGAGTTGGGTTCCGAAGtctgtgtgtgtgtgtgtg	2.7
ERF4	AT3G15210	sense antisense	TAGTTGGAATGGGTTCCGAATCAACTTTATGTGCAGCAGC TTATGGAGTTGGGTTCCGAAGtctgtgtgtgtgtgtgtg	3.0
bHLH117	AT3G22100	sense antisense	TAGTTGGAATGGGTTCCGAATgtgtgtgtgtgtgtgtg TTATGGAGTTGGGTTCCGAAGtctgtgtgtgtgtgtgtg	3.0
MBF1C	AT3G24500	sense antisense	TAGTTGGAATGGGTTCCGAAGtctgtgtgtgtgtgtgtg TTATGGAGTTGGGTTCCGAAGtctgtgtgtgtgtgtgtg	3.0
ABI3	AT3G24650	sense antisense	TAGTTGGAATGGGTTCCGAAGtctgtgtgtgtgtgtgtg TTATGGAGTTGGGTTCCGAAGtctgtgtgtgtgtgtgtg	2.9
UNE10	AT4G00050	sense antisense	TAGTTGGAATGGGTTCCGAACACTTGTgtacttctc TTATGGAGTTGGGTTCCGAAGtctgtgtgtgtgtgtgtg	3.0
MEE45	AT4G00260	sense antisense	TAGTTGGAATGGGTTCCGAAGtctgtgtgtgtgtgtgtg TTATGGAGTTGGGTTCCGAAGtctgtgtgtgtgtgtgtg	3.0
AP2B3	AT4G03170	sense antisense	TAGTTGGAATGGGTTCCGAACCAACCAAACTGTGATAATGTC TTATGGAGTTGGGTTCCGAAGtctgtgtgtgtgtgtgtg	1.5
CRK30	AT4G11460	sense antisense	TAGTTGGAATGGGTTCCGAAGaggtgtgtgtgtgtgtg TTATGGAGTTGGGTTCCGAAGtctgtgtgtgtgtgtgtg	3.0
HSP20	AT4G16560	sense antisense	TAGTTGGAATGGGTTCCGAACCTGTGTGATCTTCTCTCTC TTATGGAGTTGGGTTCCGAAGtctgtgtgtgtgtgtgtg	2.8
WRKY18	AT4G31800	sense antisense	TAGTTGGAATGGGTTCCGAAGtctgtgtgtgtgtgtgtg TTATGGAGTTGGGTTCCGAAGtctgtgtgtgtgtgtgtg	3.0
PRX52	AT5G05340	sense antisense	TAGTTGGAATGGGTTCCGAAGtctgtgtgtgtgtgtgtg TTATGGAGTTGGGTTCCGAAGtctgtgtgtgtgtgtgtg	3.1
DREB2A	AT5G05410	sense antisense	TAGTTGGAATGGGTTCCGAAGtctgtgtgtgtgtgtgtg TTATGGAGTTGGGTTCCGAAGtctgtgtgtgtgtgtgtg	2.3
ANAC082	AT5G09330	sense antisense	TAGTTGGAATGGGTTCCGAACATCTGCTGACATGAAAACG TTATGGAGTTGGGTTCCGAAGtctgtgtgtgtgtgtgtg	2.1
ANAC091	AT5G24590	sense antisense	TAGTTGGAATGGGTTCCGAAGtctgtgtgtgtgtgtgtg TTATGGAGTTGGGTTCCGAAGtctgtgtgtgtgtgtgtg	2.9
PK2	AT5G35960	sense antisense	TAGTTGGAATGGGTTCCGAAGtctgtgtgtgtgtgtgtg TTATGGAGTTGGGTTCCGAAGtctgtgtgtgtgtgtgtg	2.6
UNKN1	AT5G44570	sense antisense	TAGTTGGAATGGGTTCCGAAGtctgtgtgtgtgtgtgtg TTATGGAGTTGGGTTCCGAAGtctgtgtgtgtgtgtgtg	2.3
PERD	AT5G47000	sense antisense	TAGTTGGAATGGGTTCCGAAGtctgtgtgtgtgtgtgtg TTATGGAGTTGGGTTCCGAAGtctgtgtgtgtgtgtgtg	1.8
DUF632	AT5G54480	sense antisense	TAGTTGGAATGGGTTCCGAAGtctgtgtgtgtgtgtgtg TTATGGAGTTGGGTTCCGAAGtctgtgtgtgtgtgtgtg	2.5
MYB44	AT5G67300	sense antisense	TAGTTGGAATGGGTTCCGAAGtctgtgtgtgtgtgtgtg TTATGGAGTTGGGTTCCGAAGtctgtgtgtgtgtgtgtg	3.3







# Chapter 4

## **Auxin signaling is necessary but not sufficient for establishing vascular identity**

Margot E. Smit, Dolf Weijers

**Abstract**

Auxin plays a central role in plant development, regulating a variety of processes throughout a plant's life. Perhaps the most studied function of auxin is in initiating vascular development. Auxin maxima correlate with future vascular development and exogenous auxin can induce ectopic vascular development in adult tissues. In this chapter, the role of auxin in inducing vascular gene expression and vascular identity is investigated. We confirm that auxin treatment increases the promoter activity of vascular marker genes in the root but we find that this expression increase is limited to the vascular bundle. In the root auxin is thus not able to induce vascular identity outside its existing domain. This confirms previous findings that not all cells can be reprogrammed to vascular identity. This inability could be caused by the differentiated nature or limited auxin susceptibility of those tissues. To circumvent these limitations we ectopically expressed an unrepressable version of the MONOPTEROS (MPΔPB1) protein in the early embryo, increasing auxin signaling output in all cells of the embryo. This led to abnormal cell divisions in the protoderm but was not able to expand the expression domain of vascular marker genes, indicating that auxin signaling through MP is not sufficient for establishing vascular identity. However, we did confirm that auxin signaling is necessary for establishing vascular identity. Blocking MP activity by the expression of the undegradable *bd1* in the vascular cells abolished expression of several vascular markers. However, vascular identity was not completely lost as reported by other markers. Thus that MP activity is required for the initiation of the complete vascular identity but that MP alone is not sufficient for this initiation. Other yet unknown factors are required for initiating vascular identity.

## Introduction

Auxin was one of the first plant hormones to be extensively studied, largely because of its pronounced effects on growth and development (Went & Thimann 1937). A strong link between auxin and vascular development has been described where auxin application to the stem of pea plants resulted in the formation of vascular bundles (Sachs 1969). This link was later underlined in many studies showing that auxin production and signaling are necessary for vascular development and that auxin maxima precede the formation of vascular tissues (Fukuda & Ohashi-Ito 2019, Scarpella 2017). Strong vascular defects were seen in mutants where the activity of one of the transcription factors mediating auxin response - AUXIN RESPONSE FACTOR5/MONOPTEROS (ARF5/MP) - was impaired, either because the locus was disrupted or because the ARF-inhibitor BODENLOS was prevented from auxin-dependent degradation (Hamann et al. 1999, Hardtke & Berleth 1998). Thus, suppression of auxin signaling results in plants with vascular defects and high auxin is associated with vascular bundle formation. These findings indicate that auxin signaling, primarily through MP, is a key factor in vascular development. But it still remains an open question whether auxin response on its own is sufficient to confer vascular identity to non-vascular cells.

The transcription of vascular genes is tightly connected to auxin activity. Several vascular-specific genes were identified as transcriptional targets of auxin signaling through MP (Möller et al. 2017, Schlereth et al. 2010), while others were identified for their involvement in vascular development and later linked to MP activity (Donner et al. 2009). Although dependence on auxin signaling was not tested for all vascular marker genes, it appeared that auxin signaling is a major driver of vascular gene expression.

When auxin is applied to stems, vascular bundles are formed, but not all cells re-differentiate to form vascular cells (Sachs 1991, 2000). Similarly, not all tissues and cell types are equally competent to undergo auxin-induced reprogramming. Wounding events such as grafting or root tip regeneration result in the formation of new vascular bundles, and as such wounding might aid reprogramming (Efroni et al. 2016, Jacobs 1952, Melnyk et al. 2015). However, even in wounded tissues, auxin signaling only triggers vascular development in a subset of cells. Which cells are susceptible to auxin-induced vascular development and what molecular factors contribute to this susceptibility remains to be discovered. In adult tissues, canalization of auxin appears to be the key step in focusing auxin signaling to a specific set of cells which form vascular bundles (Rolland-Lagan & Prusinkiewicz 2005, Sachs 1981). Canalization depends on polar auxin transport facilitated by PIN efflux proteins (Gaulweiler et al. 1998), and is responsible for the proper layout of the vascular network in the leaf. Thus,

canalization creates auxin maxima in specific cells which then adopt vascular identity. This brings up the question: what are the limits to the capabilities of auxin in inducing vascular identity?

The tight correlation between auxin and vascular development is compromised by the fact that auxin triggers numerous other responses unrelated to vascular development. Auxin maxima do not precede only vascular development, they are also correlated with processes such as apical dominance, meristem maintenance and organ initiation (reviewed in Roosjen 2018). In addition, it is not just the maximum of auxin that is informative: in valve margin cells, an auxin minimum seems to inform cell identity (Sorefan et al. 2009). Therefore, it appears that different levels of auxin may have different effects on cell identity. These differences across plant tissues indicate that additional information is likely necessary to provide the context for establishing vascular identity. Given that in some contexts, vascular development can be initiated by the application of exogenous auxin, it may override other developmental programs.

In this chapter, we explore the capacity of auxin signaling to induce vascular cell identity. In auxin-treated roots, transcription of vascular genes is increased but remains limited to the vascular cells. To limit confounding factors, we next turn to the embryo where the very first auxin maxima induce vascular identity and manipulate auxin signaling to determine whether MP activity is necessary and sufficient in inducing vascular identity.

## Results

### Increased auxin levels do not induce ectopic vascular identity in the Arabidopsis root meristem

Vascular development can be triggered in the stem by application of exogenous auxin (Sachs 1969). Indeed, a large number of vascular genes was identified as targets of MP or of auxin signaling in general (Donner et al. 2009, Möller & Weijers 2009, Schlereth et al. 2010). To confirm that regulation by auxin occurs in large part via changes in transcription, transcriptional reporter lines of vascular genes were tested for auxin-responsiveness. Roots from a panel of reporters (**Chapter 3**) were treated with 1  $\mu$ M IAA for 1 hour after a pretreatment with the auxin transport inhibitor NPA to suppress transport and remove existing auxin maxima (Liao et al. 2015, Scanlon 2003). qRT-PCR was subsequently used to quantify the transcript level of the fluorescent protein, as a direct readout of promoter activity. Ex-

pression of the sensitive primary auxin responsive gene *GH3* was used as a control to confirm the effectiveness of the auxin treatment (Ulmasov et al. 1995). Compared to DMSO-treated roots, IAA-treated roots showed a 7- to 37-fold increase in *GH3* expression, which confirmed that auxin response was successfully induced (Figure 1A). Expression of a large number of vascular promoters was likewise induced by IAA treatment. Fluorescent protein transcript levels were increased in transcriptional reporter lines of *ATHB8*, *ERF4*, *GATA20*, *PEAR1*, *T5L1*, *TMO5* and *WRKY17* (Figure 1A). Induction was strongest for the *ATHB8* promoter: in the pATHB8-H2B-YFP reporter line, YFP transcript levels were increased 41-fold upon IAA treatment. Expression of the other induced reporters was increased between 1.4- and 4.5-fold (Figure 1A). In contrast, fluorescent protein transcript levels were not increased in reporter lines for *DOF6*, *IQD15*, *MIR171B* and *SOK1*. This indicates that expression of these genes is not increased by high auxin levels. All in all, we find more than half of the tested vascular reporter lines have increased reporter expression in response to a 1-hour auxin treatment. However, several of these show only marginal increases in expression and four other vascular reporter lines show no increase in expression in response to auxin treatment. This indicates that short auxin treatment increases expression levels of many but not all vascular genes.

The next question is where in the root this increase in expression occurs. Is the induction of vascular genes limited to the vascular bundle, or can auxin treatment result in expansion of the vascular domain? Confocal microscopy of roots of each vascular reporter line revealed that prolonged auxin treatment (6 and 24 hours at 0.1 and 1  $\mu$ M 2,4-D) was able to induce *ERF4* expression outside vascular cells (Figure 1B). *ERF4* expression was induced in the entire root apical meristem. This response is likely the result of the existing low activity of the *ERF4* promoter in nonvascular cells in the absence of external auxin that is amplified upon auxin treatment. The other vascular genes showed no change in expression pattern in the root meristem in response to 2,4-D treatment. These other vascular reporters were vascular-specific and did not show any expression in non-vascular cells. In addition, we could not see clear increases in fluorescence levels in the vascular bundle either: the variation in fluorescence between root for most reporters was too large to draw definitive conclusions on the effect of auxin treatment on fluorescent protein levels. The largest increase of fluorescence had been expected for *ATHB8* whose transcript was induced 41-fold after 1 hour of IAA treatment. But surprisingly, little change in fluorescence was observed in the root meristem after 6 hours of 2,4-D treatment. This could be either because roots were observed later, whilst *ATHB8* response had already declined due to feedback inhibition, or because *ATHB8* expression was induced away from the meristematic zone where it was not observed.

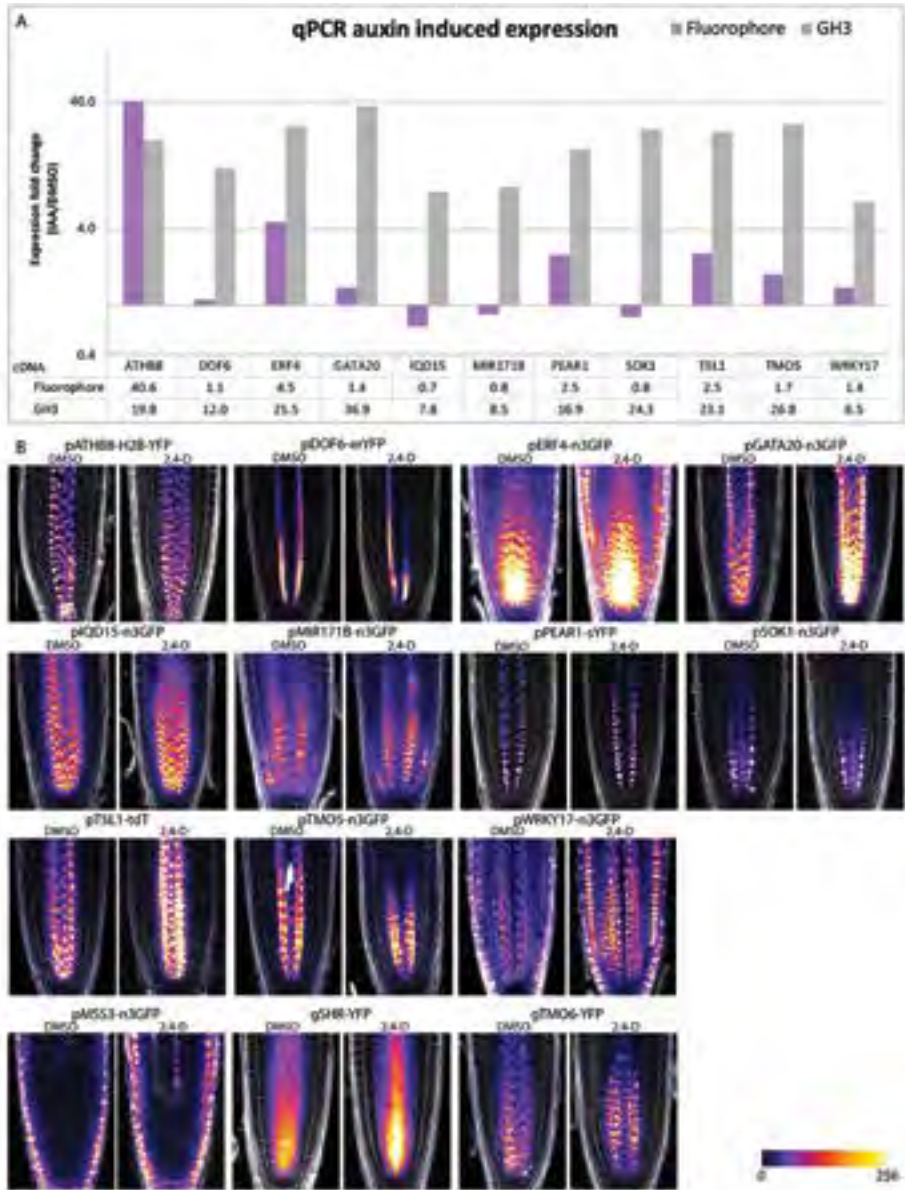


**Figure 1: Auxin treatment on roots and monitoring of vascular gene expression.** (A) Normalized cDNA levels of fluorophores (purple) and GH3 (grey) in vascular transcription reporter lines after 1 h treatment with 1  $\mu$ M IAA following pretreatment with NPA. Fluorophore cDNA detected: ATHB8, DOF6, PEAR1: YFP; ERF4, GATA20, IQD15, MIR171B, SOK1, TMO5, WRKY17: GFP; T5L1: tDT. (B) Vascular transcription domains before (left) and after (right) treatment with 2,4-D. The top 3 rows contain the 11 reporter lines used in (A) while the bottom row contains 3 additional vascular reporters, 2 of which are translational fusions. All roots were treated for 6 hours with 1  $\mu$ M 2,4-D or DMSO except for pT5L1-tDT, pWRKY17-n3GFP and gTMO6-YFP roots which were treated for 17 hours with 0.1  $\mu$ M 2,4-D. Scale bar (top left) represents 50  $\mu$ m in every picture.



Irrespective of the scenario, auxin treatment was not able to stably expand the expression domain of vascular reporter genes in the meristem. The lack of domain expansion seen for most vascular genes could indicate either that cells in the root meristem are not able to gain a new identity or that the increased auxin levels are only effective in the vascular cells, where MP is expressed, and the ARFs expressed in other cell types can not induce the expression of vascular genes (Rademacher et al. 2011, 2012).

#### In the embryo, auxin levels and signaling are high in the vascular cells

Any time vascular tissues are initiated postembryonically, their initiation is preceded by the creation of an auxin maximum (De Rybel et al. 2016, Fukuda & Ohashi-Ito 2019, Sachs 2000, Scarpella 2017). However it remains unclear whether it is the absolute amount, relative amount or flux of auxin that results in the initiation of vascular development. In the embryo, it was recently shown that not just the auxin maximum provides information (Möller et al. 2017). When auxin signaling is blocked using the undegradable bdl not only known vascular genes but also markers of the adjacent ground tissue are repressed. However auxin levels and response in the ground tissue are significantly lower than those in the vascular cells (Figure 2B,D; Möller et al. 2017). This indicates that different relative levels of auxin could lead to discrete responses.

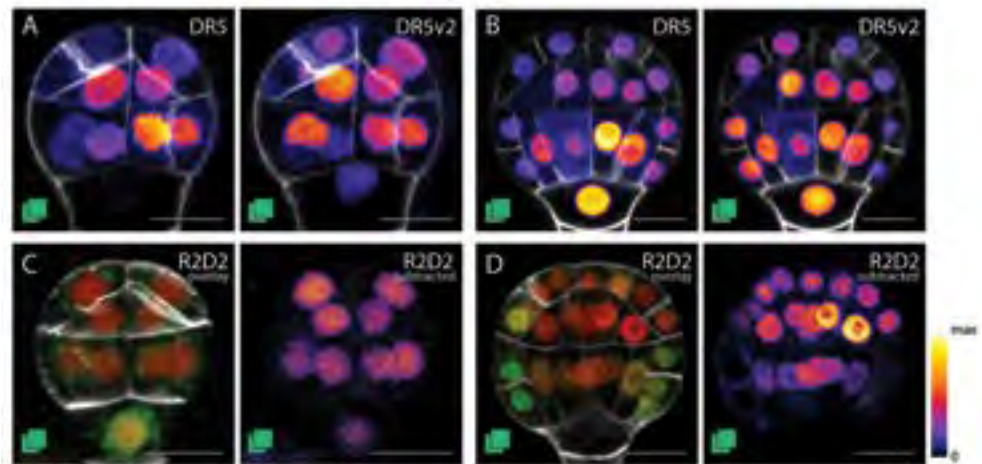


**Figure 2: Auxin levels and signaling output in the early embryo.**

Dermatogen (A,C) and early globular (B,D) stage embryos reporting the relative amount of auxin or auxin signaling per cell. (A,B) Relative amount of auxin signaling per cell output as reported by pDR5-n3GFP (left) or pDR5v2-ntdT (right). (C,D) Relative amount of auxin per cell as reported by R2D2. Left: overlay of signals from undegradable pRPS5A-mDII-tdT (red), degradable pRPS5A-DII-3xVenus (green) and Renaissance (white). Right: difference between DII signal and mDII signal per pixel. All images are stacks and all scale bars represent 10  $\mu$ m.

The vascular cells at early globular stage exhibit an auxin maximum, thus potentially providing the spatial information required for vascular cell specification. Since we now know that vascular identity is initiated one stage earlier (**Chapter 3**), we sought to confirm a similar auxin signaling maximum in the inner cells of the dermatogen stage embryo. Such a maximum was previously modeled and reported (Wabnik et al. 2013). However, we were unable to convincingly confirm increased auxin signaling in the inner cells at dermatogen stage using the ratiometric version of 2 D2's (R2D2) to determine auxin levels and using the DR5v2 reporter to measure auxin signaling output (Figure 2; Liao et al. 2015). R2D2 and DR5v2 indicate no difference between inner and outer cells while the “classical” DR5 reporter does reveal slightly higher levels of signaling in the inner cells. This indicates that at the timepoint where vascular identity is initiated during embryogenesis, auxin is not necessarily providing spatial information via a local maximum. A temporal maximum could of course be more abrupt. This leads to the question as to what kind of information auxin signaling provides in the initiation of vascular development in the early embryo.

#### Ectopic MONOPTEROS activity across the embryo does not lead to ectopic vascular identity

Increased auxin levels in the root tip were not able to expand vascular identity to other cells. This could be because tissue identity is already fixed at this stage; because MP is not present outside the vascular domain; or because the competence to respond to auxin is limited. To circumvent such restrictions, we made use of an unrepressable MP protein (MPΔPB1) to ectopically activate auxin-responsive genes. Under normal circumstances, auxin levels and signaling are highest in the vascular cells of the early globular stage embryo (Figure 2). In addition, at this stage MP expression is strongest in the lower tier of the proembryo (Crawford et al. 2015, Rademacher et al. 2011). Because auxin treatment on embryos is difficult and MP expression is not uniform we instead aimed to directly induce auxin signaling output across all cells via increased MP activity. To see if MP activity is sufficient to confer vascular identity, a constitutively active version of MP (MPΔPB1; Krogan et al. 2012) was misexpressed in the entire embryo. Because this misexpression will cause developmental defects, it was achieved via two-component gene activation. A line containing a pRPS5A-GAL4 transgene as well as a fluorescent vascular reporter, was crossed with a second line containing the UAS-MPΔPB1 transgene. The GAL4-dependent UAS promoter is only active in the F1 embryo, where the promoter is broadly activated in the *RPS5A* expression domain (Weijers et al. 2001, 2003). Crosses of the same pRPS5A-GAL4 lines with Col-0 were performed as

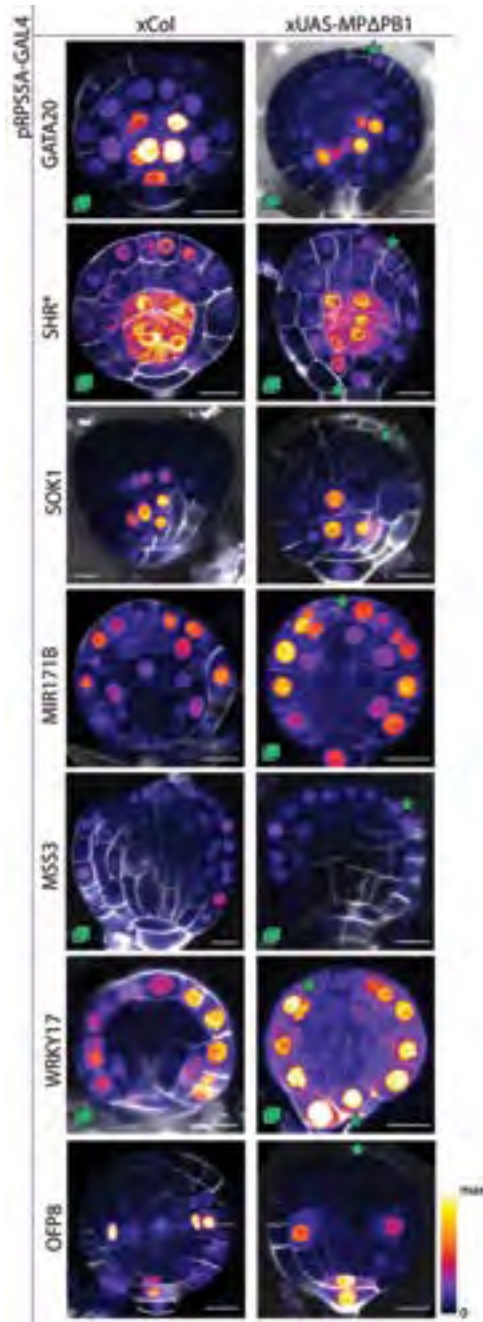


**Figure 3: Embryo-wide expression of MPΔPB1 does not alter vascular reporter expression.**

Embryos resulting from crosses between lines containing pRP5A-GAL4 and a vascular reporter (rows) and either Col-0 plants (left column) or plants containing UAS-MPΔPB1 (right column). Stars mark altered divisions caused by MPΔPB1, ## indicates images that are stacks, all scale bars represent 10  $\mu$ m.

a control. Embryos with ectopic MP activity often showed altered division planes in epidermal cells and occasionally in the hypophysis (Figure 3, green asterisks). In these embryos, expression of vascular genes (*GATA20*, *SHR*, *SOK1*) remained restricted to the vascular cells, inverse markers were still expressed in the surrounding cells (*MIR171B*, *MSS3*, *WRKY17*) and the ground tissue marker *OPF8* was still expressed in the ground tissue (Figure 3). Expression levels between embryos varied and as a result we could not determine with certainty if expression was higher or lower in the regular expression domains of these genes. Nonetheless, it is clear that ectopic MP activity was not able to induce expression of vascular genes throughout the embryo. It was able to cause changes in cell division orientation but did not lead to major cell identity defects, at least none observed until transition stage. Therefore we conclude that auxin signaling via MP activity is not sufficient for triggering vascular identity, even in young embryonic cells.

#### Blocking ARF/MP activity in vascular cells leads to reduced induction of vascular genes

If MP activity is not sufficient for initiation of vascular identity, is it required for vascular development? Previous studies have shown that *mp* mutants do not develop a root and lack expression of MP targets, and the roles of targets of MP in vascular proliferation and root apical meristem development have been studied intensively (De Rybel et al. 2014, Hardtke & Berleth 1998, Möller et al. 2017, Ohashi-Ito et al. 2014). Without MP activity, the vascular bundle does not develop properly, but the question remains whether cells not acquire vascular identity, or if they acquire some but not all traits required for further vascular development. The non-degradable *bdl* protein can be used to block ARF/MP activity (Hermann et al. 1999, Weijers et al. 2006a). Because *bdl* expression in the entire embryo leads to early developmental defects (Rademacher et al. 2011, Yoshida et al. 2014), we selectively expressed *bdl* only in the vascular cells. By crossing lines containing a Q0990-GAL4; UAS-erGFP transgene and a vascular reporter, with a second line containing UAS-*bdl*, we could observe the effect of blocking MP signaling in the vascular cells on vascular gene expression. Again, crosses of the same Q0990-GAL4 lines with Col-0 were used as a control. In these embryos, green fluorescence in the nucleus is provided by the vascular reporter, while green fluorescence in the endoplasmatic reticulum reports on Q0990 promoter activity. Embryos where *bdl* was present in the vascular cells sometimes showed altered ground tissue division orientation as previously reported (Möller et al. 2017; Figure 4, green asterisks). Inhibition of MP activity led to 96% (n=24) of the embryos lacking *SOK1* expression. As *SOK1* is a target of MP (Möller et al., 2017; Yoshida et al., 2019), this further confirms the repression

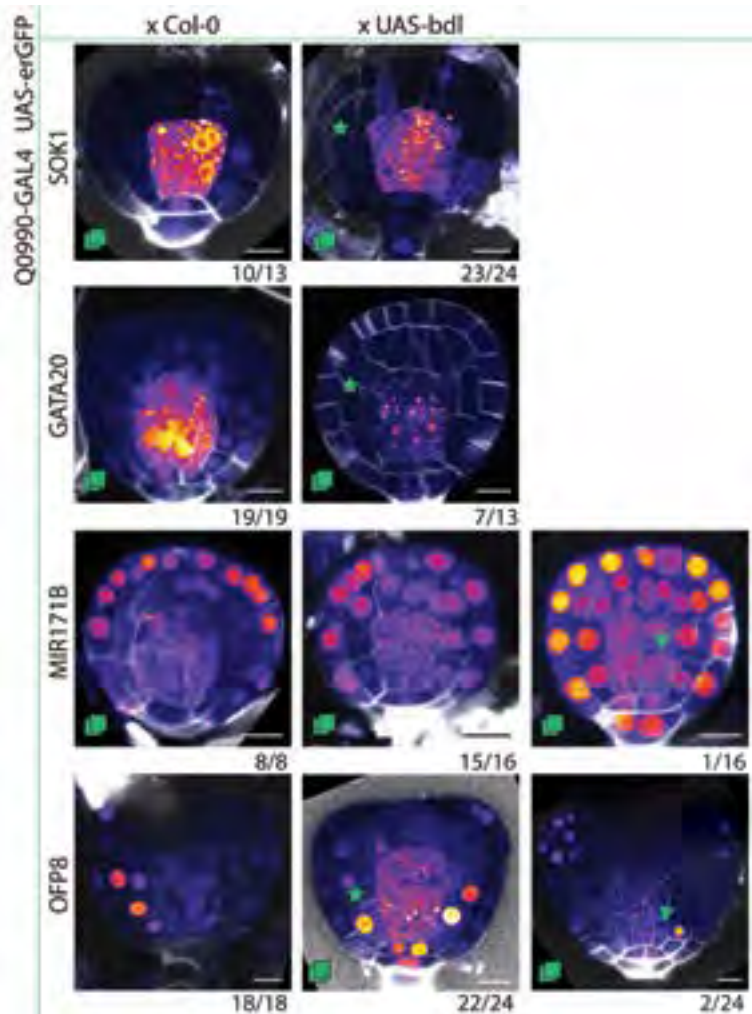


**Figure 4: Vascular expression of *bdl* partly represses vascular identity.**

Embryos resulting from crosses between lines containing Q0990-GAL4, UAS-erGFP and a vascular reporter (rows) and either Col-0 plants (left column) or plants containing UAS-*bdl* (right columns). For UAS-*bdl* crossed plants the dominant pattern is shown, if the nondominant pattern is abnormal this is also shown and marked with an arrow. Stars mark altered divisions caused by *bdl*, ## indicates images that are stacks, all scale bars represent 10  $\mu$ m.

of MP activity. In Q0990>>*bdl* embryos, *GATA20* expression is absent in about half (54%, n=13) of the embryos, but remains present in the other half, indicating that in many embryos, repression of vascular identity is incomplete. Expression of the inverse marker *MIR171B* remains mostly unchanged: in Q0990>>*bdl* embryos, expression gradients remained similar to those found in WT embryos (Figure 4). In 1 out of 16 embryos, *MIR171B* expression was seen in the vascular cells but this expression was still lower than in adjacent cells and thus

maintained a gradient. The ground tissue marker *OFP8* remained limited to ground tissue cells in most embryos, but could also be found at low levels in some vascular cells in 8% of embryos (n=24; Figure 4). This indicates that the mechanisms that separate vascular and surrounding cell identities depend in part on auxin signaling. In conclusion, MP activity is needed to initiate complete vascular identity but several vascular markers do show cell type specific expression even when MP activity is blocked in the vascular cells.

## Discussion

Auxin is intimately linked to vascular tissue development, but direct and causal links remain questionable. Here, we manipulated auxin levels and signaling activity in the Arabidopsis root and embryo to determine whether auxin is necessary and sufficient in controlling vascular development. In the root, short auxin treatment resulted in increased expression for the majority of vascular markers tested (Figure 1A). Among these, *ATHB8* and *TMO5* are confirmed direct targets of MP (Donner et al. 2009, Schlereth et al. 2010) and their promoters respond as expected, with increased expression upon auxin application. Two other targets of MP, *IQD15* and *SOK1* (Möller et al. 2017, Yoshida et al. 2019), do not show increased expression after auxin treatment. Presumably, their induction occurred either before or after the 1-hour time point that was used. Oddly enough, several genes, which are normally not associated with high auxin were also induced: in the embryo, *WRKY17* expression is lowest in the cells with high auxin activity, while *PEAR1* and *GATA20* expression in the root is in the phloem cells, away from the high auxin containing xylem axis (Brady et al. 2007, Miyashima et al. 2019; **Chapter 3**). These findings show that expression domain is a poor predictor of auxin inducibility, at least after an 1-hour treatment.

The auxin-inducibility of promoter expression appears to be limited to the existing expression domains of the genes tested here. Treatment with 2,4-D did not change the domains of expression of these vascular genes, indicating that auxin is unable to impose vascular identity within the root meristem. In addition, the increases in expression found with qPCR could not be observed when looking at fluorescence in the root. That difference was most striking for *ATHB8*, whose promoter activity was increased 41-fold after 1 hour of IAA treatment, but whose fluorescence readout appeared unchanged in root tips upon 2,4-D treatment. This could be either because a different time point was chosen for observation, 6 hours instead of 1 - to allow for translation and folding of the fluorescent protein - or because expression was not induced in the root meristem but in the elongation or differentiation zone. In addition, differences could be the result of the different treatments, cDNA



levels were measured after NPA treatment followed by 1 hour of treatment with IAA but fluorescence was observed after 6 or more hours of 2,4-D treatment. 2,4-D was used because it generally causes a stronger response due to slow degradation and lack of transportability (Eyer et al. 2016, Hošek et al. 2012). However 6 or more hours of 2,4-D treatment without NPA pretreatment could lead to different output, especially if transcriptional changes are caused by auxin flux instead of level, or if activation is transient. Of course, reprogramming of identity is expected to be a permanent output rather than a temporary change. Another confounding factor was the variation in expression levels between roots (about 20-40%), even in homozygous reporter lines. This made it difficult to draw conclusions on changes in expression level. The only clear change in root fluorescence was that of *ERF4*, whose expression was increased both in the vascular bundle and in surrounding cells. This is however not interpreted as a domain expansion as low levels of fluorescence were already observed in those cells before treatment. Taken together, it appears that in the root meristem auxin treatment can increase the level but not the domain of vascular gene expression.

The inability of auxin treatments to trigger vascular identity in roots could be either because these cells are differentiated to such an extent that they cannot be reprogrammed, or because they are less responsive to auxin in general. In the root tip, MP is expressed in the vascular bundle (Rademacher et al. 2011) and while other ARFs are expressed in the neighboring cells, these might not be able to induce the same set of vascular genes. However, even within the vascular bundle, vascular gene expression domains were not expanded, genes expressed in the xylem or phloem did not become expressed in the entire domain of MP expression (Figure 1B).

To circumvent the limitations of auxin treatment on a postembryonic tissue we instead focused on the output of auxin signaling at the stage where identities are first laid down: the early embryo. Relative amounts of auxin and auxin signaling were previously reported for early globular stage embryos (Möller et al. 2017) but not for dermatogen stage embryos, where we found vascular identity is originated (**Chapter 3**). Using sensitive auxin reporters we were not able to conclusively determine if auxin signaling in the dermatogen stage embryo formed a maximum in the inner cells (Figure 2A,C; Liao et al. 2015). A key question therefore remains whether this maximum is present and if auxin levels provide the spatial information that leads to vascular specification.

Embryo-wide ectopic activity of MP resulted in changes in cell division orientation in the protoderm and hypophysis, which suggested that MP was indeed active in those cells. But these changes in division pattern were not accompanied by changes in cell identity

as reported by transcriptional reporters of several vascular genes. Expression of *GATA20*, *SHR* and *SOK1* was still limited to the inner cells, while *MIR171B*, *MSS3* and *WRKY17* were still expressed surrounding the inner cells (Figure 3). The opposite experiment, where MP activity in the inner cells was blocked by the expression of the *bdl* protein, showed that MP activity is needed to establish complete vascular identity. Reducing MP activity in the vascular cells led to abnormal divisions in the ground tissue and resulted in the loss of expression of some vascular genes. Expression of a target of MP, *SOK1*, was absent in almost all embryos when *bdl* was introduced. Other vascular markers indicated that the loss of vascular identity was not complete in all embryos. In addition, in several embryos the ground tissue marker *OFP8* could even invade the vascular domain, indicating substantial transcriptional reprogramming. The (lack of) changes in vascular gene expression in the embryo indicate that MP activity in the inner cells is needed to establish vascular identity but that MP activity in other cells is not able to induce complete vascular identity. Thus even early in embryogenesis, either not all cells have the necessary competence or additional signals are needed to induce vascular identity. This indicates that the lack of competence in postembryonic tissues is not merely a result of age and differentiation, other properties and factors determine which cells can become vascular. The finding that tissue maturity is not always the limiting factor for vascular initiation is consistent with the finding that application of auxin to mature stems could induce vascular bundles (Sachs 1969, 2000). However, given that early embryonic cells are considered to have broad developmental potential in both plants and animals (Heidstra & Sabatini 2014), it is surprising that no ectopic vascular fate could be induced by MPΔPB1.

The finding that MP activity is not sufficient for vascular fate does indicate that an additional signal may be needed to trigger vascular identity. MP activity at early globular stage peaks in the vascular cells as these have the highest amount of auxin and could thus potentially provide spatial information. Auxin here could act as a morphogen in delimiting cell identity, but the presence of a second morphogen that results in a second, inverted signaling gradient would cause a much more robust control of cell identity (Turing 1952). Such a second signaling gradient is hypothetical at present, and could take any shape: peptide, hormone, metabolite, output of mechanical stress or any other factor that can affect gene expression. Without knowing the kind of signal that is needed, its identification is challenging. Integration of signaling will most probably occur at the DNA where the output of auxin is mediated by ARFs such as MP. DNA-binding proteins such as transcription factors can provide a starting point to uncover the mechanisms that control vascular identity.



## Materials and methods

### Plant material and growth conditions

Vascular reporter lines were obtained or generated as described in **Chapter 3**. Q0990-GAL4 UAS-erGFP, pRPS5A-GAL4 and UAS-*bd1* lines were previously described (Rademacher et al. 2011, Radoeva et al. 2016, Weijers et al. 2003, 2006b) and UAS-MPΔPB1 seeds were a gift from Gerd Jürgens (Tübingen). After surface-sterilization, Arabidopsis seeds were plated on ½ MS plates. After 2 days of seed stratification plates were placed at 21 °C under standard long-day (16:8h light:dark) conditions. After 2 weeks of growth seedlings were transferred to soil. Lines containing a GAL4 driver and a vascular reporters were generated via crossing and double homozygous F3+ plants were used for experiments. Homozygosity was confirmed by monitoring the segregation of fluorescence for Q0990-GAL4 UAS-erGFP and vascular reporters or by genotyping of the pRPS5A-GAL4 insert using primers listed in Supplementary Table 1.

### RNA isolation and qRT-PCR

For expression analysis seedlings were grown for 5 days on ½ MS plates with mesh. Seedlings were then transferred to plates containing 10 µM NPA for 12 hours and subsequently placed on plates containing 10 µM NPA and 1 µM IAA. Roots were flash frozen in liquid nitrogen and ground using a Retch machine. RNA isolation was performed using TRIzol reagent (Invitrogen) and the RNAeasy kit (Qiagen). cDNA synthesis was performed on 0,5 µg total RNA using the iScript cDNA Synthesis Kit (Biorad). Each qRT-PCR reaction was performed in triplicate using iQ SYBR Green Supermix (Biorad) and measured on a CFX384 RT-PCR detection system. qBase software was used for data analysis and gene expression levels were normalized using *CDKA* and *GAPC* expression (Hellemans et al. 2008). Primers used for qPCR are listed in Supplementary table 1.

### Microscopy and sample preparation

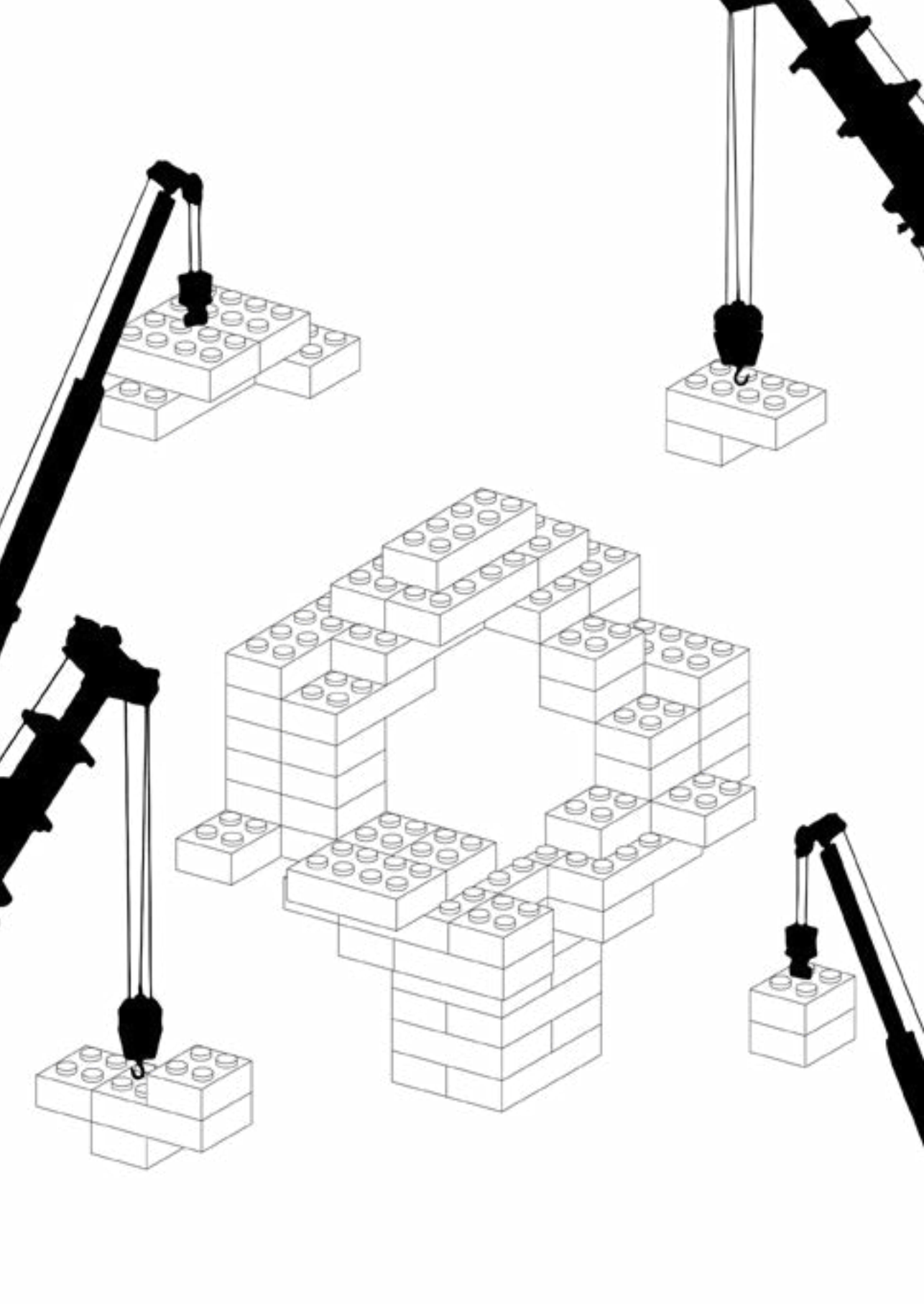
Reporter roots were moved to plates containing either 0.1 or 1 µM 2,4-D and imaged 6, 17 and 24 hours later. Roots were counterstained using 10 µg/ml propidium iodide (PI) and imaged on a Leica SP8 X SMD confocal microscope equipped with hybrid (HyD) detectors and a pulsed white-light laser. GFP, YFP, tDT and PI were excited at 488, 504 or 561 nm, and detected between 500-535 nm, 525-600 nm, 570-600 nm or 630-700 nm, respectively. Embryos were imaged 4 days after crossing, for counterstaining they were briefly incubated in 10% glucose and 0,01% SCRI Renaissance Stain 2200 (R2200; Renaissance Chemicals,

UK). Embryos were extracted from ovules by applying slight pressure on the coverslip of slides containing ovules. Confocal imaging of embryos was performed on a Leica SP5 II system equipped with Hybrid Detectors (embryos, roots). On this system in addition to GFP and YFP, the R2200 stain could be visualized by excitation at 405 nm and detection between 430-470 nm. For embryos or roots of the same construct, the same settings were used for all pictures and to allow signal comparison no brightness or contrast adjustments were made.

## Supplementary information

Supplementary Table 1: Genotyping and qRT-PCR primers used in this chapter.

Genotyping		
pRPSSA-GAL4		
Insertion site	sense	CAAGGGTAAACGGCCACGGATTGACC
	antisense	ctccacaccccccaattgcacggagc
GAL4		GCAAACGAGCGTGACCGCT
qPCR		
GAPC	sense	GAAGGGTGGTGCCAGAAGGTT
	antisense	AGGGGAGCAAGGCAGTTAGTGG
CDKA	sense	ATTGCGTATTGCCACTCTCATAGG
	antisense	TCTGACAGGGATACCGAATGC
GHS	sense	GAGACCGCTCTCCCATCTTATCTG
	antisense	GGCTGATGTTCCAGAGCTAGTG
GFP	sense	ACGTAAACGGCCACAAGTTC
	antisense	AAGTCGTGCTGCTTCATGTG
tdT	sense	ACCACTGTTCTGGGGCAT
	antisense	GGCCATGTTGTGTCTCGG



# Chapter 5

## **A Yeast One Hybrid screen for candidate regulators of vascular identity**

Margot E. Smit<sup>1</sup>, Surabissree Merialu Diwakar<sup>1</sup>, Pawel Roszak<sup>2,3</sup>, Anne-Maarit Bågman<sup>4</sup>, Allie Gaudinier<sup>4</sup>, Joel Rodriguez-Medina<sup>4</sup>, Siobhan M. Brady<sup>4</sup>, Ykä Helariutta<sup>2,3</sup>, Dolf Weijers<sup>1</sup>

1 Laboratory of Biochemistry, Wageningen University, Stippeneng 4 6708 WE Wageningen, The Netherlands

2 Institute of Biotechnology, HiLIFE/Organismal and Evolutionary Biology Research Programme, Faculty of Biological and Environmental Sciences, Viikki Plant Science Centre, University of Helsinki, Helsinki, Finland

3 The Sainsbury Laboratory, University of Cambridge, Cambridge, United Kingdom

4 Department of Plant Biology and Genome Center, University of California, Davis, Davis, CA, USA

**Abstract**

Vascular tissues play a central role in plant development. The search for regulators of this tissue has identified factors that play key roles in vascular proliferation and patterning but no genes whose mutants are defective in vascular initiation. Auxin signaling through the AUXIN RESPONSE FACTOR5/ MONOPTEROS has been shown to be key in the development of vascular tissues but it is not sufficient for inducing identity. In this chapter we use a Yeast One Hybrid screen to search for candidate regulators that might contribute to the establishment of vascular identity during embryogenesis. Transcription factors that bind to and thus potentially regulate multiple vascular specific genes could be contributing to the regulation of vascular identity. After screening the promoter sequences of 16 vascular marker genes, we have used a rational selection pipeline to select 23 DNA-binding proteins as candidate regulators of vascular identity. Translational fusions reveal that 10 of these are present at the moment and location of vascular specification. These 10 are present in all cells of the proembryo, indicating that their activity, not protein localization could be the determining factor contributing to vascular regulation. An assay designed to determine the effect of individual candidates on vascular gene expression suffers from silencing of the vascular reporter genes but is successful in misexpressing SRDX-fused candidate genes which results in moderate phenotypes in adult plants.

## Introduction

The development of vascular tissues was a key step in plant evolution around 425 million years ago (Raven 2005). Mutant plants that are defective in vascular development are at a major disadvantage: if defects do not arrest growth they result in plants that are smaller and produce reduced offspring. Because of their central role in plant development, vascular tissues have been the subject of intense study. The regulation of cell proliferation (De Rybel et al. 2014, Hirakawa et al. 2010, Miyashima et al. 2019, Ohashi-Ito et al. 2014, Vera-Sirera et al. 2015), vascular patterning (Etchells & Turner 2010, Fàbregas et al. 2015, Mähönen et al. 2006) and differentiation (Baima et al. 2001, Rodriguez-Villalon et al. 2014, Yamaguchi et al. 2010) are each understood in some detail. In addition, the first step in vascular development, the formation of new vascular bundles, is a major field of study. However, this process has for a large part been investigated during a plant's postembryonic life. New vascular bundles in adult plants emerge whenever new connections need to be formed and research has focused on vascular initiation in leaves (Donner et al. 2009, Scarpella et al. 2006) and the formation of vascular connections in graft junctions (Melnik et al. 2015, 2018).

The formation of new vascular tissues is strongly linked to auxin. The plant hormone auxin is known to play a key role in vascular development and often precedes the formation of new vascular tissues (De Rybel et al. 2013, Donner et al. 2009, Melnik et al. 2015, Sachs 1969). Application of exogenous auxin to receptive tissues can also induce the formation of vascular tissue (Sachs 1969, 1991). As a result, auxin is thought to be essential and sufficient in initiating vascular tissues. However, in **Chapter 4** we have shown that blocking auxin signaling in the future vascular cells of the early embryo does not completely prevent expression of vascular identity markers. In the reverse experiment, high auxin levels in the root or ectopic activity of AUXIN RESPONSE FACTOR 5/MONOPTEROS (ARF5/MP) in the embryo was not able to confer vascular identity characteristics to other cells. These findings suggest that while auxin signaling is a key player essential in vascular development, it is not sufficient to instruct vascular identity. This is further underlined by the diverse roles auxin plays in development: it appears that auxin can trigger a variety of processes but relies on additional pathways for creating receptive tissues and specificity (Sachs 2000).

Next to auxin signaling, it is likely that there are additional regulatory pathways that control the initiation of vascular development. Our goal is to find such additional regulators. Most probably, such regulators act either in parallel to or together with auxin signaling pathways. Integration of signaling is likely to occur at the DNA, where most downstream

effects are regulated. We expect that transcription factors or other DNA-binding proteins are the next step in unraveling the mechanism of vascular specification.

To search for regulators of vascular identity, the set of vascular marker genes established in **Chapter 3** was used. A Yeast One Hybrid screen was performed to test protein-DNA interactions between vascular promoters and DNA-binding proteins. 16 bait yeast strains were created to be screened against a collection of 2037 unique prey. After performing Yeast One Hybrid experiments we selected candidate regulators of vascular identity and tested if they could meet the base requirements of regulating vascular identity: timing, location and function.

## Results

### A Yeast One Hybrid screen identifies hundreds of transcription factors that can bind vascular promoters

An enhanced Yeast One Hybrid (eY1H) screen was performed to find candidate regulators of vascular genes. Using a semi-automated approach, thousands of transcription factor-promoter interactions could be screened efficiently (Gaudinier et al. 2011, Reece-Hoyes et al. 2011). From the vascular genes tested in **Chapter 3**, 16 vascular promoters were selected to be screened: 12 vascular genes that had been previously used to mark vascular cells and 4 newly identified vascular genes (Table 1). Using a custom collection we screened these vascular promoters against a collection of 2037 transcription factors and other DNA-binding proteins (Figure 1)(Supplementary Table 1). On average each promoter interacted with 77 proteins in the screen (Table 1). Of the 16 promoters, 13 screened well in both the LacZ and His3 test but 3 promoters (*DOF6*, *IQD15* and *WOL*) did not show any activation in the LacZ assay. As a result, less interactors could be identified for these promoters and they are dissimilar in interaction number and pattern (Table 1).

From the individual interactions recovered in the eY1H screen, an interaction network was constructed. The network with all 16 promoters contained 397 transcription factors that bound to one or more vascular promoters in 1228 interactions (Figure 2). In the network overview in Figure 2-1, the transcription factors in the network are grouped by outdegree (the number of promoters bound by each transcription factor). Transcription factors binding to one promoter are on the periphery near their target while those that could bind to multiple promoters are in the center, grouped by their outdegree. A high outdegree



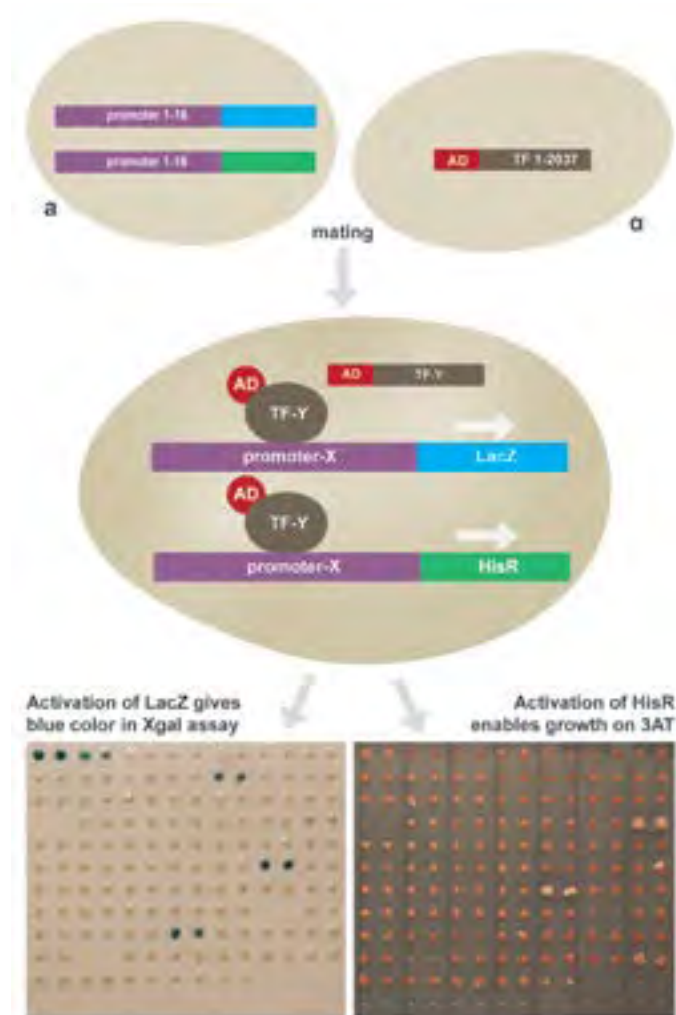


**Figure 1: Schematic overview of Yeast One Hybrid method.** After generation of bait and prey yeasts in different yeast strains, a and  $\alpha$  (Top), mating was performed for each promoter-transcription factor (TF) combination. Diploid yeasts containing both promoter and (TF) constructs were then used to check interactions. TF binding to a promoter will lead to the activation of the LacZ and His3 reporter gene (Middle). This activation was tested using an Xgal assay and growth on 3AT (3-amino-1,2,4-triazole) and interactions were called if both duplicates for each interaction were positive in either of the tests (Bottom).

could be indicative of preference for vascular promoters but could also indicate promiscuity. Certain transcription factors can bind to numerous promoters and are found in a large number of unrelated eY1H screens (Brady lab; Gaudinier et al. 2018, Sparks et al. 2016, Taylor-Teeple et al. 2015). These transcription factors are unlikely to specifically regulate vascular genes. To test whether the transcription factors that bind to many vascular promot-

**Table 1: Vascular promoters screened using Yeast One Hybrid.**

Locus and name of each of the 16 promoters screened. Per promoter the number of interactors found is indicated. Promoters of IQD15, DOF6 and WOL have lower numbers of interactors as they showed no activation in the Xgal assay.

Locus	Promoter name	Number of interactors
AT1G05577	SOK1	69
AT1G11735	MIR171B	94
AT1G68810	TSL1	125
AT2G01830	WOL	11
AT2G18380	GATA20	82
AT2G24570	WRKY17	79
AT2G37590	PEAR1	93
AT2G43290	MSS3	74
AT3G15210	ERF4	90
AT3G25710	TMO5	110
AT3G45610	DOF6	22
AT3G49380	IQD15	8
AT4G32880	ATHB8	78
AT4G37650	SHR	94
AT5G43810	ZLL	123
AT5G60200	TMO6	77

ers do so in a specific manner the frequency with which each transcription factor bound to promoters in unrelated screens was visualized (Figure 2-2). From this it appears that the majority of the transcription factors that can bind to a large number of vascular promoters, do so in a vascular-specific manner. Finally, visualizing the family to which each protein belongs reveals some interesting properties (Figure 2-3). For some families, their members show a strong preference for certain promoters: the *WRKY17* promoter is bound by a large number of GATA transcription factors and the *TARGET OF MONOPTEROS LIKE1 (TSL1)* promoter similarly by MYB transcription factors. These properties are specific to these promoters and do not inform us on the regulation of vascular identity. In contrast, members of other families (GeBP, Trihelix) can bind to many different vascular promoters, this could be of interest in identifying regulators of vascular identity. In general, within the network some transcription factor families are significantly overrepresented (G2-like, GATA, MYB) while others are underrepresented (bHLH, CO-like, MADS; Figure 3A). This could reflect either differences in ability to bind in eYIH experiments or differences in preference for vascular promoters. In the latter case, members of these families could play a role in identity regulation.

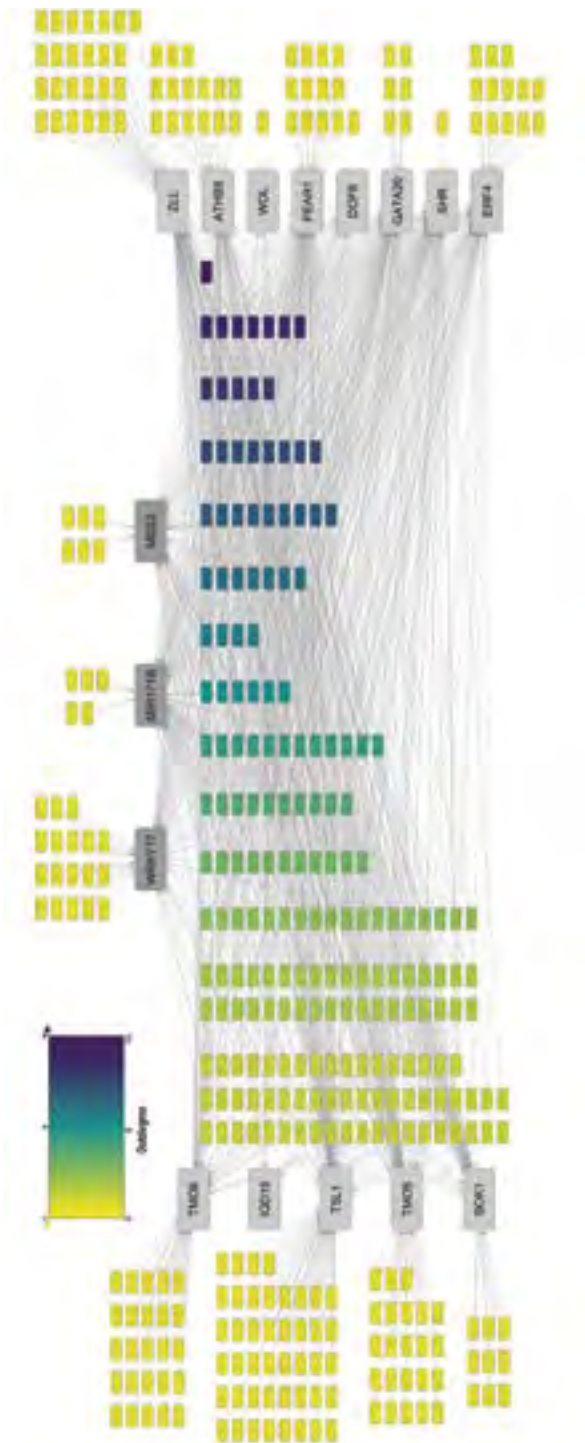


**Figure 2-1: Vascular Yeast One Hybrid network.**

Network containing all interactors of the 16 vascular promoters screened. Nodes corresponding to promoters are larger and colored grey (dark grey for inverse markers), nodes corresponding to transcription factors (TFs) are placed together based on their outdegree. TF nodes with an outdegree of 1 are placed on the periphery near their target, TF nodes with an outdegree of 2 or higher are placed in the center and are grouped based on their outdegree, nodes with a higher outdegree are located further to the right. (1) Network overview with TF nodes colored according to their outdegree (see inset).

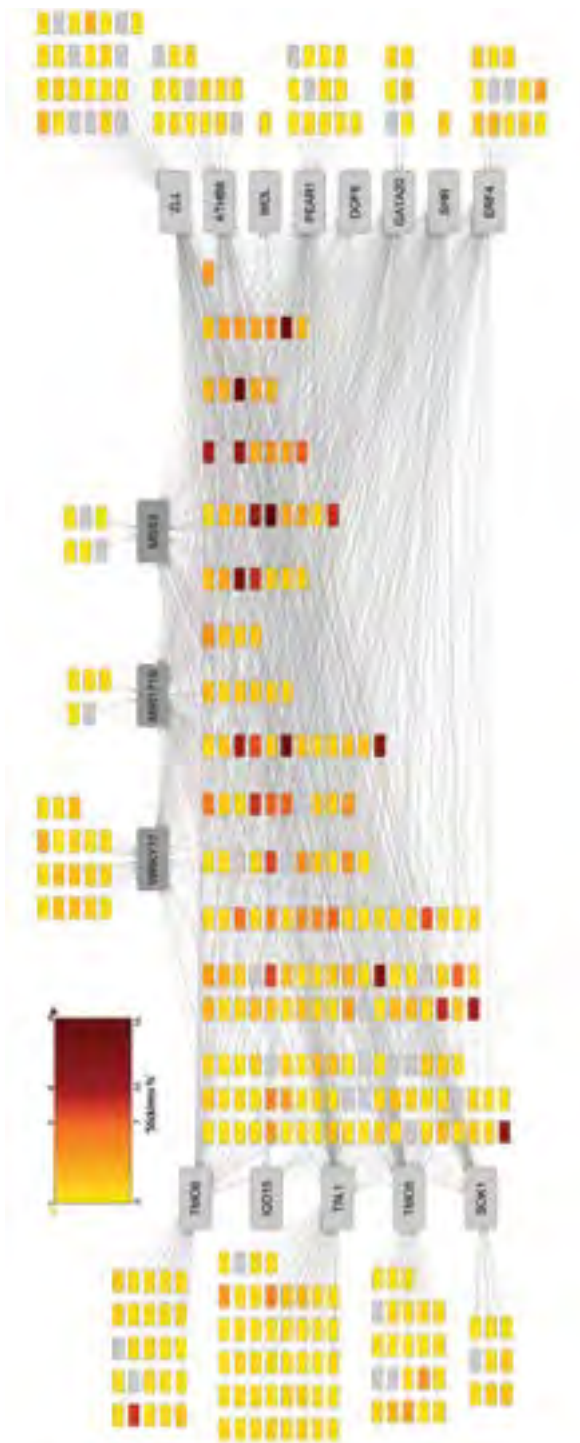


**Figure 2-2: Vascular Yeast One Hybrid network.**  
(2) Network overview with TF nodes colored according to their ‘false positive rate’ (see inset) as determined by looking at previous yeast screens performed in the Brady lab. *Full description in Figure 2-1*

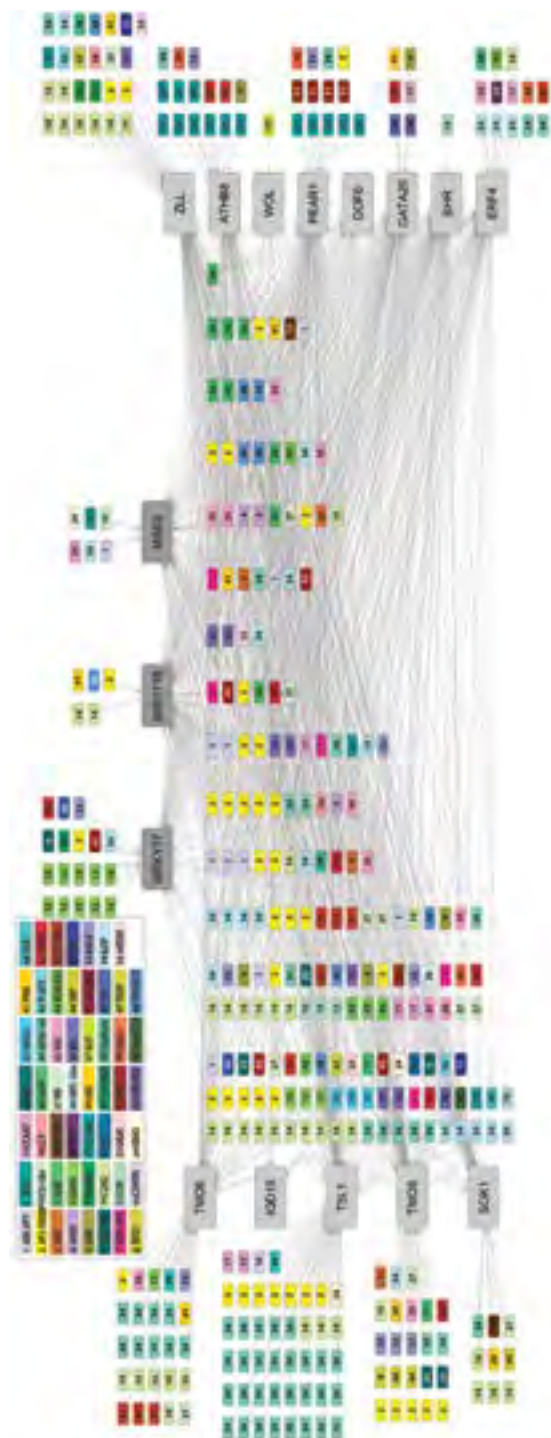
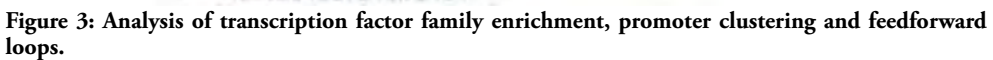


**Figure 2-3: Vascular Yeast One Hybrid network.**

Figure 2-3: Network overview with TF nodes colored according to TF family. Each TF family is represented by a color and number (see insert table). Full description in Figure 2-1





84

Next, we focused on the promoters. Clustering based on their interactors resulted in several unexpected associations (Figure 3). *IQD15*, *DOF6* and *WOL* were excluded from clustering because of their lack of LacZ activation and low number of interactors. The remaining 13 promoters could be divided into three groups with the promoters of *T5L1* and *TMO6* being outliers. These two promoters end up outside the three groups and instead more closely resemble the two unrelated TCA cycle (also citric acid cycle) promoters that were included as an outgroup (Li and Tang, unpublished)(Figure 3B). This finding underlines an observation made in **Chapter 3**: the *T5L1* and *TMO6* promoters did not mark the earliest vascular cells but instead become active later, at late globular stage. In addition, the clustering was expected to reveal differences between the vascular specific and vascular inverse promoters, as these have opposite expression patterns in the embryo. However, neither the network nor the clustering revealed such differences. The promoters of *WRKY17*, *MSS3* and *MIR171B* were bound by a similar set of transcription factors compared to the rest of the promoters and as such do not form a separate group in the clustering.

A third observation is that the network contains several promoters involved in feedforward loops (Figure 3C). These network structures arose because three of the promoters that were screened also had a corresponding transcription factor in the database that could bind to another promoter. The DOF6 protein could bind the *TMO6* promoter, the GATA20 protein interacted with the *ZLL* promoter and the ERF4 protein bound to the *TMO5* promoter (Figure 3C). Each of these combinations was in addition bound by transcription factors that bound to both promoters, this resulted in many feedforward structures. Interestingly, the three target promoters in these structures (*TMO6*, *ZLL*, *TMO5*) are all grouped in the minor groups of the promoter clustering (Figure 3B).

Summarizing, using enhanced Yeast One Hybrid screening we identified 397 transcription factors that can bind to one or more of the 16 vascular promoters. The overall network and clustering of promoters based on their interactions reveals that vascular promoters have a large amount of their potential interactors in common and that vascular specific and vascular inverse markers have highly similar interactors.

#### Rational selection of candidate regulators of vascular identity from the eY1H network

The goal of performing the eY1H screen was to find regulators of individual vascular genes but more importantly, to identify transcription factors that could regulate a large number of vascular genes and as such, vascular identity. We next aimed to select transcription factors from the network that could be regulators of vascular identity during embryogenesis. The selection process, which consists of two phases, is described below.

In the first phase, transcription factors were selected that met the base requirements for being a candidate regulator. These requirements were:

- Outdegree of 4 or more
- 'False positive score' of 8% or lower
- Expression in the early globular stage embryo

The first requirement ensured that all transcription factors selected could bind to at least 4 of the 16 promoters screened, because a regulator of vascular identity is expected to interact with multiple vascular promoters. The 'false positive score' requirement was based on data from previous screens using the same transcription factor library (Li and Tang, unpublished; Gaudinier et al. 2018, Sparks et al. 2016, Taylor-Teeples et al. 2015). Several transcription factors bind to a large number of the promoters, not just in this set of screens, but in all Yeast One Hybrid screens. As the goal was to identify vascular-specific regulators, the most 'sticky' transcription factors should be excluded. Lastly, only genes expressed in the early globular stage embryo were considered, since we searched for transcription factors that can regulate vascular identity around this stage. This criterion was not strict: in a wild type early globular stage embryo the transcription factor should be expressed in the top 80% based on the data available. By excluding the bottom 20% proteins not expressed at this stage were eliminated. This filtering step narrowed the list of transcription factors down from 397 to 50, for these 50 it was possible to perform more detailed scoring.

The next phase in selecting candidate regulators of vascular identity was to use binding and transcriptomics data to find transcription factors that might play a role in the development of vascular identity. For this purpose a scoring matrix was designed that weighed data from different sources to rank the 50 remaining transcription factors according to their likelihood of regulating vascular identity. In the scoring matrix each transcription factor was assigned points based on a combination of eY1H and transcriptomics data instead of eliminating candidates for not meeting one of the conditions (Figure 4).

First, each transcription factor was awarded points based on the number of promoters it could bind to in the eY1H screen: the higher the amount of promoters it bound, the more points awarded ('Outdegree'; Supplementary Table 2). Apart from the number of promoters bound, it was also significant with which of the promoters a transcription factor interacted. To select transcription factors that could regulate the breadth of vascular identity, points were also scored for the diversity in promoters bound ('Binding pattern'; Supplemen-



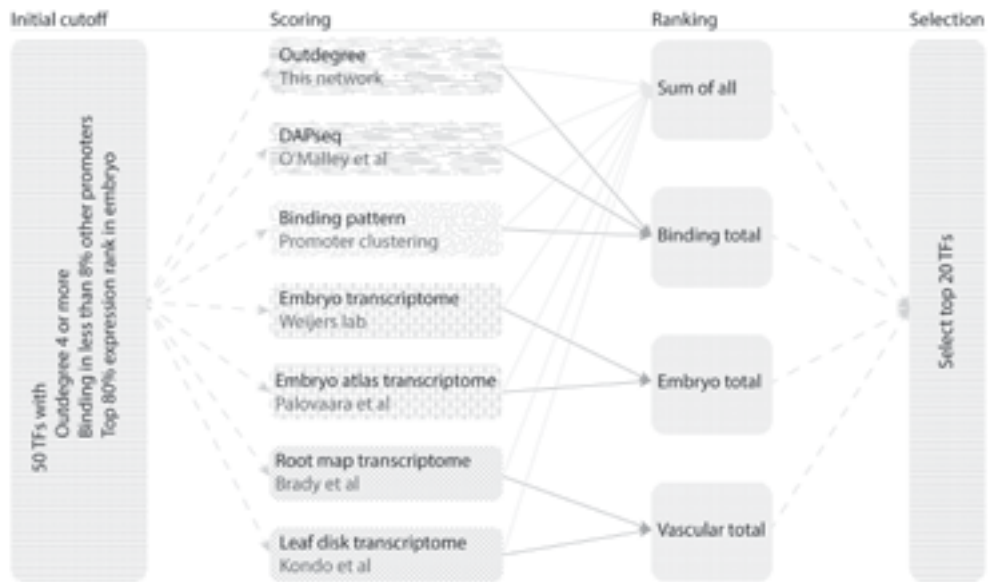


**Figure 4: Schematic overview of the procedure to select candidate regulators of vascular identity.**

Starting with 50 transcription factors (TFs) that met the criteria for the initial cutoff (left), each TF was then scored according to 7 characteristics. These scores were combined then ranked in four separate totals. The final selection of 20 candidate regulators was based on the average of the four rankings (right).

tary Table 2). This diversity was determined by looking at (1) the expression pattern of a promoter in the embryo and (2) the clustering of promoters based on their interactors. Binding to more restricted expression patterns and binding to promoters dissimilar in interactor set were prioritized. In addition to the eY1H, available DAPseq data (O'Malley et al. 2016) was used to check if each transcription factor could bind to vascular promoters in a different experimental setup. Unfortunately, this information was only available for several of the candidates ('DAPseq'; Supplementary Table 2). In addition to binding data, we used expression data to select transcription factors that were predicted to be expressed during embryogenesis and in vascular cells. To determine if a transcription factor was likely expressed during embryogenesis, transcriptomics datasets on isolated wildtype embryos was used ('Embryo transcriptome'; Supplementary Table 3; Möller et al. 2017). Here these datasets could be used to estimate if a transcription factor was expressed at the moment of characterization. Because in **Chapter 3** we found that vascular identity is first present at dermatogen stage, we used data from 8-cell, dermatogen and early globular stage embryos as we expected regulators of vascular identity to be expressed around these stages. In addition, the expectation was that a regulator of vascular identity could be expressed in vascular and adjacent cells but that ubiquitous expression was unlikely. Therefore, the embryo expression atlas was used

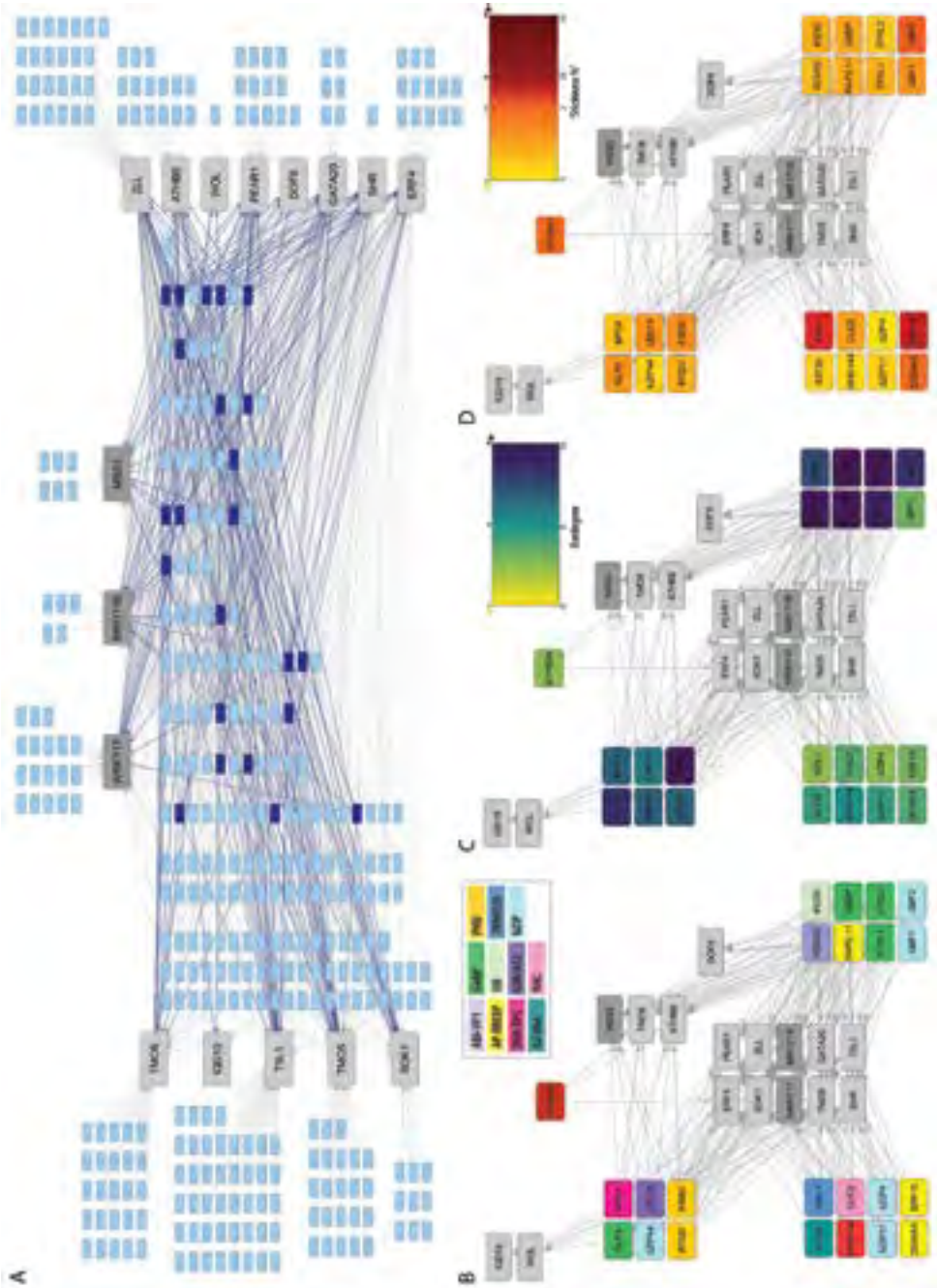


**Figure 5: Network characteristics of the 23 candidate regulators of vascular identity.**  
(A) The complete network with the 23 selected transcription factors and interactions marked in dark blue.  
(B, C, D) Partial overview of the network, containing only the 23 selected TFs and 16 promoters. Nodes are colored according to TF family (B), Outdegree (C), or False Positive Rate (D).

to score embryo expressed transcription factors that showed enrichment in the provascular cells ('Embryo atlas transcriptome'; Supplementary Table 3; Palovaara et al. 2017). Lastly, transcriptomics datasets on postembryonic tissues were used to select genes expressed in general vascular development: the root map transcriptome was used to score root vascular expressed genes ('Root map transcriptome'; Supplementary Table 4; Brady et al. 2007) and the leaf disk transcriptome was used to select genes expressed during reprogramming of leaf cells ('Leaf disk transcriptome'; Supplementary Table 4; Kondo et al. 2016).

To prevent a single characteristic from dominating the scoring outcome, four different scores were calculated: all categories combined; all binding categories; all embryo categories; and all vascular categories. The 50 transcription factors were ranked according to each score separately and finally an average ranking was used for the selection of the 20 highest ranked transcription factors overall (Supplementary Table 5). Afterwards 3 more transcription factors were added that could bind to vascular specific promoters but to none of the inverse promoters (*bZIP4*, *ERF15*, *ATHB34*).

The 23 transcription factors that were selected as candidate regulators of vascular identity could be found in different columns of the degree-organized network (Figure 5A). A closer look reveals that the selection contains transcription factors from 11 different families with the bZIP (5) and GeBP (4) families contributing the largest numbers of candidates (Figure 5B). In addition, candidates can bind many of the vascular promoters but do not indiscriminately bind in all eY1H screens, this results in a high outdegree and low 'False positive rate' (Figure 5C, D). We next characterized this core set of 23 candidate regulators.

### 10 Candidate regulators of vascular identity are present in all cells of the early embryo

In order to play a role in establishment of vascular identity, a candidate regulator needs to be present in the correct location at the correct time. To determine whether each candidate regulator was present at vascular specification, translational fusions were generated for each. The genomic fragment including a 2.1-3.0 kb promoter was C-terminally tagged with YFP and protein localization was checked in root and embryo.

For 20 of the 23 transcription factors, a translational fusion was successfully cloned and of these 20, 10 transcription factors were observed at the moment and location of vascular specification. Another five were not expressed at all during embryogenesis: RAP2.11, ERF15 and bZIP4 could not be observed in any of the roots or embryos screened. WRKY44 and AT3G12730 were observed in the root but the protein was not found in the embryo (Supplementary Figure 1). Another five transcription factors were confirmed to be present during

embryogenesis but not at the correct time or place to be involved in vascular specification. The CUC2 protein was not present until heart stage where it was present in the future shoot apical meristem (Supplementary Figure 1). DEWAX was observed early on during embryogenesis but there was no consistent pattern of expression, the protein was seen in single cells in an apparently random pattern. bZIP44, bZIP11 and GeBP were present starting before specification but their presence was limited to the suspensor at the moment of vascular specification (Figure 6-1; Figure 6-3). GeBP expression did later expand to the proembryo but not until after vascular specification. The remaining 10 transcription factors were present in the proembryo at the moment of vascular specification. All 10 were present in the nuclei of all cells of the proembryo and in some cases in the suspensor as well. None of the transcription factors showed either enrichment or depletion in the vascular cells compared to the rest of the embryo (Figure 6). With the exception of AT3G53680, all 10 proteins had similar expression levels in all cell types observed in root and embryo. AT3G53680 was expressed only in several vascular cells close to the QC in the root, but no cell type specificity or enrichment was seen in the embryo (Figure 6-2).

Translational fusions showed that the majority of the candidate transcription factors were present homogeneously in the nucleus, only excluded from the nucleolus, but the four members of the GeBP transcription factor family showed abnormal localization. They were present in spots in the nucleus, similar to previous observations in tobacco (Figure 6; Curaba et al. 2003). Each nucleus contains approximately 4-8 spots of protein but because of the low amount of fluorescence, the exact number could not be determined. For two other candidates: GBF1 and GBF2, previous reports had suggested that protein localization depends on exposure to light (Terzaghi et al. 1997). The proteins were reported to move into the nucleus upon exposure to light. However, both in the embryo and in the root and hypocotyl of dark grown seedlings, GBF1 and GBF2 were found exclusively in the nucleus (Figure 6-3; Supplementary Figure 2).

Summarizing, 10 of the 20 transcription factors for which translational fusion lines were created could be found at the moment and location of vascular specification during embryogenesis. All 10 were broadly expressed in the embryo with none showing either protein enrichment or depletion in the vascular cells. Thus, 10 of the selected transcription factors are in the correct location at the critical time to regulate vascular identity. An important question is whether they can regulate the expression of vascular genes.

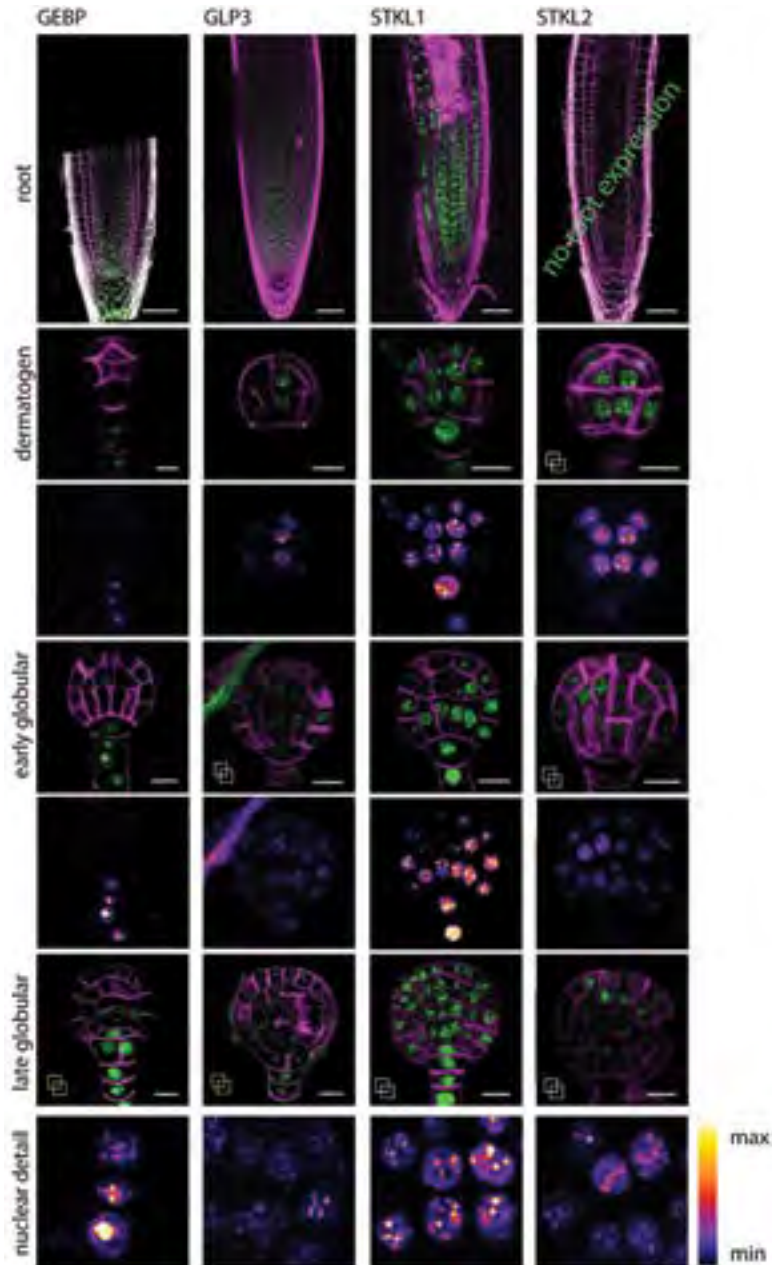


**Figure 6-1: Protein localization of the candidate regulators in root and embryo.**

In each panel localization in the root is shown at the top, followed by localization in dermatogen stage, early globular stage and one later stage. For dermatogen and early globular stage, false color images (fire LUT) are included to show the homogeneity in expression level across cell types. ## Indicates where zstacks are shown, scale bar indicates 50  $\mu$ m in roots or 10  $\mu$ m in embryos. (1) Protein localization of the 4 members of the GeBP family in the selection: GEBP, GLP3, STKL1 and STKL2.



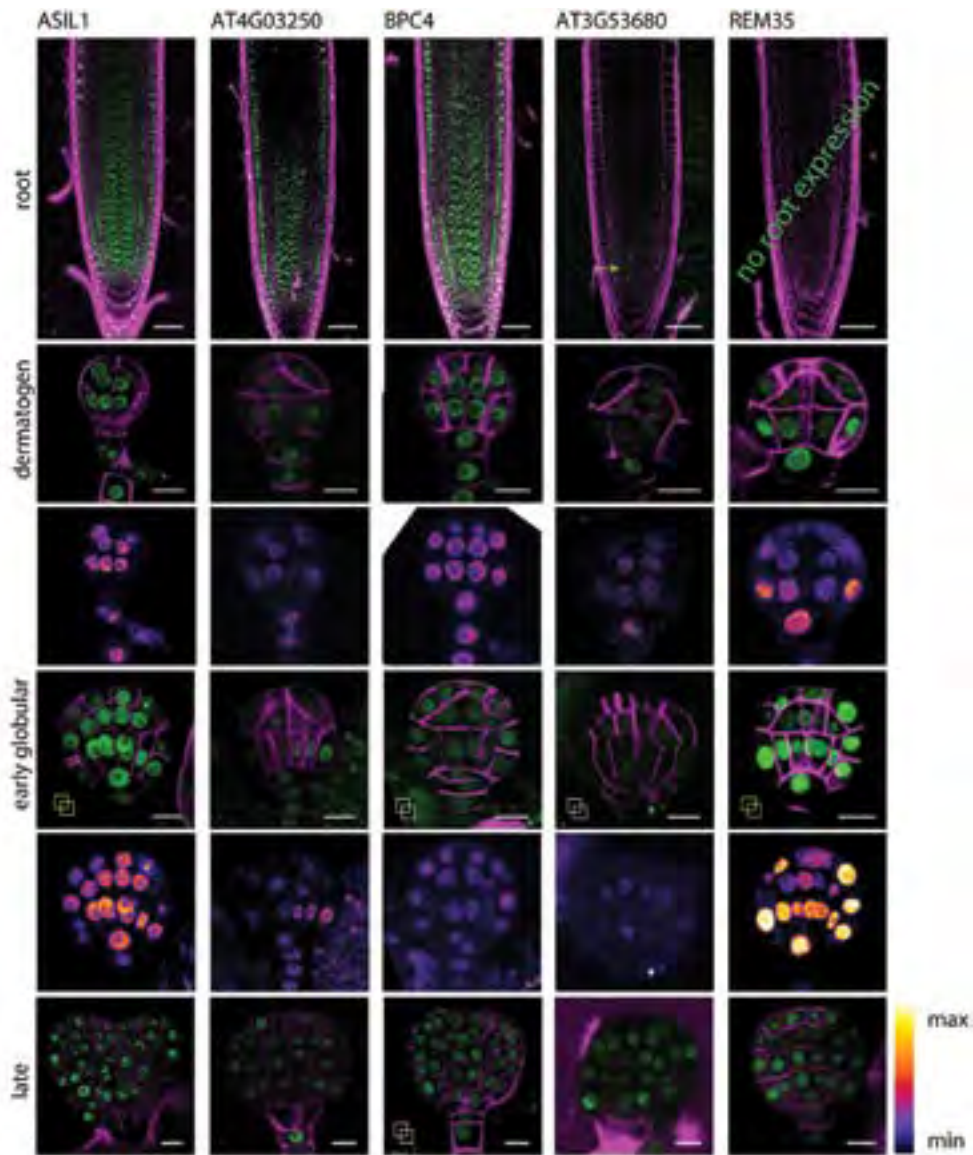


**Figure 6-2: Protein localization of the candidate regulators in root and embryo.**

(2) Broad protein localization of 5 candidate regulators.

Misexpression of candidates fused with SRDX results in mild phenotypes and reporter silencing

To investigate the function of the candidate regulators and to test their ability to bind vascular promoters, each candidate was fused to an SRDX motif and misexpressed in meristems. The SRDX motif confers transcriptional repression activity, and can act as dominant-nega-

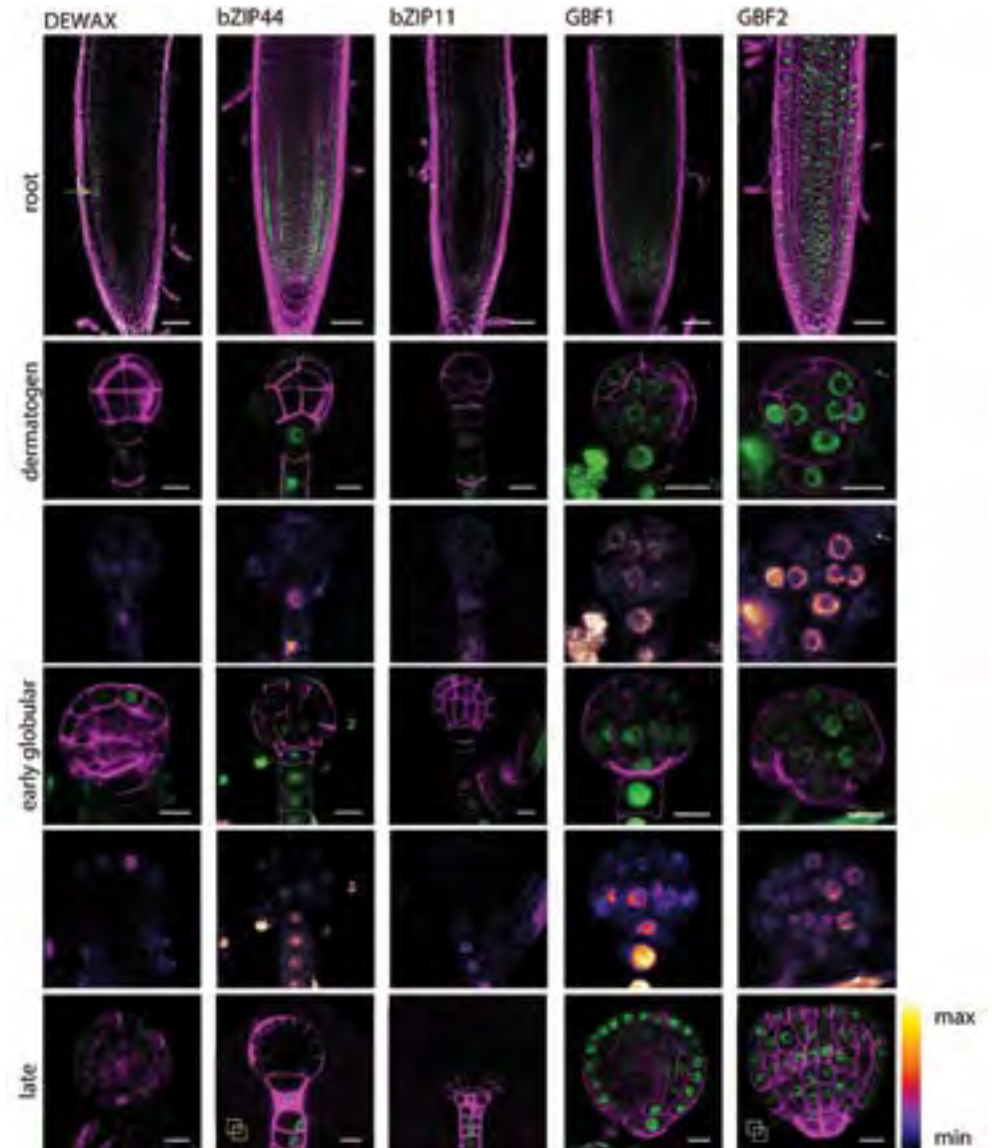


**Figure 6-3: Protein localization of the candidate regulators in root and embryo.**

(3) Protein localization of 5 candidate regulators.

rive when misexpressed (Hiratsu et al. 2003). By introducing this misexpression construct into a line containing two vascular transcriptional reporters it was possible to determine changes in vascular gene expression. The parental line used for this experiment contained a single transgene insertion with two transcriptional reporters: pTMO5-tdTomato and pWOL-sYFP (Figure 7E). In addition it contained a pRPS5A-GAL4 driver. Constructs

with each candidate regulator, fused to SRDX, and driven by the UAS promoter, were transformed directly into the parental line but also into a wildtype, Col-0, in case misexpression would cause lethality and no transformants could be recovered. The expectation was that if a candidate regulator could bind to either the *TMO5* or *WOL* promoter or to both, the fluorescence signal would decrease. This would enable quick screening to be followed up by expression quantification.

Misexpression of SRDX fused candidates did not cause major growth defects during the seedling stage but for several candidates the misexpression resulted in phenotypes such as changes in leaf shape and in some cases reduced size and fertility (Figure 7A-D; data not shown). These findings indicate that the transcription factors were misexpressed but did not severely deregulate vascular development. Adult phenotypes were often accompanied by reduced tdTomato and YFP expression in the root, as was expected for transcription factors binding to vascular promoters. However, a much higher incidence of reduced expression was found than was expected. A larger portion of T1 roots for each candidate had reduced fluorophore levels. Oddly, pWOL-YFP signal appeared linked to pTMO5-tdTomato signal: roots either had normal YFP levels but reduced tdTomato signal or both signals were decreased. No roots with normal pTMO5-tdTomato and reduced pWOL-YFP signal were found. In the next generation, the offspring of parents with reduction of only tdTomato signal included both roots lacking only tdTomato signal and roots lacking tdTomato and YFP signal (Figure 7G).

To confirm that our results were caused by changes in vascular gene regulation and not an artefact, negative control constructs were created using 4 transcription factors that were unlikely to regulate vascular genes: MGP, WER1, MUTE and SEP3. Surprisingly, introduction of these SRDX-fused candidates also resulted in fluorescence reduction (Figure 7F). Subsequent qPCR on homozygous T3 seedlings of SRDX-fused candidates containing plants confirmed that the reduction of fluorescence was not accompanied by reduction in endogenous gene expression (Figure 7H). While the candidate gene was misexpressed compared to the parental line, endogenous vascular genes including *TMO5* and *WOL* were not misregulated.

Thus, while the misexpression of candidates with SRDX tags was successful, artefactual reduction of fluorescence reporters meant that these lines could not be used as a tool to screen candidate binding to vascular promoters in plants. The lines could however still be used to further investigate the function of the candidate regulators of vascular identity in future experiments.



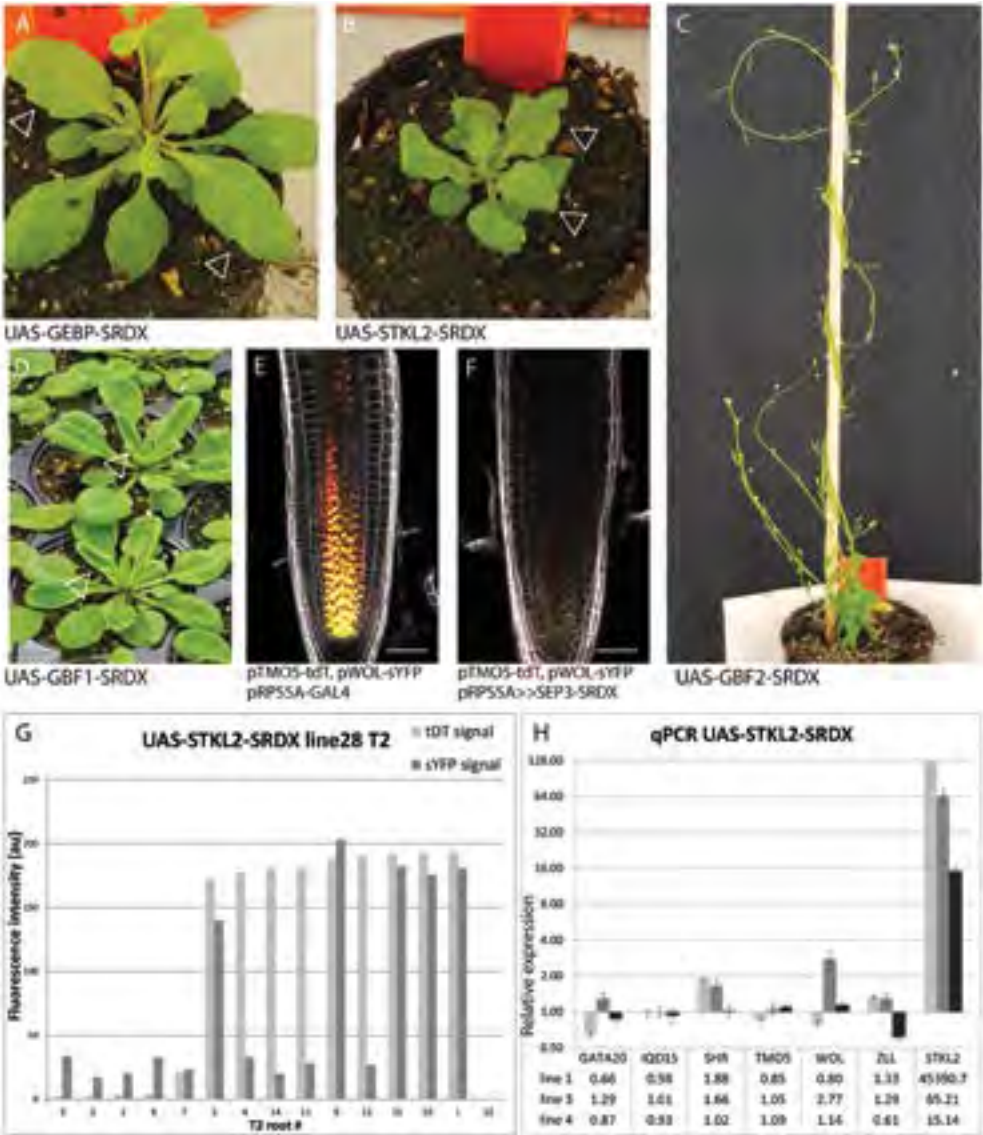


**Figure 7: Misexpression of SRDX fused candidates leads to phenotypes in adult plants and reduction in vascular reporters is unrelated to this misexpression.**

(A-D) Adult phenotypes resulting from misexpression of candidate regulators with SRDX tags. Triangles indicate abnormal leaf shapes. (E-F) Expression patterns of pTMO5-tdt and pWOL-sYFP in the root tip of WT (E) and MGP-SRDX misexpressing (F) roots. (G) Fluorescence signals in T2 roots of STKL2-SRDX misexpressing roots. Parental line showed reduced tdt signal but regular sYFP signal. (H) qPCR on STKL2-SRDX misexpressing T3 roots reveals STKL2 transcripts are increased but expression of vascular genes including TMO5 and WOL is not reduced. Expression was normalized using the parental line.

## Discussion

In this chapter, candidate regulators of vascular identity were identified using enhanced Yeast One Hybrid screening. 16 vascular promoters were screened against a collection of transcription factors and other DNA-binding proteins (Gaudinier et al. 2017; Supplementary Table 1). This eY1H screen yielded a tightly connected network in which 397 transcription factors were identified to bind one or more vascular promoters. Transcription factors that could bind to a large number of vascular promoters in the screen were often not able to bind to many promoters in unrelated screens and as such might be specific to vascular regulation. All vascular promoters were tightly connected in the network except for the promoters of *IQD15*, *DOF6* and *WOL*. For these promoters, yeast did not show any activation in the LacZ assay and as a result they have less interactions recorded. When the remaining promoters were clustered based on the proteins that could bind them, several patterns emerged. A separation was visible with the promoters of *T5L1* and *TMO6* not clustering with any other promoter in the screen, this dissimilarity reflects the difference in the timing of promoter activity found in **Chapter 3**. In addition, promoters of vascular-specific and vascular-inverse genes were not separated by clustering, which indicates that these promoters are bound by similar sets of proteins in the screen. Their opposite expression patterns could be caused by the same regulators potentially interacting with different cofactors or DNA-binding proteins not picked up in this screen.

In addition, three of the transcription factors that corresponded to promoters in our screen were able to bind to other vascular promoters. *DOF6*, *ERF4* and *GATA20* could bind to the promoters of *TMO6*, *TMO5* and *ZLL* respectively but not to other vascular promoters. This underscores the multiple levels of regulation that are expected to play a role in vascular development. However, none of the three can bind to multiple vascular promoters which makes them unlikely master regulators of vascular identity. These three pairs do share a large number of interactors, creating a large number of feedforward loops in our network. Looking at the transcription factors found in our screen we see that several transcription factor families are overrepresented in our network and others are underrepresented. This could be the result either of the preference of certain families for vascular promoters or a result of poor performance of specific families in our experimental setup. Transcription factors that require heterodimerization with other family members or interaction with unrelated cofactors do not perform well in Yeast One Hybrid screens in general (Deplancke et al. 2004). One example of a family that is underrepresented likely due to this effect is the basic Helix Loop Helix family whose members often form heterodimers (Jones 2004). In contrast, members of other families were overrepresented in our network. The cause of this is still

unknown but could be related to the mechanisms of vascular identity regulation.

The next step was to select transcription factors from the network that could regulate vascular identity. To avoid bias we employed a rational scoring mechanism to select candidate regulators of vascular identity. For 10 of these candidates translational fusion lines showed that the protein was present in the proembryo at dermatogen and early globular stage and thus could regulate the initiation of vascular identity. However, none showed tissue-specific or enriched localization. While a regulator can be broadly expressed and then locally active, we were surprised that none showed cell type-specific protein localization. This indicates that posttranscriptional regulation of RNA and posttranslational regulation protein stability do not lead to cell type specific differences in protein level for these proteins.

In addition, no differences were found in subcellular localization across cell types. Within the nucleus most candidates were present homogeneously, only excluded from a region that is likely the nucleolus, but members of the GeBP family were present in approximately 4-8 spots in the nucleus. This localization was previously reported in transient expression in tobacco (Curaba et al. 2003) but is now confirmed in Arabidopsis root and embryo. Likewise for GBF1 and GBF2 previous studies had investigated their location. Those reports had indicated that GBF1 and GBF2 were transported into the nucleus under the influence of blue light (Terzaghi et al. 1997). Interestingly, this could not be confirmed: in dark grown seedlings and dark grown cell cultures both proteins kept nucleus-specific localization (Supplementary Figure 2). Instead, signaling and subsequent protein modification could alter DNA-binding and activity as is the case for key regulators in other processes (Hamann et al. 2002, Kepinski & Leyser 2005). Indeed, redox potential has been shown to affect GBF-DNA binding (Klimczak 1992, Shaikhali et al. 2012). For other candidate regulators, similar mechanisms could also exist but remain unknown.

While eY1H is an excellent method for identifying transcription factors that can bind specific promoters, an interaction found in yeast requires confirmation in a plant system. Ectopic activation of vascular genes upon misexpression of individual candidate regulators was expected to be difficult as their regulation likely integrates multiple cues, so instead it was decided to aim at repressing expression instead. The effect of candidate regulators on vascular development was instead tested through misexpressing an SRDX fusion in the *RPS5A* expression domain, encompassing all meristematic cells. However, it appears that the locus containing both reporters was often silenced upon the introduction of an additional construct. This was confirmed by including transcription factors unlikely to regulate vascular genes as negative controls and by checking *TMO5* and *WOL* transcript levels through

qPCR. The silencing is likely the result of the introduction of a third pGREEN backbone containing vector (Martin Bayer, personal communication). Fortunately, the phenotypes observed and the qPCR results indicate that the introduced construct is active and the SRDX-fused candidates are expressed.

Misexpression of SRDX-fused candidate regulators at most led to developmental phenotypes in the adult plant, in some cases even leading to loss of fertility (GBF2, STKL2). This is the opposite of what was expected, as it was predicted that misregulation of vascular identity regulators would result in strong phenotypes that would affect early development. One explanation is that direct transformation into the pRPS5A-GAL4 containing line resulted in embryo lethality for candidates that play key roles in vascular development. In that case we would however expect to find very few transformants, but for all constructs similar numbers of transformants were found. However, the alternative of crossing the pRPS5A-GAL4 containing line with UAS-candidate-SRDX plants, to avoid embryo lethality, proved too laborious to be feasible. Another explanation for the lack of striking developmental defects is that these candidate regulators alone cannot change the development of vascular identity. Establishment of vascular identity likely depends on several cues and signaling pathways being integrated and high levels of redundancy are to be expected (Barolo & Posakony 2002, Niwa 2018, Sachs 2000, Sparks et al. 2016). However it is clear that these factors are unlikely to play a role as central as MONOPTEROS (MP) whose absence or inhibition has strong developmental repercussions (Hamann et al. 1999, Hardtke & Berleth 1998). The next step in understanding roles for the candidate regulators discovered in this chapter will be to understand the developmental interactions with auxin signaling in vascular development.

## Material and methods

### Yeast One Hybrid

Enhanced Yeast One Hybrid screens were performed as described in Gaudinier et al. 2017. The promoter used for the yeast reporter constructs (pMW2 and pMW3) was the same as the promoter used for reporting localization in Arabidopsis (except for PEAR1, where an 1.3 instead of 1.6 promoter was used for the eY1H). After yeast transformation, bait yeast was selected by testing auto-activation of both reporters and by genotyping. Auto-activation testing determined the concentration of 3-amino-1,2,4-triazole to be used in the screen. The prey collection used was the complete Arabidopsis transcription factor collection available at

the Brady lab in July 2016 (Supplementary Table 1). After yeast mating and diploid selection, growth on 3-amino-1,2,4-triazole containing plates and an X-gal assay were used to determine activation of reporter genes. Positives were scored if both duplicates showed activation in either assay. Network analysis was performed in Cytoscape (Shannon et al. 2003). Promoter clustering was performed by hierarchical clustering in R (Team & R Development Core Team 2016). TF family enrichment or depletion was calculated using the Hypergeometric distribution Calculator (<https://keisan.casio.com/exec/system/1180573201>).

### Plant material and growth conditions

All constructs for plant transformation were cloned using SliCE cloning into previously published LIC vectors (Wendrich et al. 2015, Zhang et al. 2014b). Translational fusion constructs were generated by amplifying up to 3 kb of the promoter and the gene up to but not including the stop codon and introducing this sequence into pPLV16\_v2 using the primers listed in Supplementary Table 6 (Wendrich et al. 2015). Misexpression constructs of SRDX fused candidates were created by cloning the coding sequence of each candidate and introducing this fragment into a modified pPLV32\_v2 backbone containing the SRDX tag. Translational fusion constructs were introduced into Columbia (Col-0) while misexpression constructs were introduced into the double activation line containing pRPS5A-GAL4 and a double vascular reporter construct (pTMO5-tdTomato, pWOL-sYFP).

All plants were grown at 21 °C under standard long-day (16:8h light:dark) conditions. Arabidopsis seeds were surface-sterilized, plated on ½ MS plates and underwent 2 days of stratification. For antibiotic selection seedlings were initially grown on plates containing phosphinotricin and transferred to plates without antibiotics after 7 days of growth. Seedlings were transferred to soil after emergence of the first true leaves and then continued growth under the same conditions.

### Microscopy and sample preparation

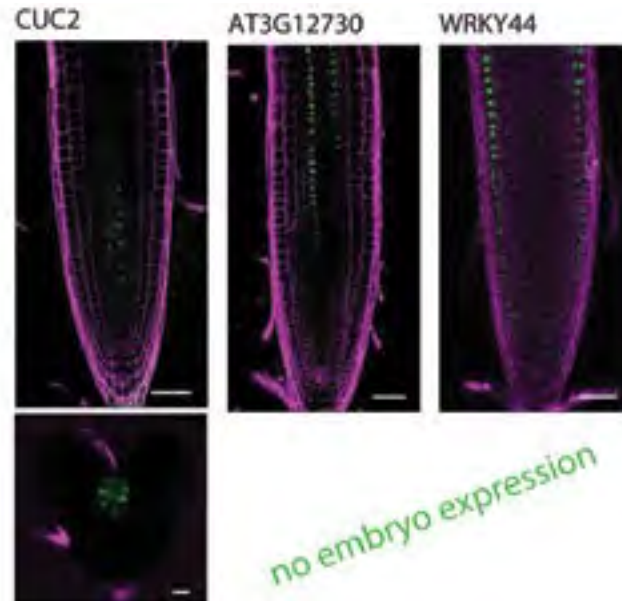
To counterstain roots and embryos they were briefly incubated in either 10 µg/ml propidium iodide (PI) or 10% glucose with 0,01% SCRi Renaissance Stain 2200 (R2200; Renaissance Chemicals, UK) respectively. Embryos were extracted from ovules by applying slight pressure on the coverslip of slides containing ovules. Confocal imaging was performed on a Leica SP5 II system equipped with Hybrid Detectors (embryos, roots) or on a Leica SP8 X SMD confocal microscope equipped with Hybrid (HyD) detectors and a pulsed white-light laser (roots). Both systems could be used for the detection of YFP, tDT and PI which were excited at 504 or 561 nm, and detected between 525-600 nm, 570-600 nm or 630-700 nm,

respectively. On the SP5 system R2200 could be visualized by excitation at 405 nm and detection between 430-470 nm.

### Expression analysis

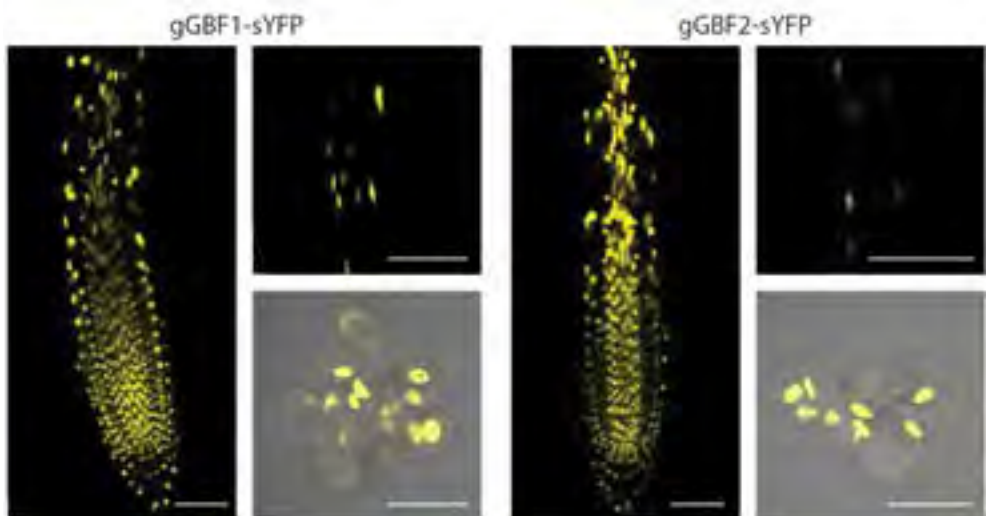
For expression analysis seedlings were grown for 5 days on  $\frac{1}{2}$  MS plates with mesh. Roots were collected, frozen in liquid nitrogen and ground using a Retch machine. RNA was isolated using TRIzol reagent (Invitrogen) and the RNAeasy kit (Qiagen). 0,5  $\mu$ g total RNA was then used for cDNA synthesis with the iScript cDNA Synthesis Kit (Biorad). qRT-PCR was performed using iQ SYBR Green Supermix (Biorad) and measured on a CFX384 RT-PCR detection system. Each reaction was performed in triplicate. Data analysis was performed using qBase software and gene expression levels were normalized using *CDKA* and *GAPC* (Hellemans et al. 2008).

## Supplementary Figures and Tables



**Supplementary Figure 1: Protein localization of candidate regulators not expressed in the early embryo.**

Green color represents YFP fused to candidate regulator protein, magenta color represents Renaissance staining, scale bar indicates 50  $\mu$ m in roots or 10  $\mu$ m in embryo.



**Supplementary Figure 2: Protein localization of GBF1 and GBF2 in dark grown root, hypocotyl and cell culture.**

Yellow color represents YFP fused to candidate regulator protein, scale bars indicate 50  $\mu$ m.



Supplementary Table 1: Full list of transcription factors used as prey.

Locus	Gene Name	Locus	Gene Name	Locus	Gene Name	Locus	Gene Name
AT1G01310	ANAC001	AT1G64860	BPCD1/SG1	AT2G39250	SN2	AT3G56520	AT3G56520
AT1G01330	NGA3	AT1G65300	AGL36/PHC2	AT2G39630	DAR2/LRD3	AT3G56570	AT3G56570
AT1G01360	LWR	AT1G65360	AGL23	AT2G39880	AMMYB25	AT3G56770	AT3G56770
AT1G01360	GIF2	AT1G65620	AS2	AT2G39900	WLM2a	AT3G56850	ARE83
AT1G01250	AT1G01250	AT1G69910	NAC038	AT2G40340	AT2G40340	AT3G56970	BH4/BB/ORG2
AT1G01260	AT1G01260	AT1G66340	ZFP4	AT2G40300	AT2G40300	AT3G56980	BH4/H39
AT1G01330	AT1G01330	AT1G66320	MYB20	AT2G40310	AGL48	AT3G57040	ANR8/ATRR4
AT1G01380	ETC4	AT1G66340	AT1G66340	AT2G40350	AT2G40350	AT3G57230	AGL36
AT1G01520	ASG4	AT1G66350	RG1	AT2G40340	AtRR48	AT3G57390	AGL18
AT1G01540	AT1G01540	AT1G66370	AtMYB113	AT2G40350	AT2G40350	AT3G57480	AT3G57480
AT1G01720	ATAF1	AT1G66380	AtMYB114	AT2G40450	AT2G40450	AT3G57600	AT3G57600
AT1G01780	PLM43b	AT1G66390	AtMYB90/PAF2	AT2G40470	AtGL1/AtGL15	AT3G57670	AtTWRP2
AT1G01920	AT1G01920	AT1G66420	AT1G66420	AT2G40620	AT2G40620	AT3G57800	AT3G57800
AT1G02030	AT1G02030	AT1G66470	AtRR46	AT2G40670	AtRR36	AT3G57920	SP15
AT1G02040	AT1G02040	AT1G66550	AtWRKY57	AT2G40740	WRKY55	AT3G58070	GIS
AT1G02065	SPB8	AT1G66600	AtWRKY63	AT2G40750	AtWRKY54	AT3G58120	AtRRP63
AT1G02170	ATMC1	AT1G66810	AT1G66810	AT2G40950	BOP17	AT3G58190	AtGL3/AtGL29
AT1G02210	AT1G02210	AT1G67030	ZFP6	AT2G40970	MYB31	AT3G58630	AT3G58630
AT1G02220	ANAC004	AT1G67100	LB040	AT2G41070	EEL	AT3G58880	AtMBP18
AT1G02230	ANAC004	AT1G67260	TCP1	AT2G41130	AT2G41130	AT3G58750	WRKY69
AT1G02250	NAC005	AT1G67370	ASY1/ATGATY1	AT2G41240	BHLH300	AT3G58780	SAF5
AT1G02340	HFR3	AT1G67710	AtRR1	AT2G41310	AtRR8/AtRR3	AT3G59060	PH5
AT1G03040	AT1G03040	AT1G67910	AT1G67910	AT2G41370	BOP2	AT3G59470	AT3G59470
AT1G03250	AT1G03250	AT1G67970	AtHFA8	AT2G41450	AT2G41450	AT3G60030	SP12
AT1G03350	AT1G03350	AT1G68030	AT1G68030	AT2G41690	AtHSP83	AT3G60190	HAT3
AT1G03650	AT1G03650	AT1G68320	AtRRP3	AT2G41710	AT2G41710	AT3G60400	SHO71
AT1G03750	CHP9	AT1G68330	AtGDI14	AT2G41835	AT2G41835	AT3G60490	AT3G60490
AT1G03790	AtZFP450M	AT1G68350	WRKY9	AT2G41900	OR52/TF27	AT3G60530	GATA4
AT1G03800	AtRRF10	AT1G68390	BOP2	AT2G41940	ZFP8	AT3G60580	AT3G60580
AT1G03840	MGP	AT1G68390	AT1G68390	AT2G42040	AT2G42040	AT3G60630	HMM2
AT1G03970	GIF4	AT1G68420	AT1G68420	AT2G42300	AtSP19	AT3G60670	AT3G60670
AT1G04050	SGG13/SA/VR1	AT1G68320	AtMYB62	AT2G42380	AtGL3/AtRR4	AT3G61130	AtGL3
AT1G04100	UAA30	AT1G68360	AT1G68360	AT2G42360	AT2G42360	AT3G61230	PLM2b
AT1G04240	SHY2	AT1G68480	LAG	AT2G42380	AtRRP34	AT3G61250	LAG2
AT1G04250	AtRRF14	AT1G68510	LB042	AT2G42400	AtVCL2	AT3G61460	BRH1
AT1G04370	AtRRF14	AT1G68520	BOP14	AT2G42410	AtRRP11	AT3G61550	AtGL3/AtGL14
AT1G04445	AT1G04445	AT1G68550	CRP23	AT2G42430	AtGL3/AtGL16	AT3G61600	AtPDR1/AtRR2
AT1G04500	AT1G04500	AT1G68640	PAN	AT2G42640	AT2G42640	AT3G61630	CRP6
AT1G04550	UAA52	AT1G68670	AT1G68670	AT2G42680	AtMBP14	AT3G61740	AtGL3/AtGL14
AT1G04850	AT1G04850	AT1G68800	BAC2/TFP12	AT2G42830	SHP2	AT3G61830	AtRR18
AT1G04880	AT1G04880	AT1G68810	AT1G68810	AT2G43000	ANAC043/UBR1	AT3G61850	DAG2
AT1G04950	AT1G04950	AT1G68840	RAT2	AT2G43010	PP4	AT3G61890	AtRR12
AT1G04990	AT1G04990	AT1G68880	AtRR2P	AT2G43060	RRH1	AT3G61910	ANAC066/NT2
AT1G05130	HOG2	AT1G68920	AT1G68920	AT2G43120	AT2G43120	AT3G61950	AtRR19/AtRR20
AT1G05380	AT1G05380	AT1G69010	BAM2	AT2G43500	AT2G43500	AT3G61970	NGA2
AT1G05420	AtRRP12	AT1G69030	AT1G69030	AT2G44020	AT2G44020	AT3G62090	PL2
AT1G05690	BT3	AT1G69120	AP1	AT2G44150	AtRR12/AtRR27	AT3G62100	UAA30
AT1G05710	AT1G05710	AT1G69170	AT1G69170	AT2G44430	AT2G44430	AT3G62240	AT3G62240
AT1G05805	AT1G05805	AT1G69180	CRC	AT2G44470	AT2G44470	AT3G62260	AT3G62260
AT1G06040	RRK2/AT10	AT1G69310	WRKY57	AT2G44470	AtWRKY52	AT3G62610	AtMYB91
AT1G06070	AT1G06070	AT1G69490	NAP	AT2G44840	AtRRP13	AT3G62670	AtRR20
AT1G06150	ORA59	AT1G69540	AGL34	AT2G44910	AtRR4	AT3G62690	AtGL3
AT1G06170	AT1G06170	AT1G69560	AtMYB105	AT2G44940	AT2G44940	AT3G63030	MBD4
AT1G06180	AtMYB13	AT1G69570	AT1G69570	AT2G45050	GATA2	AT3G63150	AtHFA78
AT1G06280	LB02	AT1G69580	AT1G69580	AT2G45120	AT2G45120	AT3G64650	AtGL3
AT1G06850	AtRRP12	AT1G69600	ZFP51	AT2G45190	HMM1	AT4G00050	UMI10
AT1G06920	AtRRP4	AT1G69690	AtRRP5	AT2G45190	YAB1	AT4G00130	At4G00130
AT1G07050	AT1G07050	AT1G69790	AtRR13	AT2G45410	LB019	AT4G00150	HAM3
AT1G07360	MACS3	AT1G69810	WRKY36	AT2G45420	LB018	AT4G00180	YAB1
AT1G07520	AT1G07520	AT1G70000	AT1G70000	AT2G45480	AtRRP9	AT4G00210	LB031
AT1G07530	SG14	AT1G70010	AT1G70010	AT2G45650	AtGL3/AtRR1	AT4G00230	GLD
AT1G07640	CHP2	AT1G70510	ENAT2	AT2G45660	SGG1/AGL20	AT4G00232	At4G00232
AT1G07700	LR1	AT1G70700	AtRRP17	AT2G45680	AT2G45680	AT4G00238	At4G00238
AT1G07880	NP-PC30	AT1G70920	AtRR18	AT2G45800	PLM2a	AT4G00250	At4G00250
AT1G08000	GATA10	AT1G71030	AtMYB92	AT2G45880	BAM7/BNM4	AT4G00270	At4G00270
AT1G08010	GATA11	AT1G71130	AtGL3/AtGL13	AT2G46040	AT2G46040	AT4G00390	At4G00390
AT1G08290	WRP1	AT1G71260	AtWRKY2	AT2G46130	AtWRKY43	AT4G00410	MBD3
AT1G08320	TGA5	AT1G71450	AT1G71450	AT2G46160	AT2G46160	AT4G00610	At4G00610
AT1G08465	YAB2	AT1G71902	AtGL12	AT2G46260	UBR1	AT4G00730	ANL2
AT1G08540	AtRR1/AtRR13	AT1G71930	VND7	AT2G46270	GFB3	AT4G00760	PRR8
AT1G08780	AtRR1/AtRR13	AT1G72010	AtRRP22	AT2G46310	CRF5	AT4G00850	GFB3
AT1G08810	AtMYB60	AT1G72030	AT1G72030	AT2G46400	WRKY46	AT4G00870	At4G00870



# A Yeast One Hybrid screen for candidate regulators of vascular identity

AT1G08880	G-H2AX/HTAS	AT1G72050	TFHA	AT2G46510	ATA8	AT4G00940	AT4G00940	AT5G18550	AT5G18550
AT1G08910	HMPSC	AT1G72060	AT1G72060	AT2G46530	AMP11	AT4G00990	AT4G00990	AT5G18560	PUCH1
AT1G09030	NF-YB4	AT1G72210	SMH96	AT2G46590	DAG2	AT4G01060	CPL4/ATC3	AT5G18680	ACT1P1
AT1G09060	AT3G09060	AT1G72310	ATL3	AT2G46670	AT2G46670	AT4G01130	GBF2	AT5G18830	SPB7
AT1G09250	AT3G09250	AT1G72350	AT1G72350	AT2G46680	ATH8-7	AT4G01250	WRKY22	AT5G18960	FRS12
AT1G09530	PF3	AT1G72360	HRE1	AT2G46735	AT2G46735	AT4G01260	AT4G01260	AT5G19280	KAPP/RAG1
AT1G09540	MYB61	AT1G72430	JAZ2/TFY118	AT2G46770	ANAC043/NS1	AT4G01280	AT4G01280	AT5G19310	ACHR23
AT1G09710	AT3G09710	AT1G72570	AT1G72570	AT2G46790	APR95/TL1	AT4G01460	AT4G01460	AT5G19330	ABA
AT1G09770	AT3G09770	AT1G72740	AT1G72740	AT2G46830	CCA1	AT4G01500	NSA4	AT5G19490	AT5G19490
AT1G10510	AT3G10510	AT1G72830	MAP2C	AT2G46870	NSA1	AT4G01540	ANAC068/NTM1	AT5G19650	ATOPB
AT1G10710	ATM9X1	AT1G73100	SGG15/SA/VR3	AT2G46970	PL1	AT4G01550	anc069	AT5G19790	RAP2.11
AT1G10700	ANWLM1	AT1G73300	AT1G73300	AT2G46990	IAA20	AT4G01580	AT4G01580	AT5G19910	ME031
AT1G10740	FRS13	AT1G73410	ATMYB54	AT2G47070	SPL1	AT4G01680	MYB55	AT5G20240	PI
AT1G10470	AMBA/RT881	AT1G73730	EL3	AT2G47190	ATMYB2	AT4G01720	ACWRKY47	AT5G20730	NPM4
AT1G10480	ZPP5	AT1G73830	BE3	AT2G47210	AT2G47210	AT4G01750	IME12	AT5G20900	JAZ13/TFY38
AT1G10580	AT3G10580	AT1G73870	AT1G73870	AT2G47260	WRKY23	AT4G01840	B2CH21	AT5G21120	EL2
AT1G10590	AT3G10590	AT1G74080	ATMYB122	AT2G47370	UPR1	AT4G01870	AUD20	AT5G21960	AT5G21960
AT1G10610	AT3G10610	AT1G74120	AT1G74120	AT2G47460	MYB12	AT4G01990	85M/RUG2	AT5G22240	ATOPF10
AT1G10720	AT3G10720	AT1G74410	AT1G74410	AT2G47520	HRE2	AT4G01170	AT4G01170	AT5G22790	anc089
AT1G11490	AT3G11490	AT1G74430	MYB95	AT2G47620	ATSW13A/CHB1	AT4G01250	AT4G01250	AT5G22380	NAC090
AT1G11510	AT3G11510	AT1G74480	ABX01/LRP4	AT2G47700	RFQ	AT4G01300	ATOPP9	AT5G22570	WRKY38
AT1G11950	AT3G11950	AT1G74510	AT1G74510	AT2G47810	NF-YB5	AT4G01450	ATMYB42	AT5G22750	RAD5/RAD5A
AT1G12260	VND4	AT1G74650	ATMYB33	AT2G47850	AT2G47850	AT4G01485	PCF34	AT5G22890	STOP2
AT1G12440	AT3G12440	AT1G74660	MY1	AT2G47890	AT2G47890	AT4G01490	POF2	AT5G22990	AT5G22990
AT1G12810	DOP1	AT1G74840	AT1G74840	AT2G47900	ACT1P3	AT4G01500	ATMYB34	AT5G23000	ATMYB37/RAK3
AT1G12830	AT3G12830	AT1G74890	ARR15	AT2G48100	AT2G48100	AT4G01570	AT4G01570	AT5G23090	NF-YB13
AT1G12860	SCRM2	AT1G74930	CHAA7	AT3G02030	AT3G02030	AT4G01630	AT4G01630	AT5G23260	AB1/AGL32
AT1G12890	AT3G12890	AT1G74950	JAZ2/TFY108	AT3G02140	ACMYB106/NOX	AT4G01664	AYY1	AT5G23280	ACTOP7
AT1G12980	DHN	AT1G75080	BZ1	AT3G02120	ATMYB2	AT4G01694	DEAR5/RAP2.9	AT5G23405	AT5G23405
AT1G13260	NAV1	AT1G75240	ARR83	AT3G02320	SAL1	AT4G01810	KNA11	AT5G23420	HMG86
AT1G13300	HRS1	AT1G75250	AT1G75250	AT3G02330	DEL3	AT4G01820	AT4G01820	AT5G23650	AT5G23650
AT1G13400	AGLNUB	AT1G75340	AT1G75340	AT3G02470	AT1H1/HA15	AT4G01845	AT4G01845	AT5G23930	AT5G23930
AT1G13450	GT-3	AT1G75390	Abd29P44	AT3G02530	ATMYB57	AT4G01910	AT4G01910	AT5G24050	AT5G24050
AT1G13600	Abd29P58	AT1G75410	Bu3	AT3G02600	NAC044	AT4G01980	FBI2	AT5G24130	ATMYB30
AT1G13960	WRKY4	AT1G75490	AT1G75490	AT3G02890	AT3G02890	AT4G01950	AT4G01950	AT5G24120	AT5G24120
AT1G14030	L3MT-4	AT1G75520	SMS5	AT3G02970	WRKY45	AT4G01960	ATMYB6	AT5G24330	ATXN6/SGD34
AT1G14150	PLP	AT1G75530	AT1G75530	AT3G02150	PT1/TCP3	AT4G01980	AT1G75540	AT5G24470	APR85
AT1G14410	ATMYB1/PTAC1	AT1G75540	STW2	AT3G02310	AGL4/SEF2	AT4G11240	Bu33	AT5G24520	ATTG1/ARM218
AT1G14440	ACHR11	AT1G75710	AT1G75710	AT3G02380	ATCOL2/RRK3	AT4G11350	ANAC070/BRN2	AT5G24590	ANAC091
AT1G14510	AL7	AT1G76110	AT1G76110	AT3G02400	AT3G02400	AT4G11600	AT4G11600	AT5G24800	AT5G24800
AT1G14580	AT3G14580	AT1G76320	CPO25/FR54	AT3G02550	UBD41	AT4G11630	KELP	AT5G24930	ATCOL4
AT1G14605	ATBP2	AT1G76350	AT1G76350	AT3G02790	AT3G02790	AT4G11670	ACWRKY41	AT5G25160	ZPP3
AT1G14687	ACHR12/ZHD14	AT1G76420	CUC3	AT3G02830	PN1/OPN1	AT4G11680	3uHMG-bbox1	AT5G25190	ESR3
AT1G14900	HMG5A	AT1G76510	AT1G76510	AT3G02860	AT3G02860	AT4G11140	CRP1	AT5G25220	KNA15
AT1G14920	GA1	AT1G76580	AT1G76580	AT3G02940	MYB107	AT4G11250	AGL52	AT5G25390	SHR2
AT1G15050	IAA34	AT1G76590	AT1G76590	AT3G02990	ATMYB41E	AT4G11400	AT4G11400	AT5G25470	AT5G25470
AT1G15340	MBD50	AT1G76710	ASAH1/SGD26	AT3G03200	anc045	AT4G11560	AT-SPB28	AT5G25475	AT5G25475
AT1G15360	SHN1	AT1G76870	AT1G76870	AT3G03450	RG2	AT4G11580	AT4G11580	AT5G25790	AT5G25790
AT1G15580	IAA5	AT1G76880	AT1G76880	AT3G03550	AT3G03550	AT4G11680	AGL13/MAJ2	AT5G25810	my
AT1G15720	YRFL3	AT1G76890	G12	AT3G03660	WOK11	AT4G11640	AUSA7	AT5G25830	GATA12
AT1G16060	ADAP/WR1	AT1G76900	AT1P1	AT3G03750	SGG15/SA/VR3	AT4G11230	AT4G11230	AT5G25890	IAA28
AT1G16490	ATMYB58	AT1G77080	AGL27/RLM	AT3G03760	UBD20	AT4G11240	AT4G11240	AT5G26170	ATMYB50
AT1G16530	UBD9	AT1G77200	AT1G77200	AT3G04030	MYB2	AT4G11250	MYB42	AT5G26210	AL4
AT1G16640	AT3G16640	AT1G77250	AT1G77250	AT3G04070	anc047	AT4G11260	ATORC18/UNE13	AT5G26610	AT5G26610
AT1G17310	AT3G17310	AT1G77300	APM42/YCR3	AT3G04100	AGL57	AT4G112670	AT4G112670	AT5G26630	AT5G26630
AT1G17380	JAZ2/TFY11A	AT1G77450	anc032	AT3G04280	ARR2	AT4G11280	AT4G11280	AT5G26650	AGL36
AT1G17460	YRFL3	AT1G77570	AT1G77570	AT3G04380	SGG15/SA/VR6	AT4G113040	AT4G113040	AT5G26660	ATMYB86
AT1G17520	AT3G17520	AT1G77640	AT1G77640	AT3G04420	NAC048	AT4G11340	SGD23/ST22	AT5G26740	AT5G26740
AT1G17590	NF-YA8	AT1G77850	AMP37	AT3G04450	AT3G04450	AT4G11380	ATMYB79	AT5G26805	AT5G26805
AT1G17950	ATMYB52	AT1G77920	AT1G77920	AT3G04670	ATWRKY39	AT4G113630	AT4G113630	AT5G26930	GATA23
AT1G18330	EPH1	AT1G77980	AGL66	AT3G04730	IAA35	AT4G11390	AT-SPB28	AT5G26950	AGL59
AT1G18335	AT3G18335	AT1G78080	RAP2.4	AT3G04930	AT3G04930	AT4G11425	AT4G11425	AT5G27050	AGL301
AT1G18400	BE1	AT1G78280	AT1G78280	AT3G05200	ATL6	AT4G114410	BuH134	AT5G27090	AGL54
AT1G18570	MYB10	AT1G78600	L2F1	AT3G05380	ATL4Y2	AT4G114490	AT4G114490	AT5G27130	AGL39
AT1G18710	ATMYB47	AT1G78700	BEH4	AT3G05670	AT3G05670	AT4G11450	NF-YB3	AT5G27580	AGL89
AT1G18750	AGL65	AT1G78930	AT1G78930	AT3G05690	AUNF-YA2	AT4G114550	IAA24	AT5G27620	ATL475
AT1G18760	AT3G18760	AT1G79000	ATHAC1	AT3G05760	AT3G05760	AT4G11460	IAA3	AT5G27820	AT5G27820
AT1G18780	AT3G18780	AT1G79180	ATMYB63	AT3G05800	AP1	AT4G114650	MDA1	AT5G27880	AT5G27880
AT1G18790	AT3G18790	AT1G79220	AT1G79220	AT3G05860	AT3G05860	AT4G114710	PPD1/TFY4A	AT5G27910	NF-YC8
AT1G18960	AT3G18960	AT1G79350	EMH135	AT3G06120	MYE1	AT4G114720	PPD2/TFY4B	AT5G27944	AT5G27944
AT1G19000	AT3G19000	AT1G79430	APL/AYOY	AT3G06230	AT3G06230	AT4G114770	YCK2	AT5G28040	AT5G28040
AT1G19040	AT3G19040	AT1G79580	ANAC011/VRM8	AT3G06250	FR57	AT4G115090	FAR2	AT5G28300	AT5G28300
AT1G19050	ARR7	AT1G79700	AT1G79700	AT3G06380	AT1P19	AT4G115240	BBOX30	AT5G28640	AN3/ATG11
AT1G19180	AMAZ1/TFY10A	AT1G79840	GL2	AT3G06410	AT3G06410	AT4G115250	BBX9	AT5G28770	B2CH20
AT1G19210	AT3G19210	AT1G80390	IAA15	AT3G06490	MYB108	AT4G115420	AT4G115420	AT5G29000	PHL1
AT1G19220	AMP19	AT1G80400	AT1G80400	AT3G06590	AT3G06590	AT4G116141	AT4G116141	AT5G29330	ATMYB2

AT1G15270	DA1	AT1G82580	AT1G82580	AT3G06740	GATA15	AT4G16430	AT4G16430	AT5G35550	AT5G35550
AT1G15950	B2R2	AT1G82590	AT1G82590	AT3G07220	AdPRA2	AT4G16610	AT4G16610	AT5G35770	SAP
AT1G15990	AT5G39490	AT1G82730	AT1G82730	AT3G07260	AT3G07260	AT4G16750	AT4G16750	AT5G35900	LB035
AT1G15910	AT1G15910	AT1G82840	AT1G82840	AT3G07340	AT3G07340	AT4G16780	AT4G16780	AT5G36020	AMR8
AT1G15900	BE120	AT1G82960	AT1G82960	AT3G07500	AT3G07500	AT4G16845	VRN2	AT5G37260	RVC2
AT1G15790	SRS7	AT1G82100	AT1G82100	AT3G07650	COL5	AT4G17230	SC133	AT5G37800	AT5G11
AT1G15850	MP	AT1G82130	AT1G82130	AT3G07670	AT3G07670	AT4G17460	HAT1	AT5G38140	NP-IC12
AT1G15860	AT5G38660	AT1G82150	AT1G82150	AT3G07740	HAC15/VRK2	AT4G17490	ATERF5	AT5G38490	AT5G38490
AT1G20640	AT5G20640	AT1G82160	AT1G82160	AT3G08020	AT3G08020	AT4G17500	ATERF-1	AT5G38740	AGL77
AT1G20693	HMG82	AT1G82170	AT1G82170	AT3G08500	MYB83	AT4G17570	GATA26	AT5G38800	Ab2P43
AT1G20696	HMG83/NFD3	AT1G82181	AT1G82181	AT3G08505	AT3G08505	AT4G17695	KAN3	AT5G38860	BM3
AT1G20700	WDX14	AT1G82190	AT1G82190	AT3G08520	AdMYB1	AT4G17785	MYB39	AT5G39010	ANAC092
AT1G20910	AT5G20910	AT1G82194	AT1G82194	AT3G08520	TAC1	AT4G17810	AT4G17810	AT5G39660	CD2
AT1G20980	AT5G14188	AT1G82200	AT1G82200	AT3G08570	MYB38-3	AT4G17880	AT4G17880	AT5G39750	AGL81
AT1G21000	AT5G21000	AT1G82207	AT1G82207	AT3G08735	AT3G08735	AT4G17900	AT4G17900	AT5G39760	AbH23
AT1G21200	AT5G21200	AT1G82208	AT1G82208	AT3G10000	IDA31	AT4G17980	NAC371	AT5G39810	AGL58
AT1G21340	AT5G21340	AT1G82209	AT1G82209	AT3G10030	AT3G10030	AT4G18030	PRR2	AT5G39820	NAC094
AT1G21450	SL2	AT1G82210	AT1G82210	AT3G10040	AT3G10040	AT4G18170	AT5G39820	AT5G39860	BH436/BNQ25
AT1G21700	AT5G39700	AT1G82211	AT1G82211	AT3G10113	AT3G10113	AT4G18390	TCF4	AT5G40220	AGL48
AT1G21780	AT5G21780	AT1G82217	AT1G82217	AT3G10390	P1D	AT4G18450	AT4G18450	AT5G40330	MYB23
AT1G21910	HEK26	AT1G82240	AT1G82240	AT3G10470	AT3G10470	AT4G18470	SN1	AT5G40370	AT5G40370
AT1G21970	AMEC1/NF-YB9	AT1G82240	AT1G82240	AT3G10480	ANAC050	AT4G18770	MYB98	AT5G40880	AT5G40880
AT1G22070	TGA3	AT1G82280	AT1G82280	AT3G10500	anac053	AT4G18830	ATOPP5	AT5G41030	AT5G41030
AT1G22130	AGL504	AT1G82280	AT1G82280	AT3G10580	AT3G10580	AT4G18880	AT-IF5AAA	AT5G41090	NAC095
AT1G22190	AT5G22190	AT1G82300	AT1G82300	AT3G10590	AT3G10590	AT4G18890	BEH3	AT5G41200	AGL75
AT1G22310	AT5G22310	AT1G82340	AT1G82340	AT3G10595	AT3G10595	AT4G18960	AG	AT5G41315	GL3
AT1G22490	AT5G22490	AT1G82340	AT1G82340	AT3G10760	AT3G10760	AT4G19630	AT4G19630	AT5G41380	AT5G41380
AT1G22590	AGL87	AT1G82350	AT1G82350	AT3G10800	B2P28	AT4G19985	AT4G19985	AT5G41410	BE13
AT1G22640	AT5G22640	AT1G82370	AT1G82370	AT3G11020	ORF628	AT4G20280	TAF11	AT5G41580	AT5G41580
AT1G22810	AT5G22810	AT1G82438	AT1G82438	AT3G11090	UBQ21	AT4G20380	USD1	AT5G41590	AT5G41590
AT1G22985	AT5G22985	AT1G82440	AT1G82440	AT3G11100	AT3G11100	AT4G20400	JM114	AT5G42630	KAN4
AT1G23080	KNA16	AT1G82440	AT1G82440	AT3G11200	AL2	AT4G20970	AT4G20970	AT5G42640	AT5G42640
AT1G23420	INO	AT1G82445	AT1G82445	AT3G11260	WDR1/WDR58	AT4G21030	ATDOF4.2	AT5G42700	AT5G42700
AT1G23810	AT5G23810	AT1G82480	AT1G82480	AT3G11280	AT3G11280	AT4G21040	ATDOF4.3	AT5G42780	AbH27/J24013
AT1G24030	AT5G24030	AT1G82480	AT1G82480	AT3G11440	AT5G24030	AT4G21080	ATDOF4.5	AT5G42820	AT5G42820
AT1G24040	AT5G24040	AT1G82510	AT1G82510	AT3G11580	AT3G11580	AT4G21340	R70	AT5G42950	AT5G42950
AT1G24190	AT5G24190	AT1G82530	AT1G82530	AT3G12130	AT3G12130	AT4G21430	B160	AT5G43170	A2F3
AT1G24210	AT5G24210	AT1G82590	AT1G82590	AT3G12250	TGA6	AT4G21440	AT5G43170	AT5G43250	NP-IC13
AT1G24230	AT5G24230	AT1G82600	AT1G82600	AT3G12270	AT3G12270	AT4G21610	LDL2	AT5G43270	SP2
AT1G24250	AT5G24250	AT1G82650	AT1G82650	AT3G12280	AT3G12280	AT4G22070	AT5G43270	AT5G43290	AT5G43290
AT1G24260	SEF3	AT1G82640	AT1G82640	AT3G12480	NP-IC13	AT4G22140	EB5	AT5G43540	AT5G43540
AT1G24580	AT5G24580	AT1G82670	AT1G82670	AT3G12680	HUA1	AT4G22360	AT4G22360	AT5G43620	AT5G43620
AT1G24590	DMN1	AT1G82670	AT1G82670	AT3G12720	AT5G24590	AT4G22680	MYB85	AT5G43650	BH492
AT1G24610	AT5G24610	AT1G82690	AT1G82690	AT3G12730	AT3G12730	AT4G22700	LB032	AT5G43700	AT5G43700
AT1G24620	ZYP2	AT1G82710	AT1G82710	AT3G12820	AT5G24620	AT4G22745	MYB1	AT5G43840	AT-IF5A4C
AT1G25280	ACTP10	AT1G82760	AT1G82760	AT3G12890	ASAL2	AT4G22820	AT4G22820	AT5G43990	SDG18/SLVR2
AT1G25310	MEK8	AT1G82880	AT1G82880	AT3G12910	AT3G12910	AT4G22950	AGL19	AT5G44080	AT5G44080
AT1G25330	C3HAP	AT1G82880	AT1G82880	AT3G12977	AT3G12977	AT4G23050	AT5G44080	AT5G44160	NUC
AT1G25340	MYB9216	AT1G82890	AT1G82890	AT3G13040	AT3G13040	AT4G23070	CRF2	AT5G44180	AT5G44180
AT1G25440	BBH15	AT1G82910	AT1G82910	AT3G13350	AT3G13350	AT4G23800	3eHMG-box2	AT5G44190	AT5G44190
AT1G25470	CRF12	AT1G82940	AT1G82940	AT3G13445	TBP1/TTPD-1	AT4G23810	WRKY53	AT5G44210	ERF5
AT1G25550	AT5G25550	AT1G82970	AT1G82970	AT3G13540	AT5G25550	AT4G23860	AT4G23860	AT5G44260	ACT2F5
AT1G25560	TEM3	AT1G82970	AT1G82970	AT3G13680	LDL2	AT4G23980	AMF9	AT5G44500	AT5G44500
AT1G25580	TEM3	AT1G82980	AT1G82980	AT3G13810	AUD013	AT4G24030	NP7	AT5G44510	AT5G44510
AT1G25580	SOE1	AT1G82980	AT1G82980	AT3G13840	AT3G13840	AT4G24060	AT4G24060	AT5G44560	AT5G44560
AT1G26270	AT5G26270	AT1G83130	AT1G83130	AT3G13960	AGR5	AT4G24240	WRKY7	AT5G44580	AT5G44580
AT1G26260	CIB5	AT1G83180	AT1G83180	AT3G14000	AT5G26260	AT4G24470	TIF1	AT5G44580	AT5G44580
AT1G26300	AT5G26300	AT1G83180	AT1G83180	AT3G14030	NP-186	AT4G24540	AGL24	AT5G44580	AT5G44580
AT1G26310	CAL	AT1G83180	AT1G83180	AT3G14180	AT3G14180	AT4G24660	AT5G26310	AT5G44580	AT5G44580
AT1G26590	AT5G26590	AT1G83180	AT1G83180	AT3G14230	RAIP2.2	AT4G25110	AT5G26590	AT5G44580	AT5G44580
AT1G26610	AT5G26610	AT1G83180	AT1G83180	AT3G14700	AT3G14700	AT4G25210	AT5G26610	AT5G44580	AT5G44580
AT1G26780	AT5G26780	AT1G83180	AT1G83180	AT3G14740	AT3G14740	AT4G25380	AT5G26780	AT5G44580	AT5G44580
AT1G26840	KDM9/PR6	AT1G83180	AT1G83180	AT3G15030	MEK15/TCF4	AT4G25400	AT4G25400	AT5G44680	BH4971
AT1G26960	AbH23	AT1G83180	AT1G83180	AT3G15170	CUC1	AT4G25410	AT4G25410	AT5G44730	AT5G44730
AT1G27050	AT5G27050	AT1G83180	AT1G83180	AT3G15210	ATERF-4	AT4G25440	ZPWO1	AT5G44760	AT5G44760
AT1G27280	AT5G27280	AT1G83180	AT1G83180	AT3G15270	SP15	AT4G25470	CBF2	AT5G44830	AT5G44830
AT1G27360	SP11	AT1G83180	AT1G83180	AT3G15500	AT5G27360	AT4G25490	CBF1	AT5G44880	AT5G44880
AT1G27370	SP120	AT1G83180	AT1G83180	AT3G15510	AT5G27370	AT4G25560	AT5G27370	AT5G44915	AT5G44915
AT1G27650	AT5G27650	AT1G83180	AT1G83180	AT3G15540	GA19	AT4G25610	AT4G25610	AT5G44915	AT5G44915
AT1G27660	AT5G27660	AT1G83180	AT1G83180	AT3G15790	AT5G27660	AT4G25990	CL	AT5G44915	AT5G44915
AT1G27730	STZ	AT1G83180	AT1G83180	AT3G16160	AT3G16160	AT4G26030	AT4G26030	AT5G44915	AT5G44915
AT1G27740	RSR4	AT1G83180	AT1G83180	AT3G16280	AT3G16280	AT4G26110	GATA22/GRN	AT5G44915	AT5G44915
AT1G28050	BBH15	AT1G83180	AT1G83180	AT3G16350	AT3G16350	AT4G26640	WRKY20	AT5G44915	AT5G44915
AT1G28060	AT5G28060	AT1G83180	AT1G83180	AT3G16500	PAP1	AT4G27230	W5A2	AT5G44915	AT5G44915
AT1G28080	ABH22	AT1G83180	AT1G83180	AT3G16770	RAIP2.3	AT4G27240	AT4G27240	AT5G44915	AT5G44915
AT1G28090	BBH13	AT1G83180	AT1G83180	AT3G16810	ABH1	AT4G27310	BBH28	AT5G44915	AT5G44915

# A Yeast One Hybrid screen for candidate regulators of vascular identity

AT1G28370	ERF11	AT2G18670	AT2G18670	AT3G16870	GATA17	AT4G27330	N2Z5PL	AT5G47790	AT5G47790
AT1G28450	AGL58	AT2G18850	AT2G18850	AT3G17010	HEM22	AT4G27410	RD26	AT5G48150	PAT1
AT1G28470	ANAC015	AT2G19260	AT2G19260	AT3G17100	AT3G17100	AT4G27900	AT4G27900	AT5G48250	AT5G48250
AT1G28520	ATV035	AT2G19380	AT2G19380	AT3G17600	UA31	AT4G27950	CRF4	AT5G48500	AT5G48500
AT1G29160	AT3G29160	AT2G19520	ACG5/ATM54	AT3G17600	HHH	AT4G28030	AT4G28030	AT5G48560	AT5G48560
AT1G29280	WRRY5	AT2G19810	AGD2/LN1/T2	AT3G17730	anac057	AT4G28110	AIMY84	AT5G48670	FEM311
AT1G29860	ATWRRY71	AT2G20100	AT2G20100	AT3G18010	WOK1	AT4G28140	AT4G28140	AT5G48890	LATE
AT1G29950	AT5G29950	AT2G20210	AT2G20210	AT3G18400	NAC058	AT4G28190	UL1	AT5G49200	AT5G49200
AT1G30135	IAZ6/THY5A	AT2G20480	PP1	AT3G18550	AsbM21	AT4G28500	ANAC073	AT5G49300	GATA16
AT1G30210	ATTCP24	AT2G20750	AT2G20750	AT3G18640	AT3G18640	AT4G28530	NAC074	AT5G49330	ATMYB111/PW1
AT1G30330	ARF6	AT2G20800	AT2G20800	AT3G18650	AGL303	AT4G28610	AIMY81	AT5G49420	AT5G49420
AT1G30460	ATCP5F30	AT2G20570	AT2G20570	AT3G18870	AT3G18870	AT4G28640	UA31	AT5G49450	AIMY81
AT1G30490	PHV	AT2G20825	UL2	AT3G18960	AT3G18960	AT4G29080	PAP2	AT5G49490	AGL83
AT1G30500	NF-YA7	AT2G20880	AT2G20880	AT3G18990	VNN1	AT4G29100	AT4G29100	AT5G49520	WRRY48
AT1G30650	ATWRRY14	AT2G21060	AT2G21060	AT3G19070	AT3G19070	AT4G29190	AsC3H49	AT5G49620	AsMYB78
AT1G30810	AT5G30810	AT2G21230	AT2G21230	AT3G19184	AT3G19184	AT4G29230	anac075	AT5G50010	AT5G50010
AT1G30970	SUR4	AT2G21240	AT2G21240	AT3G19210	AT3G19210	AT4G29410	AT4G29410	AT5G50020	AIMY83
AT1G31040	AT5G31040	AT2G21320	AT2G21320	AT3G19290	AIMY84	AT4G29930	AT4G29930	AT5G50070	NF-YC7
AT1G31050	AT5G31050	AT2G21400	SMS3	AT3G19500	AT3G19500	AT4G30080	AIMY85	AT5G50480	NF-YC6
AT1G31140	AGL53/UGA	AT2G21530	AT2G21530	AT3G19510	HA3.1	AT4G30080	AIMY85	AT5G50570	SP13
AT1G31320	LB04	AT2G21650	AT2G21650	AT3G19580	AZF2	AT4G30410	AT4G30410	AT5G50670	SP13B
AT1G31330	AGL86	AT2G21710	IMR2213	AT3G19860	SHLH121	AT4G30835	WRRY33	AT5G50835	anac087
AT1G31760	AT5G31760	AT2G21900	AT2G21900	AT3G20110	AT2F7-7	AT4G30980	UL2	AT5G50915	AT5G50915
AT1G32070	ATN50	AT2G22200	AT2G22200	AT3G20590	DCX	AT4G31080	AT4G31080	AT5G51190	AT5G51190
AT1G32130	FW1	AT2G22300	CAM1A1/5A3	AT3G20640	AT3G20640	AT4G31420	AT4G31420	AT5G51230	EMF2
AT1G32150	hnp58	AT2G22430	AT2G22430	AT3G20670	hTA13	AT4G32150	WRRY13	AT5G51780	AT5G51780
AT1G32240	KAN2	AT2G22540	SVP	AT3G20770	U303	AT4G32180	SAG22	AT5G51790	AT5G51790
AT1G32330	ATWRRY3D	AT2G22630	AGL17	AT3G20800	AT3G20800	AT4G32610	AT4G32610	AT5G51860	AGL72
AT1G32360	AT5G32360	AT2G22670	AGL18	AT3G20810	IMY80/IMY85	AT4G32615	AT4G32615	AT5G51870	AGL71
AT1G32510	ANAC011	AT2G22740	SGS2/SGH46	AT3G20840	PL71	AT4G32620	AT4G32620	AT5G51910	AT5G51910
AT1G32540	LCK1	AT2G22750	AT2G22750	AT3G20910	NP-18	AT4G32660	AT4G32660	AT5G51980	AT5G51980
AT1G32640	ATMYC2	AT2G22760	AT2G22760	AT3G21150	ABR032/UP4	AT4G32680	AT4G32680	AT5G51990	CRF4
AT1G32700	AT5G32700	AT2G22770	NA1	AT3G21175	ZM1	AT4G32690	AT4G32690	AT5G52010	AT5G52010
AT1G32770	ANAC012/MS1	AT2G22800	HA79	AT3G21270	ADOF2	AT4G32710	AT4G32710	AT5G52020	AT5G52020
AT1G32810	AT5G32810	AT2G22840	AsMY81	AT3G21330	AT3G21330	AT4G32730	ARR10	AT5G52170	HOG7
AT1G32870	ANAC13	AT2G22850	AsMY86	AT3G21350	MD06	AT4G32810	hSL1	AT5G52230	MD03
AT1G33060	ANAC014	AT2G22900	AT2G22900	AT3G21430	AT4Y3	AT4G32840	KNA75	AT5G52260	AsMY81
AT1G33240	AT-GT1	AT2G23060	AT2G23060	AT3G21880	RR033	AT4G32780	UA29	AT5G52510	SC18
AT1G33280	ANAC015/BN1	AT2G23290	AsMY87	AT3G21890	AT3G21890	AT4G32790	TYR8	AT5G52600	AsMY82
AT1G33760	AT5G33760	AT2G23320	WRRY15	AT3G21900	AT3G21900	AT4G32730	AT4G32730	AT5G52660	AT5G52660
AT1G34170	ARF13	AT2G23340	DEAR3	AT3G22170	CP04G/THY3	AT4G32800	AT4G32800	AT5G52830	ATWRRY27
AT1G34180	anac005	AT2G23380	CLY/COU/SG1	AT3G22560	AT3G22560	AT4G32880	AT4G32880	AT5G53040	AT5G53040
AT1G34190	anac017	AT2G23660	LD03	AT3G22760	SOL1	AT4G32890	GAT38	AT5G53200	TRY
AT1G34310	ARF12	AT2G23760	BUH4	AT3G22830	AT-HSP468	AT4G32980	AT4G32980	AT5G53210	SPCH
AT1G34370	STOP1	AT2G24260	UL1	AT3G23030	UA2	AT4G33280	AT4G33280	AT5G53290	CRF3
AT1G34390	ARF22	AT2G24430	ANAC008	AT3G23050	UA3	AT4G33450	AT4G33450	AT5G53420	AT5G53420
AT1G34470	AsMY89	AT2G24500	F2F	AT3G23130	FLO10	AT4G33880	RS2	AT5G53430	AT5G53430
AT1G35240	ARF20	AT2G24570	WRRY17	AT3G23140	URO	AT4G34000	ABF3	AT5G53660	AsMY87
AT1G35460	IRH5	AT2G24590	As-AS22a	AT3G23150	CTR2	AT4G34290	AT4G34290	AT5G53950	CLC2
AT1G35490	AT5G35490	AT2G24790	COL3	AT3G23210	hSLH34	AT4G34400	AT4G34400	AT5G53980	ATWRRY2
AT1G35515	HOG10/MyB8	AT2G25000	ATWRRY60	AT3G23220	ISE1	AT4G34410	RRF11	AT5G54067	AT5G54067
AT1G35540	ARF14	AT2G25180	ARR12	AT3G23230	AsMY88	AT4G34430	AT4G34430	AT5G54070	AT-HSP48
AT1G35560	AT5G35560	AT2G25620	AsMY81	AT3G23240	IRF1	AT4G34530	CR1	AT5G54230	MYB48
AT1G36060	AT5G36060	AT2G25630	AT2G25630	AT3G23250	MYB15	AT4G34590	AsMY81/UGF6	AT5G54360	AT5G54360
AT1G42990	AT2G2990	AT2G25820	ISE2	AT3G23690	AT3G23690	AT4G34630	BUH6	AT5G54470	AT5G54470
AT1G43000	AT5G43000	AT2G25900	AT2G25900	AT3G24010	AT3G24010	AT4G34680	GAT33	AT5G54630	AT5G54630
AT1G43160	RAP2.6	AT2G26150	AT-HSP42	AT3G24050	GATA1	AT4G34990	AsMY82	AT5G54640	AT-HSP42
AT1G43700	VSP1	AT2G26580	YAB5	AT3G24120	AT3G24120	AT4G35040	BZF19	AT5G54680	CR3
AT1G43770	AT5G43770	AT2G26940	AT2G26940	AT3G24140	FMA	AT4G35270	NLP2	AT5G54930	AT5G54930
AT1G43860	AT5G43860	AT2G26960	AsMY88	AT3G24310	MYB105	AT4G35280	GAZ2	AT5G55690	AT5G55690
AT1G43950	ARF23	AT2G27050	EL1	AT3G24490	AT3G24490	AT4G35550	HB-4	AT5G56110	AsMY83
AT1G44810	AT5G44810	AT2G27100	SE	AT3G24500	AT4MYB3C	AT4G35570	HMGR5/NF15	AT5G56200	AT5G56200
AT1G44830	AT5G44830	AT2G27110	FBS3	AT3G24520	AT-HSP43	AT4G35580	CRNAC/NT13	AT5G56270	WRRY2
AT1G45249	ARF2	AT2G27220	BUH5	AT3G24650	AsMY81	AT4G35610	AT4G35610	AT5G56780	AT1T2
AT1G46480	WDR4	AT2G27230	UHW	AT3G24820	AT3G24820	AT4G35700	GA2	AT5G56880	AT5G56880
AT1G46768	RAP2.1	AT2G27300	ANAC040	AT3G24860	AT3G24860	AT4G35900	FDZ	AT5G56860	GNC
AT1G47270	AsMY86	AT2G27470	NF-YB13	AT3G25710	hSLH12	AT4G36020	AsMY81/CSG1	AT5G56900	AT5G56900
AT1G47655	AT5G47655	AT2G27580	AT2G27580	AT3G25730	EDF3	AT4G36060	hSLH11	AT5G56930	EMR1789
AT1G47760	AGL502	AT2G27760	ATWRRY97	AT3G25790	AT3G25790	AT4G36160	ANAC076	AT5G57180	CA2
AT1G47870	AT2F22	AT2G27930	AT2G27930	AT3G25890	CRF11	AT4G36240	GAT37	AT5G57390	AsMY83
AT1G48000	MYB12	AT2G27990	BUH9/PH	AT3G25990	AT3G25990	AT4G36260	SR52/STY2	AT5G57990	PLT5
AT1G48040	AT5G48040	AT2G28160	AT-HSP29	AT3G26620	UBQ23	AT4G36540	BE2	AT5G57420	UA33
AT1G48350	AT5G48350	AT2G28200	AT2G28200	AT3G26744	ICE1	AT4G36570	AT4G36570	AT5G57520	AT2F22
AT1G48395	AT5G48395	AT2G28350	ARF30	AT3G26790	FUS3	AT4G36590	AT4G36590	AT5G57620	MYB36
AT1G48310	CHAL1/CH18	AT2G28450	AT2G28450	AT3G27010	AT-TCF20	AT4G36620	GATA19	AT5G57660	AT2F25
AT1G48500	AsMY82/THY5A	AT2G28500	LD01	AT3G27650	UBQ25	AT4G36710	AT4G36710	AT5G58010	ULR3



AT1G49010	AT5G49000	AT2G28510	AT2G28510	AT3G27785	ATMYB118	AT4G31670	GBF1	AT5G58080	ARR38
AT1G49120	CRP9	AT2G28550	RAP2.7	AT3G27810	ATMYB21	AT4G31670	HB-5	AT5G58140	AT5G58140
AT1G49130	BBP17	AT2G28610	PR5, WOX3	AT3G27920	ATGL1/ATMYB0	AT4G31780	BEH2	AT5G58360	ATOPF3
AT1G49475	AT5G49475	AT2G28710	AT2G28710	AT3G27940	LR026	AT4G31880	AT4G31880	AT5G58620	TDF9
AT1G49480	KTV1	AT2G28810	AT2G28810	AT3G28730	ATHMG/WFD	AT4G31670	BLH2	AT5G58850	ATMYB119
AT1G49520	AT5G49520	AT2G28910	COP4	AT3G28810	PR5	AT4G31690	RAP2.30	AT5G58890	AGL82
AT1G49560	AT5G49560	AT2G28930	AT2G28930	AT3G28910	MYB30	AT4G31690	AP2	AT5G58900	AT5G58900
AT1G49720	ANF1	AT2G29060	AT2G29060	AT3G28917	MY2	AT4G31690	SPT	AT5G59140	WOX2
AT1G49830	AT5G49830	AT2G29580	MACS8	AT3G28920	AsH34	AT4G31690	AT4G31690	AT5G59180	ATM806
AT1G49950	TRB1	AT2G29660	AT2G29660	AT3G29015	ATNAC3	AT4G31710	AT4G31710	AT5G59430	ATTRP1
AT1G50410	AT5G50410	AT2G30130	AS5.1/BO12	AT3G30210	ATMYB121	AT4G31720	MYB73	AT5G59450	AT5G59450
AT1G50420	SC3	AT2G30250	WRKY5	AT3G30260	AGL79	AT4G31750	LR039	AT5G59570	BOA
AT1G50600	SC5	AT2G30340	LR039	AT3G30350	AT2G2942	AT4G31750	COP1/HLS1	AT5G59780	MYB93
AT1G50640	ERF3	AT2G30400	ATOPF2	AT3G30420	AL3	AT4G31760	BT5	AT5G59800	ATM807
AT1G50670	AT5G50670	AT2G30420	ETC2	AT3G30460	AT3G30460	AT4G31760	SHR	AT5G59820	RH41
AT1G50680	AT5G50680	AT2G30424	TCL2	AT3G30420	AT3G30420	AT4G31760	NAO52	AT5G59990	AT5G59990
AT1G50680	HTA30	AT2G30432	TCL1	AT3G30430	AT3G30430	AT4G31770	Atb2P7	AT5G60120	APR83
AT1G50730	BH4H15	AT2G30470	H52/VALL	AT3G30440	JA211/TFYJA	AT4G31770	Atb2P2	AT5G60120	TCE2
AT1G51120	AT5G51120	AT2G30580	BM1A/DRP2	AT3G30450	NAC061	AT4G31770	ANT	AT5G60130	AT5G60130
AT1G51140	AT5G51140	AT2G30590	WRKY21	AT3G30460	Atb2P57	AT4G31770	ATMYB87	AT5G60140	AT5G60140
AT1G51290	PLT2	AT2G31070	TPC10	AT3G30470	HO2A	AT4G31770	Atb2P2	AT5G60142	AT5G60142
AT1G51290	AT5G51290	AT2G31180	ATMYB14	AT3G30475	AT3G30475	AT4G31780	AT4G31780	AT5G60200	TM06
AT1G51220	Atb2P5	AT2G31210	AT2G31210	AT3G30510	TCF16	AT4G31790	AGL25	AT5G60440	AGL82
AT1G51600	ZML2	AT2G31220	AT2G31220	AT3G30510	GA7A14	AT4G31800	DOF4.7	AT5G60440	Atb2P2
AT1G51700	Atb2P1	AT2G31230	AT2G31230	AT3G30520	AT3G30520	AT4G31810	Atb2P1	AT5G60480	Atb2P2/DOF2
AT1G51950	UAA18	AT2G31280	CPUC077	AT3G30560	AT3G30560	AT4G31810	FR55	AT5G60600	REV
AT1G51970	AT5G51970	AT2G31310	LR034	AT3G30580	AT3G30580	AT4G31810	FR55	AT5G60850	OBP4
AT1G52250	ATb2P15	AT2G31370	AT2G31370	AT3G30600	AT3G30600	AT4G31820	ATMYB84	AT5G60880	ATMYB34
AT1G52880	UAA6	AT2G31380	Atb2P5/TFY	AT3G30600	ZAT7	AT4G31860	ATCSP2/WRP2	AT5G60910	AGL8
AT1G52880	NAM	AT2G31460	AT2G31460	AT3G30610	ATMYB48	AT4G31890	AT4G31890	AT5G60910	FUA
AT1G52890	ANAC019	AT2G31550	ATCQ/DOF27	AT3G30610	ATMYB48	AT4G31890	BP5	AT5G60910	TCPS
AT1G53160	SP4	AT2G31720	AT2G31720	AT3G30690	AT3G30690	AT4G31890	AT4G31890	AT5G61270	PP7
AT1G53170	ATb2P8	AT2G31730	AT2G31730	AT3G30690	AT3G30690	AT4G31900	AT4G31900	AT5G61380	TDC1
AT1G53230	TOP3	AT2G32020	AT2G32020	AT3G30660	UUR/PC1	AT4G31910	SHL1	AT5G61420	MYB28
AT1G53320	Atb2P7	AT2G32030	AT2G32030	AT3G30710	AT3G30710	AT4G31910	AT4G31910	AT5G61430	ANAC300
AT1G53810	RAP2.32	AT2G32100	ATOPF5	AT3G30750	CDH3	AT4G31920	ATb2P5/TFY	AT5G61470	AT5G61470
AT1G54080	ASL1	AT2G32250	FR52	AT3G30760	ATMYB94	AT4G31940	ATb2P5/TFY	AT5G61590	AT5G61590
AT1G54140	TFY/TFY21	AT2G32460	ATMYB101	AT3G30760	Atb2P14	AT4G31940	ATb2P5/TFY	AT5G61620	ERF104
AT1G54160	NPYK1	AT2G32550	AT2G32550	AT3G30760	PYE	AT4G30060	Atb2P16	AT5G61620	AT5G61620
AT1G54330	ANAC020	AT2G32600	AT2G32600	AT3G30770	BHLH181/BNQ2	AT5G01160	AT5G01160	AT5G61890	LFY
AT1G54360	ATb2P8	AT2G32700	UUR	AT3G30780	Atb2P14/DOF27	AT5G01200	AT5G01200	AT5G61890	AT5G61890
AT1G54390	IMG2	AT2G32905	AT2G32905	AT3G30810	ARR5/WRK6	AT5G01380	AT5G01380	AT5G62000	APF2
AT1G54690	H2A9B/HTA3	AT2G32930	ZNF2	AT3G30810	DEL1/CTF2	AT5G01380	AT5G01380	AT5G62000	APF2
AT1G54760	AGL85	AT2G32960	AT2G32960	AT3G30860	ATb2P2	AT5G01380	AT5G01380	AT5G62000	APF2
AT1G54830	NP-PC3	AT2G33110	UAA13	AT3G30860	ATb2P2	AT5G01380	AT5G01380	AT5G62000	APF2
AT1G55110	Atb2P7	AT2G33150	AT2G33150	AT3G30860	NP-PC1	AT5G01380	AT5G01380	AT5G62000	APF2
AT1G55460	AT5G55460	AT2G33480	ANAC041	AT3G30860	AT3G30860	AT5G01380	AT5G01380	AT5G62000	APF2
AT1G55520	ATb2P2	AT2G33500	BBX23	AT3G30860	Atb2P2	AT5G01380	AT5G01380	AT5G62000	APF2
AT1G55580	LAS	AT2G33550	AT2G33550	AT3G30860	ANAC062	AT5G01380	AT5G01380	AT5G62000	APF2
AT1G55600	ATb2P5/TFY	AT2G33610	ATb2P5/TFY	AT3G30860	RAX3	AT5G01380	AT5G01380	AT5G62000	APF2
AT1G55650	AT5G55650	AT2G33710	AT2G33710	AT3G30860	Atb2P5	AT5G01380	AT5G01380	AT5G62000	APF2
AT1G55750	AT5G55750	AT2G33720	AT2G33720	AT3G30860	AT3G30860	AT5G01380	AT5G01380	AT5G62000	APF2
AT1G55760	AT5G55760	AT2G33810	SP13	AT3G30860	ATb2P2	AT5G01380	AT5G01380	AT5G62000	APF2
AT1G55950	AT5G55950	AT2G33835	FE3	AT3G30860	ATb2P2	AT5G01380	AT5G01380	AT5G62000	APF2
AT1G56010	NAC1	AT2G33860	ETT	AT3G30860	LR038	AT5G01380	AT5G01380	AT5G62000	APF2
AT1G56160	ATMYB72	AT2G33880	WOK9	AT3G30860	AT3G30860	AT5G01380	AT5G01380	AT5G62000	APF2
AT1G56170	HAP58	AT2G34140	AT2G34140	AT3G30860	MYB77	AT5G01380	AT5G01380	AT5G62000	APF2
AT1G56650	ATMYB75/TFY	AT2G34440	AGL29	AT3G30860	CT15	AT5G01380	AT5G01380	AT5G62000	APF2
AT1G57560	Atb2P5	AT2G34450	AT2G34450	AT3G30860	HEC2	AT5G01380	AT5G01380	AT5G62000	APF2
AT1G58100	AT5G58100	AT2G34600	JA21/TFY58	AT3G30860	OMP1	AT5G01380	AT5G01380	AT5G62000	APF2
AT1G58110	AT5G58110	AT2G34620	AT2G34620	AT3G30860	LR038	AT5G01380	AT5G01380	AT5G62000	APF2
AT1G58220	AT5G58220	AT2G34710	PH8	AT3G30860	AT3G30860	AT5G01380	AT5G01380	AT5G62000	APF2
AT1G59530	ATb2P4	AT2G34720	NP-RR4	AT3G30860	Atb2P2	AT5G01380	AT5G01380	AT5G62000	APF2
AT1G59640	ZCWS3	AT2G34830	Atb2P5/TFY	AT3G30860	BEH1	AT5G01380	AT5G01380	AT5G62000	APF2
AT1G59750	ARF1	AT2G35000	ATb2P5	AT3G30860	HAN/MNP	AT5G01380	AT5G01380	AT5G62000	APF2
AT1G59810	AGL50	AT2G35160	SGO9/TFY5	AT3G30860	Atb2P2/DOF27	AT5G01380	AT5G01380	AT5G62000	APF2
AT1G59890	SN3	AT2G35310	AT2G35310	AT3G30860	AGL7Y/TFY5	AT5G01380	AT5G01380	AT5G62000	APF2
AT1G59940	ARR3	AT2G35430	AT2G35430	AT3G30860	GA7A6	AT5G01380	AT5G01380	AT5G62000	APF2
AT1G60040	AGL49	AT2G35530	SGO9/TFY	AT3G30860	ATb2P5	AT5G01380	AT5G01380	AT5G62000	APF2
AT1G60240	AT5G60240	AT2G35550	ATb2P2/TFY	AT3G30860	ATb2P5	AT5G01380	AT5G01380	AT5G62000	APF2
AT1G60260	RRK26	AT2G35605	AT2G35605	AT3G30860	Atb2P5/TFY	AT5G01380	AT5G01380	AT5G62000	APF2
AT1G60350	NAC024	AT2G35700	ATb2P5	AT3G30860	ATb2P5	AT5G01380	AT5G01380	AT5G62000	APF2
AT1G60380	AT5G60380	AT2G35910	AT2G35910	AT3G30860	ATb2P5	AT5G01380	AT5G01380	AT5G62000	APF2
AT1G60700	AT5G60700	AT2G35940	BOH5	AT3G30860	ATb2P24	AT5G01380	AT5G01380	AT5G62000	APF2
AT1G60880	AGL56	AT2G36000	EMH3134	AT3G30860	ATb2P24	AT5G01380	AT5G01380	AT5G62000	APF2
AT1G60920	AGL55	AT2G36010	ETP3	AT3G30860	ATb2P24	AT5G01380	AT5G01380	AT5G62000	APF2

# A Yeast One Hybrid screen for candidate regulators of vascular identity

AT1G61660	AT5G61660	AT2G16036	AT2G16036	AT3G52525	ATCFP6	AT5G06160	ATD	AT5G65670	IAA9
AT1G61730	AT5G61730	AT2G16050	ATCFP15	AT3G52540	ATCFP18	AT5G06250	EPH4	AT5G65790	ATMYB88
AT1G61970	AT5G61970	AT2G16080	AT2G16080	AT3G52910	AGRF4	AT5G06430	AT5G06430	AT5G65910	AT5G65910
AT1G61980	AT5G61980	AT2G16270	AB5	AT3G53200	AIMYB27	AT5G06500	AGL96	AT5G66160	ATRMH1
AT1G61990	AT5G61990	AT2G16340	AT2G16340	AT3G53310	AT3G53310	AT5G06550	JM122	AT5G66270	AT5G66270
AT1G62010	AT5G62010	AT2G16400	AGRF3	AT3G53340	NP-YB10	AT5G06650	G52	AT5G66300	ANAC305
AT1G62085	AT5G62085	AT2G16720	AT2G16720	AT3G53370	AT3G53370	AT5G06710	HA154	AT5G66320	GATA5
AT1G62110	AT5G62110	AT2G16740	AT5WIC2	AT3G53440	AT3G53440	AT5G06770	AT5G06770	AT5G66350	SH
AT1G62120	AT5G62120	AT2G16890	ATMYB18/WT1	AT3G53600	AT3G53600	AT5G06800	AT5G06800	AT5G66630	DAR5
AT1G62130	AT5G62130	AT2G16930	AT2G16930	AT3G53680	AT3G53680	AT5G06839	TGA50	AT5G66700	AT1H53/PH8-8
AT1G62300	WRKY6	AT2G16960	TRO1	AT3G53820	AT3G53820	AT5G06950	AHRP-18	AT5G66730	AT5G66730
AT1G62310	AT5G62310	AT2G16990	AT5G6656G	AT3G53920	SG3/SGC	AT5G06960	OMF5	AT5G66750	ATDMM1/CH43
AT1G62360	STN4	AT2G17000	AT2G17000	AT3G54220	SCR	AT5G07100	WRKY26	AT5G66770	AT5G66770
AT1G62700	VND5	AT2G17060	NP-YB8	AT3G54320	ASML1/ATMYB1	AT5G07310	EPF115	AT5G66870	ASL1/ABD36
AT1G62830	ATL5D5	AT2G17120	AT2G17120	AT3G54340	AP5	AT5G07400	AT5G07400	AT5G66940	AT5G66940
AT1G62975	AT5G62975	AT2G17260	ATWRKY44	AT3G54350	em61967	AT5G07500	AT2F6/PE11	AT5G66980	AT5G66980
AT1G62990	KNA77	AT2G17430	AT2G17430	AT3G54390	AT3G54390	AT5G07580	AT5G07580	AT5G67000	AT5G67000
AT1G63030	dH2	AT2G17520	AT2G17520	AT3G54430	SR56	AT5G07680	ANAC080	AT5G67060	HBC1
AT1G63040	AT5G63040	AT2G17590	ATDGF2.4	AT3G54610	BGT/PCN5	AT5G07690	MYB29	AT5G67110	AuC
AT1G63100	AT5G63100	AT2G17630	ATPHAN	AT3G54620	ATB2F25	AT5G07700	MYB76	AT5G67180	TOE3
AT1G63170	AT5G63170	AT2G17740	AT2F920	AT3G54810	BME3-2F	AT5G07900	AT5G07900	AT5G67190	DEAR2
AT1G63490	AT5G63490	AT2G18090	AT2G18090	AT3G54990	SAZ	AT5G08070	TCP17	AT5G67300	ATMYB83
AT1G63650	ATMYC-2	AT2G18130	ATMAK3	AT3G55080	AT3G55080	AT5G08130	BIM1	AT5G67415	AT5G67415
AT1G63820	AT5G63820	AT2G18250	AT2G18250	AT3G55210	NAC063	AT5G08190	NP-YB12	AT5G67420	BD37
AT1G63840	AT5G63840	AT2G18300	AT2G18300	AT3G55370	OMF9	AT5G08330	ATTCP11	AT5G67430	AT5G67430
AT1G63910	ATMYB035	AT2G18340	SHB39	AT3G55530	ACSDH1	AT5G08520	AT5G08520	AT5G67450	AZF1
AT1G64000	ATWRKY56	AT2G18470	WRKY33	AT3G55730	MYB109	AT5G08630	AT5G08630	AT5G67480	ATB4
AT1G64105	ANAC027	AT2G18880	ATNF-YB1	AT3G55770	WUM2b	AT5G08790	anac083/ATAF2	AT5G67580	TRB2
AT1G64380	AT5G64380	AT2G18950	AT2G18950	AT3G55980	AT5Z91	AT5G09240	AT5G09240		
AT1G64530	AT5G64530	AT2G19000	AT2G19000	AT3G56130	AT3G56130	AT5G09250	KW1		
AT1G64620	AT5G64620	AT2G19020	NATA2	AT3G56380	ARR17	AT5G09330	anac082		
AT1G64625	AT5G64625	AT2G19030	NATA1	AT3G56400	WRKY70	AT5G09430	CAMTA1		

**Supplementary Information: Scoring algorithm for node scoring**

Ranking of nodes  
All awarded points

Outdegree

14+ = +4

12+ = +3

9+ = +2

6+ = +1

DAPseq

in DAPseq = +4

high BS = -2 ( $>10000$ )

EMB

4 sets: 8-cell, 16-cell EMB, 16-cell nEMB, EG Q

per set:

top10% = -1

top40% = +1

total score = sum from 3 stages (average 16-cell)

INTACT

3 sets: ILT, EG, LG

more than 2 fold up vasc/inner cells = +2

more than 1.5 fold up vasc/inner cells = +1

more than 2 fold down vasc/inner cells = -1

total score = sum from 3 stages

VASC

2 sets: Kondo and Brady

Kondo

more than 2 fold up = +2

more than 1.5 fold up = +1

Brady, subsets for phloem, xylem, stele

top10% = +2

top30% = +1

bottom10% = -1 (only for stele)

total score = sum from each tissue (averages for phloem and xylem)

Binding

A: binding to ERF4/WOL (wider pattern) = +1 each

B: not binding to T5L1 or TMO6 = +1

C: not binding to TMO5 or ZLL = +1

D: not binding to WRK or GATA or SOK or MIR = +2

E: not binding to MSS or EPM or ERF or ATHB or SHR = +2

F: not binding to MP targets = +1

G: not binding to inverted pattern = +1

total score = sum of all categories

Total score

Create 4 rankings to prevent strong bias

A = sum of all – binding/2

B = EMB and INTACT only

C = VASC only

D = outdegree – binding/1,5

Use average position of 4 rankings for selection

**Supplementary table 2: Ranking of and scores awarded to the 50 initially selected transcription factors.** Final results of the 4 scoring totals and average total ranking. \* HTA2 and ESE3 were excluded.

IGGid	TF name	Score all	Rank all	Score embryo	Rank embryo	Score vascular	Rank vascular	Score pattern	Rank pattern	Average rank
AT1G75390	BZIP44	13.0	1	6.0	1	6.0	2	1.0	17	5.3
AT5G19790	RAP2.11	9.5	6	1.0	21	2.0	5	3.5	1	8.3
AT2G36340	GLP3	12.0	3	6.0	1	0.0	26	3.0	5	8.8
AT2G37520	AT2G37520	8.5	9	3.0	7	2.0	6	1.5	14	8.8
AT2G21240	BPC4	9.0	8	3.0	7	3.0	4	1.0	17	9.0
AT3G51680	AT3G51680	10.0	5	5.0	3	0.0	26	3.0	5	9.8
AT2G45420	LOB18	11.0	3	2.0	14	1.5	10	1.5	14	10.3
AT4G34590	BZIP11	12.0	2	3.0	21	6.5	1	0.5	23	11.5
AT4G00270	GBF8	9.5	6	5.0	3	-1.0	41	3.5	1	12.6
AT4G00250	STKL2	8.5	9	1.5	19	0.0	26	3.5	1	13.8
AT4G36730	GBF1	7.0	12	4.0	5	2.0	5	-1.0	34	14.0
AT2G37260	WRKY44	6.0	15	3.0	7	1.0	13	0.0	29	16.0
AT5G61590	DEWAX	5.7	18	3.0	7	0.7	23	1.0	17	16.3
AT4G01120	GBF2	11.0	11	3.0	7	-0.5	40	2.5	8	16.5
AT4G00238	STKL1	5.0	21	1.0	21	0.5	24	2.5	8	18.5
AT3G12730	AT3G12730	5.5	19	1.0	21	1.0	13	0.5	22	18.8
AT1G54060	ASL1	5.8	17	3.0	7	1.1	11	-1.5	44	19.8
AT4G31615	REM35	4.5	23	0.5	31	0.0	26	3.5	1	20.3
AT4G03250	AT4G03250	4.0	25	1.5	19	0.0	26	2.0	13	20.8
AT5G53950	CUC2	3.5	28	1.0	21	1.0	13	0.5	22	21.0
AT2G01370	AT2G01370	4.5	23	2.0	14	0.0	26	0.5	22	21.3
AT1G76420	CUC3	6.0	15	0.0	34	0.0	26	2.0	13	22.0
AT1G62120	AT1G62120	3.0	29	1.0	21	0.0	26	1.0	17	23.1
AT2G36270	AB5	5.0	21	2.0	14	0.0	26	-1.0	34	23.8
AT4G00390	AT4G00390	1.0	38	-2.5	48	2.0	5	3.0	5	24.0
AT4G00210	LOB31	2.5	31	1.0	21	0.0	26	0.5	22	25.0
AT5G06960	DBF5	2.0	33	1.0	21	1.0	13	-1.0	34	25.3
AT5G05550	AT5G05550	5.5	19	0.0	34	-1.0	41	2.5	8	25.5
AT1G14687	ATHB32	4.0	25	0.5	31	1.0	13	-1.0	34	25.8
AT1G55650	AT1G55650	1.5	35	0.0	34	0.0	26	1.5	14	27.3
AT1G66420	AT1G66420	-0.5	42	-2.5	48	1.0	13	2.5	8	27.8
AT2G30470	HSF2	3.0	29	3.5	9	0.0	26	-3.0	50	27.8
AT5G25470	AT5G25470	2.5	31	2.5	13	-1.0	41	-0.5	30	28.8
AT1G65620	AS2	1.5	35	1.0	21	-1.0	41	0.5	22	29.8
AT3G25730	EDF3	0.3	40	0.0	34	1.3	11	-1.0	34	29.8
AT3G61970	NGA2	1.5	35	2.0	14	-1.0	41	-0.5	30	30.0
AT3G28920	ATHB34	4.0	25	0.5	31	0.5	24	-1.5	44	31.0
AT5G51990	CBF4	2.0	33	1.0	21	-1.0	41	-1.0	34	32.3
AT3G13350	AT3G13350	-0.5	42	0.0	34	0.0	26	-0.5	30	33.0
AT5G44210	ERF9	0.3	40	0.0	34	-0.2	39	0.5	22	33.8
AT1G05230	HDG2	-1.0	44	0.0	34	1.0	13	-2.0	48	34.8
AT1G12980	DRN	-0.0	47	-1.5	47	1.0	13	-1.0	34	35.3
AT5G06250	DPA4	-1.5	45	0.0	34	1.0	13	-2.5	49	35.3
AT5G19760	ATHB73	1.0	38	-1.0	45	1.0	13	-2.0	48	36.0
AT4G33280	AT4G33280	-1.5	45	0.0	34	-1.0	41	-0.5	30	37.5
AT3G61830	ARF18	-4.0	48	0.0	34	-1.0	41	-1.0	34	39.3
AT1G50680	AT1G50680	-4.0	48	-1.0	45	-1.0	41	-1.0	34	42.0
AT4G04890	PDF2	-9.5	50	-4.0	50	-1.0	41	-1.5	44	46.3

**Supplementary table 3: Ranking of and scores awarded to the 50 initially selected transcription factors.** Scores awarded based on binding pattern. Includes data on outdegree and binding pattern from the network and DAPseq data from O'Mally. \* HTA2 and ESE3 were excluded.

Locus	TF name	Outdeg	Score	DAPseq	BS_Count	Score	A	B	C	D	E	F	G	H	I	Binding score
AT1G75390	bZIP44	10	2		2679		1	1								2
AT5G19790	RAV2.11	14	4	Y	13538	2	1									1
AT2G36340	GLP3	12	3													0
AT2G37520	AT2G37520	10	2					1								1
AT2G21240	BPC4	10	2				2									2
AT3G53680	AT3G53680	14	4				2									2
AT2G45420	LBD18	9	2	Y	5578	4	1									1
AT4G34590	bZIP11	7	1	Y	9894	4	1									1
AT4G00270	GE8P	14	4				1									1
AT4G00250	STKL3	14	4	Y	11654	2	1									1
AT4G36730	GRF1	5								2						2
AT2G37260	WRKY44	8	1				1	1								2
AT5G61590	DEWAX	6	1													0
AT4G01120	GBF2	12	3				1									1
AT4G00190	GLC3	5	1													1
AT4G00238	STKL1	13	3				1									1
AT3G12730	AT3G12730	7	1	Y	10750	2	1									1
AT1G54060	ASL1	4						1			2					3
AT4G31615	REM35	14	4				1									1
AT4G03250	AT4G03250	11	2													0
AT5G53950	CUC2	6	1		2465										1	1
AT2G01370	AT2G01370	8	1					1								1
AT1G75420	CUC3	11	2	Y	5385	4										0
AT1G62120	AT1G62120	9	2				1	1								2
AT2G36270	AB15	4		Y	4178	4	1	1								2
AT4G00390	AT4G00390	16	4				2									2
AT4G00210	LBD11	7	1						1							1
AT5G05960	QBF5	4			2604						2					2
AT5G05550	AT5G05550	13	3	Y	8441	4	1									1
AT1G14687	ATHB32	4		Y	21104	2	1	1								2
AT1G55650	AT1G55650	11	2				1									1
AT1G66420	AT1G66420	13	3				1									1
AT2G30470	HS12	5					1	1	1	2				1		6
AT5G25470	AT5G25470	7	1				1	1						1		3
AT1G66620	AS2	9	2				2	1								3
AT3G25730	EDF3	4								2						2
AT3G61970	NGA1	4						1								1
AT3G28920	ATHB34	4		Y	7200	4	1			2						3
AT5G51990	CBF4	4		Y	10898	2					2					2
AT3G13350	AT3G13350	6	1				1	1						1		3
AT5G44210	ERF9	7	1				1									1
AT1G05710	HOG3	4					1	1	1					1		4
AT1G12980	DRN	4									1					2
AT5G06250	DPA4	5					1	1	1	2						5
AT5G39760	ATHB23	4		Y		4	1	1		2						4
AT4G33280	AT4G33280	7	1				1	1						1		3
AT3G61830	ARF1A	5									1					2
AT1G50680	AT1G50680	5								2						2
AT4G04890	PDF2	4			2150			1			2					3



**Supplementary table 4: Ranking of and scores awarded to the 50 initially selected transcription factors.** Scores awarded based on embryo expression. Includes expression percentile data on embryo expression levels of whole WT embryos (Weijers lab) and fold changes from the embryo expression atlas (Palovaara). \* HTA2 and ESE3 were excluded.

Spot	TF name	Rank 16cH EMV		Rank 16cH nEMV		Rank 16cH B-cell		Rank 16cH D990		Total EMVH1 Score	FC H1P 16cH	FC VSC H1	FC VSC AG	Total INFAC3 score		
AT1G75190	WDF44	0.92	-1	0.95	-1	0.60	1	0.21		0	2.50	2	2.22	2	2	0
AT5G19790	RAF2.11	0.52		0.32		0.38		0.79	1	1	3.20		-1.66		-1.38	0
AT2G36340	GAP5	0.90	-1	0.60		0.82	1	0.77	1	2	-1.01	3.48	2	2.45	2	4
AT2G37520	AT2G37520	0.58		0.56		0.63	1	0.88	1	2	1.10	1.61	1	1.11	1	1
AT2G21240	BPC4	0.78	1	0.83	1	0.74	1	0.65		2	1.54	1	1.43	1	1.23	1
AT2G53680	AT2G53680	0.80	1	0.83	1	0.87	1	0.53		2	-1.18	2.28	2	1.77	1	2
AT2G45420	IRD38	0.18		0.12		0.04	1	0.80	1	1	-1.56		-1.05		1.13	0
AT4G34590	SDF11	0.90	-1	1.00	-1	0.72	1	0.37		0	1.29	1.06		1.90	1	1
AT4G00170	GRRP	0.86	1	0.65	1	0.69	1	0.22		2	1.03	2.24	2	1.28	1	1
AT4G00050	SRK2	0.82	1	0.18		0.76	1	0.52		1.5	1.27	1.03		-1.41		0
AT4G36750	GRR1	0.80	1	0.82	1	0.61	1	0.39		2	0.67	2.56	2	1.18	2	2
AT2G37200	WRKY64	0.75	1	0.86	1	0.41		0.69	1	2	1.55	1	-1.21	-1.45	1	1
AT5G61590	DFWAX	0.41		0.27		0.21		0.87	1	1	-1.25	2.68	1	1.05		2
AT4G01120	GRR2	0.54	1	0.67	1	0.67	1	0.81	1	1	1.14	-1.28		-1.25		0
AT4G00158	SRK1	0.89	1	0.83	1	0.83	1	0.95	1	1	-1.51	1.15		-1.14		0
AT3G12730	AT3G12730	0.24		0.30		0.11		0.84	1	1	1.00	1.01		1.10		0
AT1G54060	ASL1	0.73	1	0.77	1	0.70	1	0.71	1	1	1.17	-1.13		1.08		0
AT4G38615	HEM35	0.85	1	0.46		0.91		0.35		0.5	-1.83	1.17		-1.48		0
AT4G01250	AT4G01250	0.62	1	0.50		0.51		0.57		0.5	1.55	1	1.18	-1.20	-1.20	1
AT5G51950	CUC2	0.18		0.16		0.13		0.81	1	1	-1.12	-1.18		1.01		0
AT2G01370	AT2G01370	0.46		0.25		0.80	1	0.80	1	2	-1.13	1.18		-1.18		0
AT1G76470	CUC3	0.53		0.47		0.43		0.50		0	-1.58	1.06		-1.09		0
AT1G61120	AT1G61120	0.44		0.38		0.44		0.68	1	1	1.10	1.13		1.14		0
AT2G36170	ARE5	0.66	1	0.65	1	0.44		0.94	-1	0	1.78	2	1.08	-1.11	2	2
AT4G00390	AT4G00390	0.98	-1	0.30		0.98	-1	0.44		-1.5	-4.32	-1	-1.04	-1.01	-1	-1
AT4G00110	IRD31	0.61	1	0.68	1	0.92	1	0.79	1	1	1.25	-1.05		-1.07		0
AT5G06960	GRR5	0.62	1	0.60	1	0.53		0.28		1	1.03	1.07		1.14		0
AT5G06150	AT5G06150	0.57		0.25		0.59		0.29		0	1.01	1.11		-1.11		0
AT1G14687	ATHB32	0.60	1	0.50		0.66	1	0.55		1.5	-2.11	-1	1.07	-1.18	1	1
AT1G51660	AT1G51660	0.53		0.17		0.57		0.47		0	1.30	-1.27		-1.22		0
AT1G66420	AT1G66420	0.94	-1	0.46		0.99	-1	0.50		-1.5	-1.88	-1	-1.18	-1.11	-1	-1
AT2G30470	HUB1	0.77	1	0.57		0.69	1	0.72	1	2.5	1.05	1.53	1	1.06	1	1
AT5G25470	AT5G25470	0.61	1	0.53		0.61	1	0.31		1.5	1.30	-1.09		1.35	1	1
AT1G66670	AS2	0.31		0.05		0.05		0.75	1	1	0.05	-1.22		-1.14		0
AT3G25730	EDF3	0.09		0.15		0.05		0.27		0	-1.06	1.04		1.10		0
AT3G61970	NGA2	0.28		0.52		0.21		0.69	1	1	-1.32	-1.14		-1.72	1	1
AT3G28920	ATHB34	0.59		0.77	1	0.51		0.53		0.5	1.68	1	-1.10	-1.17	-1	0
AT5G51990	CER4	0.30		0.47		0.13		0.77	1	1	1.06	1.28		1.18		0
AT3G13350	AT3G13350	0.91	-1	0.73	1	0.80	-1	0.73	1	0	-1.33	1.14		1.10		0
AT5G44210	ERF9	0.45		0.50		0.44		0.52		0	-1.51	-1.14		-1.15		0
AT1G05130	HMG2	0.62	1	0.77	1	0.46		0.05	-1	0	1.07	-1.05		-1.27		0
AT1G17980	DRN	0.06	-1	0.43		0.01	-1	0.40		-1.5	-1.36	1.03		-1.38		0
AT5G06150	DRP4	0.30		0.45		0.51		0.30		0	1.06	-1.45		1.13		0
AT5G39700	ATHB21	0.22		0.14		0.20		0.51	-1	1	1.07	-1.05		-1.12		0
AT4G31280	AT4G31280	0.43		0.46		0.51		0.51		0	1.12	1.02		1.06		0
AT3G61830	ARF11	0.97	1	0.90	1	0.97	1	0.57		2	1.28	2.07	2	1.00	2	2
AT1G50600	AT1G50600	0.40		0.54		0.19		0.80	-1	1	1.14	-1.25		-1.27		0
AT4G04890	PDF2	0.97	-1	0.94	-1	0.88	-1	0.88	-1	-1	-1.79	-2.11	-1	-1.52	-1	-1

**Supplementary table 5: Ranking of and scores awarded to the 50 initially selected transcription factors.** Scores awarded based on vascular expression. Includes expression fold changes from leaf disk (Kondo) and expression percentile data from root transcriptome atlas (Brady)(Phloem, Stele, Xylem). \* HTA2 and ESE3 were excluded.

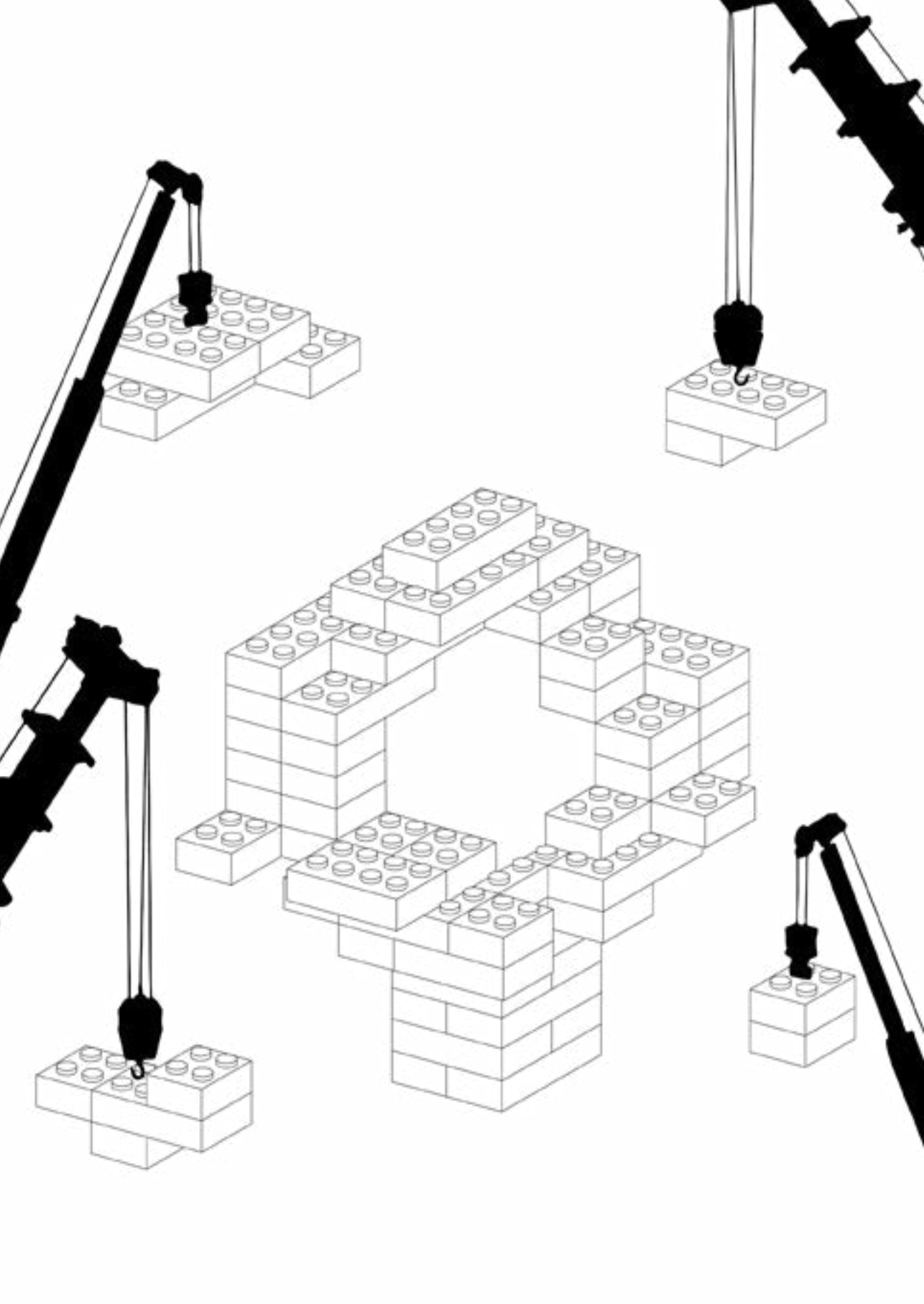
Locust	TJ name	FC Kilom		Point Percent1	Point Percent2	Point Percent3	Pres Score	Pres Kilom1	Pres Kilom2	Pres Kilom3	Total VAS Score					
AT1G75390	L2P14	1.37	1	0.99	1	0.96	2	1.09	2	0.92	2	0.80	1	0.77	1	6.0
AT6G10790	RAF2.11	2.48	1	0.42		0.32		0.45		0.42		0.35		0.33		2.0
AT2G36340	CUP3															0.0
AT2G37520	AT2G37520	1.94	1	0.45		0.44		0.43		0.50		0.59		0.51		2.0
AT2G21240	BPC4	-1.50		0.80	1	0.83	1	0.87	1	0.81	1	0.87	1	0.83	1	8.0
AT3G53680	AT3G53680	-1.52		0.49		0.57		0.47		0.57		0.59		0.60		0.0
AT2G45470	IBD18	-1.17		0.22		0.14		0.21		0.27		0.88	2	0.71	1	1.0
AT4G34530	L2P11	2.25	1	0.98	1	0.97	1	0.99	1	0.87	1	0.74	1	0.50		6.0
AT4G00270	GEPF	1.00		0.08		0.06		0.22		0.00	-1	0.09		0.23		-1.0
AT8G00250	STR12															0.0
AT4G36730	GEP1	-4.80	-1	0.74	1	0.72	1	0.77	1	0.74	1	0.81	1	0.79	1	2.0
AT2G37260	WKEY44	5.16	1	0.11		0.04		0.07		0.06	-1	0.05		0.06		1.0
AT5G61980	DEWAX	-20.63	-1	0.70	1	0.73		0.74	1	0.42		0.65		0.36		0.7
AT4G01120	CBF2	-3.15	1	0.58		0.57		0.58		0.48		0.65		0.72	1	0.5
AT8G00730	STR11			0.95		0.99		0.93		0.62		0.38		0.83	1	0.5
AT3G12730	AT3G12730	-1.91		0.83	1	0.70	1	0.80	1	0.40		0.34		0.25		4.0
AT1G54090	ASA1	-1.60		0.71	1	0.63		0.69		0.63		0.79	1	0.79	1	1.0
AT4G11635	REV35	1.51														0.0
AT4G03250	AT4G03250															0.0
AT5G53950	CUC2	1.19		0.33		0.36		0.34		0.41		0.37		0.37		1.0
AT2G01370	AT2G01370															0.0
AT3G76420	CUC3	-1.60	-1	0.17		0.19		0.16		0.10		0.19		0.16		0.0
AT1G62120	AT1G62120															0.0
AT2G36270	AMS	1.16		0.11		0.14		0.18		0.36		0.40		0.41		0.0
AT6G00390	AT6G00390	1.51	1	0.40		0.42		0.08		0.06	-1	0.50		0.10		2.0
AT4G00210	IBD31															0.0
AT5G06960	CBF3	1.86	1	0.59		0.48		0.50		0.51		0.58		0.63		1.0
AT5G05550	AT5G05550	-4.84	-1	0.27		0.23		0.17		0.27		0.27		0.35		-1.0
AT1G14687	ATH32	11.59	1	0.06		0.01		0.10		0.07	1	0.08		0.09		1.0
AT3G55650	AT3G55650															0.0
AT3G66420	AT3G66420															1.0
AT2G30470	HS2	1.18		0.31		0.34		0.16		0.15		0.40		0.58		0.0
AT5G25470	AT5G25470	-3.07	-1	0.22		0.31		0.22		0.20		0.48		0.21		1.0
AT1G65630	AS2	-4.96	-1	0.50		0.48		0.51		0.52		0.59		0.43		-1.0
AT3G25780	EDF3	1.77	1	0.60		0.71	1	0.69		0.66		0.68		0.38		1.0
AT3G61970	NGA2	-2.18	-1	0.21		0.17		0.18		0.27		0.19		0.19		-1.0
AT3G28920	ATH34	1.46		0.52		0.60		0.45		0.38		0.80	1	0.59		0.0
AT5G51990	CBF4	-15.86	-1	0.63		0.64		0.67		0.61		0.65		0.54		-1.0
AT3G18350	AT3G18350	1.77		0.30		0.81		0.38		0.38		0.28		0.57		0.0
AT5G44230	EDF9	-2.21	-1	0.50		0.75	1	0.51		0.64		0.58		0.75	1	-0.7
AT1G05230	HDC2	-1.61		0.45		0.51		0.40		0.53		0.51		0.45		1.0
AT3G12980	DWN															1.0
AT5G06250	DN44	1.44		0.09		0.19		0.11		0.16		0.23		0.14		1.0
AT5G38760	ASH33	1.89	1	0.30		0.29		0.37		0.27		0.62		0.28		1.0
AT4G33280	AT4G33280	-5.74	-1	0.31		0.35		0.16		0.13		0.31		0.27		-1.0
AT3G61830	ARY18	-6.91	-1	0.59		0.64		0.53		0.56		0.48		0.46		-1.0
AT3G50680	AT3G50680			0.06		0.04		0.05		0.06	-1	0.05		0.09		1.0
AT4G04890	PDF2	-1.42	-1	0.24		0.24		0.14		0.33		0.37		0.27		-1.0

Supplementary table 6: Primers used in this chapter for cloning promoter fragments and translational fusions.

Gene Name	Locus		Sequence	Promoter length (kb)
SOK1	AT1G05577	sense	CGTCCGTGGTGATCAAG	2
		antisense	CICCTTCTTTTGTGTGCT	
MIR171B	AT1G11735	sense	agggaaaagagfcaac	2
		antisense	taaaacacitgtttgac	
TSU1	AT1G68810	sense	acggaaaatgttgatllg	1.2
		antisense	aaggaaaggtttgaaagpagg	
WOL	AT2G01830	sense	cggtttatctctctacaaaatcc	2
		antisense	cacttcaaatgaggtatctc	
GATA20	AT2G18380	sense	tacaaatcgatctgacac	3
		antisense	gaattgagactacagatagag	
WRKY17	AT2G24570	sense	caataattatctgtgtgag	3
		antisense	ggttggaacacagagag	
PEAR1	AT2G37590	sense	ccacatcgataatgaaatgac	1.3
		antisense	agttatctcttttgatattcttc	
ME53	AT2G43290	sense	cattgtacatcagatgtataac	3
		antisense	aactgttgatcacaactc	
ERF4	AT3G15210	sense	ATCAACTTATGTCACGAC	3
		antisense	tcttgatgataatgataag	
TM05	AT3G25710	sense	tgatttcaaatataggttgg	2.9
		antisense	ttttgctttttgtttttagttttgg	
DOF6	AT3G45610	sense	tctggatctcaatcac	
		antisense	tctcaacgaattgagaac	
IQD15	AT3G49380	sense	cggagatcttaaatatatagc	1.4
		antisense	caagatgatcaactgtctgc	
ATH1B	AT4G32880	sense	cttggatctctgacatctc	1.2
		antisense	ctgtgtgacatacacattgg	
SHR	AT4G37650	sense	agaaagagagtgatggttc	2.5
		antisense	ttttatgataagaaatgg	
ZLL	AT5G43810	sense	AGGCCGGTGGTTGCATAC	2.9
		antisense	TTTTGTGTGTGGATTTCAAAATC	
TM06	AT5G60200	sense	gaaatagctgataag	
		antisense	aagagtgatctgag	

Gene Name	Locus		Sequence	Promoter length (kb)
ArbZP44	AT1G75390	sense	tataagttcactaagcaacttgatoc	3
		antisense	CAGTTGAAAACATCACCAGC	
RAP2.11	AT5G19790	sense	tttcttgtaugctcccttttagagg	2.9
		antisense	CGTAGCCGAGAAAGATTGG	
AT3G53680	AT3G53680	sense	agaagtgatgagagtgagc	2.8
		antisense	TCCCTGATACTCTCGGCTTGAGC	
BPC4	AT2G21240	sense	ctaggaacctgttcaatacc	3
		antisense	CTTGATAGTGATGTAGCGTTTGTC	
GLP3	AT2G36340	sense	gatatataccaacactgtatatgacc	3
		antisense	AGGAGAACTCCTAAGTTTGC	
GE8P	AT4G00270	sense	aaatacatgaatgggtcttgg	2.6
		antisense	ACTATCATTAGCTGCTCTGTC	
STKL2	AT4G00250	sense	AGAGTCGTTAAOCCACTTCACACC	3
		antisense	GTTGGTTTGAGCAAGCACC	
GBF1	AT4G36730	sense	CTATAAAGTCGGAGATGATGG	3
		antisense	ATTGTTCCTTCACCATCTTCG	
WRKY44	AT2G37260	sense	tctgttactgtgttctgtatgg	3
		antisense	AATTGTTTGCTTAGAAAGTTGTGG	
bZIP11	AT4G34590	sense	ctcagattcttttgaggatggc	2.9
		antisense	ATACATTAAAGCATCAAGACG	
GBF2	AT4G01120	sense	gatacttctatacatgcatcg	3
		antisense	GCTAGCCCGGACAGGATCGTTATCG	
DEWAX	AT5G61590	sense	gactaacgaagtgttaacagg	3
		antisense	GTTTGATGACGATGATGAAGTAC	
STKL1	AT4G00238	sense	CAATCGATTCAAACCTCTGTGAAAGG	3
		antisense	GTTGGTTTGAGTAAGCACTGAAGTC	
AT4G03250	AT4G03250	sense	GTATACAAAGATGTGAAGAGAGG	3
		antisense	ATCCATTGACGAGCTAGATTGG	
AT3G12730	AT3G12730	sense	CAGAACAAAGCTTCTTCTTC	3
		antisense	ACCGAGACAAACCGTACG	
ASL1	AT1G54060	sense	cagcttgacttttagctaaagg	3
		antisense	GCTACTTACATTGCCGTTATTCTTGC	
REM35	AT4G31615	sense	gaccaggtaactttatgtttgc	3
		antisense	TTGACCTGACTTGAGCATGTAAGG	
CUC2	AT5G53950	sense	gacgtttcttacacaattgc	3
		antisense	GTAGTTCCAAATACAGTCAAGTC	
bZIP4	AT1G59530	sense	gtctatatgttttgctactc	2.1
		antisense	AATCTCGAGCETTGTGATG	
ERF15	AT2G31230	sense	gaataagggatttcaagttcg	3
		antisense	ACATGAGCTCATAAGAAGTTG	





# Chapter 6

## **Candidate regulators of vascular identity modulate auxin-dependent expression of vascular genes**

Margot E. Smit<sup>1</sup>, Frederique Polder<sup>1</sup>, Henriette van Beijnum<sup>1\*</sup>, Mark  
Roosjen<sup>1</sup>, Daria Novikova<sup>1,2,3</sup>, Victor Levitsky<sup>2,3</sup>, Victoria Mironova<sup>2,3</sup> and  
Dolf Weijers<sup>1</sup>

1. Laboratory of Biochemistry, Wageningen University, Stippeneng 4, 6708WE Wageningen, the Netherlands

2. Novosibirsk State University, 2 Pirogova Street, Novosibirsk 630090, Russian Federation

3. Institute of Cytology and Genetics, 10 Lavrentyeva avenue, Novosibirsk 630090, Russian Federation

\* Present adress: Hubrecht Institute, Uppsalalaan 8, 3584 CT Utrecht, Nederland

## Abstract

Initiation of vascular development requires auxin signaling but auxin is not enough for creating ectopic vascular identity. In the previous chapter we have identified transcription factors that can bind to vascular promoters in yeast and might play a role in the control of vascular gene expression. In this chapter we find that misexpression of single candidate regulators cannot induce vascular identity, probably because identity requires integration of multiple signals. Misexpression of three individual candidates (*ASIL1*, *AT2G37520* and *GLP3*) does however affect auxin response: decreasing auxin sensitivity as measured by the inhibition of root growth and vascular gene expression. This suggests that candidate regulators might act by modulating response to auxin, potentially through interaction with ARF proteins. Using split-YFP (BiFC) assays we confirm the interaction between two candidates (GBF1 and GBF2) with the ARF DNA-BINDING DOMAIN. We confirmed that GBF1 and GBF2 can bind to G-box motifs in several vascular promoters and three of these promoters contained G-boxes and AuxREs in close proximity. Truncated promoters where both the G-box and AuxRE motifs were missing displayed large decreases in expression level in the vascular bundle. In contrast, removal of only the G-box increased the variation in expression level between independent transgenic lines. These findings suggest a role for G-box binding proteins such as G-class bZIP proteins in modulating auxin-dependent gene expression. However, due to gene redundancy in the G-class of bZIP proteins we were unable to confirm a role for GBF1 and GBF2 in regulation of vascular identity.



## Introduction

Auxin plays a central role in plant development. Its effects on plant growth have been studied in a number of tissues and in a variety of plant species (Aloni et al. 2010, de Jong et al. 2009, Kato et al. 2017, Sachs 1969). A central question that emerges from its many functions is how auxin can control a wide variety of responses while triggering specific downstream effects for each response. In *Arabidopsis*, 23 AUXIN RESPONSE FACTORS (ARFs) interact with the DNA to control auxin-dependent gene expression. Diverse expression patterns among these *ARF* genes contribute to diversity in cellular auxin responses, since ARF proteins differ in function and are not all interchangeable, indicating specialized roles (Rademacher et al. 2011, 2012). This can in part be explained by differences in protein structure: within the ARF family, three distinct classes exist which appear to have different effects on gene regulation (Finet et al. 2013, Guilfoyle & Hagen 2007, Mutte et al. 2018, Okushima 2005). Intriguingly, it appears that the same ARF proteins can have either an activating or a repressing role, depending on developmental context (Brackmann et al. 2018, Guilfoyle & Hagen 2007, Zhang et al. 2014a), but mechanisms underlying this biochemical multifunctionality are unknown.

Given the opposing action ARFs can have on gene expression, it remains difficult to predict ARF-dependent regulation of target genes. DNA motif specificity appears to have limited influence as divergent ARFs can bind to similar DNA elements (Boer et al. 2014). ARFs can bind to inverted repeats of Auxin Response Elements (AuxREs) in the DNA as homodimers (Boer et al. 2014, Franco-Zorrilla et al. 2014, O'Malley et al. 2016) and binding specificity in part stems from differences in preference for spacing between the AuxREs (Boer et al. 2014). Specificity might be further modulated via protein interactions and the resulting cooperative DNA binding or cooperative recruitment of cofactors. Several interactions between ARFs and other transcription factors have been identified (reviewed in Roosjen et al. 2018). Furthermore the co-occurrence of specific DNA motifs near AuxREs (Berendzen et al. 2012, Cherenkov et al. 2018, Weiste & Dröge-Laser 2014) indicates that specificity may be influenced by other transcription factors, whose binding sites are associated with an AuxRE in composite elements.

While auxin is involved in a wide range of processes, a long-recognized activity is in promoting the formation of vascular tissues. Auxin maxima and fluxes are correlated with vascular development and exogenous auxin induces the formation of new vascular bundles (Lee et al. 2014, Sachs 1969, Smit & Weijers 2015). While it remains unclear whether it is the absolute level of auxin or the flux of auxin that determines cell fate, it is evident that

the auxin response machinery is critically required. Without ARF5/MP, root development is arrested and the vascular bundle does not develop (Hardtke & Berleth 1998, Mayer et al. 1991). The vascular role of MP is further underlined by the vascular specificity of many of its target genes (Möller et al. 2017, Schlereth et al. 2010; **Chapter 3**). Whilst MP is present in a broad domain (Crawford et al. 2015, Rademacher et al. 2011), it activates target gene expression in vascular cells, though not all targets are specific to vascular cells (Möller et al. 2017). Vascular development does not only depend on auxin: a dominant active version of MP can cause vascular defects in leaves (Krogan et al. 2012) but was not able to induce expression of vascular genes in the non-vascular cells of the embryo (**Chapter 4**). This indicates that additional modifications or interactors restrict ARF activity to the vascular cells.

In previous chapters we have searched for transcription factors that can bind to vascular promoters and affect their activity. In **Chapter 5** we explored the function of these factors by misexpressing them while fused to an SRDX tag. While this experiment did produce abnormal phenotypes, no clear effects on vascular development were observed. This could be because the candidate does not function in vascular development; a result of embryo lethality; or an effect of the absence of additional components. We hypothesize that the initiation of vascular development depends on the integration of multiple signaling modules, including auxin response. In this chapter we test the relation between our candidate regulators of vascular identity (**Chapter 5**) and auxin response. Several candidates are found to affect auxin responsive root growth and the induction of vascular genes in response to auxin. In addition, we confirm the interaction between G-BOX BINDING FACTOR (GBF) proteins and ARFs and look at the role of ARF and GBF binding sites in the regulation of vascular gene expression.

## Results

### Overexpressing candidate regulators of vascular identity affects response to auxin

In the previous chapter, several candidate regulators of vascular identity were identified through screening a set of vascular-enriched promoters against a transcription factor library in yeast (**Chapter 5**). These candidates were able to bind to vascular promoters in yeast and 10 of them were found to be expressed during embryogenesis at the time and location where vascular identity emerges. To address the function of these candidate regulators, each was misexpressed in meristematic tissues using the *RPS5A* promoter (Weijers et al.

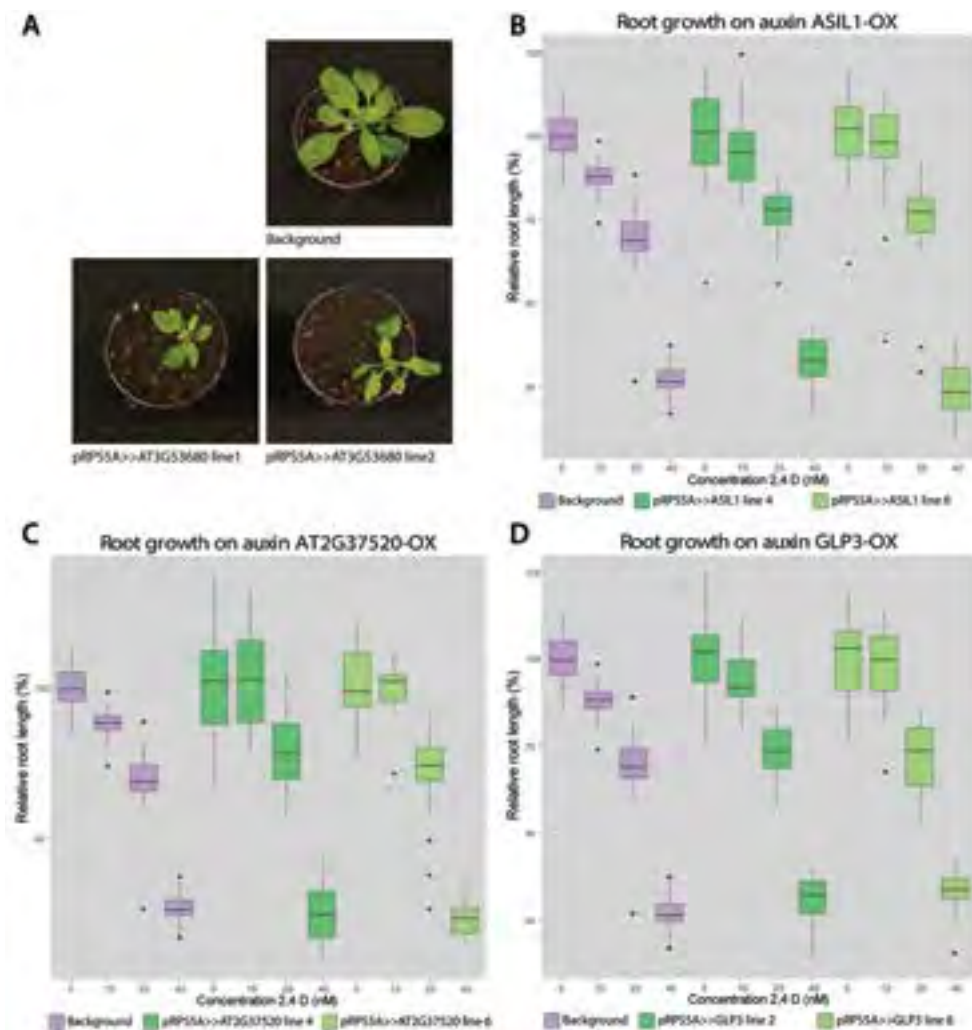


**Figure 1: Effects of overexpression of candidate regulators of vascular identity.**

(A) Overexpression of *AT3G53680* causes slower development and altered leaf morphology in the adult plant. (B-D) overexpression of *ASIL1* (B), *AT2G37520* (C) and *GLP3* (D) causes reduced sensitivity to the auxin 2,4-D as measured by root elongation. Roots were moved to plates containing different concentrations of 2,4-D and increase in root length was measured 3 days later. Root growth on 0 nM 2,4-D is set to 100% for each line.

2001, 2003). The misexpression of most of the 10 candidate regulators did not lead to strong developmental phenotypes, but misexpression of *AT3G53680* resulted in visible abnormalities. Adult plants showed retarded growth and abnormal leaf development (Figure 1A). Since all 10 candidates are generally broadly expressed in the embryo (**Chapter 5**), it is plausible that their DNA binding or potential activity in regulating vascular gene expression would depend on additional signals that result in cell type-specific activity.

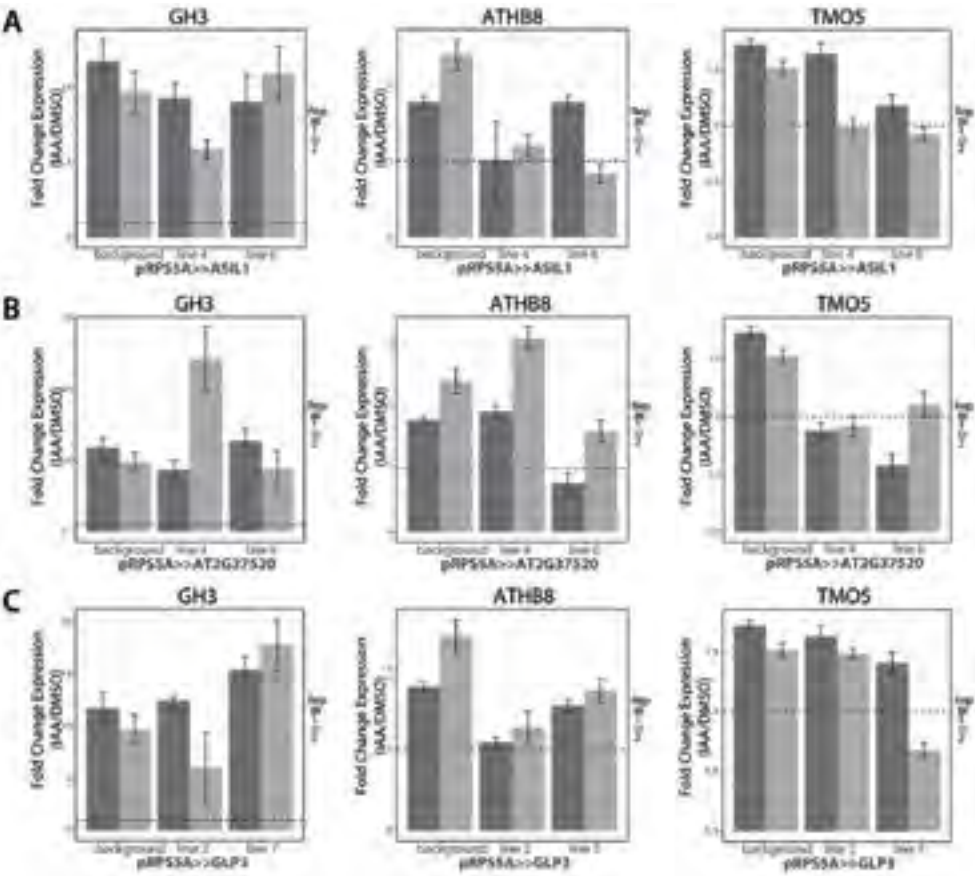


**Figure 2: Overexpression of candidate regulators reduced auxin induced expression.**

Expression levels of the auxin response gene GH3 and two vascular genes ATHB8 and TMO5 after 1 hour of 1  $\mu$ M IAA after 12 hours of pretreatment with 10  $\mu$ M NPA. (A) Overexpression of ASIL1 results in reduced induction of ATHB8 expression by auxin. (B) Overexpression of AT2G37520 results in reduced induction of TMO5 expression by auxin. (C) Overexpression of GLP3 results in reduced induction of ATHB8 expression by auxin. Dark grey and grey bars indicate two independent biological replicates.

One signal required for vascular development is auxin signaling. To test for interaction between the candidate regulators and auxin action, misexpression lines of the 10 candidates were tested for their responsiveness to auxin by assaying root elongation on auxin. 4-day old seedlings were transferred to plates containing different concentrations of auxin and the increase in root length was measured after 3 days of growth. Increasing concentrations of 2,4-D resulted in reduction of root growth (Figure 1B-D). Misexpression of 3 candidates (*ASIL1*, *AT2G37520* and *GLP3*) resulted in reduced auxin sensitivity: at low auxin concentrations root growth was less affected. We next tested if the altered root growth on auxin-containing media reflected a change in auxin-dependent gene expression. A short (1 hour) auxin treatment led to induction of vascular genes in wild-type, but the degree of

induction of the vascular genes *ATHB8* or *TMO5* was reduced in misexpression lines for *ASIL1*, *AT2G37520* and *GLP3* (Figure 2). In contrast, general auxin response, reported by the *GH3* primary response gene (Ulmasov et al. 1995) remained unchanged in these lines (Figure 2). This indicates that these candidate regulators may modulate transcription of auxin-responsive vascular genes.

#### LBD18 regulates vascular differentiation, but not vascular initiation

When constitutively misexpressing a candidate regulator, it is possible that strong expressors are selected against, when these would have strong, potential lethal phenotypes. In this case, a role in vascular development would go unnoticed. Therefore, we generated inducible misexpression lines for several candidate regulators. Glucocorticoid Receptor (GR) tagged versions of these candidate regulators were expressed in meristematic cells from the *RPS5A* promoter. By keeping the candidate protein contained in the cytoplasm with the GR domain, activity is suppressed. Treatment with dexamethasone (DEX) triggers nuclear translocation, allowing activity of the transcriptional regulator. Germination and growth on plates containing DEX did not visibly affect root or seedling development for most of the candidates tested. Only the induction of LBD18-GR caused severe developmental abnormalities (Figure 3). LBD18 was previously reported as a regulator of lateral root development and xylogenesis (Lee et al. 2009, Soyano et al. 2008) and indeed the induction of LBD18 led to lateral root and xylem-related phenotypes. Germination on plates containing DEX resulted in cells in the cotyledons transdifferentiating to xylem vessels with spiral cell walls (Figure 3A-B). In addition, the root meristem collapsed: ground tissue and epidermal cells disappeared and the remaining vascular cells were swollen (Figure 3C). Higher up in the root, the regions where LBD18 was not misexpressed appeared normal and at the transition we could see clear effects on cell size, shape and adhesion (Figure 3D). The different effects of LBD18 in the root and cotyledons indicates that LBD18 target regulation depends on tissue context. Nonetheless, in both tissues LBD18 induction led to impaired development. After 10 days of growth, many seedlings remained small and cotyledons largely lost their green color (Figure 3E-F).

When seedlings were instead first grown without induction for 4 days and next transferred to DEX-containing plates, more subtle effects of LBD18 induction became clear. After 44 hours of growth on DEX, the cortical cells higher up in the meristem were swollen and altered division planes were observed in both cortex and epidermis (Figure 3G-H). In addition, lateral roots no longer emerged, after initiation their development became disorganized and stalled (data not shown).

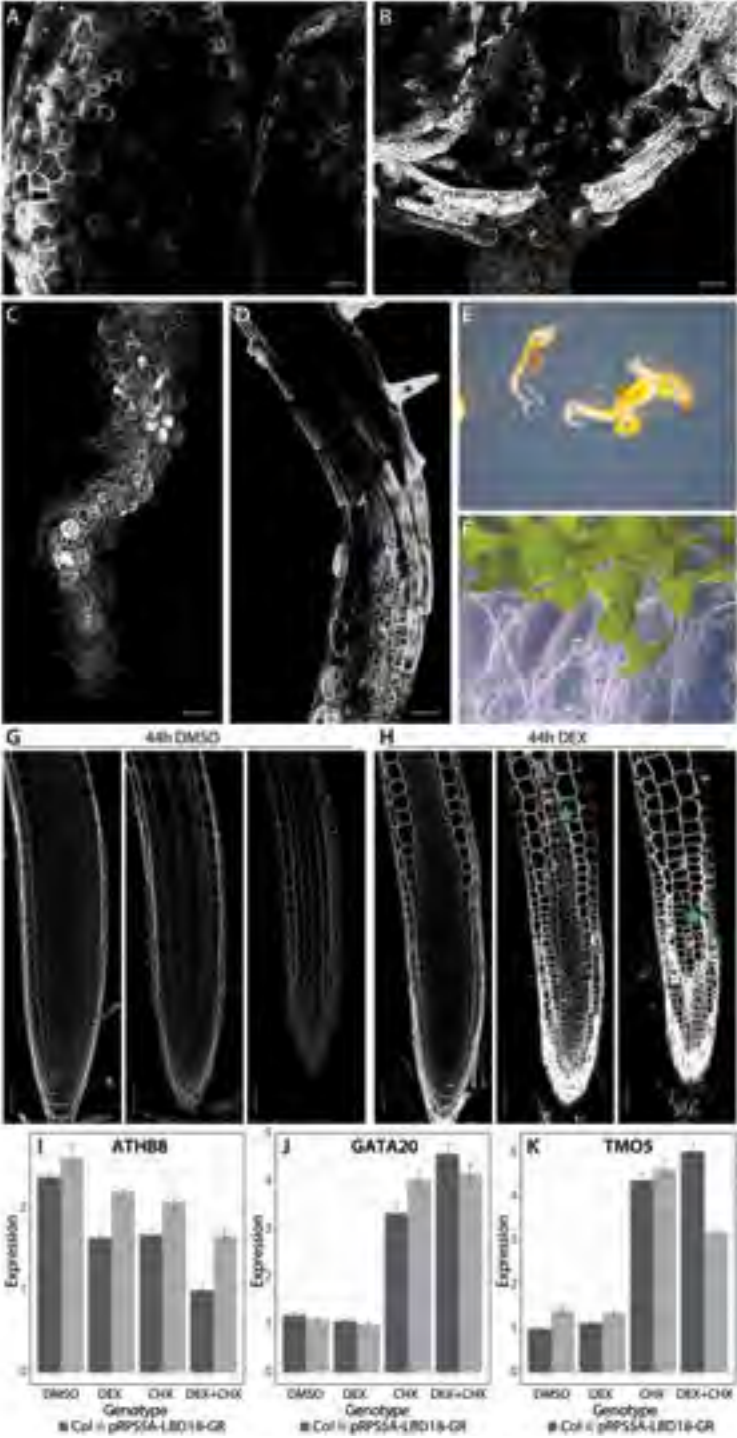




**Figure 3: Misexpression of LBD18 can induce xylogenesis but does not induce expression of early vascular genes.**

(A-E) Germination of pRPS5A-LBD18-GR seeds on DEX plates causes strong developmental defects while seedlings grown on DMSO (F) look like wildtype. (A-B) Z-stacks of cotyledons with ectopic xylogenesis. (C,D) LBD18 degrades the root meristem (z-stacks), at the boundary of misexpression abnormal cell divisions and cell shapes are observed. (E-F) pRPS5A-LBD18-GR seedlings 10 days after germination on DEX (E) or DMSO (F). (G-H) Roots of 5-day old seedlings 44 hours after being transferred to DMSO (G) or DEX (H). Panels are cross-sections through the vascular bundle (lef), cortex (middle) and epidermis (right). Stars mark changed division planes. (I-K) Expression of *ATHB8*, *GATA20* and *TMO5* after 1 hour of treatment with DMSO, 20  $\mu$ M DEX, 10  $\mu$ M CHX or both DEX and CHX. All scale bars are 50  $\mu$ m.

While the induced xylogenesis indicated a role for LBD18 in vascular development it remained unclear at what stage of vascular development LBD18 acts. LBD18-GR roots were harvested after a short (1 hour) treatment with DEX and cycloheximide (CHX) to determine whether LBD18 directly controls expression of early vascular genes. If LBD18 controls the expression of early vascular genes, one would expect expression levels of these genes to be altered after 1 hour of DEX treatment compared to the DMSO control. If this is caused by direct regulation by LBD18, the effect should persist even in the presence of CHX, which blocks translation and thus the activation of secondary target genes. DEX induction did not cause altered expression of vascular genes such as *ATHB8*, *GATA20* and *TMO5* (Figure 2I-K). CHX treatment did lead to induction of several vascular genes (Figure 3). This is in line with expectations since these genes are activated by auxin (**Chapter 4**) and thus inhibited by Aux/IAA proteins. These are labile repressor proteins and inhibition of their synthesis by CHX would lift the repression of such target genes (Soeno et al. 2010). These results indicate that LBD18 does not directly control the expression of early vascular genes and it likely acts further downstream in vascular development. However, LBD18 is the first candidate resulting from the vascular Yeast One Hybrid screen to have a distinct vascular phenotype, indicating that we were able to find regulators of vascular development.

GBF proteins can heterodimerize and can interact with ARFs

To better understand the roles that some of our candidate regulators might play in vascular development, we next focused on protein interactions, searching for mechanisms that could be responsible for the integration with auxin signaling. Preliminary IP-MS/MS (Immunoprecipitation followed by tandem MS) data on ARF5/MP had indicated that G-BOX BINDING FACTOR 2 (GBF2) could interact with MP (Llavata-Peris 2013). GBF1 and GBF2 are two candidates that were selected from our Yeast One Hybrid screen that both are broadly expressed in embryo and root (**Chapter 5**). Both are G-class bZIP transcription factors of which Arabidopsis has five (Dröge-Laser et al. 2018, Jakoby et al.



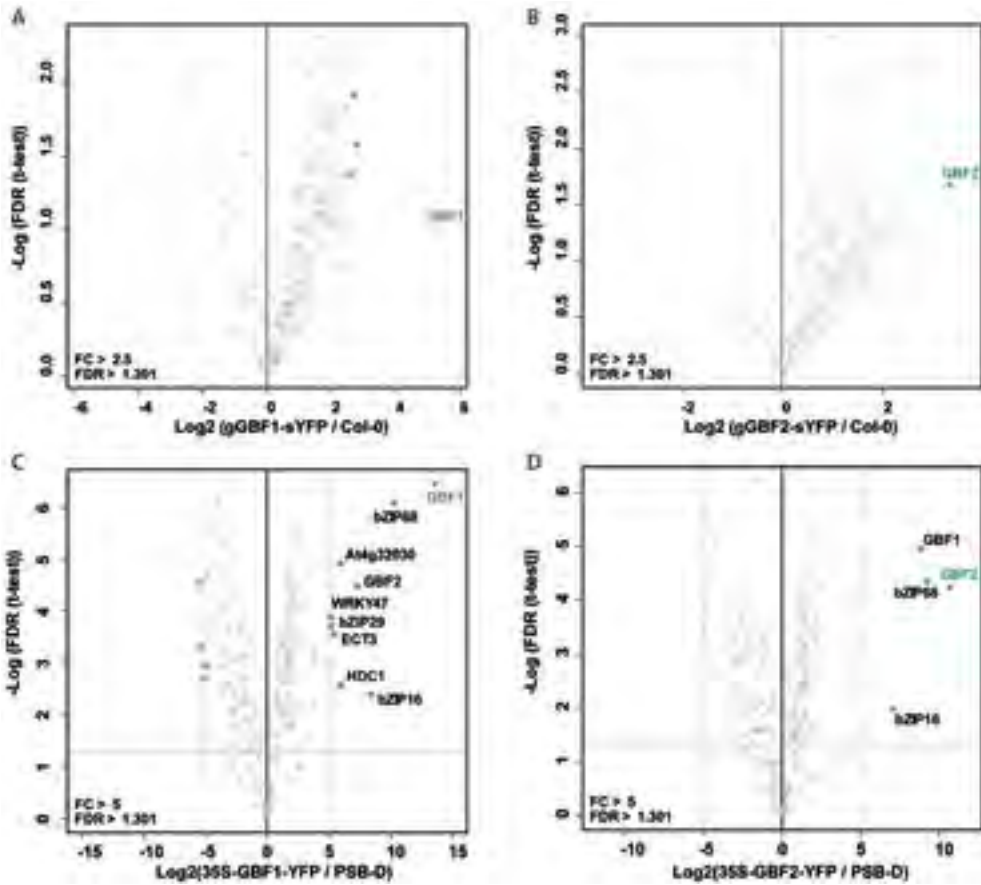


**Figure 4: IP-MS/MS experiments reveal GBF1 and GBF2 can heterodimerize with G-class bZIPs**

Results of immunoprecipitation followed by tandem MS (IP-MS/MS). Volcano plots show fold change (FC, x-axis) and significance (FDR, y-axis) of each detected protein. Proteins with a p-value below 0.05 ( $-\log(\text{FDR}) > 1.301$ ) and a fold change above 2.5 (A-B) or 5 (C-D) are marked and have their name displayed. (A-B) Plots generated from IP-MS/MS results on Arabidopsis roots expressing GBF1-YFP (A) or GBF2-YFP (B) under their native promoters compared to Col-0 seedlings. (C-D) Plots generated from IP-MS/MS results on Arabidopsis cell cultures expressing GBF1-YFP (C) or GBF2-YFP under the 35S promoter compared to wildtype (PSB-D) cell cultures.

2002). We next performed IP-MS/MS experiments on the GBF1-YFP and GFP2-YFP translational reporter lines (**Chapter 5**) to identify interaction partners and see if the GBF-ARF interaction could be confirmed. Pull-downs on root material expressing GBFs under their native promoter did retrieve the bait GBF but enrichment was insufficient to identify interactors (Figure 4A-B). Therefore we generated plant cell cultures overexpressing GBF-YFP under the control of the 35S promoter, and repeated the IP-MS/MS experiments on these cells cultures. With this setup, we identified other G-class bZIP transcription factors: next to GBF1 and GBF2, bZIP16 and bZIP68 were found in both pulldowns. GBF proteins

had indeed been shown previously to be able to heterodimerize (Menkens & Cashmore 1994, Schindler et al. 1992). In addition, the pulldown of GBF1 also recovered HISTONE DEACETYLASE COMPLEX1 (HDC1), hinting at a function in regulating chromatin state (Perrella et al. 2016). Using the IP-MS/MS, no ARF proteins were identified as GBF interactors, perhaps because these proteins are not expressed or not abundant in cell cultures. Alternatively, the stoichiometry of GBF-ARF interaction may be substantially different from the heterodimeric nature of bZIP dimers. We therefore used a more direct approach to validate interactions between GBF proteins and MP.

Split-YFP (Bimolecular Fluorescence Complementation; BiFC) assays can reveal protein interactions (Ghosh et al. 2000, Horstman et al. 2014), by reconstituting the N- and C-terminal halves of YFP upon bringing both in close proximity through the interaction between the two proteins to which the YFP halves were fused. We expressed fusions of YFP halves to GBF1, GBF2 and MP in the *Nicotiana benthamiana* leaf epidermis and assessed fluorescence. Fluorescence complementation was observed when GBF1 or GBF2 was combined with MP, indicating interaction, but not when either was combined with TMO5, another transcription factor (Supplementary Figure 1). This complementation did not depend on the location of the tag: both N-terminal and C-terminal fusions of GBF or MP with NtYFP or CtYFP resulted in YFP signal (Supplementary Figure 1). To determine if this interaction was specific to MP or more general with ARF proteins, interactions between GBFs and other ARFs were tested as well. Two ARFs from each of the 3 major classes (A, B and C; Finet et al. 2013, Mutte et al. 2018) were tested and all could interact with both GBF1 and GBF2 (Supplementary Figure 1). In addition, we found that the DNA-binding domain of each ARF was sufficient for the interaction with the GBFs (Figure 5; Supplementary Figure 1). In summary, GBF1 and GBF2 can interact with other G-class bZIP transcription factors and directly interact with ARFs from all three major classes, likely by interacting with the ARF DNA-binding domain.

### G-boxes modulate vascular gene activity

The direct interaction between GBFs and the DNA-binding domain of ARF proteins indicates that protein interactions potentially occur at the DNA and that GBF and ARF might bind DNA together. Furthermore, this result suggests that GBF's may co-regulate auxin-responsive genes. DNA-binding motifs for ARFs and GBFs are known, identified both through protein binding microarrays and DAPseq experiments (Boer et al. 2014, O'Malley et al. 2016). In addition, AuxREs and G-boxes were shown to often co-occur in

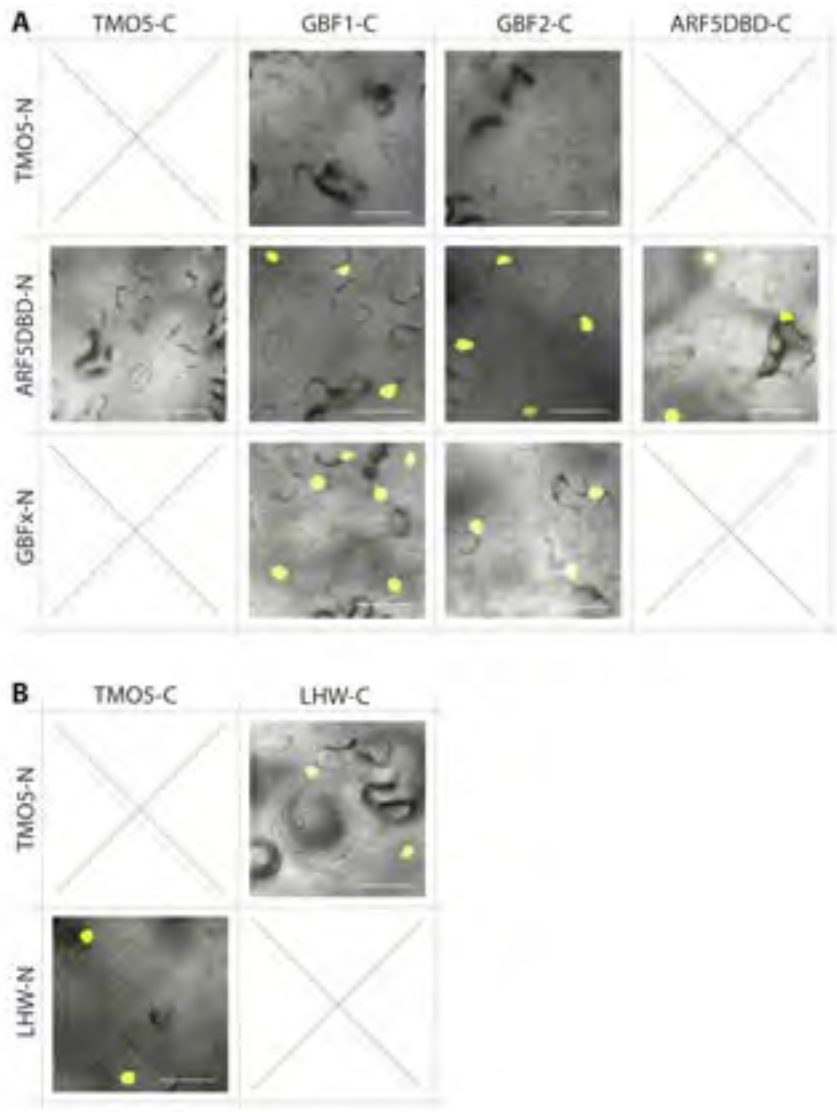


**Figure 5: Split-YFP experiments confirm interaction of GBF1 and GBF2 with ARF5/MP.** Selection of split-YFP experiments performed using Tobacco leaves to confirm GBF-ARF interactions. Upper panel shows complementation caused by interaction GBF1/2-CrYFP and ARF5dbd-NrYFP. TMO5 is used as a negative control while homodimerization for GBF and ARF was used as a positive control. LHW was used as a positive control for TMO5. Crosses indicate interactions that were not tested. Scale bars represent 10  $\mu$ m.

auxin-dependent promoters (Berendzen et al. 2012, Cherenkov et al. 2018, Ulmasov et al. 1995, Weiste & Dröge-Laser 2014). To confirm that ARFs and G-class bZIPs can indeed bind close to each other we applied the MCOT (Motif co-Occurrence Tool) to ARF5 and

ARF2 peaks taken from Dap-Seq data (O'Malley et al. 2016). We then analyzed all possible combinations of the AuxREs (ARF2/5) and G-boxes (GBF3, bZIP16/68) with spacer lengths below 30 nucleotides across the genome. Indeed bZIP68 binding sites overlapped with ARF5 binding sites (Figure 6A-B).

We next selected four vascular promoters to confirm GBF binding: the *GATA20*, *TMO5* and *WRKY17* promoters each contain predicted G-boxes and AuxREs in close proximity, while in contrast the *ERF4* promoter contains G-boxes without adjacent AuxREs. ChIP-qPCR on Arabidopsis cell cultures expressing a 35S-GBF1/2-YFP transgene revealed that both GBF1 and GBF2 can bind to the G-boxes in the *ERF4* and *WRKY17* promoters (Figure 6C-D). Enrichment was however not found for the potential G-boxes in the *GATA20* and *TMO5* promoters (Figure 6C-D). It should be noted that misexpression of only a GBF proteins would be insufficient for binding if this relies on interaction with an ARF protein. Hence, we can conclude that GBF1 and GBF2 bind vascular promoters *in vivo*, but the interdependence between GBFs and ARFs remains to be tested.

The role of the G-boxes and AuxREs in regulating gene expression was next investigated by removing these motifs from vascular promoters and determining the effect on expression pattern and level. Lines containing truncated promoters driving n3GFP expression were generated and compared to lines containing full length promoters. Because transgene insertion location can significantly affect expression intensity among transgenic plants, we measured fluorescence intensity in the vascular cells of various T1 roots.

In the *ERF4* promoter, two regions containing G-boxes were removed (Figure 7-1A). Truncated *ERF4* promoters did not result in clearly altered fluorescence in the young vascular cells compared to the full-length promoter. In contrast, removing two short regions in the *WRKY17* promoter caused a significant reduction of fluorescence intensity in the vascular bundle (Figure 7-1F). However, the amount of fluorescence in surrounding cell types did not decrease as strongly. As a result, roots containing the truncated promoter on average had a different signal ratio in signal between the vascular and surrounding cells (Figure 7-1G). The vascular-specific decrease in *WRKY17* expression suggests that the mutated elements act in vascular specific gene expression. Because the AuxRE and G-box overlap in the *WRKY17* promoter and this truncated promoter also missed a predicted GATA binding site, it remains to be seen if the reduction in promoter activity is a result of the missing GATA binding site, AuxRE or Gbox.

The *GATA20* and *TMO5* promoters each have distinct G-boxes and AuxREs in close proximity. Truncated promoters where both binding elements had been removed

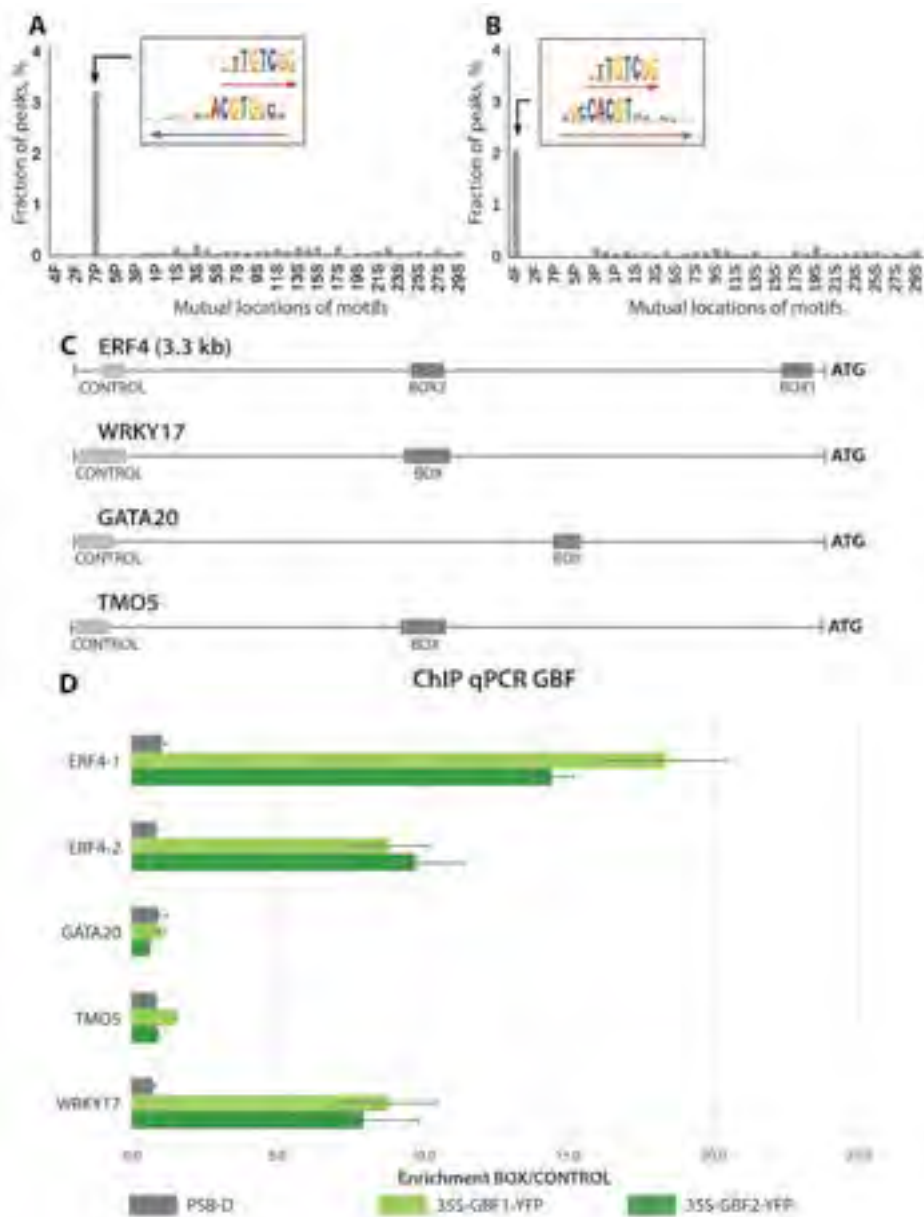


**Figure 6: Gboxes occur close to AuxREs in vascular promoters and are bound by GBFs.** (A-B) Distribution of potential ARF5/bZIP68 composite elements within ARF5 binding regions taken from Dap-Seq. Y axis numbers reflect number of nucleotides, F - full overlap, P - partial overlap, S - spacer. (A) ARF5/bZIP68 everted composite element distribution. (B) ARF5/bZIP68 direct composite element distribution. (C) Schematic representation of control regions and regions containing Gboxes in the promoters of ERF4, WRKY17, GATA20 and TMO5. (D) Relative enrichment of the BOX regions compared to CONTROL regions. Scale bars represent standard error.

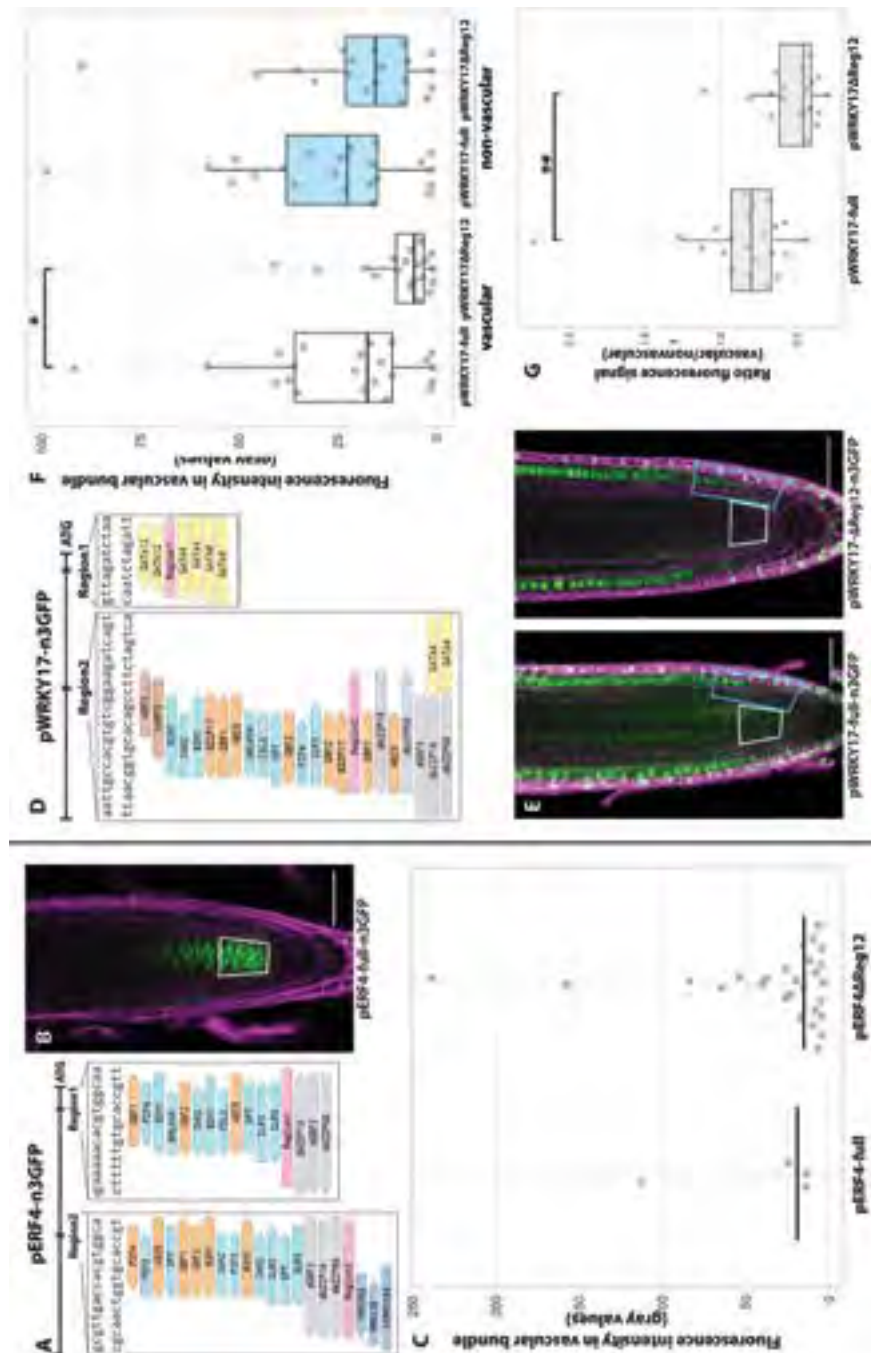


**Figure 7-1: AuxRE and Gboxes in vascular promoters control expression in the vascular bundle.** Comparison of fluorescence signal in the early vascular cells of the root between T1 roots containing full length and truncated promoters driving n3GFP expression. *Description continued on next page*

*Continued description Figure 7-1.* In each panel (A&D) show the location of the deleted regions within the 3 kb promoter. The pink bar marks the removed region (the outer two bases remain) while the other bars represent predicted and experimentally confirmed TF binding sites. Orange bars represent predicted GBF binding sites based on Position Weight Matrices (PWMs), brown bars represent predicted ARF binding sites based on PWMs. Dark blue, light blue and yellow bars represent predicted WRKY, bHLH and GATA binding sites respectively. Grey bars represent DAPseq confirmed G-class bZIP binding sites. (B&E) show the expression pattern of representative T1 roots, boxes indicate the region in which fluorescent signal was measured. (C&F) shows a plot comparing the mean fluorescence in the measured cells for T1 roots containing full length or truncated promoters, each point is the mean fluorescence measured from 1 independent T1 root. Boxplots are shown if  $n > 10$ . For the WRKY17 promoter two areas were measured, the vascular bundle (white) and adjacent non-vascular cells (blue). (G) Ratio of WRKY17 driven GFP signal in the vascular cells compared to signal in the non-vascular cells. Scale bars represent 50  $\mu\text{m}$ . \* indicates  $p < 0.05$ , \*\* indicates  $p < 0.001$  as calculated by a two-sided Student's ttest.

displayed significant and strong reductions in expression (Figure 7-2). In contrast, removing only the G-box led to a weaker reduction in average expression for *GATA20* or no reduction for *TMO5*. While the effect on the mean expression was less pronounced, the variation between individual transgenics increased dramatically (Figure 7-2), suggesting that the G-box is required for stable expression of these genes. Altogether, it appears that G-box elements play a role in the expression level and pattern of vascular promoters, potentially through their proximity to AuxREs, perhaps facilitating interactions between ARFs and GBFs.

### GBF overexpression affects leaf shape and results in delayed flowering

Given that GBF proteins interact directly with ARFs and can bind vascular gene promoters, we next further explored their biological activity. Overexpression of *GBF1* using the *RPS5A* promoter did not result in a visible phenotype. However, the *RPS5A* promoter is specific to young and dividing cells (Weijers et al. 2001, 2003), and perhaps GBF activity is not limiting in these cells. To test activity in more mature cells, we next overexpress the GBF proteins from the ubiquitous *35S* promoter, and found this to induce changes in development. Early in development, leaves appeared rounder, having a smaller length/width ratio (Figure 8). Older leaves showed more pronounced serration and in addition the major veins could be clearly seen within the leaf blade (Figure 8). Nonetheless, direct observation of the venation pattern in cleared leaves did not reveal a remarkable change in venation pattern (Figure 8). *35S::GBF1* plants developed leaves slower than wildtype Columbia and as a result flowered much later. These results indicate that GBF misexpression does affect plant development, but no distinct effect on vascular development was observed.



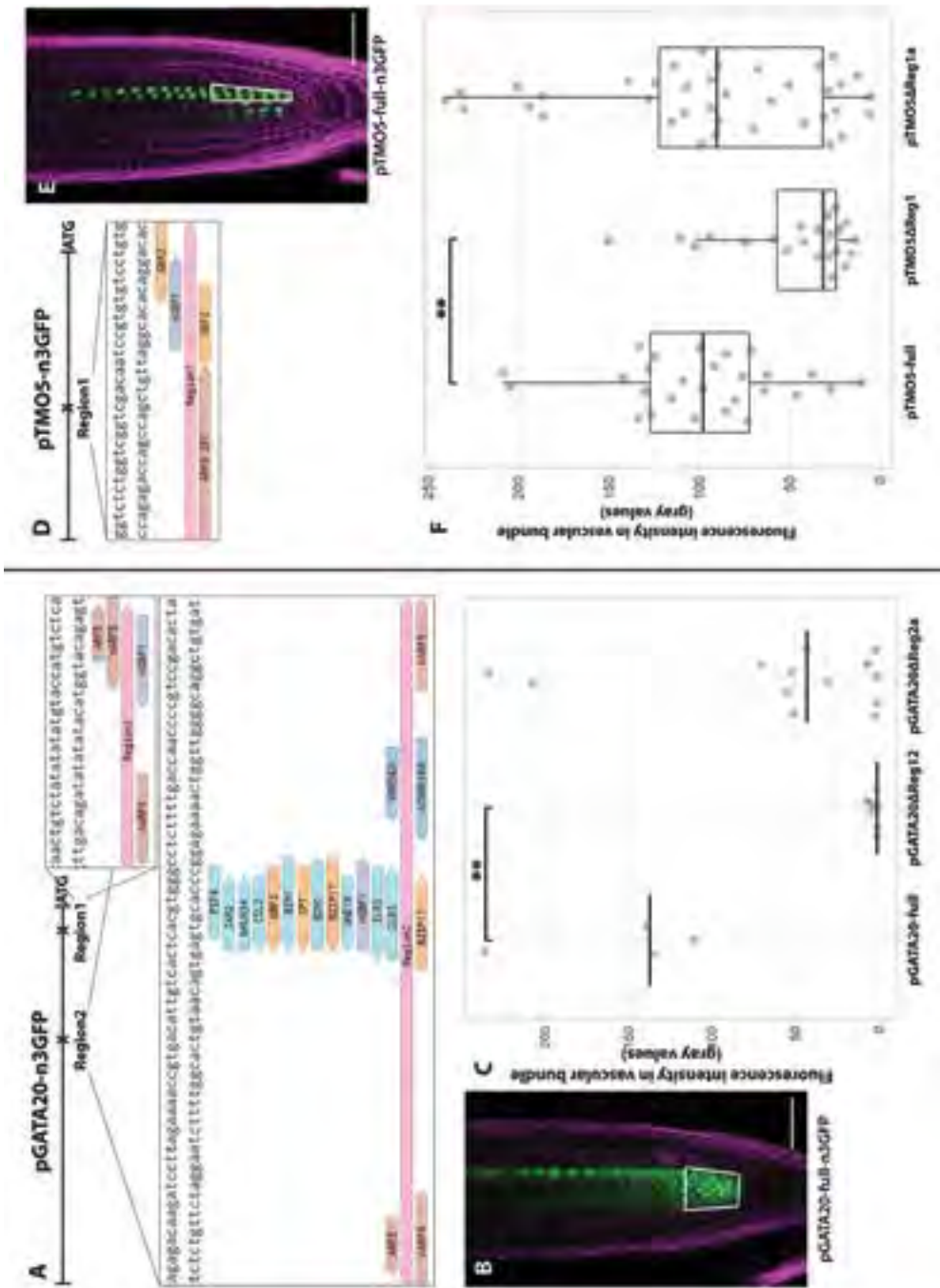
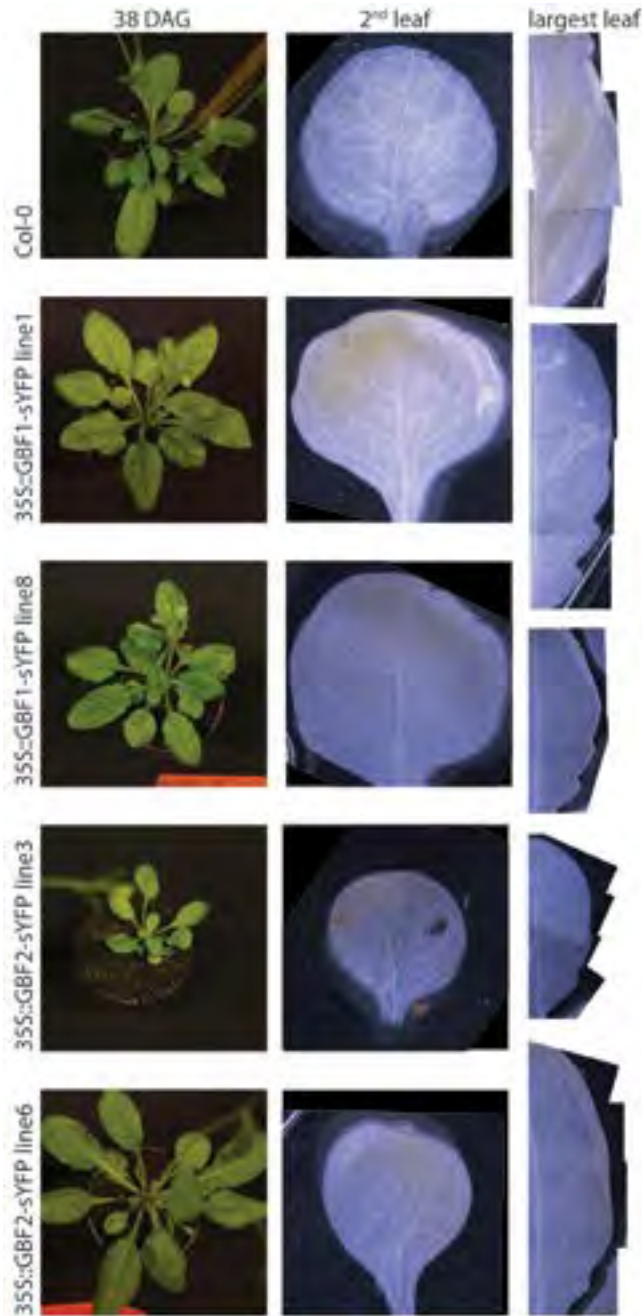


Figure 7-2: AuxRE and Gboxes in vascular promoters control expression in the vascular bundle. Full description in figure 1-1.



**Figure 8: Overexpression of GBF1 results in abnormal leaf morphology.** 35S-GBF1 and Col-0 plants 38 DAG. 2 independent 35S-GBF1 lines show early leaves have increased width/length ratio and late leaves show increased serration, leaves have more pronounced veins and slower development resulting in delayed flowering. No obvious changes in veination pattern were observed.

### GBF double mutants do not display vascular defects

Because single GBF mutants did not show abnormalities in vascular development, double mutants were generated (Figure 9A-B). However, these double mutants similarly were not visibly affected in vascular development. This could be caused by the high homology between G-class bZIP transcription factors; the overlapping expression domains of GBF1 and 2 (**Chapter 5**); and compensation by the increased expression of close family members upon the removal of one or more homologs (Figure 9D). To determine if GBFs play a role in auxin-dependent vascular development we next tested the auxin-responsiveness of the GBF double mutants. The *gbf1gbf3* double mutant shows less reduction in root growth in response to low levels of 2,4-D compared to the wildtype background (Figure 9C). This reduced auxin sensitivity was not found when we measured the transcriptional response to auxin: both single and double mutants showed increased induction of *ATHB*, *GATA20* and *TMO5* transcripts by auxin (Figure 9E). This indicates that *gbf1gbf3* roots have increased response to auxin. Finally, *ERF4* and *WRKY17* transcripts are not differentially induced by auxin between mutant lines, but their expression is higher in the *gbf1gbf3* double mutant (Figure 9E). Altogether, *gbf1gbf3* double mutants have altered auxin response, both in root growth and regulation of vascular genes. While the exact role of GBF proteins in auxin response and vascular development remains unclear, they do appear to play a role in the regulation of vascular gene expression.

## **Discussion**

In this chapter the function of candidate regulators that were identified in **Chapter 5** is further investigated. Overexpression of candidates in meristematic cells using the *RPS5A* promoter did not result in vascular defects. This could be because these proteins do not play a role in vascular development; because high overexpression results in embryo lethality; or because an additional signal is needed to control protein activity. By creating GR-fused overexpression lines we confirmed that embryo lethality is probably not the cause of the lack of developmental phenotypes. DEX induction of LBD18 activity resulted in ectopic xylogenesis in cotyledons but not in the alteration of early vascular gene expression, indicating that LBD18 is involved in vascular differentiation as described previously (Soyano et al. 2008), but not vascular induction. The option of an additional signal being required for candidate function is more challenging to test, but maybe the candidate regulators act in modulating auxin response. Overexpression of *ASIL1*, *AT2G37520* and *GLP3* indeed altered response to auxin. Root growth on low concentrations of the auxin 2,4-D is less



*Description figure 8.* (A) Insert locations of the T-DNA lines used. (B) 24-day old plants of 3 sets of GBF double mutants, single mutants and background plants. (C) Relative root growth on auxin. Sensitivity to the auxin 2,4-D is measured by root elongation. Roots were moved to plates containing different concentrations of 2,4-D and increase in root length was measured 3 days later. Root growth on 0 nM 2,4-D is set to 100% for each line. (D) Relative expression levels of GBF1, GBF2 and GBF3 in the *gbf1gbf3* double mutant and single mutants. (E) Relative expression levels of GH3, ATHB8, GATA20, TMO5, WRKY17 and ERF4 under mock conditions (white-green) and fold induction upon when treated with IAA (grey).

reduced and auxin induction of some vascular genes is also cut back. This indicates that these candidate regulators share target genes with auxin signaling and potentially regulate gene expression together, with *ASIL1*, *AT2G37520* and *GLP3* negatively regulating auxin-dependent gene expression.

Several candidate regulators of vascular development appeared to act in parallel to auxin signaling. These proteins affect vascular gene expression by binding to vascular promoters either close to or independently of ARFs. We find that one set of candidate regulators, GBF proteins, directly interact with MP. GBF1 and GBF2 can interact with the DNA binding domain (DBD) of MP but also with the DBD of other ARFs. Previously interactors of ARF7 and ARF6/8 were found to affect auxin response by binding close to ARFs and interacting with the ARF PB1 domain (Ripoll et al. 2015, Shin et al. 2007, Varaud et al. 2011). In addition to the GBF-ARF interaction, G-boxes and AuxREs were found close together in several vascular promoters, indicating that these proteins could regulate expression together. Promoter truncations indeed indicated that these motifs contribute to expression level in the vascular bundle and hint that the G-box modulates gene expression. However, other bZIPs and bHLH transcription factors can also bind to the G-box motif (Kim et al. 2016, Oh et al. 2012). While ChIP-qPCR confirmed GBF binding to G-boxes in the promoters of *ERF4* and *WRKY17*, we were not able to confirm GBF binding in *TMO5* and *GATA20* promoter sequences. In conclusion, GBF1 and GBF2 can interact with ARFs and can bind to G-boxes in some vascular promoters, these G-boxes together with AuxREs contribute to the vascular expression of these promoters.

No vascular defects were observed for either GBF overexpression lines or single or double knockout mutants. While *p35S::GBF* and *pRPS5A>>GBF1-SRDX* (**Chapter 4**) lines resulted in changes in leaf appearance, no clear vascular defects were found. Because of the already ubiquitous expression of GBFs, it is likely that overexpression does not equal overactivation and some signal might be required to induce ectopic GBF activity. The specifics of such a signal remain unknown but previous experiments indicated that redox potential affects GBF DNA-binding (Klimczak 1992, Shaikhali et al. 2012). It should be noted that in general, the processes that are regulated by auxin can not simply be induced

by providing more external auxin. In part, this is probably due to the strong feedbacks in auxin-dependent gene regulation (Dreher 2006, Okushima 2005, Sauer et al. 2006). Auxin treatment will activate ARFs, but these in turn activate expression of their own Aux/IAA inhibitors. Therefore, an interesting future direction would be to test if GBFs and ARFs together are sufficient to induce vascular gene expression and vascular tissue specification. This could be achieved by misexpressing both GBF and e.g. MP, potentially even the auxin-independent MPΔPB1 (**Chapter 4**). Similarly, for the obligate TMO5/LHW bHLH heterodimer, neither induces clear defects when misexpressed, but joint misexpression is highly potent in inducing cell divisions (De Rybel et al. 2013).

The double loss of function mutants in GBF genes did not show defects beyond a very mild change in auxin-dependent root growth. Here, it is very likely that functions are obscured by genetic redundancy among the closely related G-class bZIP factors (Dröge-Laser et al. 2018). Differential response to auxin was observed for one of the GBF double mutant s (*gbf1gbf3*), but only a marginal difference. In addition, in the *gbf1gbf3* double mutant expression of *ERF4* and *WRKY17* is higher and auxin treatment increases *ATHB*, *GATA20* and *TMO5* expression levels more strongly than in the background. These findings suggests that GBFs contribute to the regulation of several vascular marker genes. Mutation of several other G-class bZIP genes simultaneously could reveal a more distinct function in vascular tissue development.

In summary, the approach used in this thesis towards identifying new regulators of vascular gene expression succeeded in isolating proteins that bind vascular genes *in vivo*, and participate in auxin-dependent gene regulation. Their role in establishing vascular tissue identity however, remains to be established.

## Material and Methods

### Plant material, growth conditions and treatments

Misexpression lines were generated by introducing UAS-gene constructs into a background containing the pRPS5A-GAL4 driver. pRPS5A-gene-GR and promoter truncation constructs were transformed into the Col-0 wildtype background. Insertion lines (*gbf1* SALK\_027691, *gbf2-1* SALK\_206654, *gbf2-2*, SALK\_205706, *gbf3* SALK\_067963) were obtained from the Arabidopsis Biological Resource Center (ABRC).

Plants were grown at 21 °C under standard long-day (16:8h light:dark) conditions.



Arabidopsis seeds were surface-sterilized, plated on ½ MS plates and underwent 2 days of stratification at 4 °C before being placed in the growth chamber. For antibiotic selection seedlings were initially grown on plates containing phosphinotricin or kanamycin and transferred to plates without antibiotics after 7 days of growth. Seedlings were transferred to soil after emergence of the first true leaves and then continued growth under the same conditions. Leaves were cleared by incubation in methanol for several hours after which methanol was replaced by ethanol. Leaves were subsequently rehydrated and cleared with chloral hydrate.

Dexamethasone treatment was performed either by letting seeds germinate on plates containing 20 µM DEX or by transferring 4 day old seedlings to DEX plates. Seedlings for expression analysis in response to DEX treatment were moved to plates containing 20 µM DEX and/or 10 µM CHX or plates containing DMSO for 1 hour before material was harvested. Root growth in response to auxin was determined by transferring 4 day old seedlings to plates containing 0, 10, 20 or 40 nM 2,4-D. Root length at transfer was marked on the plate, after 3 days of growth pictures were taken of the roots and the NeuronJ plugin in ImageJ was used to trace root length (Popko et al. 2009, Schneider et al. 2012). Auxin treatment for expression analysis was performed by transferring seedlings to plates containing 10 µM NPA for 12 hours of NPA pretreatment before transferring those seedlings to plates containing 1 µM IAA and 10 µM NPA for 1 hour after which root material was harvested (Liao et al. 2015).

### Cloning

All primers used for cloning can be found in Supplementary Table 1. UAS overexpression constructs were cloned by introducing the amplified cDNA sequence without stop codon into a modified pPLV32\_v2 backbone containing a Myc tag using SLICE cloning (Wendrich et al. 2015, Zhang et al. 2014b). DEX-inducible overexpression constructs were generated using stitch PCR to fuse the cDNA with the GR coding sequence and introducing the fragment into pPLV28 (Aoyama & Chua 1997, De Rybel et al. 2011). 35S overexpression constructs were generated by introducing the cDNA sequence into a modified pPLV26 containing c-terminal YFP. Truncated promoters were introduced into the pPLV04\_v2 backbone. These beforementioned constructs were all introduced using the simplified flora dip method (De Rybel et al. 2011). BiFC constructs were generated by introducing amplified cDNA sequences into modified pPLV26 vectors containing NtYFP or CtYFP either before or after the insertion site.

### Expression analysis



Plant material for expression analysis was flash frozen in liquid nitrogen and ground using a Retch machine. RNA isolation was performed using TRIzol reagent (Invitrogen) and an RNAeasy kit (Qiagen). cDNA synthesis was performed on 0.5 µg total RNA using the iScript cDNA Synthesis kit (Biorad). iQ SYBR Green Supermix (Biorad) and a CFX384 RT-PCR detection system were used to perform qRT-PCR. Each reaction was performed in triplicate and qBase software was used for data analysis, gene expression levels were normalized using *CDKA* and *GAPC* (Hellemans et al. 2008). Primers used for qPCR are listed in Supplementary Table 1.

### Confocal microscopy and Split-YFP/BiFC assays

Confocal imaging was performed on a Leica SP5 II system equipped with Hybrid Detectors. Roots were counterstained with 10 µg/mL propidium iodide. GFP, YFP and PI were excited at 488, 504 and 514 nm, and detected between 500-535 nm, 525-600 and 630-700 nm, respectively.

Split-YFP was performed by infiltrating *Nicotiana bentamiana* leaves with *Agrobacterium tumefaciens*. *Agrobacterium* containing BiFC plasmids were grown overnight in LB containing 20 mg/L gentamycin, 50 mg/L kanamycin, 25 mg/L rifampicin and 2 mg/L tetracyclin. After centrifugation the bacterial pellet was resuspended in MMAi (5 g/L MS salts, 2 g/L MES, 20 g/L sucrose, pH 5.6, 0.2mM acetosyringone). Infiltration samples were mixed 1:1 at a total OD<sub>600</sub> of 0.8 and then incubated at room temperature for 2 hours and subsequently infiltrated into the underside of tobacco leaves using a 1 mL syringe. Two days after infiltration leaf sections were cut and imaged using the confocal microscope. Positive controls were designed based on known interactions: GBF homodimerization, ARF homodimerization and interaction with IAA. Both empty vector controls and TMO5 were used as negative controls. LHW was included as a positive control for TMO5.

### Arabidopsis cell suspension cultivation and transformation

Wild type *Arabidopsis Landsberg erecta* and transgenic PSB-D cell suspension cultures were weekly maintained in MSMO medium (4.43 g/liter MSMO (Sigma-Aldrich), 30 g/liter sucrose, 0.5 mg/liter α-naphthaleneacetic acid, 0.05 mg/liter kinetin, pH 5.7, adjusted with 0.1 M KOH) in the dark at 25°C gently shaking at 130rpm. Cells were sub cultured every 7 days in a 1:10 dilution. Transformations were conducted without callus selection as described by (Van Leene et al. 2007). In brief, *Agrobacterium* and PSB-D cells were co-cultivated in MSMO medium supplemented with 200 µM 4'-Hydroxy-3',5'-dimethoxyacetophenone (Sigma-Aldrich). After two days, PSB-D cells were washed twice in MSMO medium

containing 25 µg/ml kanamycin, 500 µg/ml carbenicillin, and 500 µg/ml vancomycin (MSMO-KVC) for 10 minutes at 800 rpm. Cells were subsequently weekly maintained in MSMO-KVC. After two weeks cells were weekly maintained in MSMO containing only 25 µg/ml kanamycin. Agrobacterium clearance was confirmed on a RGTK plate.

#### Affinity purification and sample preparation of mass spectrometry

For affinity purification either 4 g root material or 50 ml of 3 day old transgenic PSB-D cell suspension cultures was used. Material was directly frozen in liquid nitrogen and ground to a fine powder. For protein extraction, ground cells were suspended in 2 volumes lysis buffer (50mM Tris pH8, 150mM NaCl, 2mM MgCl<sub>2</sub>, 0.2 mM EDTA, 0.2%NP40, 20% Glycerol, 10mM DTT and 1xCPI) and sonicated in a Biorupter (Diagenode) at 4°C for three cycles (15s ON, 60s OFF). After sonication, lysate was spun down for 30 minutes at 14.000xg at 4°C. Supernatant was collected and protein concentration measured by the Bradford assay (Bio-rad).

Affinity purifications were conducted in technical triplicate. For each reaction 50µl GFP-TRAP agarose beads (Chromotek) were equilibrated by washing beads three times in lysis buffer for 2min at 2000xg at 4°C. For each replicate 10mg of whole cell lysate was used and incubated with beads at 4°C while rotating head over tail. After 90 minutes beads were sedimented by centrifugation for 2min at 2000xg at 4°C, washed twice in lysis buffer, twice in lysis buffer without NP40 and trice in 50mM Ammonium Bicarbonate (ABC). After the last wash, bead precipitated proteins were alkylated in 50mM ABC supplemented with 50mM Acrylamide (Sigma-Aldrich) and incubated in the dark at 25°C for 30 minutes. After alkylation, on-bead trypsin digestion was performed by using 0.35µg trypsin (Roche) and incubated overnight at 25°C. After overnight digestion peptides were desalted and concentrated by C18 Stagetips as described previously (Rappsilber et al. 2007) with the modification that extra 1mg C18 Lichoprep beads were added. After C18 desalting peptides were vacuum dried and resuspended in 50µl 0.1% formic acid.

#### LC-MS/MS and data analysis

Peptides were applied to online nano LC-MS/MS mass spectrometer (Thermo Scientific) using a 60 minute acetonitrile gradient from 5-50%. Spectra were recorded on a LTQ-XL mass spectrometer (Thermo Scientific) and analysed according to (Wendrich et al. 2017). Maxquant output Proteingroups.txt was filtered in Perseus v1.6.2.3.. Volcano plots were generated in R and further visualized in Adobe Illustrator.

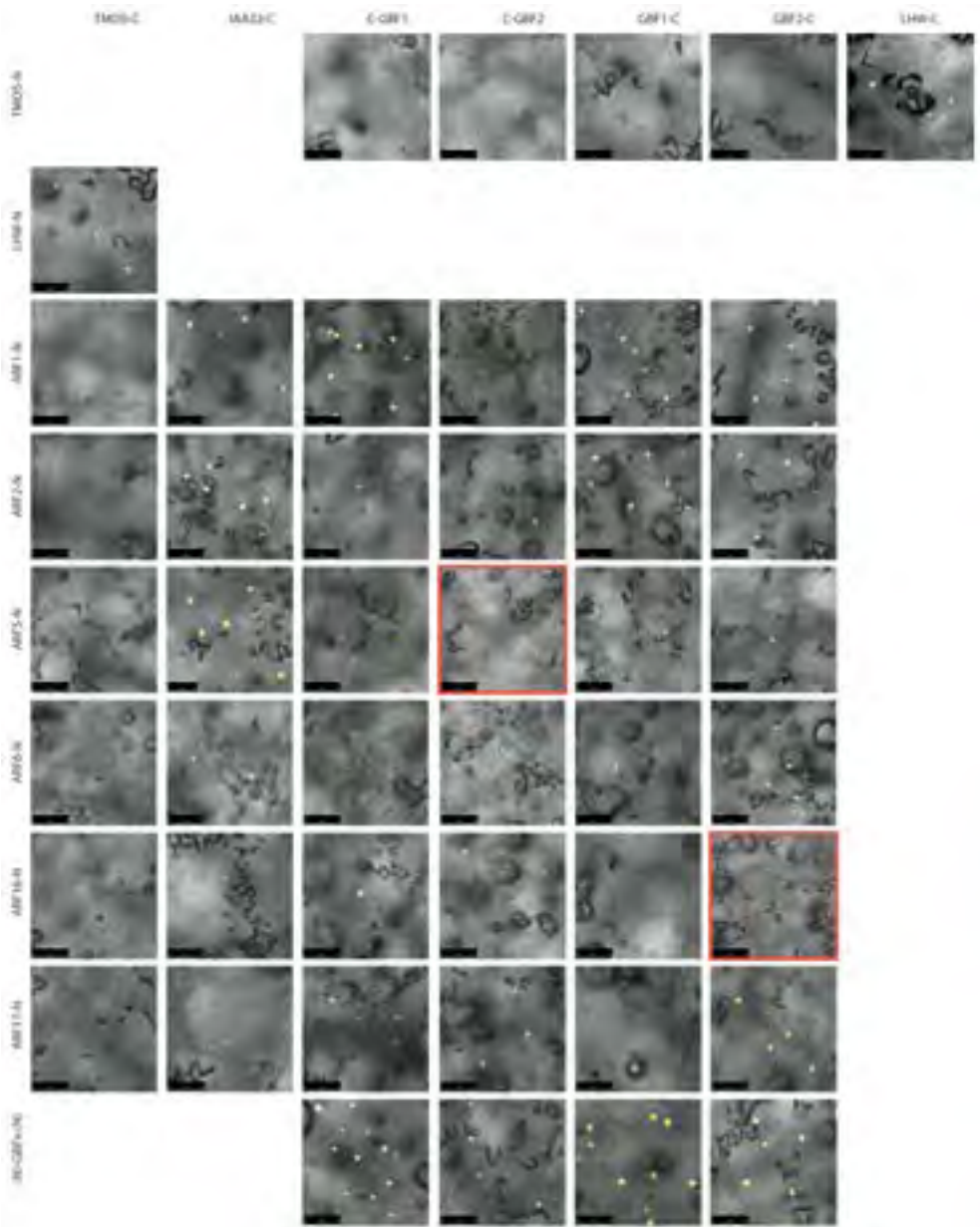
### Motif analysis

Analysis of potential binding sites presence was performed with position weight matrices taken from Plant TFDB database (Jin et al., 2017) for GBF3 (MP00318), bZip16 (MP00291) and bZip68 (MP00173). According to their occurrence we checked if some of them could be ARF partners with the MCOT tool (Levitsky et al., 2018) using data on ARF binding regions from Dap-Seq analysis (O'Malley et al., 2016) for following transcription factors ARF2 (GSM1925138, GSM1925826) and ARF5 (GSM1925827). We took upstream regions [-1500;+1] of 27202 protein-coding genes including 16 vasculature-related genes and overlapped them with Dap-Seq peaks of mentioned above transcription factors (GSE60141). MCOT applies the recognition model of Position Weight Matrix for mapping motifs in peaks. For each matrix, MCOT uses five thresholds  $\{t_1, \dots, t_5\}$  according to the unified set of five expected false positive rates for a whole-genome dataset of promoters,  $\{5E-4, 3.33E-4, 1.9E-4, 1.02E-04, 5.24E-5\}$ . The profile of the most stringent hits contains matrix scores  $t \geq t_1$ , the next profile comprises PWM scores in the range  $t_2 \geq t > t_1$ , etc.

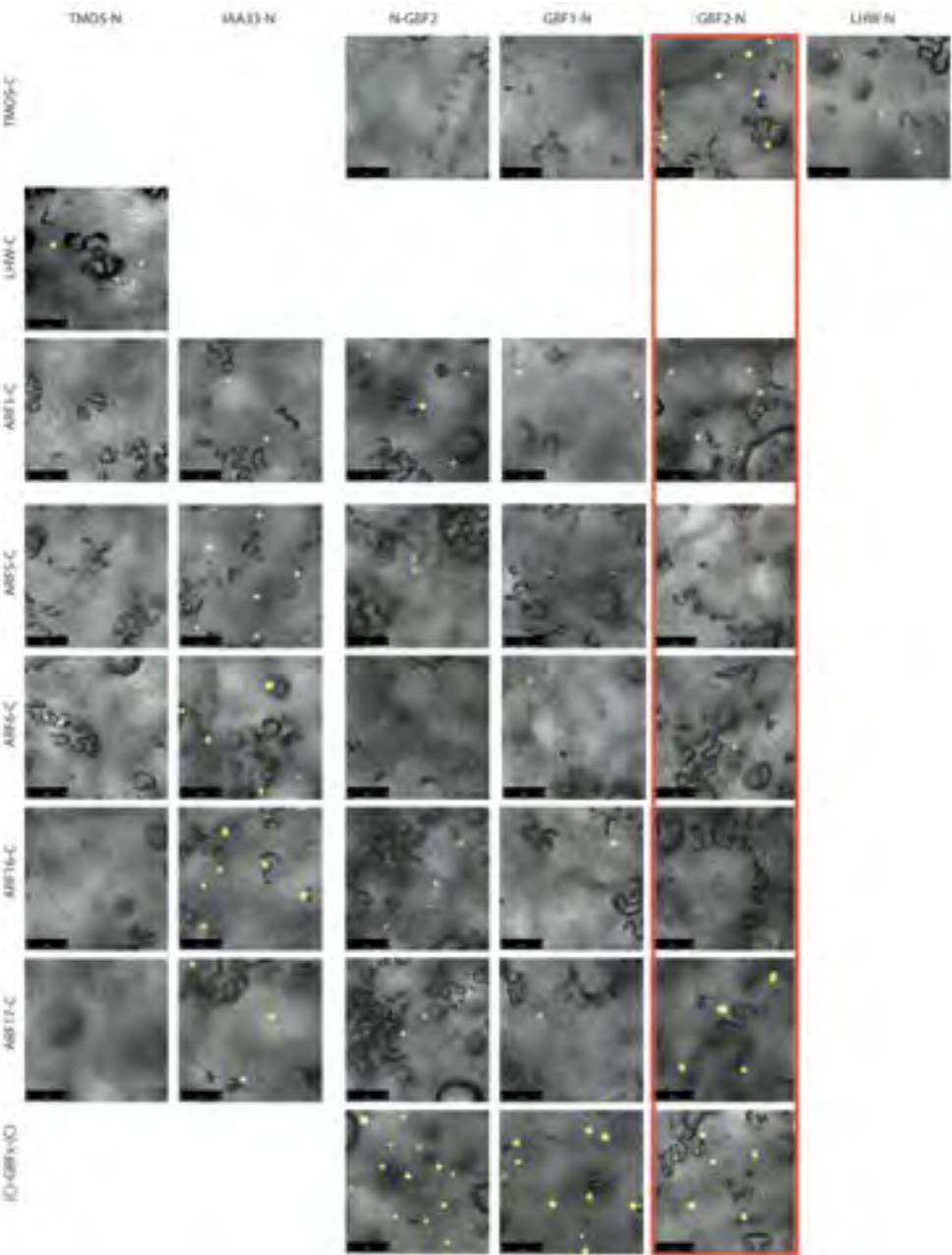
### ChIP-qPCR

ChIP-qPCR was performed on Arabidopsis cell cultures using a protocol adapted from (Gendrel et al. 2005). 3-4 grams of filtered cell culture material was used as input material. After crosslinking and DNA fragmentation, the sample was split and GFP-Trap beads (Chromotek) were used to pull down GBF-YFP complexes while Myc-Trap beads (Chromotek) were used for the negative control sample. qRT-PCR was performed using primers listed in Supplementary Table 1. Ct values were then used to calculate fold enrichment and relative fold enrichment compared to the control regions.

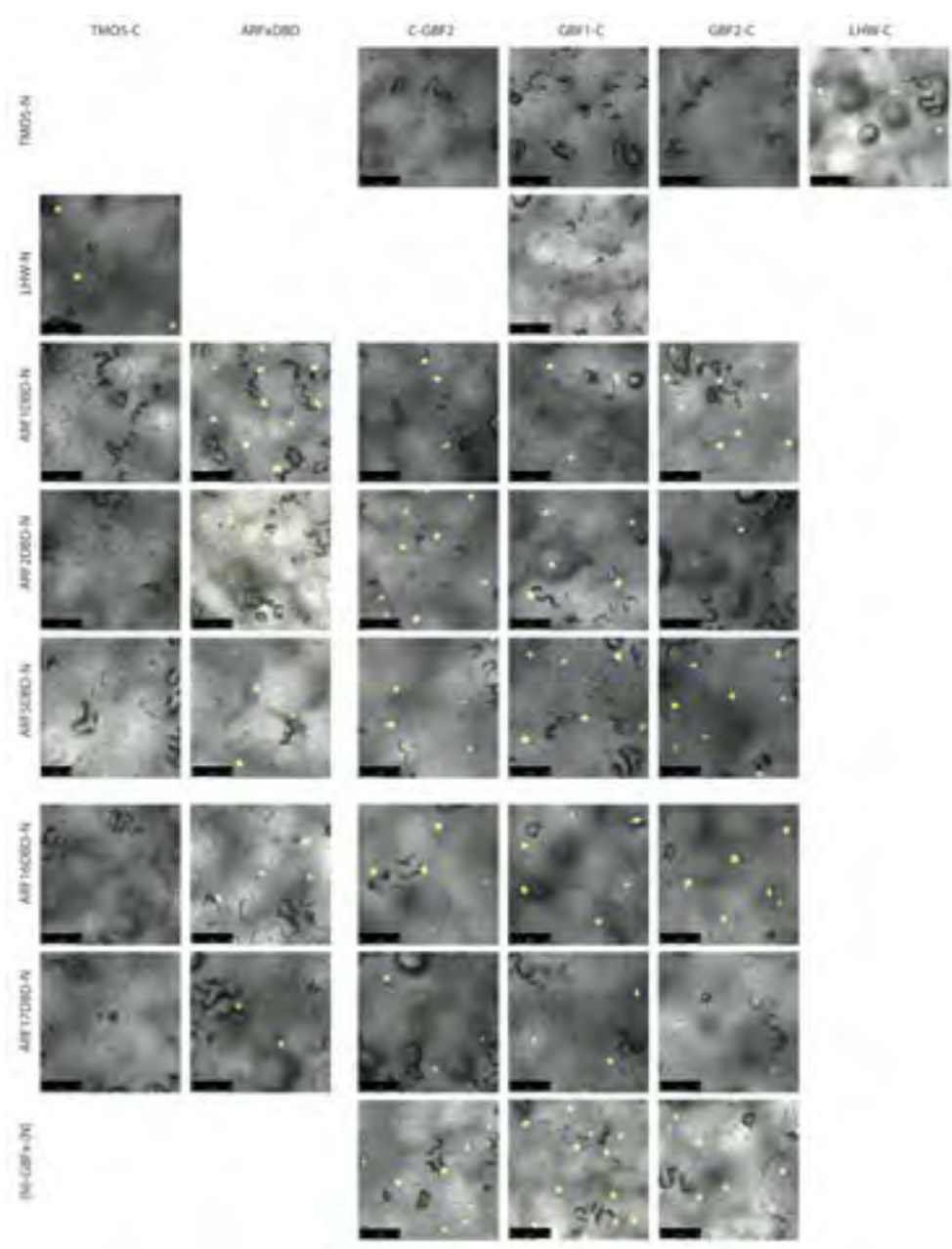
Supplementary Figures and Tables



**Supplementary Figure 1-1 Split-YFP experiments confirm interaction of GBF1 and GBF2 with ARF5/MP.** Split-YFP experiments performed using tobacco leaves to confirm GBF-ARF interactions. Interactions GBF1/2-CtYFP and ARF-NtYFP. TMO5 was used as a negative control, homodimerization was used as a positive control for GBF and IAA33 was used as a positive control for ARFs. LHW was used as a positive control for TMO5.

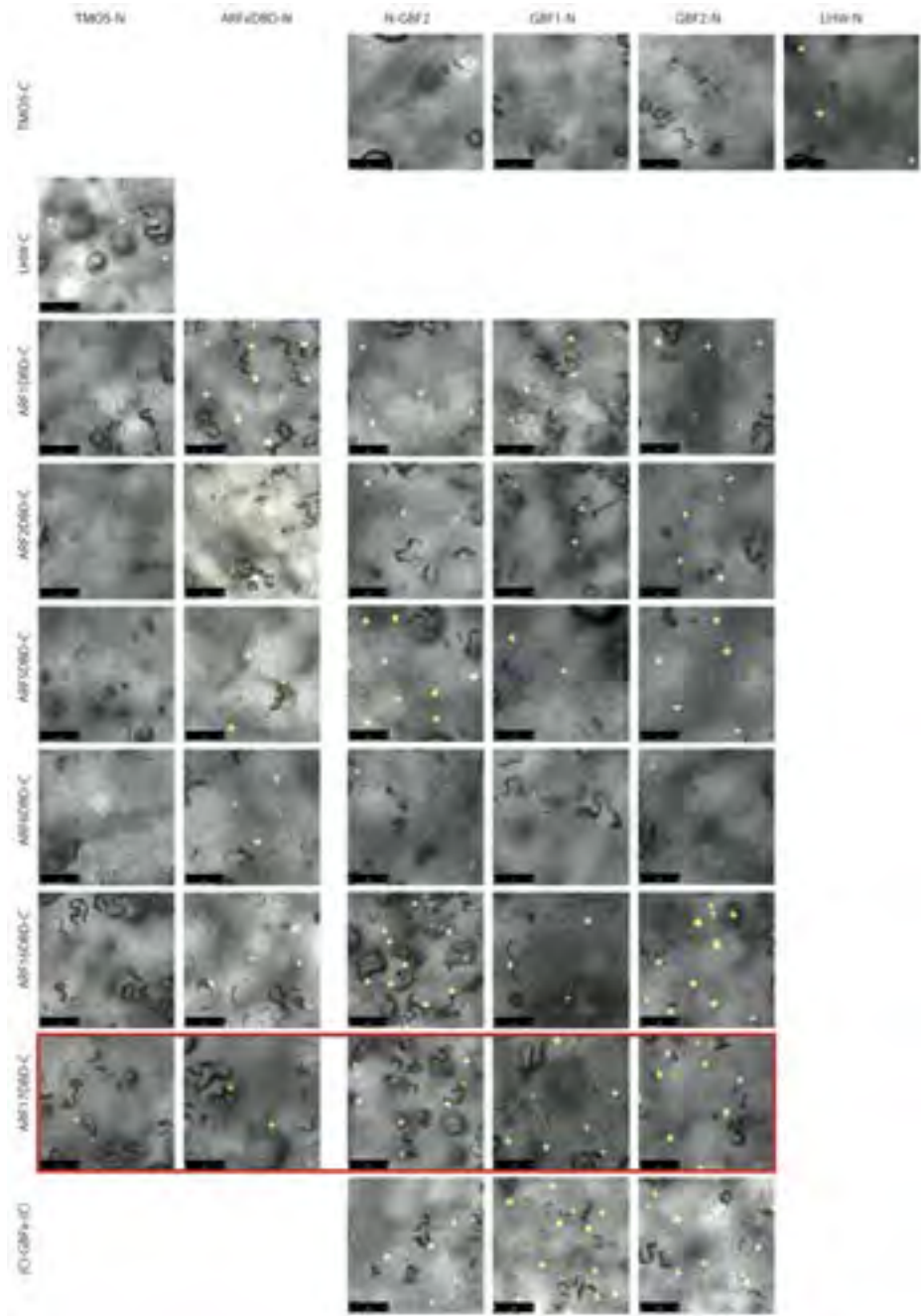


**Supplementary Figure 1-2 Split-YFP experiments confirm interaction of GBF1 and GBF2 with ARF5/MP.** Split-YFP experiments performed using tobacco leaves to confirm GBF-ARF interactions. Interactions GBF1/2-NtYFP and ARF-CtYFP. TMO5 was used as a negative control, homodimerization was used as a positive control for GBF and IAA33 was used as a positive control for ARFs. LHW was used as a positive control for TMO5.



**Supplementary Figure 1-3 Split-YFP experiments confirm interaction of GBF1 and GBF2 with ARF5/MP.** Split-YFP experiments performed using tobacco leaves to confirm GBF-ARF interactions. Interactions GBF1/2-CtYFP and ARFXdbd-NtYFP. TMO5 was used as a negative control and homodimerization was used as a positive control for GBF and for ARFs. LHW was used as a positive control for TMO5.





**Supplementary Figure 1-4 Split-YFP experiments confirm interaction of GBF1 and GBF2 with ARF5/MP.** Split-YFP experiments performed using tobacco leaves to confirm GBF-ARF interactions. Interactions GBF1/2-NtYFP and ARFXdbd-CtYFP. TMO5 was used as a negative control and homodimerization was used as a positive control for GBF and for ARFs. LHW was used as a positive control for TMO5.

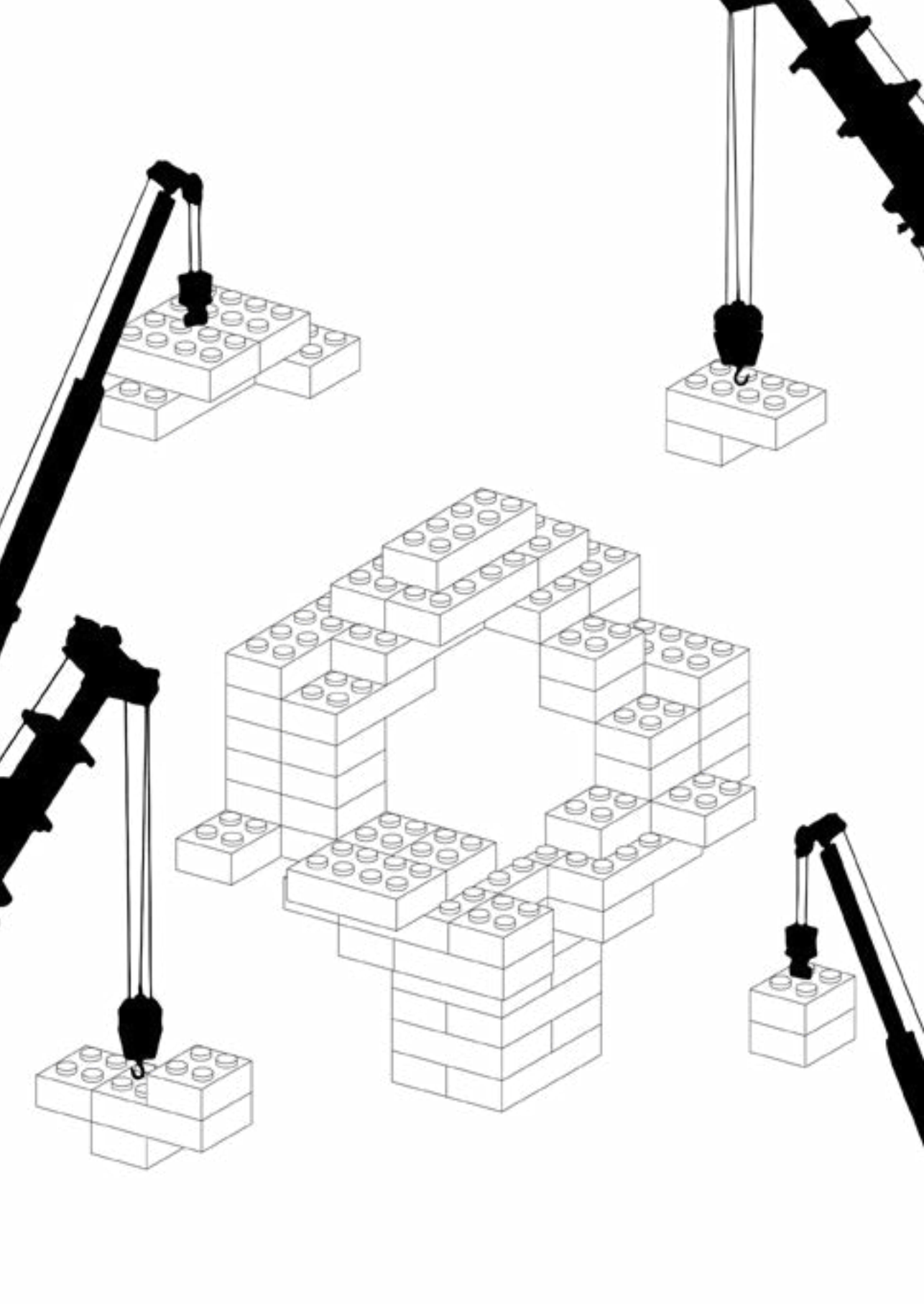


Supplementary Table 1: Primers used in this chapter

Cloning primers misexpression		
LBD18_GR	sense	TAGTTGGAATAGGTTTCATGAGCGGTGGTGGGAACACAATCAC
	antisense	ccaacactaccaccaccaccaccaccaccTCTAGACATAGTTGAGAC
AT3G53680	sense	agaagatgatgagagtgaagc
	antisense	TCCTGATACTCTCGGCTTGTAGC
BIFC		
GBF1	sense	ctagtggaaataggttcATGGGAACGAGCGAAGACAGATGC
	antisense	tatggagttgggttaattaATTGTTCCTTCACCATCTTTG
GBF2	sense	ctagtggaaataggttcATGGGTAGCAACGAAGAAGG
	antisense	tatggagttgggttaatacaGCTAGCCGCGACAGGATCG
TM05	sense	TAGTTGGAATAGGTTTCATGTACGCAATGAAGA
	antisense	GTATGGAGTTGGGTTCAATATAACATCGATTCACCATC
LHW	sense	TAGTTGGAATAGGTTTCATGGGAGTTTACTAAGAGA
	antisense	GTATGGAGTTGGGTTCCATTGAACAGCCACAGTAAC
ARF1	sense	TAGTTGGAATAGGTTTCATGGCAGCTTCCATCATTCTCT
	antisense	AGTATGGAGTTGGGTTCTCATCTTGATCCCGCATAG
	DBDanti	AGTATGGAGTTGGGTTCCagaccagatggaccagtggc
ARF2	sense	TAGTTGGAATAGGTTTCATGGCGAGTTCCGAGGTTTC
	antisense	AGTATGGAGTTGGGTTCTTAAGAGTTCCAGCGCTGGACA
	DBDanti	AGTATGGAGTTGGGTTCAACAGGACTCAAGCAGGAGG
ARF5	sense	TAGTTGGAATAGGTTTCATGATGGCTTCATTGTCTTG
	antisense	agtatggagttgggttcTGAACAGAGTCTTAAGATC
	DBDanti	AGTATGGAGTTGGGTTGctaccccaatcagtttcaac
ARF6	sense	TAGTTGGAATAGGTTTCATGAGATTATCTTCAGCTGG
	antisense	agtatggagttgggttcGTAGTTGAATGAACCCCAAC
	DBDanti	AGTATGGAGTTGGGTTCAAGGCCATGGAAGATGGGAG
ARF16	sense	TAGTTGGAATAGGTTTCATGATAAATGTGATGAATCC
	antisense	AGTATGGAGTTGGGTTCTTATACTACAACGCTCTCAC
	DBDanti	AGTATGGAGTTGGGTTGatcagattgttgtatctg
ARF17	sense	TAGTTGGAATAGGTTTCATGTCAACCGCGTCGGCAAC
	antisense	AGTATGGAGTTGGGTTCTTAACCTGGGAGCTAGAAC
	DBDanti	AGTATGGAGTTGGGTTTccactcaagaacctctctc
Genotyping		
SALK LB		ATTTTGCCGATTTCGGAAC
SALK_027691	WT LB	TATTATGTTCAAGCAGTCCCGG
	WT RB	TCGTTGAGTGTGGTTTCG
SALK_206654	WT LB	TGGTGATCTTGTGTGCTTC
	WT RB	TGGTGGAGTTTATGCTCATCC
SALK_205706	WT LB	TGGATATGGTGCTCCATAAGG
	WT RB	CGCTCTGTTTCTCGAGAAAG
SALK_067963	WT LB	ATAGCTGCCCAATCAGGGTAG
	WT RB	CTCAAGGAGCTTTCGGATTC

qPCR		
GAPC	sense	GAAGGGTGGTGCCAGAAGGTT
	antisense	AGGGGAGCAAGGCAGTTAGTGG
CDKA	sense	ATTGCGTATTGCCACTCTCATAGG
	antisense	TCCTGACAGGGATACCGAATGC
GBF1	sense	ATGGTGCTCTCATAGTG
	antisense	CCTGTTCTGTTGATTGG
GBF2	sense	CAATGTCAATAGCAATAAC
	antisense	CCAGTTGTATTACCATCA
GBF3	sense	CTTGCTATGTCTTAGGAA
	antisense	CCATCAGTAGAACCATCA
GIG3	sense	GAGACCGCTCTCCATCTTATCTG
	antisense	GGCTGATGTTCCAGAGCTAGTG
ATHB8	sense	AACACCACTTGACCCCTCAACATCAG
	antisense	CACGCAACCAACAAGGCTTATCC
TMD5	sense	CGATAGAAGAAGCGTTAA
	antisense	CGATTCAACATCTTACTA
GATA20	sense	TACAACGGAGGTGGAAC
	antisense	GAAGTCGGACTTGCTCAC
ERF4	sense	GTGTTATCAGATCCGATGTC
	antisense	TCACAGGAGGAGGCTGAC
WRKY17	sense	TTCAGGCAAAATCAACAAA
	antisense	GCAAGAAAGATCGAAGAG
ChIP qPCR		
WRKY17 box	sense	ATTAGATCGAGCTGCAAAATG
	antisense	TTTACCACGGCAACTGAT
WRKY17 control	sense	GAGGTTACATTGACTTCT
	antisense	ATTAGTTAGTGGATGATAGA
GATA20 box	sense	TTGGTAATCTAAGAGAGA
	antisense	ATAAGTGTGTGTATCTG
GATA20 control	sense	TACCAATCCGATCTTGAT
	antisense	TGATTAACTCGCATCTTG
TMD5 box	sense	GGTTTGGCTATACGAAAC
	antisense	AGAAATTCATTGGCTGC
TMD5 control	sense	CACAATTTAAGGGTCGGAAA
	antisense	AATATAATTGACTCCACCATGT
ERF4 box2	sense	GCCAAATTAACAACCAAT
	antisense	AGAATGGATGAAGAGAGA
ERF4 box1	sense	AAAGATAAGTGAGGTAA
	antisense	TGTGATAGATAATTGAAGG
ERF4 control	sense	ACACCACCGTTGAGAAT
	antisense	TTGAATTTGCGGAAACTTTGTT

Cloning promoter deletions		
WRKY17_full	sense	TAGTTGGAAATGGGTTCGAACaataatttctctgtggagg
	antisense	TTATGGAGTTGGGTTCGAAGatgagaaccagaggag
WRKY17_reg1	sense	cttcaactcaatctcagcgtaagcaccgatttgactaaactcc
	antisense	ggagtttagtcaaatcgggtcttacggctgagattgagttgaag
WRKY17_reg2	sense	gacaatttatgagtcagccagaattagatcagttgccgtagtaaaagg
	antisense	ccttttaccacggcaactgactaattctggctgactcatabaattgtc
TMO5_full	sense	TAGTTGGAAATGGGTTCGAATgattttcacaaatttaagggtcgg
	antisense	TTATGGAGTTGGGTTCGAATttttggtttttttagttttttgggt
TMO5_reg1	sense	gattaaaagtaaaagtcctttttgggtcagtggtttgttttttttc
	antisense	gaataaaaaacaacacagaccccaaaaagacttttacttttaatc
TMO5_reg1a	sense	GTCTCTGGTCGGTCGACAGGTGAGTGTGTGTTTTTATTC
	antisense	GAATAAAAACAAACACTGACCTGTCGACCGACCAAGAGAC
GATA20_full	sense	TAGTTGGAAATGGGTTCGAATaccaatccgactctgaccc
	antisense	TTATGGAGTTGGGTTCGAAGaaattgaagactacagatagag
GATA20_reg1	sense	gtcgttacttaagtttccacagtttgaacttgtaac
	antisense	gttacaagttacaactgtggaacttaagtaacgac
GATA20_reg2	sense	gtgaaggagcttggtatctaaagaaaaactgagatcacacaac
	antisense	gtgtgtgtatctgcagttttcttagattaccaagctcctttcac
GATA20_reg2a	sense	CCTTAGAAAACCGTGACATTGTCACGCTCTTTTGACCAACCCCG
	antisense	CGGGGTTGGTCAAAGAGGCGTGACAATGTCACGGTTTTCTAAGG
ERF4_full	sense	TAGTTGGAAATGGGTTCGAATCAACTTATGTGCAGCAGC
	antisense	TTATGGAGTTGGGTTCGAATctcggatagatagattagag
ERF4_reg1	sense	caaaattctttgaagaggaaagaaagataagtggaagtaaaaaag
	antisense	cttttttacctccacttacttttttcttcttttcaagaattttg
ERF4_reg2	sense	ccattctccacgctgcgactatcacatcttttaaaactc
	antisense	gagttttaagatgtatagtcgcacgcgtggagaaatgg



# Chapter 7

## **Parallels in vascular tissue specification across tissues and species**

Margot E. Smit<sup>1</sup>, Sumanth Mutte<sup>1</sup>, Taco Jesse<sup>2</sup>, Ilse Wolthuis<sup>2</sup>, Paul van Drongelen<sup>2</sup>, Peter de Heer<sup>2</sup>, Petra van Ham<sup>2</sup>, Gerald Freymark<sup>2</sup> and Dolf Weijers<sup>1</sup>

1. Laboratory of Biochemistry, Wageningen University, Stippeneng 4, 6708WE Wageningen, the Netherlands

2. Rijk Zwaan Breeding B.V., Eerste Kruisweg 9, 4793 RS Fijnaart, The Netherlands

## Abstract

Vascular development starts during embryogenesis but is reinitiated as the plant undergoes developmental transitions. New vascular bundles are formed when new organs develop but also in response to wounding. Studies in *Arabidopsis* have revealed parallels in the mechanisms that control vascular development. For example, several early vascular marker genes that are active in the embryo are also induced upon grafting. Separating the pathways that control vascular development from those that regulate other morphological transitions is challenging in most tissue contexts but can be done in the graft. While compatible grafts develop vascular connections, incompatible grafts lack or lag behind in this development. We have identified several compatible and incompatible grafting combinations in cucumber and used an RNAseq approach to identify transcriptome differences between a successful and an unsuccessful graft. Upon grafting genes are upregulated whose *Arabidopsis* homologs are involved in auxin response and developmental reprogramming. These findings further underline the parallels in vascular tissue specification across species. In addition we find that most graft-induced transcripts originate from the rootstock and that in incompatible grafts the rootstock appears to be contributing less to transcript abundance. Thus it appears that rootstock activation and grafting success are correlated. These results could form a starting point both for identifying factors that control vascular development and for developing molecular markers for grafting success.

## Introduction

Plants have extraordinary developmental plasticity and, unlike most animals, they continue changing shape and growing new organs as they age. In this thesis, we have focused on embryogenesis, during which vascular identity is established for the first time. However, later during the plant life cycle, new vascular bundles are also formed. When new organs are initiated and grow, new vascular tissues connect these to the existing vascular system. Superficially, the *de novo* establishment of vascular tissue during the development of new organs appears to be similar to the formation of vascular tissues in the embryo, involving overlapping genetic pathways and gene expression markers (De Rybel et al. 2016, Scarpella 2017). For example, new vascular networks in leaves rely on auxin flux and perception, and involve many of the same pathways and markers as vascular development in other tissues (Donner et al. 2009). However, development of vascular bundles during organogenesis is coordinated with many other morphological changes, which make it challenging to study the genetic components controlling of *de novo* vascular tissue formation during organogenesis. The new organ tightly controls its shape, expansion and differentiation, involving numerous gene activities. Because there are no mutants that form new organs that entirely lack vascular development, it is challenging to separate factors controlling vascular identity from those regulating other aspects of organogenesis.

An extreme case of the developmental flexibility typical for plants is the regeneration of tissues after injury. The ability to generate new tissues is also used agronomically, in the grafting process. Grafting is performed to combine a strong root system (rootstock) with a desirable shoot system (scion), for example to combine resistance to soil-borne pathogens from one species (or variety) with high fruit yield from another species or variety (Lee & Oda 2010). Critical to grafting success is the reconnection of the vascular systems of the two severed parts, for which cells need to be reprogrammed towards vascular identity, followed by the differentiation of new bundles. Therefore, grafting represents an interesting case of *de novo* vascular tissue formation, similar to vascular development in new organs and in the embryo. Indeed, analysis of gene expression markers and transcriptome analysis on graft junctions in *Arabidopsis* has shown that graft development involves the accumulation of auxin, similar to vascular patterning in other tissues (Melnik et al. 2015). In addition, provascular (*TMO6*) and cambial (*WOX4*) genes were found to be induced during graft reconnection (Melnik et al. 2018). Although additional processes, such as wound response and callus formation, do occur in the graft junction, the grafting process allows the separation of the process of vascular development from organogenesis. Given that incompatible grafts undergo wound response and callus formation without vascular development (Aloni et al.



2010, Jeffree & Yeoman 1983), one should be able to dissect these processes when compatible and incompatible grafts are compared. Such a comparison, on a transcriptome level, has not yet been performed, to our knowledge.

While grafting is often used in horticulture and crop production, it is still unclear what determines whether a graft will succeed (Aloni et al. 2010, Pina et al. 2012). As a rule of thumb, more closely related species are more likely to form successful grafts, but the precise determinants of grafting success remain elusive (Goldschmidt 2014, Moore & Walker 1983). Cucumber (*Cucumis sativus*) is one of the crops that is often grafted when grown in the greenhouse (Lee & Oda 2010) and for which grafting success is usually assumed, but not systematically explored. Understanding the genetic components that control vascular development, and as a result grafting success, can contribute to the increase of grafting efficiency. By investigating the parallels between vascular development in embryo and graft it will be possible to identify genes that are needed for vascular initiation and thus contribute to grafting success. Molecular markers linked to these vascular related genes, either their regulation or function, can in the future help identify compatible grafting combinations.

In this chapter we start by focusing on the similarities in regulation of vascular genes in *Arabidopsis* embryos and grafts by looking at available transcriptomics data (Melnik et al. 2018). After identifying such parallels, we perform RNAseq analysis of empirically defined incompatible and compatible grafts of cucumber to identify genes associated with the formation of vascular connections during graft development. We identify several genes that are differentially expressed between incompatible and compatible grafts. The expression origins of these genes and the developmental programs they potentially control point to parallels in *Arabidopsis* vascular development that can with future experiments be used to better understand and predict grafting success.

## Results

### Vascular markers are induced below the graft junction in *Arabidopsis* grafts

In **Chapter 3**, we have established a set of *Arabidopsis* genes that mark vascular cells during embryogenesis and in the root. To better understand the parallels between vascular initiation in an embryo and in a graft, we looked at the behavior of these genes during vascular reconnection in graft development. A valuable transcriptome dataset has previously been published, where grafted and ungrafted plants are followed over time (Melnik et al.

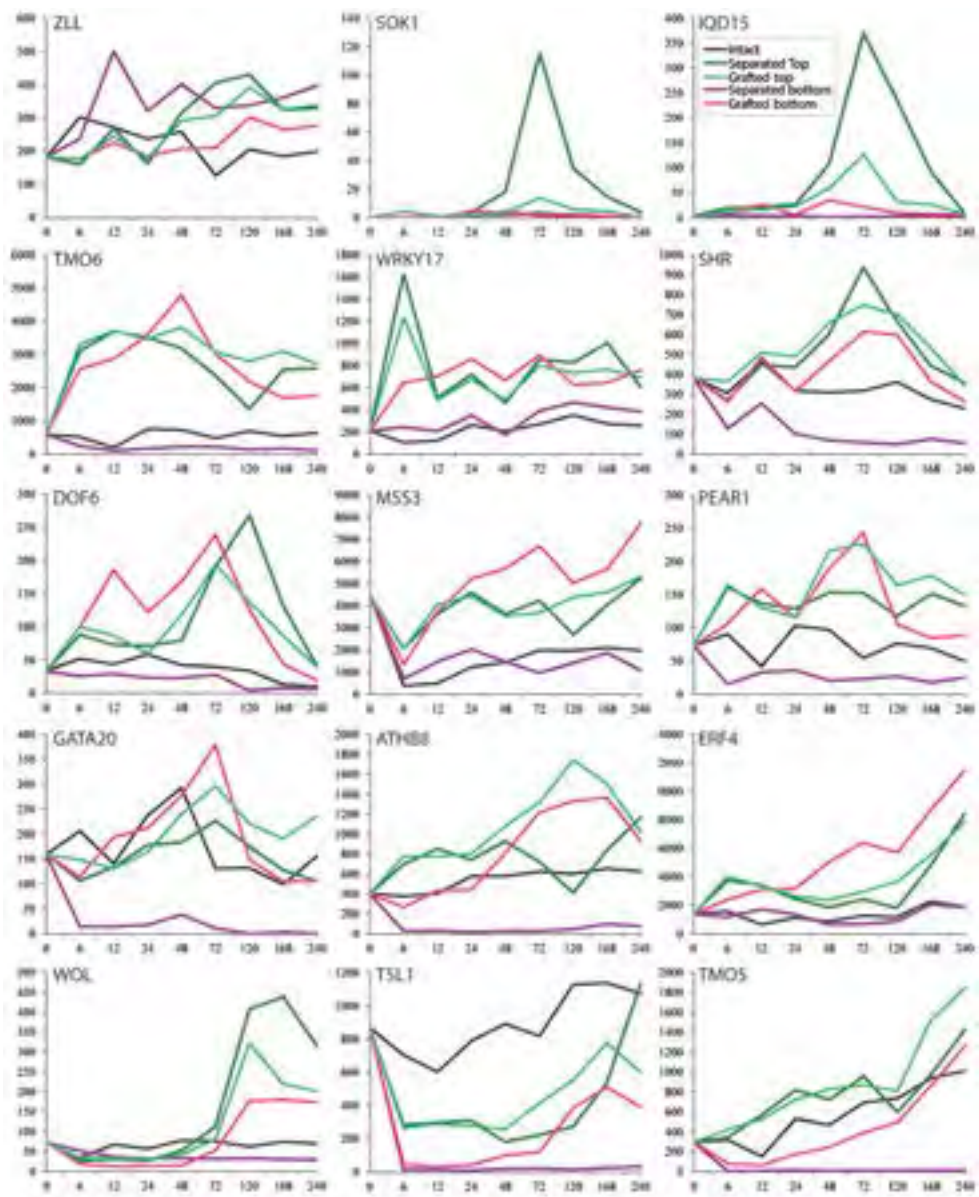


**Figure 1: Induction of vascular genes upon grafting.**

Expression profiles over time of vascular genes after cutting or grafting of Arabidopsis compared to intact seedlings (Melnik et al, 2017). Genes are organized based on pattern and speed of induction. Expression of several auxin inducible vascular genes is found in graphs in the top half of cut or grafted seedlings (green) and graft specific induction of vascular genes was found the bottom half of grafted seedlings (pink).

2018). In this experiment, Arabidopsis seedlings were cut at the hypocotyl and grafted with plants of the same genotype. The top and bottom part of the graft were collected at regular

intervals over the next few days until after vascular connections were formed. As a control, samples were also collected from uncut seedlings and from cut but ungrafted seedlings, allowing for the separation of wound-induced and graft-induced gene activity. We explored the regulation of the set of “embryonic” vascular genes (**Chapter 3**) in this dataset and found that several early vascular genes are upregulated in the scion upon cutting: both grafted and ungrafted tops have increased vascular gene expression (Figure 1). This is likely the result of auxin accumulation above the graft, given that several of the vascular marker genes were originally identified as auxin-dependent genes (Donner et al. 2009, Schlereth et al. 2010). The differences between the formation of a vascular connection and wound response become clear when comparing ungrafted and grafted bottoms. Most of the vascular marker genes that are induced by grafting were induced in the bottom half of the graft, but not or barely in the cut but ungrafted bottom half (Figure 1). While the timing on this response varies, the induction of most vascular genes occurs before xylem and phloem transport are re-established at 6-8 days and 3-4 days respectively (Melnik et al. 2015). This indicates that the formation of vascular bundles in the graft is accompanied by the induction of genes, that start their vascular expression during early embryogenesis, in the bottom half of the graft. This demonstrates a parallel between the two processes and shows that a common genetic program may be shared by both.

#### Cucumber as a model for graft development

A successful graft requires that physical and vascular connections are established between rootstock and scion. Grafting success depends on many factors including plant age, fitness and growth conditions. In addition, success depends on compatibility between varieties or species (Irisarri et al. 2015, Moore & Walker 1983). The available Arabidopsis dataset did contain controls for the wounding response (cut, but not grafted), but not for an incompatible graft, analogous to those found in horticultural practice. To allow such an analysis, we explored grafting in cucumber. Ten genotypes of *Cucumis sativus* representing different types of cucumbers, gherkin or rootstock material from the breeder Rijk Zwaan were selected and reciprocal grafting combinations were made for varieties with similar stem diameter (Figure 2A,B). Most grafts had a high success rate, but several combinations were consistently unsuccessful, leading to wilting of the grafted scion (Figure 2C). Grafting of scion I on rootstock J (IJ) or scion E on rootstock G (EG) resulted in only 20% of grafted plants surviving (Figure 2B). This is not due to a principal incompatibility between these genotypes, because the reverse grafts between the same varieties led to a 70-80% success rate (n=20; Figure 2B). In the case of the EG graft, the incompatibility also did not reflect general poor performance of the E scion or G rootstock, because each performed well in

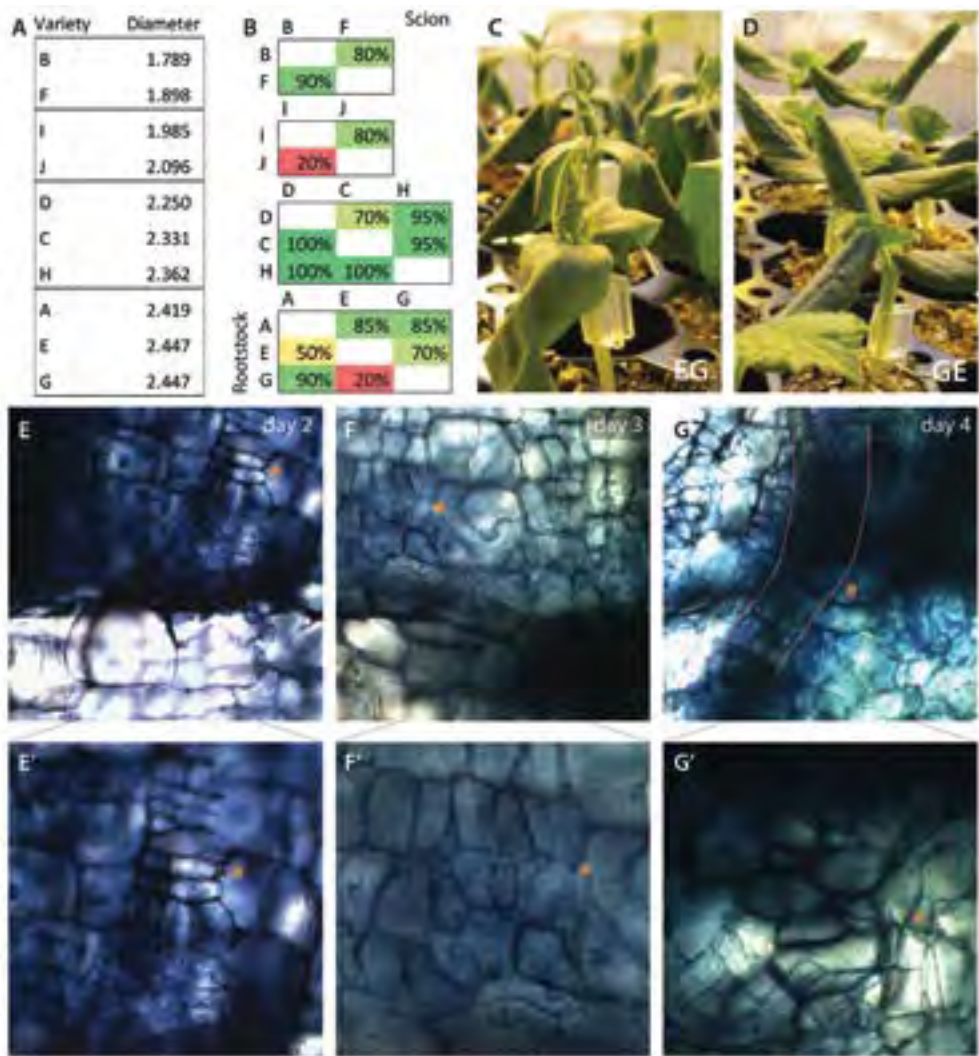


**Figure 2: (In)Compatible of cucumber grafting combinations and speed of reconnection.** (A) Overview of the hypocotyl diameter of the 10 cucumber varieties. (B) Grafting success of different combinations of cucumber varieties, n=20. (C-D) Grafted EG (C) and GE (D) seedlings 6 days after grafting. (E-G) Sections of GE graft junctions. (E) Graft junction 2 days after grafting, orange asterisk indicates new cell divisions above the graft junction, (E') shows a detail of (E). (F) Graft junction 3 days after grafting, orange asterisk indicates single differentiated xylem cells, (F') shows a detail of (F). (G) Graft junction 4 days after grafting, orange asterisk and line indicate newly formed xylem bundle connecting scion and rootstock, (G') is a different picture taken in the same graft junction that shows connected xylem cells.

these roles when combined with variety A. Combinations EG and GE were selected for further analysis, to better understand what makes a successful graft (Figure 2C,D).

While the timing of vascular reconnection in *Arabidopsis* grafts was reported in

(Melnik et al. 2015), it is not known when vascular tissues reconnect in a cucumber graft. To identify at which time point vascular connection was complete, junctions of EG and GE grafts were cleared and stained with toluidine blue before hand-sectioning. During sample preparation, older EG grafts often fell apart, likely a result of poor adhesion and connection. Sections of GE grafts revealed induction of cell division above the graft junction 2 days after grafting (Figure 2E). The first single differentiated xylem cells above the junction were observed at day 3 and at day 4 xylem bundles connecting scion and rootstock were visible. Thus, vascular reconnection is established earlier in cucumber grafts compared to *Arabidopsis* where xylem connections are completed after 6-8 days. This helps define a window for gene expression analysis prior to completion of the graft.

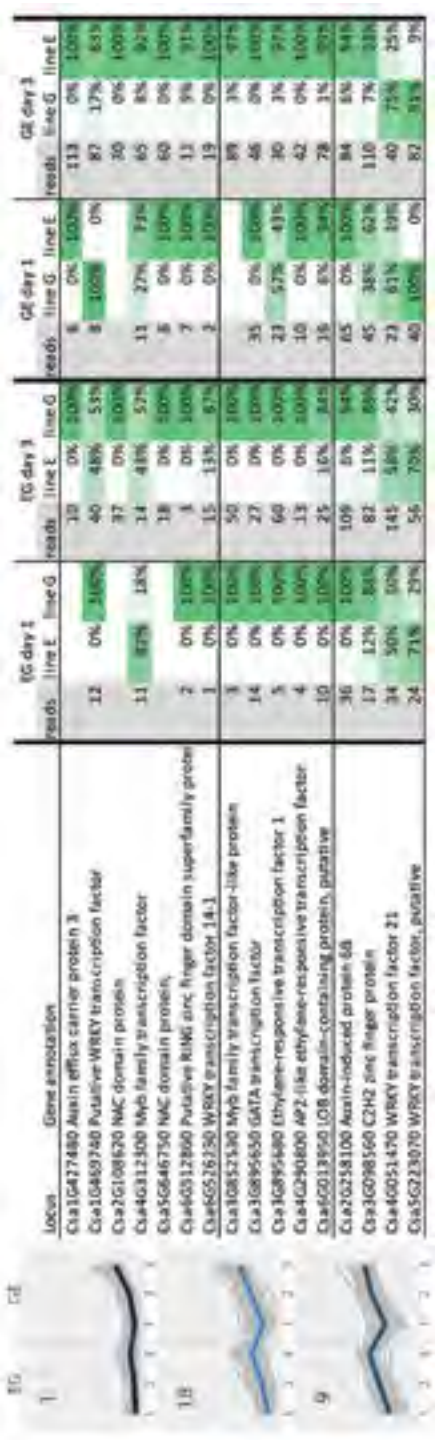
#### Transcriptome profiling reveals genes differentially regulated between compatible and incompatible cucumber grafts

To identify transcriptional differences between compatible and incompatible grafts, we performed an RNAseq experiment on EG and GE cucumber graft junctions. Compatible grafts such as GE undergo a typical wound response before and while forming vascular tissues. Therefore it is unclear which genes coordinate and reflect each of the two processes. In contrast, in EG grafts wound response occurs but vascular reconnection is absent. By comparing transcriptional changes in both types of grafts, it should be possible to identify genes associated with vascular reconnection. Graft junctions, spanning the hypocotyl of both rootstock and scion were collected 1, 2 and 3 days after grafting. RNAseq libraries were prepared for each, followed by next-generation sequencing. Reads were mapped to a cucumber reference genome (Chinese Long v2; (Huang et al. 2009)), followed by read counting per gene and normalization to Fragments Per Kilobase per Million (FPKM) values. To identify dominant expression profiles across samples, K-means clustering was performed using the FPKM values. Clustering revealed several groups of genes that were induced upon grafting (Figure 3A; Supplementary Figure 1). Genes from clusters 1, 9 and 18 were selected for further analysis based on induction in GE grafts. Genes in cluster 1 were only upregulated in successful grafts while genes in clusters 9 and 18 were induced in both GE and EG combinations. Therefore we expected clusters 9 and 18 to contain genes mostly involved in wound response and callus formation while cluster 1 was expected to contain genes involved in vascular development.

A closer look at the types of genes in these clusters revealed parallels with graft formation in *Arabidopsis*. GO term analysis revealed that clusters 9 and 18 are enriched for genes with functions in oxidation-reduction processes. Wound response and grafting



**Figure 3: Rootstock enriched expression of genes in compatible and incompatible cucumber grafts.**  
(left) Expression profiles of the three clusters induced after grafting. (right) Graft induced cucumber genes for which SNPs between E and G were available. Information on reads and sequence variation 1 and 3 days after grafting are shown. Genes from clusters 1 and 18 (top and middle) were generally induced mostly in the rootstock (right column).



were previously reported to result in the accumulation of ROS, supporting the need for oxidoreductase activity (Irisarri et al. 2015, León et al. 2001). In contrast, cluster 1 was not enriched for GO terms involved in gene regulation or vascular development, only for genes in the extracellular region and genes involved in flavonoid production. Particularly the latter may be linked to auxin accumulation, as several Arabidopsis flavonoids were shown to inhibit auxin transport (Brown 2001). From the three clusters we have selected several genes that are likely involved in vascular reconnection based on the prior knowledge. These include transcription factors and auxin-related genes found in each cluster (Supplementary Table 2-4). Based on their Arabidopsis homologs, we identified several genes of interest including: homologs of targets of auxin signaling (*SOK4* and *PIN2* in cluster 1; *IQD17* in cluster 18)(Adamowski & Friml 2015, Möller et al. 2017, Schlereth et al. 2010, Yoshida et al. 2019); transcription factors regulating cell proliferation (*FEZ* in cluster 1 and 18; *SMB* and *BBM* in cluster 9)(Boutilier 2002, Willemsen et al. 2008), and transcription factors regulating patterning and boundary formation (*MNP/HAN* in cluster 1; *PLT2* in cluster 18; *BIB* in cluster 9)(Aida et al. 2004, Long et al. 2015, Zhao 2004)(Table 1-3). These indicate that similar developmental programs seem to be recruited in the formation of a vascular connection in both cucumber and Arabidopsis.

We next asked if transcription of the genes selected from the clusters was induced in the scion or in the rootstock of the cucumber grafts. In Arabidopsis grafts, it is clear that auxin accumulation in the top half induces expression of genes in both grafted and ungrafted (cut) plants, but the differences between grafted and ungrafted plants are most clear in the bottom half of the graft, where vascular genes were only induced in grafted plants (Melnik et al. 2018)(Figure 1). For several cucumber genes, we could infer their expression origin through polymorphisms (SNP's) between variety E and G. Some sequence information of the two genotypes was available (Rijk Zwaan, unpublished), and this information was used to identify SNP's in the genes in cluster 1, 9 and 18. Based on the differential abundance of polymorphic sequences, we concluded that most of the grafting-induced genes were exclusively induced in the bottom half of the graft, both in graft EG and in GE (Figure 3A). We were interested in genes that behaved differently between EG and GE grafts. Several genes were induced only in the rootstock, but this induction was often larger in graft GE compared to graft EG (cluster 1: *Csa1G427480*, *Csa5G646750*). In contrast, *Csa1G469740* and *Csa4G312300* (cluster 1) were induced in both the top and bottom of both grafts, while in GE a much higher percentage of transcripts was found to originate from the rootstock than in EG (Figure 3A). As an exception: *Csa3G895680* (cluster 18) was only found in the rootstock in EG grafts, while in GE grafts, more than half



of the transcripts on day 1 originated from the scion, at day 3 this contribution was close to none. A clear trend we found was that transcripts that derive mainly from the rootstock have a higher scion contribution in the EG graft compared to the GE graft. This difference in contribution is most apparent on day 3, indicating reduced activation of the rootstock of EG grafts. Contrary to all other genes, transcripts from *Csa4G051470* and *Csa5G223070* (cluster 9) originate primarily from the scion at all time points. The dominance of scion-derived transcripts for these genes is stronger in GE grafts compared to EG grafts (Figure 3B). Summarizing, scion and rootstock both contribute transcripts in the grafts but most genes are induced specifically in rootstock. This mirrors similar findings in *Arabidopsis*. Furthermore, when GE and EG grafts are compared, we find differences between scion and rootstock contribution indicating that graft compatibility affects rootstock activation and scion response.

The next question was whether the *Arabidopsis* homologs of the cucumber genes for which the origins could be tracked, behaved in a similar matter in *Arabidopsis*. Many of the orthologous genes showed induction in the upper half of *Arabidopsis* ungrafted samples, similar to some vascular marker genes (Supplementary Figure 2). Only two *Arabidopsis* homologs were induced in the lower half of grafted samples, and those were both induced in the upper half of cucumber samples. These findings indicate that while in grafts of both species induction of genes in the bottom half is key, homologous protein sequences do not infer homologous regulation.

## Discussion

Vascular development in a graft starts after auxin accumulates above the graft junction (Melnyk et al. 2015, Yin et al. 2012). In *Arabidopsis*, this accumulation of auxin is accompanied by the induction of auxin-responsive genes above the graft junction, followed by graft-specific induction of vascular genes below the graft junction (Figure 1). However, the timing of induction of vascular genes varies. Some are induced quickly after grafting (*TMO6*, *WRKY17*) while expression of others is not induced until vascular connections are established (*WOL*, *TMO5*). These differences highlight that while vascular establishment in embryo and graft use similar components, their regulation is dissimilar and details from either process cannot be extrapolated. However, it is expected that key factors and regulatory steps, such as an increase in auxin signaling, are conserved between the processes.

The comparison of incompatible grafts, where no vascular connection is formed,

with compatible grafts allowed us to focus on the genetic components involved in vascular development. Analysis of cucumber RNAseq data comparing the compatible GE graft with the incompatible EG graft was the starting point to finding genes associated with grafting success and thus vascular development. Gene clustering identified several groups of genes induced by grafting. When it came to distinguishing between a successful and failed graft, several genes induced in rootstocks in cluster 1 were the best predictors of a future vascular connection (Figure 3A). These genes were induced to a higher degree in compatible GE grafts than in incompatible EG counterparts, suggesting that these genes are involved in (or reporting on) vascular development and graft connection. Similar to vascular genes in Arabidopsis grafts, graft-responsive genes in cucumber were induced predominantly in the bottom half of the graft. The reduced contribution of the rootstock in incompatible EG grafts indicates that grafting success is correlated with rootstock activation. This activation occurs before vascular connections are formed, indicating that it is not a result of long-distance transport. However, it remains unclear what causes rootstock activation. A future challenge would be to determine if the types of genes induced during graft formation can help us understand the regulation that is needed to form a vascular connection.

A closer look at the genes in the three induced clusters revealed that the two clusters upregulated in both compatible and incompatible grafts are enriched with genes associated with oxidoreductase activity according to GO term analysis (Supplementary table 1). The activation of such genes in both types of grafts indicates that these are involved in regular wound response (León et al. 2001). However these clusters also contain several genes that are spatially differently regulated in compatible and incompatible grafts (Figure 3). Therefore, while these genes are not exclusive to successful grafts, their location and exact degree of induction appears to be compatibility-dependent. GO term analysis in addition revealed that the compatible-specific cluster 1 was enriched with genes encoding proteins with extracellular localization. The function of this remains unclear but could be related to the finding that adhesion of incompatible EG grafts decreased quickly while GE graft junctions remained strong even before vascular connections were established. In addition, looking at individual genes in all three clusters reveals homologs of genes that in Arabidopsis either are targets of auxin signaling or that play key roles in regulating patterning and proliferation. This could point to the mechanisms recruited in the process of graft vascular connection but without experimental validation it is unclear if these factors determine grafting success or merely report on it. However, the patterns and genes identified in this experiment could form a starting point for future experiments.

Additional experiments can help identify genes robustly associated with grafting

success. The first step would be to determine how reproducible the results found in this chapter are. By repeating this same experiment with more grafting combinations, genes consistently associated with grafting success can be identified. By also comparing the IJ and JI grafting combination (Figure 2) a similar dataset can be generated and genes that are induced in both GE and JI could be regarded as more general markers of grafting success. In addition, mis-sense SNPs in coding regions could point to proteins whose activity might be impaired in incompatible grafts while SNPs in regulatory regions could point to regulatory elements that are needed for the induction of genes that determine grafting success. Furthermore, a wider dataset involving more grafting comparisons would with more certainty point to molecular markers of grafting success that could potentially predict grafting success. In addition, mapping populations of ExG or IxJ crosses could lead to the identification of Quantitative Trait Loci (QTLs) responsible for grafting success. In this chapter we raise the question as to which part(s) of the graft determines compatibility. Does the scion or the rootstock determine success or are specific combinations incompatible? Grafting the scions E and I with a variety of rootstocks and the rootstocks G and J with a variety of scions can get us closer to unraveling those mechanisms and to genes involved in this process.

All in all, in this chapter we have identified parallels between vascular specification in embryo and grafts and we have used cucumber grafting combinations to identify genes associated with grafting success. These findings can form a starting point for both the identifications of molecular markers and QTLs associated with grafting success and for the unraveling of molecular mechanisms that control vascular development in the graft.

## **Materials and methods**

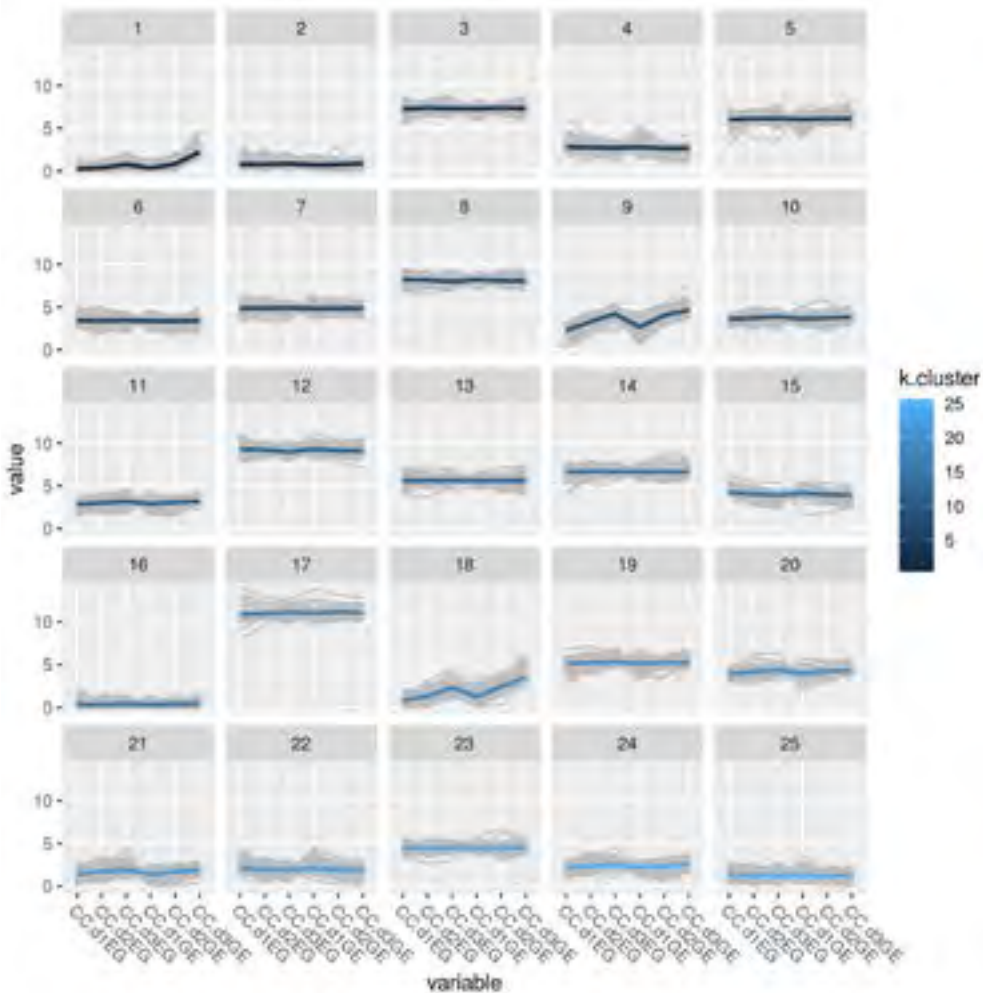
### Plant materials, growth, sectioning and staining

Cucumber varieties were selected by Rijk Zwaan and experiments were performed at the breeding company's location in Fijnaart. Plants were grown under regular greenhouse (soil blocks covered with vermiculite) conditions. Seedlings were grafted 9 days after germination and kept together with soft plastic clips. Graft junctions for imaging were collected 2, 3 and 4 days after grafting. After fixation in 4% paraformaldehyde, grafts were staining using 0.1% of toluidine blue and hand-sectioned.

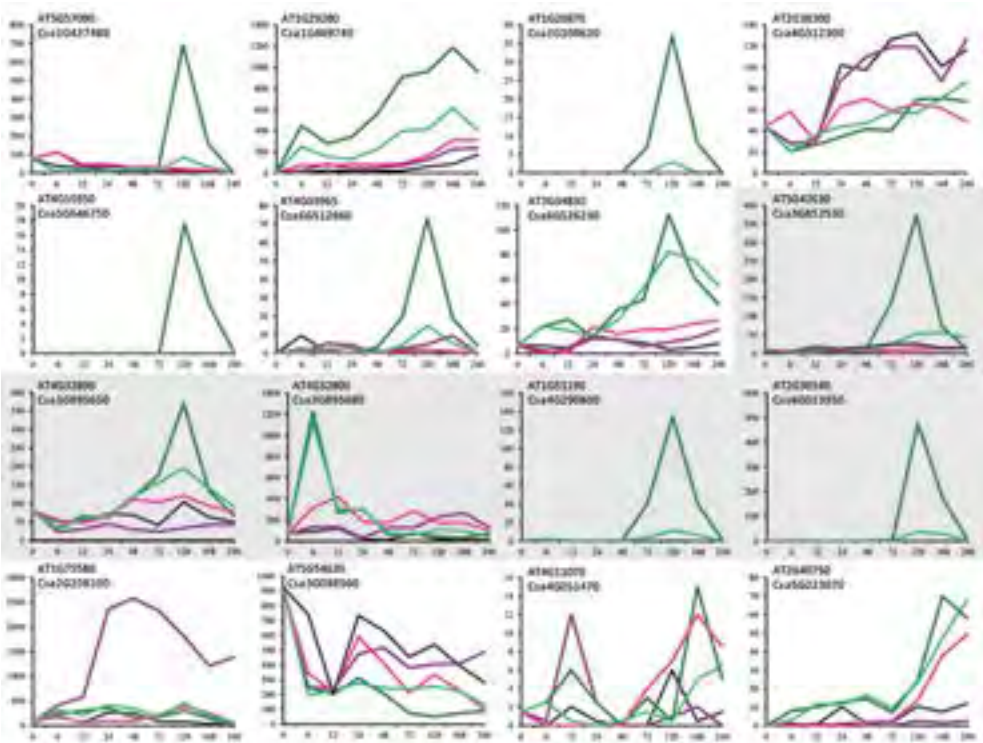
### RNAseq: material collection and data analysis

Samples for RNA extraction were collected 1, 2 and 3 days after grafting and consisted of 20 graft junctions. Each graft junction was about 1 cm with equal contributions from top and bottom. Quality check for the raw RNAseq reads was performed using FastQC ([www.bioinformatics.babraham.ac.uk/projects/fastqc](http://www.bioinformatics.babraham.ac.uk/projects/fastqc)). Illumina adapters at the 3' end of the reads and the biased 5' end (10 bp from start) were cleaned up using TrimGalore (v0.5.0; <https://github.com/FelixKrueger/TrimGalore>). The cleaned FASTQ reads were mapped onto the Cucumber genome (Chinese Long v2; <http://cucurbitgenomics.org/>) using HISAT2 (v2.1.0; Kim et al. 2015) with default parameters. The obtained mapping (SAM) files were converted to binary (BAM) format and further indexed using SAMTOOLS (v1.9; Li et al. 2009). FeatureCounts (v1.6.2; Liao et al. 2014) was used to count the raw reads corresponding to each gene, with the parameters `"-t 'exon' -g 'gene_id' -Q 30 -p --primary"`. These raw counts were normalized using Fragments Per Kilobase per Million (FPKM) metric. The normalized data was used for generating 25 clusters using k-means clustering in R (v3.5; [www.r-project.org](http://www.r-project.org)). Plots were generated using `'ggplot2'` module in R. GO term enrichment was performed with a Bonferroni correction for p-values and a cutoff of 0.05 (<http://cucurbitgenomics.org/goenrich>). To identify the corresponding Arabidopsis homologs of the cucumber genes, the aminoacid sequences of cucumber genes were matched against the Arabidopsis proteome using 'blastp' with the parameters `"-max_target_seqs 1 -evalue 0.001"` to identify the best hit in Arabidopsis.

Supplementary Figures and Tables



**Supplementary figure 1: Expression profiles of the 25 clusters.**  
Clusters were generated by k-means clustering. Clusters 1, 9 and 18 were selected for further analysis.



**Supplementary figure 2: Expression profiles of Arabidopsis homologs of Cucumber graft induced genes.**  
Expression after grafting in Arabidopsis of homologs of the cucumber genes of which expression origin could be determined.

Supplementary table 1: GO term enrichment clusters 1, 18 and 9.  
GO terms enriched in each of the 3 selected clusters.

	Function	Process	Component
Cluster 1	GO:0047213 anthocyanidin 3-O-glucosyltransferase activity	None	GO:0005576 extracellular region
	GO:0003935 GTP cyclohydrolase II activity		GO:0044421 extracellular region part
	GO:0006668 3,4-dihydroxy-2-butanone-4-phosphate synthase activity		
Cluster 18	GO:0016491 oxidoreductase activity	GO:0005114 oxidative reduction process	None
	GO:0051213 dehydrogenase activity		
	GO:0046872 metal ion binding		
	GO:0043169 cation binding		
	GO:0020037 heme binding		
	GO:0016705 oxidoreductase activity, acting on paired donors, with incorporation or reduction of molecular oxygen		
Cluster 9	GO:0046906 tetrapyrrole binding	GO:0044710 single-organism metabolic process GO:0005114 oxidative reduction process	None
	GO:0016491 oxidoreductase activity		
	GO:0020037 heme binding		
	GO:0047911 galacturan 1,4-alpha-galacturonidase activity		
	GO:0005506 iron ion binding		
	GO:0004497 monooxygenase activity		
	GO:0016705 oxidoreductase activity, acting on paired donors, with incorporation or reduction of molecular oxygen		



**Supplementary table 2: Selected genes from cluster 1.**

A list of cucumber genes related to transcriptional regulation and auxin response and their Arabidopsis homologs.

Locus Csa	Description Csa	Locus At	Description Ath
Csa1G004170	LOB domain-containing protein	AT5G63090	LATERAL ORGAN BOUNDARIES (LOB)
Csa1G042180	Transcription factor CYCLOIDEA	AT3G18550	BRANCHED 1 (BRC1)
Csa1G045430	DNA-binding protein-like	AT1G74500	BRU1-SUPPRESSOR 1 (BS1)
Csa1G427480	Auxin efflux carrier protein 3	AT5G57090	ETHYLENE INSENSITIVE ROOT 1 (EIR1)
Csa1G469740	Putative WRKY transcription factor	AT1G29280	WRKY DNA-BINDING PROTEIN 65 (WRKY65)
Csa1G497300	Zinc finger CONSTANS-like protein	AT5G59990	CCT motif family protein
Csa2G006080	Putative zinc finger protein	AT2G26695	Ran BP2/NZF zinc finger-like protein
Csa2G049890	Myb transcription factor-like protein	AT5G65790	MYB DOMAIN PROTEIN 68 (MYB68)
Csa2G108620	NAC domain protein	AT1G26870	FEZ (FEZ)
Csa3G127050	AT-hook DNA-binding protein	AT4G17800	AT-HOOK NUCLEAR PROTEIN 23 (AHL23)
Csa3G134010	MYB transcription factor	AT4G13480	MYB DOMAIN PROTEIN 79 (MYB79)
Csa3G178570	Transcription factor bHLH36	AT5G51790	basic helix-loop-helix (bHLH) protein
Csa3G212490	WRKY transcription factor, putative	AT1G68150	WRKY DNA-BINDING PROTEIN 9 (WRKY9)
Csa3G592130	MYB transcription factor	AT5G14340	MYB DOMAIN PROTEIN 40 (MYB40)
Csa3G865440	MADS box transcription factor	AT3G54340	APETALA 3 (AP3)
Csa3G883020	Auxin-induced protein 6B	AT2G24400	SMALL AUXIN UPREGULATED RNA38 (SAUR38)
Csa4G027920	Auxin-regulated protein	AT3G46110	UPSTREAM OF FLC-like protein (DUF966)
Csa4G043850	Homeobox-leucine zipper protein	AT2G18550	HOMEODOMAIN PROTEIN 21 (HB21)
Csa4G046650	GATA transcription factor, putative	AT3G50870	MONOPOLE (MNP)
Csa4G312300	Myb family transcription factor	AT2G38300	myb-like HTH transcriptional regulator family
Csa4G639900	Transcription factor, putative	AT3G50330	HECATE 2 (HEC2)
Csa5G156170	MADS box transcription factor	AT4G22950	AGAMOUS-LIKE 19 (AGL19)
Csa5G605050	NAC domain-containing protein	AT1G26870	FEZ (FEZ)
Csa5G646750	NAC domain protein,	AT4G10350	NAC DOMAIN CONTAINING 70 (NAC070)
Csa6G148250	FER-LIKE IRON DEFICIENCY-INDUCED	AT2G28160	FER-LIKE REGULATOR OF IRON UPTAKE (FRU)
Csa6G157640	Putative MYB transcription factor	AT2G38300	myb-like HTH transcriptional regulator family
Csa6G445020	Zinc finger protein	AT5G66730	INDETERMINATE DOMAIN 1 (IDD1)
Csa6G489970	B3 domain-containing protein	AT3G18990	REDUCED VERNALIZATION RESPONSE 1 (VRN1)
Csa6G497330	Mads box protein, putative	AT3G57230	AGAMOUS-LIKE 16 (AGL16)
Csa6G512860	Putative RING zinc finger domain	AT4G03965	RING/U-box superfamily protein
Csa6G526230	WRKY transcription factor 14-1	AT2G34830	WRKY DNA-BINDING PROTEIN 35 (WRKY35)
Csa7G041360	BZIP transcription factor family protein	AT3G58120	(BZIP61)
Csa7G452960	GATA transcription factor, putative	AT4G32890	GATA TRANSCRIPTION FACTOR 9 (GATA9)

**Supplementary table 3: Selected genes from cluster 18.**

A list of cucumber genes related to transcriptional regulation and auxin response and their Arabidopsis homologs.

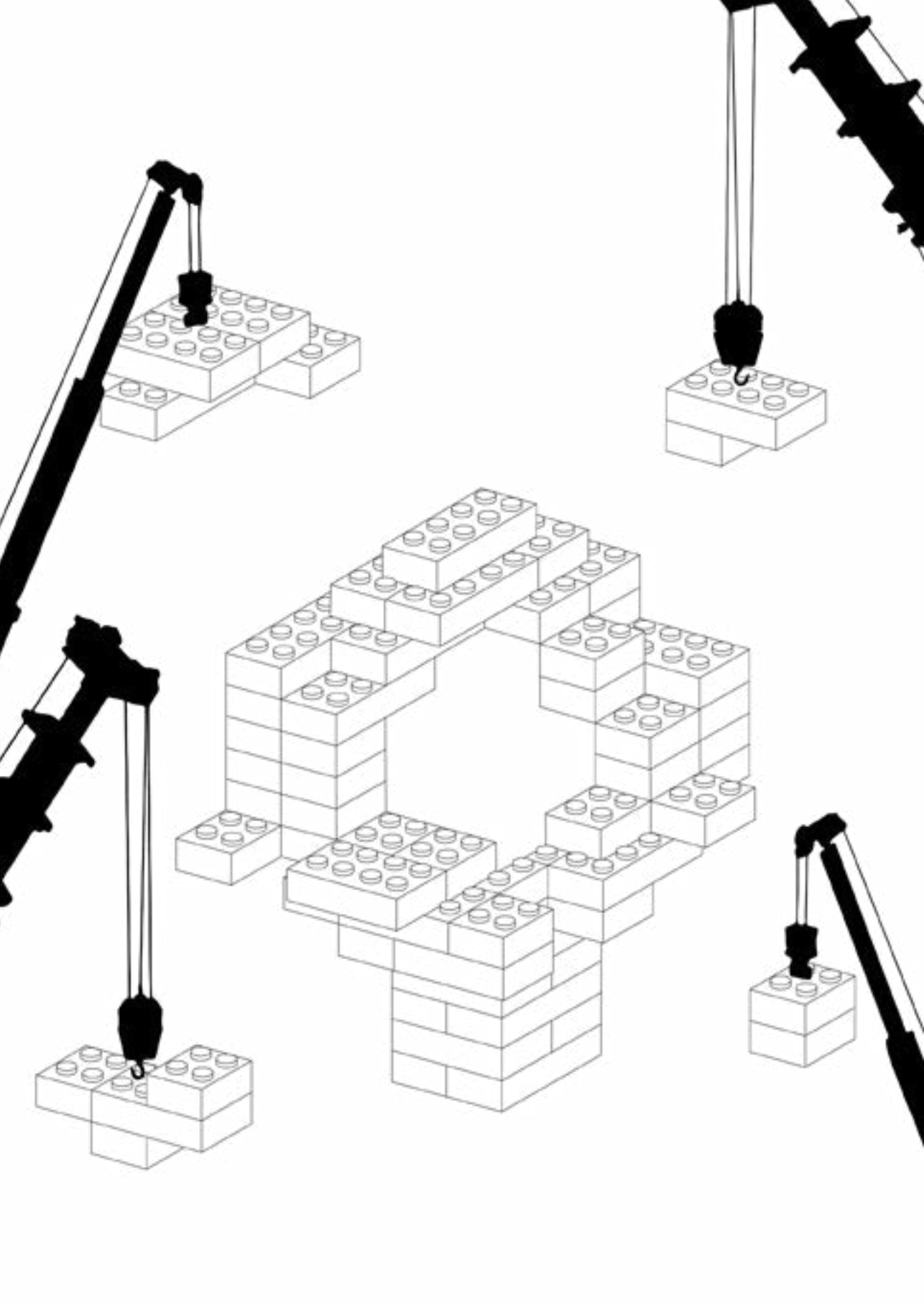
Locus Csa	Description Csa	Locus At	Description Ath
Csa1G043020	Putative zinc finger protein	AT2G01940	SHOOT GRAVITROPISM 5 (SGR5)
Csa2G009420	Zinc-binding protein	AT2G12646	PLAT2 transcription factor family protein
Csa2G247590	Transcription factor	AT4G36540	BR ENHANCED EXPRESSION 2 (BEE2)
Csa2G351740	Putative MYB transcription factor	AT5G56840	myb-like transcription factor family protein
Csa2G416070	BZIP transcription factor family protein	AT2G42380	(BZIP34)
Csa2G423560	Zinc finger protein CONSTANS-like	AT3G21890	B-BOX DOMAIN PROTEIN 31 (BBX31)
Csa3G019400	Ethylene-responsive 7	AT2G44940	DREB subfamily A-4 of ERF/AP2 protein
Csa3G126090	LOB domain-containing protein	AT2G45420	LOB DOMAIN PROTEIN 18 (LBD18)
Csa3G180430	Homeobox-leucine zipper protein ROC7	AT4G00730	ANTHOCYANINLESS 2 (ANL2)
Csa3G379740	NAC domain protein,	AT4G28530	NAC DOMAIN PROTEIN 74 (NAC074)
Csa3G457670	GATA transcription factor	AT4G32890	GATA TRANSCRIPTION FACTOR 9 (GATA9)
Csa3G510960	Homeobox-leucine zipper protein 22	AT4G37790	(HAT22)
Csa3G536650	Transcription factor UPBEAT1	AT2G47270	UPBEAT1 (UPB1)
Csa3G637990	Myb family transcription factor-related	AT5G45580	Homeodomain-like superfamily protein
Csa3G852530	Myb family transcription factor-like	AT5G42630	ABERRANT TESTA SHAPE (ATS)
Csa3G895650	GATA transcription factor	AT4G32890	GATA TRANSCRIPTION FACTOR 9 (GATA9)
Csa3G895680	Ethylene-responsive 1	AT4G32800	DREB subfamily A-4 of ERF/AP2 protein
Csa3G902390	AT-hook DNA-binding protein	AT2G35270	AT-HOOK NUCLEAR PROTEIN 21 (AHL21)
Csa4G181200	MADS-box transcription factor	AT2G14210	AGAMOUS-LIKE 44 (AGL44)
Csa4G290800	AP2-like ethylene-responsive	AT1G51190	PLETHORA 2 (PLT2)
Csa5G201310	Auxin transporter-like protein	AT2G38120	AUXIN RESISTANT 1 (AUX1)
Csa5G641610	MYB transcription factor	AT3G30210	MYB DOMAIN PROTEIN 121 (MYB121)
Csa6G013950	LOB domain-containing protein	AT2G30340	LOB DOMAIN PROTEIN 13 (LBD13)
Csa6G076850	LOB domain-containing protein	AT4G00210	LOB DOMAIN PROTEIN 31 (LBD31)
Csa6G103520	Dof zinc finger protein	AT3G61850	DOF AFFECTING GERMINATION 1 (DAG1)
Csa6G107880	IQ-domain 17	AT4G00820	IQ-DOMAIN 17 (iqd17)
Csa6G401350	Ring finger protein, putative	AT5G07040	RING/U-box superfamily protein
Csa6G501990	Homeobox-leucine zipper protein	AT2G18550	HOMEODOMAIN PROTEIN 21 (HB21)
Csa6G524000	TCP transcription factor	AT4G18390	CYCLOIDEA AND PCF 2 (TCP2)
Csa7G447000	Homeobox-leucine zipper ATHB-9	AT1G79840	GLABRA 2 (GL2)
CsaUNG003730	Ethylene-responsive TF	AT5G13910	LEAFY PETIOLE (LEP)

**Supplementary table 4: Selected genes from cluster 9.**

A list of cucumber genes related to transcriptional regulation and auxin response and their Arabidopsis homologs.

Locus Csa	Description Csa	Locus At	Description Ath
Csa1G043040	Zinc finger-homeodomain protein 3	AT4G24650	HOMEODOMAIN PROTEIN 22 (HB22)
Csa2G009360	RING finger protein 126	AT2G15580	RING/U-box superfamily protein
Csa2G010120	DNA-binding protein	AT4G14465	AT-HOOK NUCLEAR PROTEIN 20 (AHL20)
Csa2G047780	Transcription factor UPBEAT1	AT2G47270	UPBEAT1 (UPB1)
Csa2G092800	AP2-like ethylene-responsive	AT5G17430	BABY BOOM (BBM)
Csa2G258100	Auxin-induced protein 68	AT1G75580	SMALL AUXIN UPREGULATED RNA51 (SAUR51)
Csa3G098560	C2H2 zinc finger protein	AT5G54630	zinc finger protein-like protein
Csa3G396920	LOB domain-containing protein	AT3G58190	LATERAL ORGAN BOUNDARIES-DOMAIN 29 (LBD29)
Csa3G727990	WRKY transcription factor	AT3G56400	WRKY DNA-BINDING PROTEIN 70 (WRKY70)
Csa3G738980	Zinc finger protein	AT3G45260	BALDIBIS (BIB)
Csa3G872040	Auxin-induced protein 68	AT2G21220	SMALL AUXIN UPREGULATED RNA 12 (SAUR12)
Csa4G051470	WRKY transcription factor 21	AT4G11070	(WRKY41)
Csa4G193250	NAC-domain containing protein	AT5G18270	NAC DOMAIN CONTAINING PROTEIN 87 (ANAC087)
Csa5G152860	Homeobox protein BEL1 homolog	AT5G41410	BELL 1 (BEL1)
Csa5G223070	WRKY transcription factor	AT2G40750	WRKY DNA-BINDING PROTEIN 54 (WRKY54)
Csa5G642710	BZIP transcription factor	AT3G30530	BASIC LEUCINE-ZIPPER 42 (bZIP42)
Csa6G013900	DNA binding protein	AT2G40435	SCREAM-like protein
Csa7G252700	NAC domain-containing protein	AT1G79580	SOMBRERO (SMB)





# Chapter 8

## **General Discussion**





Early during plant embryogenesis, cells acquire one of three distinct cell identities, each contributing unique cell types that, upon differentiation, contribute to plant development, adaptation and survival. The dominant presence of multi-cellular organisms - such as land plants - in ecosystems, is likely aided by their ability to form specialized tissues. Instead of each cell acting alone, large collectives of cells act together to ensure their survival, with groups of cells adopting fates dedicated to a singular task. The division of labor in multicellular organisms however, needs to be under tight control. In plants, three overarching tissue identities exist: epidermal identity, ground tissue identity and vascular identity are each first specified during embryogenesis and will each contribute to all tissues and organs the plant will form during its life. Each of these three cell identities will give rise to several sub-identities (cell types), and mutations that result in the impaired development of a single tissue sub-type can cause aberrant development and reduced fertility (MacAlister et al. 2007, Mähönen et al. 2000, Mayer et al. 1991, Okada et al. 1991). This suggests that failure to initiate a major cell identity, and as a consequence the loss of all its sub-types, will be lethal. While it is known that the specification of cell identity during plant embryogenesis is crucial, at this moment the mechanisms responsible remain elusive, and the genetic master switches are unknown. In this thesis we started unraveling the mechanisms that are responsible for the specification and development of vascular identity in the *Arabidopsis* embryo.

### Vascular identity establishment is a multi-step process

The origin of the first vascular cells in *Arabidopsis* have been traced back to the early globular stage embryo using lineage tracing (Dolan et al. 1993, Scheres et al. 1994). This stage corresponds to the one where a dedicated tissue layer is formed that will only later generate the pericycle, xylem, phloem and cambium. In **Chapter 3**, we concluded that vascular identity is instead laid down one stage earlier: in the dermatogen stage embryo, where a large number of vascular marker genes start showing cell-type specific expression. This finding confirms an earlier report that made this same suggestion based on global tissue-specific transcriptome analysis (Palovaara et al. 2017): those findings had indicated that the vascular cells at early globular stage are highly similar to the inner dermatogen stage cells (16-cell stage) in their transcriptome, as measured by GO term analysis. This is surprising, since the inner cells at 16-cell stage will not only generate vascular cell types, but are also the precursor to the ground tissue, from which endodermis and cortex differentiate (Raven et al. 2005, Scheres et al. 1994). The genetic regulation responsible for this specification step is unknown, nor have models been proposed for the establishment of other tissue identities

during early embryogenesis. In this respect, there is more information on metazoan embryogenesis. Single cell sequencing of mouse embryos has revealed that gaining cell type specificity commonly occurs through the local repression of cell identity markers (Guo et al. 2010). During mouse embryogenesis at 32-cell stage the trophectoderm (TE) and inner cell mass (ICE) are specified (Rossant & Tam 2009). TE-specific transcription factors are first expressed equally across all cells, before their expression is inhibited specifically in the inner cells (Guo et al. 2010). Similarly, in the Arabidopsis embryo, the inverse markers of vascular identity start expression before the distinction between vascular and non-vascular cells is made, and gain specificity to non-vascular cells at dermatogen stage, potentially through repression in the inner cells. In contrast, the vascular-specific genes are not expressed before the first vascular cells are specified. These observations indicate that vascular identity probably arises through a combination of both location-specific activation and location-specific repression of transcription.

The quick and local distinction between the inner and outer cells of the Arabidopsis embryo might depend on the differential activation of components that are already present, rather than through the slower induction of newly synthesized components. In **Chapter 5** we found that the 10 candidate regulators of vascular identity, identified using Yeast One Hybrid, were expressed at similar levels across the embryo and their expression precedes vascular initiation. Similar patterns exist in the Drosophila embryo where the TEAD4 transcription factor is present in all cells (Nishioka et al. 2009). Here, cell-specific activity is caused by differential localization of the TEAD4 co-activator: YAP (Nishioka et al. 2009). YAP localization is nuclear in the outer cells but cytoplasmic in the inner cells as a result of differential phosphorylation (Nishioka et al. 2009). A similar mechanism in the embryo Arabidopsis could allow a broadly expressed regulator to restrict vascular fate through cell-specific differences in activity. An important future question therefore is if any of these potential regulators of vascular tissue specification is regulated in its activity by cofactor binding or post-translational modification.

A second step in the establishment of discrete cell identities entails the transition of vascular identity from a diffuse to a discrete trait. Since ground tissue identity appears to arise from a prior vascular-like identity (**Chapter 3**; Möller et al. 2017, Palovaara et al. 2017), vascular marker genes will need to be suppressed in several cells just one division after their activation. However, it appeared that this is not an instant change. Many vascular marker genes remained active in ground tissue cells until several cell divisions later, around transition stage (**Chapter 3**). The subsequent step-by-step restriction of vascular markers to the vascular cells indicates that the emergence of discrete cell identities may depend on

feedback mechanisms. Indeed, gene regulatory networks involving extensive feedback were found to be necessary for creating discrete cell fate outputs across multicellular organisms (Briscoe & Small 2015, Rossant & Tam 2009, Stathopoulos & Levine 2002, ten Tusscher 2013). While the existence of such a gene regulatory network restricting vascular identity in the Arabidopsis embryo remains unconfirmed, the components and outputs identified in this thesis indicate that a broadly present set of regulators can modulate the response to a signaling molecule, auxin, which then over the course of several divisions could help create discrete cell identities.

### The role of auxin in vascular tissue specification

The plant hormone auxin instructs and drives a broad variety of responses in plant development and adaptation (Roosjen et al. 2018, van den Berg & ten Tusscher 2017). A strong link exists between auxin signaling and vascular development: auxin maxima are strongly correlated with vascular initiation and were suggested to trigger vascular development (Ohashi-Ito & Fukuda 2010, Sachs 1969, Scarpella 2017, Weijers et al. 2006). In **Chapter 4** we found that auxin levels and signaling are unlikely to be only the spatial cue that limits vascular identity to the inner cells at dermatogen stage. Both inner and outer cells have high levels of auxin as measured by the R2D2 and DR5v2 reporters (**Chapter 4**; Liao et al. 2015). The notion that auxin triggers vascular identity comes largely from experimental work that links high auxin to vascular development (reviewed in De Rybel et al. 2016, Fukuda & Ohashi-Ito 2019, Scarpella 2017). Induction of vascular development in grafts (Melnik et al. 2015), after wounding (Efroni et al. 2016, Jacobs 1952), or upon application of auxin to the stem (Sachs 1969), all underline the link between auxin signaling and vascular development. Yet, in each of these experiments vascular cells originate not from the existing tissues but from the de-differentiated (callus) tissue that is formed whenever a plant is wounded. It is clear that auxin is needed for the formation of vascular bundles in these situations and auxin maxima caused by canalization do indeed overlap with the future location of vascular bundles. However, our attempts in **Chapter 4** to induce vascular identity in the root and embryo showed that auxin alone is not able to confer vascular identity during regular development.

In the embryo, we found that while ectopic MONOPTEROS (MP/MPΔPB1) activity could trigger cell divisions, it could not induce vascular identity outside its regular domain. However, previously the expression of MPΔPB1 under the *MP* promoter was shown to cause ectopic and aberrant vascular development in leaves (Krogan et al. 2012). It can be argued that in this case ectopic auxin signaling did result in ectopic vascular

development, but only in the context of the developing leaf. The *MP* promoter is active outside the vascular domain in the embryo and root (Rademacher et al. 2011) but in both tissues no ectopic vascular development was reported when *MPΔPB1* was introduced in this domain. Instead of auxin triggering vascular development it is imaginable that both transdifferentiation caused by wounding and organogenesis result in the formation of naive cells that will then use auxin as a positional cue to create centrally located vascular tissue. Indeed, blocking auxin signaling in the inner cells of the embryo resulted in incomplete establishment of vascular identity (**Chapter 4**) which will then cause in aberrant vascular development (Hamann et al. 1999, Schlereth et al. 2010). Since auxin is not the spatial cue that limits identity, the question remains which factors add to auxin signaling response to provide spatial specificity during the initiation of vascular development.

### Modulation of auxin response

As auxin response is needed for the initiation vascular identity during embryogenesis, but is not sufficient to induce ectopic vascular identity, it might instead be the differences in response to the same level of auxin that limit identity. Cell-specific responses to auxin could be caused by protein interactions that alter AUXIN RESPONSE FACTOR (ARF) DNA binding or activity at the DNA. In addition to ARF homo- and heterodimerization, members of other transcription factor families were found to interact with ARF proteins (reviewed in Roosjen et al. 2018). Interactions with MYB DOMAIN PROTEIN77 (MYB77), FRUITFULL (FUL) and BIGPETAL (BPE) occur via the PB1 domain of ARFs and appear to modulate response to auxin in the context of lateral root development (MYB77-ARF7) and fruit morphogenesis (FUL-ARF6/8 and BPE-ARF6/8) (Ripoll et al. 2015, Shin et al. 2007, Varaud et al. 2011). In **Chapter 6**, we find that the bZIP transcription factors G-BOX BINDING FACTOR 1 and 2 (GBF1 and GBF2) can interact with the DNA-binding domain of ARFs, including MP. The expression of GBF1 and GBF2 during embryogenesis (**Chapter 5**) nominates these transcription factors as potential contributors to auxin response in vascular specification.

In **Chapter 6** we found that several vascular promoters contained both putative Auxin Response Elements (AuxREs) and G-boxes. G-boxes are often found in the promoters of auxin response genes and appear close to AuxREs (**Chapter 6**; Berendzen et al. 2012, Cherenkov et al. 2018, Menkens et al. 1995, Ulmasov et al. 1995). Removing the putative AuxREs and flanking G-boxes from the promoters of *GATA20*, *TMO5* and *WRKY17* resulted in large decreases in root promoter activity. The separate removal of G-boxes did not result in similarly strong decreases in promoter activity but instead increased the

variation in expression level between transformants, indicating a role for these elements in stabilizing expression. The removal of a combined AuxRE/G-box motif in the *WRKY17* promoter resulted in a vascular-specific reduction of expression, indicating that this motif confers vascular-specific gene expression. In both cases, it appears that the presence of G-box elements near AuxREs in vascular promoters contributes to vascular expression, specifically to the stabilization of expression levels in the vascular bundle. Stabilization of expression levels in response to signal fluctuations plays a key role in patterning and is essential in maintaining patterning (Briscoe & Small 2015, ten Tusscher & Scheres 2011). On the protein level, G-class bZIPs could alter binding of ARF proteins to the DNA or be involved in the recruitment of specific cofactors and in these ways help restrict vascular specific gene expression. It will be interesting to find if and how these factors contribute to vascular identity specification during embryogenesis. However, we were unable to determine the role of GBFs during vascular specification.

G-class bZIPs can bind G-box motifs in vascular promoters (**Chapter 6**; Giuliano et al. 1988, Schindler et al. 1992), but other bZIP family members and bHLH transcription factors can bind to the same G-box motif (Berendzen et al. 2012, Kim et al. 2016). Thus, using promoter truncations it was not possible to separate the role of GBF in vascular specific gene expression from that of other G-box binding transcription factors. Knockout of one or two G-class bZIPs only caused marginal changes in development or auxin response (**Chapter 6**). This may in part be due to the redundancy that likely exists in the G-class of bZIP transcription factors, and in part to the lack of knowledge on factors that regulate GBF activity. Arabidopsis has 5 G-class bZIP transcription factors (Dröge-Laser et al. 2018, Jakoby et al. 2002) and a knockout of one member results in upregulation of others (**Chapter 6**). While overexpression of GBFs using the *35S* promoter altered leaf shape, overexpression from the *RPS5A* promoter caused no observable effect on development (**Chapter 6**) unless fused to an SRDX repressor domain (**Chapter 5**). This indicates that unmodified GBF alone cannot activate or repress vascular identity. A higher order GBF knockout mutant or a constitutively active version GBF would allow to help elucidate the role of GBF proteins in vascular development. Creating a constitutively active version of GBF requires understanding of the factors that regulate GBF activity. Theoretically, mechanisms altering GBF activity might be the result of differential protein localization as reported for cell specification in *Drosophila* (Nishioka et al. 2009), but we found that GBF1 and GBF2 were present in the nucleus in all cells. However, previous work has shown that GBF DNA-binding is redox-dependent (Klimczak 1992, Shaikhali et al. 2012) and this could contribute to cell type-specific GBF activity. Additional work is needed to determine what role, if any, GBFs

play in the initiation of vascular identity.

In addition to the GBFs we were able to link several other candidate regulators to modulation of auxin response. *ASILI*, *AT2G37520* and *GLP3* can bind to vascular specific promoter sequences in yeast (**Chapter 5**) and their misexpression can affect auxin response in Arabidopsis (**Chapter 6**). The mechanisms that these genes use to modulate auxin responsive gene expression remain unclear as their binding sites and protein interactions remain obscure. However, their effects appear to be context-dependent, as overexpression did not result in strong developmental phenotypes. All in all, the search for the master regulator of vascular identity is not yet concluded.

### Is there a master regulator of vascular identity?

In this thesis we aimed to identify a master regulator that is both necessary and sufficient for the initiation of vascular tissue identity. Our search has not yielded a master identity regulator. While there can be many technical reasons why the strategy chosen did not deliver a master regulator, an important question is whether such a regulator exists. An important assumption was the existence of a unifying vascular identity. The three major tissue types (vascular, ground, epidermis), which are initiated during embryogenesis, are thought to be distinct identities that persist post-embryonically (Raven et al. 2005). It is possible to induce aspects of vascular tissue development or differentiation, such as periclinal cell division or xylogenesis, in other cell types through misexpression of their key regulators (**Chapter 6**; De Rybel et al. 2013, Kondo et al. 2014, Smet et al. 2019, Soyano et al. 2008). Thus, aspects of vascular tissue development are indeed under control of master regulators, but this may not be the case for vascular tissue identity itself. Vascular cells are thought to possess unique ‘vascular’ characteristics that are shared among the different vascular cell types. Such characteristics would include the factor that restricts vascular marker expression outside of the vascular tissues upon auxin treatment (**Chapter 4**). However, expression of even xylem- or phloem-specific markers can not be induced in other vascular cell types (**Chapter 4**), suggesting that these identities might not be as similar as assumed.

This separation between different vascular cell types is also found in a single-cell RNAseq (scRNA-seq) experiment performed on Arabidopsis root tips, which found distinct groups of xylem and phloem cells (Ryu et al. 2019). Clustering revealed that the vascular cells were clustered close to other cell types such as the lateral root cap and root hair cells; xylem cells even appeared more similar to root hair cells than to the phloem (Ryu et al.

2019). In addition, other recent scRNA-seq studies on *Arabidopsis* root tips similarly find that the distance between the subtypes of each major identity (vascular, ground, epidermis) might be larger than the distance between the major identities (Denyer et al. 2018, Jean-Baptiste et al. 2019, Shulze et al. 2018). This leads to the question as to whether there is a unified vascular identity or if vascular cell types only share a set of common precursor cells. Based on vascular marker expression patterns (**Chapter 3**) we hypothesize that a common vascular identity does exist during early embryogenesis in the cells that share xylem and phloem markers but that as soon as there are enough cells in the vascular bundle, these identities separate. Altogether, vascular identity appears to be a temporary state from which vascular subtypes quickly depart and its specification might be one module that is recruited early on instead of a constant driving force. Following this argument, it is perhaps unrealistic to assume the presence of a master switch for vascular identity that persists beyond the initial stage of tissue ontogeny.

## Outlook

In this thesis, we set out to describe the initiation of vascular identity during embryogenesis and to find factors that control this developmental transition. While none of the transcription factors identified in this thesis are the master regulator of vascular identity, they do fit into the view that regulation of identity depends on the interpretation of a positional gradient by a broadly present gene regulatory network (Bhalerao & Bennett 2003, Briscoe & Small 2015). Future research into the nature of plant cell identity and its regulation will bring us closer to truly understanding the process of identity specification. Firstly, characterization of the factors identified in this thesis using higher order mutants and identification of mechanisms controlling their cell type-specific activity will help understand the factors that regulate vascular identity. At the moment, single cell sequencing is being applied to a variety of plant tissues (Efroni & Birnbaum 2016) and advances from the animal field indicate that single cell transcriptome profiling of embryonic cells can teach us about the components that contribute to cell identity (Cao et al. 2019; Guo et al. 2010, 2017). Single cell RNAseq of the early *Arabidopsis* embryo can provide spatial and temporal resolution of the specification process. However, because identity is probably regulated by the regulated activity of a broadly transcribed transcription factor, transcriptome profiling and network inference might not be sufficient to identify the regulators of cell fate initiation. Additionally, the analysis of regulatory elements that determine promoter activity and thus cell type-specific transcription using data from DAPseq and protein binding microarrays



(Franco-Zorrilla et al. 2014, O'Malley et al. 2016) can point in the direction as to which regulatory proteins could contribute. The investigation into the modifications that alter protein activity remains restricted by the size and accessibility of the early embryo which prevents proteomics studies. Progress in understanding regulation of protein activity will thus depend on the parallels between embryonic and post-embryonic development. In the end, understanding the control of vascular identity during embryogenesis will depend on and might contribute to a myriad of related processes, once again with auxin at its center.

# References

- Adamowski, M., & Friml, J. (2015).** PIN-Dependent Auxin Transport: Action, Regulation, and Evolution. *The Plant Cell*, 27(1), 20–32. <https://doi.org/10.1105/tpc.114.134874>
- Aida, M., Beis, D., Heidstra, R., Willemsen, V., Blilou, I., Galinha, C., Nussaume, L., Noh, Y. S., Amasino, R., & Scheres, B. (2004).** The PLETHORA genes mediate patterning of the Arabidopsis root stem cell niche. *Cell*, 119(1), 109–120. <https://doi.org/10.1016/j.cell.2004.09.018>
- Akam, M. (1987).** The molecular basis for metameric pattern in the Drosophila embryo. *Development*, 101(1), 1–22.
- Aoyama, T., & Chua, N. H. (1997).** A glucocorticoid-mediated transcriptional induction system in transgenic plants. *Plant Journal*, 11(3), 605–612. <https://doi.org/10.1046/j.1365-313X.1997.11030605.x>
- Ashe, H. L., & Briscoe, J. (2006).** The interpretation of morphogen gradients. *Development*, 133(3), 385–394. <https://doi.org/10.1242/dev.02238>
- Baima, S., Nobili, F., Sessa, G., Lucchetti, S., Ruberti, I., & Morelli, G. (1995).** The expression of the Athb-8 homeobox gene is restricted to provascular cells in Arabidopsis thaliana. *Development*, 121(12), 4171–4182. <https://doi.org/10.3732/ajb.89.6.908>
- Baima, S., Possenti, M., Matteucci, A., Wisman, E., Altamura, M. M., Ruberti, I., & Morelli, G. (2001).** The Arabidopsis ATHB-8 HD-Zip Protein Acts as a Differentiation-Promoting Transcription Factor of the Vascular Meristems. *Plant Physiology*, 126(2), 643–55. <https://doi.org/10.1104/pp.126.2.643>
- Barolo, S., & Posakony, J. W. (2002).** Three habits of highly effective signaling pathways: Principles of transcriptional control by developmental cell signaling. *Genes and Development*, 16(10), 1167–1181. <https://doi.org/10.1101/gad.976502>
- Bauby, H., Divol, F., Truernit, E., Grandjean, O., & Palauqui, J. C. (2007).** Protophloem differentiation in early Arabidopsis thaliana development. *Plant and Cell Physiology*, 48(1), 97–109. <https://doi.org/10.1093/pcp/pcl045>
- Beck, C. B. (2010).** *An introduction to plant structure and development : plant anatomy for the twenty-first century*. Cambridge University Press.
- Belmonte, M. F., Kirkbride, R. C., Stone, S. L., Pelletier, J. M., Bui, A. Q., Yeung, E. C., Hashimoto, M., Fei, J., Harada, C. M., Munoz, M. D., Le, B. H., Drews, G. N., Brady, S. M., Goldberg, R. B., & Harada, J. J. (2013).** Comprehensive developmental profiles of gene activity in regions and subregions of the Arabidopsis seed. *Proceedings of the National Academy of Sciences*, 110(5), E435–E444. <https://doi.org/10.1073/PNAS.1222061110>
- Bennett, M. J., Marchant, A., Green, H. G., May, S. T., Ward, S. P., Millner, P. A., Walker, A. R., Schulz, B., & Feldmann, K. A. (1996).** Arabidopsis AUX1 gene: A permease-like regulator of root gravitropism. *Science*, 273(5277), 948–950. <https://doi.org/10.1126/science.273.5277.948>
- Bennett, T., Hines, G., & Leyser, O. (2014).** Canalization: What the flux? *Trends in Genetics*. <https://doi.org/10.1016/j.tig.2013.11.001>
- Berendzen, K. W., Weiste, C., Wanke, D., Kilian, J., Harter, K., Dröge-Laser, W., & Dröge-Laser, W. (2012).** Bioinformatic cis-element analyses performed in Arabidopsis and rice disclose bZIP- and MYB-related binding sites as potential AuxRE-coupling elements in auxin-mediated transcription. *BMC Plant Biology*, 12(125). <https://doi.org/10.1186/1471-2229-12-125>
- Berleth, T., & Jürgens, G. (1993).** The role of the monopteros gene in organising the basal body region of the Arabidopsis embryo. *Development*, 118, 575–587. [https://doi.org/10.1016/0168-9525\(93\)90246-E](https://doi.org/10.1016/0168-9525(93)90246-E)
- Besson, S., & Dumais, J. (2011).** Universal rule for the symmetric division of plant cells. *Proceedings of the National Academy of Sciences*, 108(15), 6294–6299. <https://doi.org/10.1073/pnas.1011866108>
- Bhalerao, R. P., & Bennett, M. J. (2003).** The case for morphogens in plants. *Nature Cell Biology*, 5(11), 939–943. <https://doi.org/10.1038/ncb1103-939>

- Bishopp, A., Help, H., El-Showk, S., Weijers, D., Scheres, B., Friml, J., Benková, E., Mähönen, A. P., & Helariutta, Y. (2011). A mutually inhibitory interaction between auxin and cytokinin specifies vascular pattern in roots. *Current Biology*, 21(11), 917–926. <https://doi.org/10.1016/j.cub.2011.04.017>
- Boer, D. R., Freire-Rios, A., Van Den Berg, W. A. M., Saaki, T., Manfield, I. W., Kepinski, S., López-Vidrieo, I., Franco-Zorrilla, J. M., De Vries, S. C., Solano, R., Weijers, D., & Coll, M. (2014). Structural basis for DNA binding specificity by the auxin-dependent ARF transcription factors. *Cell*, 156(3), 577–589. <https://doi.org/10.1016/j.cell.2013.12.027>
- Bonke, M., Thitamadee, S., Mähönen, A. P., Hauser, M. T., & Helariutta, Y. (2003). APL regulates vascular tissue identity in Arabidopsis. *Nature*, 426(6963), 181–186. <https://doi.org/10.1038/nature02100>
- Boutillier, K. (2002). Ectopic Expression of BABY BOOM Triggers a Conversion from Vegetative to Embryonic Growth. *Plant Cell*, 14(8), 1737–1749. <https://doi.org/10.1105/tpc.001941>
- Brackmann, K., Qi, J., Gebert, M., Jouannet, V., Schlamp, T., Grünwald, K., Wallner, E.-S., Novikova, D. D., Levitsky, V. G., Agustí, J., Sanchez, P., Lohmann, J. U., & Greb, T. (2018). Spatial specificity of auxin responses coordinates wood formation. *Nature Communications*, 9(1), 875. <https://doi.org/10.1038/s41467-018-03256-2>
- Brady, S. M., Orlando, D. A., Lee, J. Y., Wang, J. Y., Koch, J., Dinneny, J. R., Mace, D., Ohler, U., & Benfey, P. N. (2007). A high-resolution root spatiotemporal map reveals dominant expression patterns. *Science*, 318(5851), 801–806. <https://doi.org/10.1126/science.1146265>
- Briscoe, J., & Small, S. (2015). Morphogen rules: design principles of gradient-mediated embryo patterning. *Development*, 142(23), 3996–4009. <https://doi.org/10.1242/dev.129452>
- Brown, D. E. (2001). Flavonoids Act as Negative Regulators of Auxin Transport in Vivo in Arabidopsis. *Plant Physiology*, 126(2), 524–535. <https://doi.org/10.1104/pp.126.2.524>
- Brunoud, G., Wells, D. M., Oliva, M., Larrieu, A., Mirabet, V., Burrow, A. H., Beeckman, T., Kepinski, S., Traas, J., Bennett, M. J., & Vernoux, T. (2012). A novel sensor to map auxin response and distribution at high spatio-temporal resolution. *Nature*, 482(7383), 103–106. <https://doi.org/10.1038/nature10791>
- Calderón Villalobos, L. I. A., Lee, S., De Oliveira, C., Ivetac, A., Brandt, W., Armitage, L., Sheard, L. B., Tan, X., Parry, G., Mao, H., Zheng, N., Napier, R., Kepinski, S., & Estelle, M. (2012). A combinatorial TIR1/AFB-Aux/IAA co-receptor system for differential sensing of auxin. *Nature Chemical Biology*, 8(5), 477–485. <https://doi.org/10.1038/nchembio.926>
- Cao, J., Spielmann, M., Qiu, X., Huang, X., Ibrahim, D. M., Hill, A. J., Zhang, F., Mundlos, S., Christiansen, L., Steemers, F. J., Trapnell, C., & Shendure, J. (2019). The single-cell transcriptional landscape of mammalian organogenesis. *Nature*, 566(7745), 496–502. <https://doi.org/10.1038/s41586-019-0969-x>
- Carlsbecker, A., Lee, J. Y., Roberts, C. J., Dettmer, J., Lehesranta, S., Zhou, J., Lindgren, O., Moreno-Risueno, M. A., Vátén, A., Thitamadee, S., Campilho, A., Sebastian, J., Bowman, J. L., Helariutta, Y., & Benfey, P. N. (2010). Cell signalling by microRNA165/6 directs gene dose-dependent root cell fate. *Nature*, 465(7296), 316–321. <https://doi.org/10.1038/nature08977>
- Chen, X., Grandont, L., Li, H., Hauschild, R., Paque, S., Abuzeineh, A., Rakusová, H., Benkova, E., Perrot-Rechenmann, C., & Friml, J. (2014). Inhibition of cell expansion by rapid ABP1-mediated auxin effect on microtubules. *Nature*, 516(729), 90–93. <https://doi.org/10.1038/nature13889>
- Cheng, Y., Dai, X., & Zhao, Y. (2006). Auxin biosynthesis by the YUCCA flavin monooxygenases controls the formation of floral organs and vascular tissues in Arabidopsis. *Genes & Development*, 20(13), 1790–1799. <https://doi.org/10.1101/gad.1415106>
- Cherenkov, P., Novikova, D., Omelyanchuk, N., Levitsky, V., Grosse, I., Weijers, D., & Mironova, V. (2018). Diversity of cis-regulatory elements associated with auxin response in Arabidopsis thaliana. *Journal of Experimental Botany*, 69(2), 329–339. <https://doi.org/10.1093/jxb/erx254>
- Corish, P., & Tyler-Smith, C. (1999). Attenuation of green fluorescent protein half-life in mammalian cells. *Protein Engineering, Design and Selection*, 12(12), 1035–1040. <https://doi.org/10.1093/protein/12.12.1035>

- Crawford, B. C. W., Sewell, J., Golembeski, G., Roshan, C., Long, J. A., & Yanofsky, M. F. (2015). Genetic control of distal stem cell fate within root and embryonic meristems. *Science*, 347(6222), 655–659. <https://doi.org/10.1126/science.aaa0196>
- Curaba, J., Herzog, M., & Vachon, G. (2003). GeBP, the first member of a new gene family in Arabidopsis, encodes a nuclear protein with DNA-binding activity and is regulated by KNAT1. *The Plant Journal: For Cell and Molecular Biology*, 33(2), 305–317. <https://doi.org/10.1046/j.1365-3113.2003.00162.x> [pii]
- de Jong, M., Mariani, C., & Vriezen, W. H. (2009). The role of auxin and gibberellin in tomato fruit set. *Journal of Experimental Botany*, 60(5), 1523–1532. <https://doi.org/10.1093/jxb/erp094>
- de Luis Balaguer, M. A., Fisher, A. P., Clark, N. M., Fernandez-Espinosa, M. G., Möller, B. K., Weijers, D., Lohmann, J. U., Williams, C., Lorenzo, O., Sozzani, R., Lorenzo, O., Lohmann, J. U., Möller, B. K., Fisher, A. P., Williams, C., Clark, N. M., Weijers, D., ... Sozzani, R. (2017). Predicting gene regulatory networks by combining spatial and temporal gene expression data in Arabidopsis root stem cells. *Proceedings of the National Academy of Sciences*, 114(36), E7632–E7640. <https://doi.org/10.1073/pnas.1707566114>
- De Rybel, B., Adibi, M., Breda, A. S., Wendrich, J. R., Smit, M. E., Novák, O., Yamaguchi, N., Yoshida, S., Van Isterdael, G., Palovaara, J., Nijse, B., Boeckschoten, M. V., Hooiveld, G., Beeckman, T., Wagner, D., Ljung, K., Fleck, C., & Weijers, D. (2014). Integration of growth and patterning during vascular tissue formation in Arabidopsis. *Science*, 345(6197), 1255215. <https://doi.org/10.1126/science.1255215>
- De Rybel, B., Breda, A. S., & Weijers, D. (2014). Prenatal plumbing-vascular tissue formation in the plant embryo. *Physiologia Plantarum*, 151(2), 126–133. <https://doi.org/10.1111/pl.12091>
- De Rybel, B., Mähönen, A. P., Helariutta, Y., & Weijers, D. (2016). Plant vascular development: From early specification to differentiation. *Nature Reviews Molecular Cell Biology*, 17(1), 30–40. <https://doi.org/10.1038/nrm.2015.6>
- De Rybel, B., Möller, B., Yoshida, S., Grabowicz, I., Barbier de Reuille, P., Boeren, S., Smith, R. S., Borst, J. W., & Weijers, D. (2013). A bHLH Complex Controls Embryonic Vascular Tissue Establishment and Indeterminate Growth in Arabidopsis. *Developmental Cell*, 24(4), 426–437. <https://doi.org/10.1016/j.devcel.2012.12.013>
- De Rybel, B., van den Berg, W., Lokerse, A. S., Liao, C.-Y., van Mourik, H., Moller, B., Llavata-Peris, C. I., & Weijers, D. (2011). A Versatile Set of Ligation-Independent Cloning Vectors for Functional Studies in Plants. *Plant Physiology*, 156(3), 1292–1299. <https://doi.org/10.1104/pp.111.177337>
- Denyer, T., Ma, X., Klesen, S., Scacchi, E., Nieselt, K., & Timmermans, M. (2018). Spatiotemporal Developmental Trajectories in the Arabidopsis Root Revealed Using High-Throughput Single Cell RNA Sequencing. *SSRN Electronic Journal*. <https://doi.org/10.2139/ssrn.3300042>
- Deplancke, B., Dupuy, D., Vidal, M., & Walhout, A. J. M. (2004). A gateway-compatible yeast one-hybrid system. *Genome Research*, 14(10B), 2093–2101. <https://doi.org/10.1101/gr.2445504>
- Depuydt, S., Rodriguez-Villalon, A., Santuari, L., Wyser-Rmili, C., Ragni, L., & Hardtke, C. S. (2013). Suppression of Arabidopsis protophloem differentiation and root meristem growth by CLE45 requires the receptor-like kinase BAM3. *Proceedings of the National Academy of Sciences*, 110(17), 7074–7079. <https://doi.org/10.1073/pnas.1222314110>
- Di Laurenzio, L., Wysocka-Diller, J., Malamy, J. E., Pysh, L., Helariutta, Y., Freshour, G., Hahn, M. G., Feldmann, K. A., & Benfey, P. N. (1996). The SCARECROW gene regulates an asymmetric cell division that is essential for generating the radial organization of the Arabidopsis root. *Cell*, 86(3), 423–433. [https://doi.org/10.1016/S0092-8674\(00\)80115-4](https://doi.org/10.1016/S0092-8674(00)80115-4)
- Dinesh, D. C., Kovermann, M., Gopalswamy, M., Hellmuth, A., Calderón Villalobos, L. I. A., Lilie, H., Balbach, J., & Abel, S. (2015). Solution structure of the PsIAA4 oligomerization domain reveals interaction modes for transcription factors in early auxin response. *Proceedings of the National Academy of Sciences*, 112(19), 6230–6235. <https://doi.org/10.1073/pnas.1424077112>
- Dolan, L., Duckett, C. M., Grierson, C., Linstead, P., Schneider, K., Lawson, E., Dean, C., Poethig, S., & Roberts, K. (1994). Clonal relationships and cell patterning in the root epidermis of Arabidopsis. *Development*, 120, 2465–2474.

- Dolan, L., Janmaat, K., Willemsen, V., Linstead, P., Poethig, S., Roberts, K., & Scheres, B. (1993). Cellular organisation of the Arabidopsis thaliana root. *Development*, 119(1), 71–84. <https://doi.org/VL-119>
- Donner, T. J., Sherr, I., & Scarpella, E. (2009). Regulation of preprocambial cell state acquisition by auxin signaling in Arabidopsis leaves. *Development*, 136(19), 3235–3246. <https://doi.org/10.1242/dev.037028>
- Dreher, K. A. (2006). The Arabidopsis Aux/IAA Protein Family Has Diversified in Degradation and Auxin Responsiveness. *Plant Cell*, 18(3), 699–714. <https://doi.org/10.1105/tpc.105.039172>
- Dröge-Laser, W., Snoek, B. L., Snel, B., & Weiste, C. (2018). The Arabidopsis bZIP transcription factor family — an update. *Current Opinion in Plant Biology*, 45(PtA), 36–49. <https://doi.org/10.1016/j.pbi.2018.05.001>
- Efroni, I., & Birnbaum, K. D. (2016). The potential of single-cell profiling in plants. *Genome Biology*, 17, 65. <https://doi.org/10.1186/s13059-016-0931-2>
- Efroni, I., Ip, P. L., Nawy, T., Mello, A., & Birnbaum, K. D. (2015). Quantification of cell identity from single-cell gene expression profiles. *Genome Biology*, 16, 9. <https://doi.org/10.1186/s13059-015-0580-x>
- Efroni, I., Mello, A., Nawy, T., Ip, P. L., Rahni, R., Delrose, N., Powers, A., Satija, R., & Birnbaum, K. D. (2016). Root Regeneration Triggers an Embryo-like Sequence Guided by Hormonal Interactions. *Cell*, 165(7), 1721–1733. <https://doi.org/10.1016/j.cell.2016.04.046>
- Enders, T. A., Oh, S., Yang, Z., Montgomery, B. L., & Strader, L. C. (2015). Genome Sequencing of Arabidopsis *abp1-5* Reveals Second-Site Mutations That May Affect Phenotypes. *The Plant Cell*, 27(7), 1820–1826. <https://doi.org/10.1105/tpc.15.00214>
- Errera, L. (1888). Über Zellformen und Siefenblasen. *Botanisches Centralblatt*, 34, 395–398.
- Etchells, J. P., Mishra, L. S., Kumar, M., Campbell, L., & Turner, S. R. (2015). Wood Formation in Trees Is Increased by Manipulating PXY-Regulated Cell Division. *Current Biology*, 25(8), 1050–1055. <https://doi.org/10.1016/j.cub.2015.02.023>
- Etchells, J. P., Provost, C. M., Mishra, L., & Turner, S. R. (2013). WOX4 and WOX14 act downstream of the PXY receptor kinase to regulate plant vascular proliferation independently of any role in vascular organisation. *Development*, 140(10), 2224–2234. <https://doi.org/10.1242/dev.091314>
- Etchells, J. P., & Turner, S. R. (2010). The PXY-CLE41 receptor ligand pair defines a multifunctional pathway that controls the rate and orientation of vascular cell division. *Development*, 137(5), 767–774. <https://doi.org/10.1242/dev.044941>
- Eyer, L., Vain, T., Pařízková, B., Oklestkova, J., Barbez, E., Kozubíková, H., Pospíšil, T., Wierzbicka, R., Kleine-Vehn, J., Fránek, M., Strnad, M., Robert, S., & Novak, O. (2016). 2,4-D and IAA Amino Acid Conjugates Show Distinct Metabolism in Arabidopsis. *PloS One*, 11(7), e0159269. <https://doi.org/10.1371/journal.pone.0159269>
- Fàbregas, N., Formosa-Jordan, P., Confraria, A., Siligato, R., Alonso, J. M., Swarup, R., Bennett, M. J., Mähönen, A. P., Caño-Delgado, A. I., & Ibañez, M. (2015). Auxin Influx Carriers Control Vascular Patterning and Xylem Differentiation in Arabidopsis thaliana. *PLoS Genetics*, 11(4), e1005183. <https://doi.org/10.1371/journal.pgen.1005183>
- Farcot, E., Lavedrine, C., & Vernoux, T. (2015). A modular analysis of the auxin signalling network. *PLoS ONE*, 10(3), e0122231. <https://doi.org/10.1371/journal.pone.0122231>
- Finet, C., Berne-Dedieu, A., Scutt, C. P., & Marlétaz, F. (2013). Evolution of the ARF gene family in land plants: Old domains, new tricks. *Molecular Biology and Evolution*, 30(1), 45–56. <https://doi.org/10.1093/molbev/mss220>
- Fisher, K., & Turner, S. (2007). PXY, a Receptor-like Kinase Essential for Maintaining Polarity during Plant Vascular-Tissue Development. *Current Biology*, 17(12), 1061–1066. <https://doi.org/10.1016/j.cub.2007.05.049>
- Franco-Zorrilla, J. M., López-Vidriero, I., Carrasco, J. L., Godoy, M., Vera, P., & Solano, R. (2014). DNA-binding specificities of plant transcription factors and their potential to define target genes. *Proceedings of the National Academy of Sciences*, 111(6), 2367–2372. <https://doi.org/10.1073/pnas.1316278111>
- Friml, J., Vieten, A., Sauer, M., Weijers, D., Schwarz, H., Hamann, T., Offringa, R., & Jürgens, G. (2003).

- Efflux-dependent auxin gradients establish the apical-basal axis of Arabidopsis. *Nature*, 426(6963), 147–153. <https://doi.org/10.1038/nature02085>
- Fukuda, H., & Ohashi-Ito, K. (2019).** Vascular tissue development in plants. *Current Topics in Developmental Biology*, 131, 141–160. <https://doi.org/10.1016/BS.CTDB.2018.10.005>
- Ga lweiler, L., Guan, C., Mu ller, A., Wisman, E., Mendgen, K., Yephremov, A., & Palme, K. (1998).** Regulation of Polar Auxin Transport by AtPIN1 in Arabidopsis Vascular Tissue. *Science*, 282(5397), 2226–2230. <https://doi.org/10.1126/science.282.5397.2226>
- Gao, Y., Zhang, Y., Zhang, D., Dai, X., Estelle, M. and Z. (2015).** Auxin binding protein 1 (ABP1) is not required for either auxin signaling or Arabidopsis development. *Proceedings of the National Academy of Sciences of the United States of America*, 112, 2275–2280. <https://doi.org/10.1073/pnas.1500365112>
- Gardiner, J., Donner, T. J., & Scarpella, E. (2011).** Simultaneous activation of SHR and ATHB8 expression defines switch to preprocambial cell state in Arabidopsis leaf development. *Developmental Dynamics*, 240(1), 261–270. <https://doi.org/10.1002/dvdy.22516>
- Gardiner, J., Sherr, I., & Scarpella, E. (2010).** Expression of DOF genes identifies early stages of vascular development in Arabidopsis leaves. *International Journal of Developmental Biology*, 54(8–9), 1389–1396. <https://doi.org/10.1387/ijdb.093006jg>
- Gaudinier, A., Rodriguez-Medina, J., Zhang, L., Olson, A., Liseron-Monfils, C., Bågman, A. M., Foret, J., Abbitt, S., Tang, M., Li, B., Runcie, D. E., Kliebenstein, D. J., Shen, B., Frank, M. J., Ware, D., & Brady, S. M. (2018).** Transcriptional regulation of nitrogen-associated metabolism and growth. *Nature*, 563(7730), 259–264. <https://doi.org/10.1038/s41586-018-0656-3>
- Gaudinier, A., Tang, M., Bågman, A. M., & Brady, S. M. (2017).** Identification of protein–DNA interactions using enhanced yeast one-hybrid assays and a semiautomated approach. In *Methods in Molecular Biology* (pp. 187–215). [https://doi.org/10.1007/978-1-4939-7003-2\\_13](https://doi.org/10.1007/978-1-4939-7003-2_13)
- Gaudinier, A., Zhang, L., Reece-Hoyes, J. S., Taylor-Teeple, M., Pu, L., Liu, Z., Breton, G., Pruneda-Paz, J. L., Kim, D., Kay, S. A., Walhout, A. J. M., Ware, D., & Brady, S. M. (2011).** Enhanced Y1H assays for Arabidopsis. *Nature Methods*, 8(12), 1053–1055. <https://doi.org/10.1038/nmeth.1750>
- Gendrel, A. V., Lippman, Z., Martienssen, R., & Colot, V. (2005).** Profiling histone modification patterns in plants using genomic tiling microarrays. *Nature Methods*, 2(3), 213–218. <https://doi.org/10.1038/nmeth0305-213>
- Ghosh, I., Hamilton, A. D., Regan, L., Indraneel Ghosh, Andrew D. Hamilton, \* and, & Regan\*, L. (2000).** Antiparallel leucine zipper-directed protein reassembly: Application to the green fluorescent protein. *Journal of the American Chemical Society*, 122, 5658–5659. <https://doi.org/10.1021/ja994421w>
- Giuliano, G., Pichersky, E., Malik, V. S., Timko, M. P., Scolnik, P. a, & Cashmore, a R. (1988).** An evolutionarily conserved protein binding sequence upstream of a plant light-regulated gene. *Proceedings of the National Academy of Sciences of the United States of America*, 85(19), 7089–7093. <https://doi.org/10.1073/pnas.85.19.7089>
- Goldschmidt, E. E. (2014).** Plant grafting: new mechanisms, evolutionary implications. *Frontiers in Plant Science*, 5, 727. <https://doi.org/10.3389/fpls.2014.00727>
- Grones, P., Chen, X., Simon, S., Kaufmann, W. A., De Rycke, R., Nodzyński, T., Zažímalová, E., & Friml, J. (2015).** Auxin-binding pocket of ABP1 is crucial for its gain-of-function cellular and developmental roles. In *Journal of Experimental Botany* (Vol. 66, pp. 5055–5065). <https://doi.org/10.1093/jxb/erv177>
- Grones, P., & Friml, J. (2015).** ABP1: Finally docking. *Molecular Plant*, 8(3), 356–358. <https://doi.org/10.1016/j.molp.2014.12.013>
- Guilfoyle, T. J., & Hagen, G. (2007).** Auxin response factors. *Current Opinion in Plant Biology*, 10(5), 453–460. <https://doi.org/10.1016/J.PBI.2007.08.014>
- Guo, F., Li, L., Li, J., Wu, X., Hu, B., Zhu, P., Wen, L., & Tang, F. (2017).** Single-cell multi-omics sequencing of mouse early embryos and embryonic stem cells. *Cell Research*, 27(8), 967–988. <https://doi.org/10.1038/cr.2017.82>



- Guo, G., Huss, M., Tong, G. Q., Wang, C., Li Sun, L., Clarke, N. D., & Robson, P. (2010). Resolution of Cell Fate Decisions Revealed by Single-Cell Gene Expression Analysis from Zygote to Blastocyst. *Developmental Cell*, 18(4), 675–685. <https://doi.org/10.1016/j.devcel.2010.02.012>
- Hamann, T., Benkova, E., Bäurle, I., Kientz, M., & Jürgens, G. (2002). The Arabidopsis BODENLOS gene encodes an auxin response protein inhibiting MONOPTEROS-mediated embryo patterning. *Genes and Development*, 16(13), 1610–1615. <https://doi.org/10.1101/gad.229402>
- Hamann, T., Mayer, U., & Jürgens, G. (1999). The auxin-insensitive bodenlos mutation affects primary root formation and apical-basal patterning in the Arabidopsis embryo. *Development (Cambridge, England)*, 126(7), 1387–1395.
- Han, M., Park, Y., Kim, I., Kim, E.-H., Yu, T.-K., Rhee, S., & Suh, J.-Y. (2014). Structural basis for the auxin-induced transcriptional regulation by Aux/IAA17. *Proceedings of the National Academy of Sciences*, 111(52), 18613–18618. <https://doi.org/10.1073/pnas.1419525112>
- Hardtke, C. S., & Berleth, T. (1998). The Arabidopsis gene MONOPTEROS encodes a transcription factor mediating embryo axis formation and vascular development. *EMBO Journal*, 17(5), 1405–1411. <https://doi.org/10.1093/emboj/17.5.1405>
- Heidstra, R., & Sabatini, S. (2014). Plant and animal stem cells: Similar yet different. *Nature Reviews Molecular Cell Biology*, 15(5), 301–312. <https://doi.org/10.1038/nrm3790>
- Hellemans, J., Mortier, G., De Paepe, A., Speleman, F., & Vandesompele, J. (2008). qBase relative quantification framework and software for management and automated analysis of real-time quantitative PCR data. *Genome Biology*, 8(2), R19. <https://doi.org/10.1186/gb-2007-8-2-r19>
- Hirakawa, Y., Kondo, Y., & Fukuda, H. (2010). TDIF Peptide Signaling Regulates Vascular Stem Cell Proliferation via the WOX4 Homeobox Gene in Arabidopsis. *The Plant Cell*, 22(8), 2618–2629. <https://doi.org/10.1105/tpc.110.076083>
- Hiratsu, K., Matsui, K., Koyama, T., & Ohme-Takagi, M. (2003). Dominant repression of target genes by chimeric repressors that include the EAR motif, a repression domain, in Arabidopsis. *Plant Journal*, 34(5), 733–739. <https://doi.org/10.1046/j.1365-313X.2003.01759.x>
- Horstman, A., Tonaco, I. A. N., Boutillier, K., & Immink, R. G. H. (2014). A Cautionary note on the use of split-YFP/BiFC in plant protein-protein interaction studies. *International Journal of Molecular Sciences*, 15(6), 9628–9643. <https://doi.org/10.3390/ijms15069628>
- Hošek, P., Kubeš, M., Laňková, M., Dobrev, P. I., Klíma, P., Kohoutová, M., Petrášek, J., Hoyerová, K., Jiřina, M., & Zažímalová, E. (2012). Auxin transport at cellular level: new insights supported by mathematical modelling. *Journal of Experimental Botany*, 63(10), 3815–3827. <https://doi.org/10.1093/jxb/ers074>
- Huang, S., Li, R., Zhang, Z., Li, L., Gu, X., Fan, W., Lucas, W. J., Wang, X., Xie, B., Ni, P., Ren, Y., Zhu, H., Li, J., Lin, K., Jin, W., Fei, Z., Li, G., ... Li, S. (2009). The genome of the cucumber, *Cucumis sativus* L. *Nature Genetics*, 41, 1275–1281. <https://doi.org/10.1038/ng.475>
- Irisarri, P., Binczycki, P., Errea, P., Martens, H. J., & Pina, A. (2015). Oxidative stress associated with rootstock-scion interactions in pear/quince combinations during early stages of graft development. *Journal of Plant Physiology*, 176, 25–35. <https://doi.org/10.1016/j.jplph.2014.10.015>
- Jacobs, W. P. (1952). The Role of Auxin in Differentiation of Xylem Around a Wound. *American Journal of Botany*, 39(5), 301. <https://doi.org/10.2307/2438258>
- Jakoby, M., Weisshaar, B., Dröge-Laser, W., Vicente-Carbajosa, J., Tiedemann, J., Kroj, T., Parcy, F., & bZIP Research Group. (2002). bZIP transcription factors in Arabidopsis. *Trends in Plant Science*, 7(3), 106–111. [https://doi.org/10.1016/S1360-1385\(01\)00223-3](https://doi.org/10.1016/S1360-1385(01)00223-3)
- Jean-Baptiste, K., McFaline-Figueroa, J. L., Alexandre, C. M., Dorrity, M. W., Saunders, L., Bubb, K. L., Trapnell, C., Fields, S., Queitsch, C., & Cuperus, J. T. (2019). Dynamics of gene expression in single root cells of *A. thaliana*. *BioRxiv*, 448514. <https://doi.org/10.1101/448514>
- Jeffree, C. E., & Yeoman, M. M. (1983). Development of intercellular connections between opposing cells in a



- graft union. *New Phytologist*, 93(4), 491–510. <https://doi.org/10.1111/j.1469-8137.1983.tb02701.x>
- Jin, J., Tian, F., Yang, D. C., Meng, Y. Q., Kong, L., Luo, J., & Gao, G. (2017).** PlantTFDB 4.0: Toward a central hub for transcription factors and regulatory interactions in plants. *Nucleic Acids Research*, 45(D1), D1040–D1045. <https://doi.org/10.1093/nar/gkw982>
- Jones, S. (2004).** An overview of the basic helix-loop-helix proteins. *Genome Biology*, 5(6), 226. <https://doi.org/10.1186/gb-2004-5-6-226>
- José Ripoll, J., Bailey, L. J., Mai, Q.-A., Wu, S. L., Hon, C. T., Chapman, E. J., Ditta, G. S., Estelle, M., & Yanofsky, M. F. (2015).** microRNA regulation of fruit growth. *Nature Plants*, 1(4), 15036. <https://doi.org/10.1038/nplants.2015.36>
- Journot-Catalino, N., Somssich, I. E., Roby, D., & Kroj, T. (2006).** The transcription factors WRKY11 and WRKY17 act as negative regulators of basal resistance in *Arabidopsis thaliana*. *The Plant Cell*, 18(11), 3289–3302. <https://doi.org/10.1105/tpc.106.044149>
- Kato, H., Kouno, M., Takeda, M., Suzuki, H., Ishizaki, K., Nishihama, R., & Kohchi, T. (2017).** The roles of the sole activator-type auxin response factor in pattern formation of marchantia polymorpha. *Plant and Cell Physiology*, 58(10), 1642–1651. <https://doi.org/10.1093/pcp/pcx095>
- Kepinski, S., & Leyser, O. (2005).** The *Arabidopsis* F-box protein TIR1 is an auxin receptor. *Nature*, 435(7041), 446–451. <https://doi.org/10.1038/nature03542>
- Kim, J., Kang, H., Park, J., Kim, W., Yoo, J., Lee, N., Kim, J., Yoon, T.-Y., & Choi, G. (2016).** PIF1-Interacting Transcription Factors and Their Binding Sequence Elements Determine the in Vivo Targeting Sites of PIF1. *The Plant Cell*, 28(6), 1388–1405. <https://doi.org/10.1105/tpc.16.00125>
- Klimczak, L. J. (1992).** DNA Binding Activity of the *Arabidopsis* G-Box Binding Factor GBF1 Is Stimulated by Phosphorylation by Casein Kinase II from Broccoli. *Plant Cell*, 4(1), 87–98. <https://doi.org/10.1105/tpc.4.1.87>
- Kondo, Y., Fujita, T., Sugiyama, M., & Fukuda, H. (2015).** A novel system for xylem cell differentiation in *arabidopsis thaliana*. *Molecular Plant*, 8(4), 612–621. <https://doi.org/10.1016/j.molp.2014.10.008>
- Kondo, Y., Ito, T., Nakagami, H., Hirakawa, Y., Saito, M., Tamaki, T., Shirasu, K., & Fukuda, H. (2014).** Plant GSK3 proteins regulate xylem cell differentiation downstream of TDIF-TDR signalling. *Nature Communications*, 5(3504), 3504. <https://doi.org/10.1038/ncomms4504>
- Kondo, Y., Nurani, A. M., Saito, C., Ichihashi, Y., Saito, M., Yamazaki, K., Mitsuda, N., Ohme-Takagi, M., & Fukuda, H. (2016).** Vascular Cell Induction Culture System Using *Arabidopsis* Leaves (VISUAL) Reveals the Sequential Differentiation of Sieve Element-Like Cells. *The Plant Cell*, 28(6), 1250–1262. <https://doi.org/10.1105/tpc.16.00027>
- Konishi, M., Donner, T. J., Scarpella, E., & Yanagisawa, S. (2015).** MONOPTEROS directly activates the auxin-inducible promoter of the Dof5.8 transcription factor gene in *Arabidopsis thaliana* leaf provascular cells. *Journal of Experimental Botany*, 66(1), 283–291. <https://doi.org/10.1093/jxb/eru418>
- Korasick, D. A., Westfall, C. S., Lee, S. G., Nanao, M. H., Dumas, R., Hagen, G., Guilfoyle, T. J., Jez, J. M., & Strader, L. C. (2014).** Molecular basis for AUXIN RESPONSE FACTOR protein interaction and the control of auxin response repression. *Proceedings of the National Academy of Sciences*, 111(14), 5427–5432. <https://doi.org/10.1073/pnas.1400074111>
- Krogan, N. T., Ckurshumova, W., Marcos, D., Caragea, A. E., & Berleth, T. (2012).** Deletion of MP/ARF5 domains III and IV reveals a requirement for Aux/IAA regulation in *Arabidopsis* leaf vascular patterning. *New Phytologist*, 194(2), 391–401. <https://doi.org/10.1111/j.1469-8137.2012.04064.x>
- Lau, S., Jurgens, G., & De Smet, I. (2008).** The Evolving Complexity of the Auxin Pathway. *Plant Cell*, 20(7), 1738–1746. <https://doi.org/10.1105/tpc.108.060418>
- Lawrence, P. A., & Struhl, G. (1996).** Morphogens, compartments, and pattern: Lessons from *Drosophila*? *Cell*, 85(7), 951–961. [https://doi.org/10.1016/S0092-8674\(00\)81297-0](https://doi.org/10.1016/S0092-8674(00)81297-0)
- Lee, H. W., Kim, N. Y., Lee, D. J., & Kim, J. (2009).** LBD18/ASL20 Regulates Lateral Root Formation in Combination with LBD16/ASL18 Downstream of ARF7 and ARF19 in *Arabidopsis*. *Plant Physiology*, 151(3),

- 1377–1389. <https://doi.org/10.1104/pp.109.143685>
- Lee, J.-M., & Oda, M. (2010). Grafting of Herbaceous Vegetable and Ornamental Crops. In *Horticultural Reviews* (p. 63). <https://doi.org/10.1002/9780470650851.ch2>
- Lee, S. W., Feugier, F. G., & Morishita, Y. (2014). Canalization-based vein formation in a growing leaf. *Journal of Theoretical Biology*, 353, 104–120. <https://doi.org/10.1016/j.jtbi.2014.03.005>
- León, J., Rojo, E., & Sánchez-Serrano, J. J. (2001). Wound signalling in plants. *Journal of Experimental Botany*, 52(354), 1–9. <https://doi.org/10.1093/jxb/52.354.1>
- Levitsky V.G., Oshchepkov D.Y., Zemlyanskaya E.V., Mironova V.V., Ignatieva E.V., Podkolodnaya O.A., Merkulova T.I. (2018). The overlapped motifs co-occurrence in ChIP-seq data. *The 11th International Conference "On Bioinformatics of Genome Regulation and Structure" Systems Biology (BGRS\SB'2018) 20-25 August 2018*. p.58.
- Liao, C.-Y., Smet, W., Brunoud, G., Yoshida, S., Vernoux, T., & Weijers, D. (2015). Reporters for sensitive and quantitative measurement of auxin response. *Nature Methods*, 12(3), 207–210. <https://doi.org/10.1038/nmeth.3279>
- Llavata-Peris, C. I. (2013). *Proteomic and mechanistic analysis of Auxin Response Factors in the Arabidopsis embryo*. Wageningen University.
- Long, Y., Smet, W., Cruz-Ramírez, A., Castelijn, B., de Jonge, W., Mähönen, A. P., Bouchet, B. P., Perez, G. S., Akhmanova, A., Scheres, B., & Blilou, I. (2015). Arabidopsis BIRD Zinc Finger Proteins Jointly Stabilize Tissue Boundaries by Confining the Cell Fate Regulator SHORT-ROOT and Contributing to Fate Specification. *The Plant Cell*, 27(4), 1185–1199. <https://doi.org/10.1105/tpc.114.132407>
- MacAlister, C. A., Ohashi-Ito, K., & Bergmann, D. C. (2007). Transcription factor control of asymmetric cell divisions that establish the stomatal lineage. *Nature*, 445, 537–540. <https://doi.org/10.1038/nature05491>
- Maher, K. A., Bajic, M., Kajala, K., Reynoso, M., Pauluzzi, G., West, D., Zumstein, K., Woodhouse, M., Bubb, K. L., Dorrity, M. W., Queitsch, C., Bailey-Serres, J., Sinha, N., Brady, S. M., & Deal, R. (2018). Profiling of Accessible Chromatin Regions across Multiple Plant Species and Cell Types Reveals Common Gene Regulatory Principles and New Control Modules. *Plant Cell*, 30(1), 15–36. <https://doi.org/10.1105/tpc.17.00581>
- Mähönen, A. P., Bishopp, A., Higuchi, M., Nieminen, K. M., Kinoshita, K., Törmäkangas, K., Ikeda, Y., Oka, A., Kakimoto, T., & Helariutta, Y. (2006). Cytokinin signaling and its inhibitor AHP6 regulate cell fate during vascular development. *Science*, 311(5757), 94–98. <https://doi.org/10.1126/science.1118875>
- Mähönen, A. P., Bonke, M., Kauppinen, L., Riikonen, M., Benfey, P. N., & Helariutta, Y. (2000). A novel two-component hybrid molecule regulates vascular morphogenesis of the Arabidopsis root. *Genes and Development*, 14(23), 2938–2943. <https://doi.org/10.1101/gad.189200>
- Marchant, A. (1999). AUX1 regulates root gravitropism in Arabidopsis by facilitating auxin uptake within root apical tissues. *The EMBO Journal*, 18(8), 2066–2073. <https://doi.org/10.1093/emboj/18.8.2066>
- Martínez-García, J. F., Huq, E., & Quail, P. H. (2000). Direct targeting of light signals to a promoter element-bound transcription factor. *Science*, 288(5467), 859–863. <https://doi.org/10.1126/science.288.5467.859>
- Mashiguchi, K., Tanaka, K., Sakai, T., Sugawara, S., Kawaide, H., Natsume, M., Hanada, A., Yaeno, T., Shirasu, K., Yao, H., McSteen, P., Zhao, Y., Hayashi, K. -i., Kamiya, Y., & Kasahara, H. (2011). The main auxin biosynthesis pathway in Arabidopsis. *Proceedings of the National Academy of Sciences*, 108(45), 18512–18517. <https://doi.org/10.1073/pnas.1108434108>
- Mattsson, J., Ckurshumova, W., & Berleth, T. (2003). Auxin signaling in Arabidopsis leaf vascular development. *Plant Physiology*, 131(3), 1327–1339. <https://doi.org/10.1104/pp.013623>
- Mayer, U., Ruiz, R. a. T., Berleth, T., Miseéra, S., & Jüürgens, G. (1991). Mutations affecting body organization in the Arabidopsis embryo. *Nature*, 353, 402–407. <https://doi.org/10.1038/353402a0>
- McConnell, J. R., Emery, J., Eshed, Y., Bao, N., Bowman, J., & Barton, M. K. (2001). Role of PHABULOSA and PHAVOLUTA in determining radial patterning in shoots. *Nature*, 411(6838), 709–713. <https://doi.org/10.1038/35079635>
- Medford, J. I., Elmer, J. S., & Klee, H. J. (2007). Molecular Cloning and Characterization of Genes Expressed

in Shoot Apical Meristems. *The Plant Cell*, 3(4), 359–370. <https://doi.org/10.2307/3869211>

**Melnyk, C. W., Gabel, A., Hardcastle, T. J., Robinson, S., Miyashima, S., Grosse, I., & Meyerowitz, E. M. (2018).** Transcriptome dynamics at Arabidopsis graft junctions reveal an intertissue recognition mechanism that activates vascular regeneration. *Proceedings of the National Academy of Sciences*, 115(10), E2447–56. <https://doi.org/10.1073/pnas.1718263115>

**Melnyk, C. W., Schuster, C., Leyser, O., & Meyerowitz, E. M. (2015).** A developmental framework for graft formation and vascular reconnection in arabidopsis thaliana. *Current Biology*, 25(10), 1306–1318. <https://doi.org/10.1016/j.cub.2015.03.032>

**Menkens, a E., & Cashmore, a R. (1994).** Isolation and characterization of a fourth Arabidopsis thaliana G-box-binding factor, which has similarities to Fos oncoprotein. *Proceedings of the National Academy of Sciences of the United States of America*, 91(7), 2522–2526. <https://doi.org/10.1073/PNAS.91.7.2522>

**Menkens, A. E., Schindler, U., & Cashmore, A. R. (1995).** The G-box: a ubiquitous regulatory DNA element in plants bound by the GBF family of bZIP proteins. *Trends in Biochemical Sciences*, 20(12), 506–510. [https://doi.org/10.1016/S0968-0004\(00\)89118-5](https://doi.org/10.1016/S0968-0004(00)89118-5)

**Miyashima, S., Roszak, P., Seville, I., Toyokura, K., Blob, B., Heo, J., Mellor, N., Help-Rinta-Rahko, H., Otero, S., Smet, W., Boeckschoten, M., Hooiveld, G., Hashimoto, K., Smetana, O., Siligato, R., Wallner, E.-S., Mähönen, A. P., ... Helariutta, Y. (2019).** Mobile PEAR transcription factors integrate positional cues to prime cambial growth. *Nature*, 565(7740), 490–494. <https://doi.org/10.1038/s41586-018-0839-y>

**Möller, B. K., ten Hove, C. A., Xiang, D., Williams, N., López, L. G., Yoshida, S., Smit, M., Datla, R., & Weijers, D. (2017).** Auxin response cell-autonomously controls ground tissue initiation in the early Arabidopsis embryo. *Proceedings of the National Academy of Sciences*, 114(12), E2533–E2539. <https://doi.org/10.1073/pnas.1616493114>

**Möller, B., & Weijers, D. (2009).** Auxin control of embryo patterning. *Cold Spring Harbor Perspectives in Biology*. <https://doi.org/10.1101/cshperspect.a001545>

**Moore, R., & Walker, D. B. (1983).** Studies of vegetative compatibility-incompatibility in higher plants - VI. Grafting of Sedum and Solanum callus tissue in vitro. *Protoplasma*, 115(2–3), 114–121. <https://doi.org/10.1007/BF01279803>

**Mouchel, C. F., Osmont, K. S., & Hardtke, C. S. (2006).** BRX mediates feedback between brassinosteroid levels and auxin signalling in root growth. *Nature*, 443(7110), 458–461. <https://doi.org/10.1038/nature05130>

**Moussian, B., Schoof, H., Haecker, A., Jürgens, G., & Laux, T. (1998).** Role of the ZWILLE gene in the regulation of central shoot meristem cell fate during Arabidopsis embryogenesis. *EMBO Journal*, 17(6), 1799–1809. <https://doi.org/10.1093/emboj/17.6.1799>

**Mutte, S. K., Kato, H., Rothfels, C., Melkonian, M., Wong, G. K. S., & Weijers, D. (2018).** Origin and evolution of the nuclear auxin response system. *ELife*, 7, e33399. <https://doi.org/10.7554/eLife.33399>

**Nakajima, K., Sena, G., Nawy, T., & Benfey, P. N. (2001).** Intercellular movement of the putative transcription factor SHR in root patterning. *Nature*, 413(6853), 307–311. <https://doi.org/10.1038/35095061>

**Nanao, M. H., Vinos-Poyo, T., Brunoud, G., Thévenon, E., Mazzoleni, M., Mast, D., Lainé, S., Wang, S., Hagen, G., Li, H., Guilfoyle, T. J., Parcy, F., Vernoux, T., & Dumas, R. (2014).** Structural basis for oligomerization of auxin transcriptional regulators. *Nature Communications*, 5, 3617. <https://doi.org/10.1038/ncomms4617>

**Nishioka, N., Inoue, K., Adachi, K., Kiyonari, H., Ota, M., Ralston, A., Yabuta, N., Hirahara, S., Stephenson, R. O., Ogonuki, N., Makita, R., Kurihara, H., Morin-Kensicki, E. M., Nojima, H., Rossant, J., Nakao, K., Niwa, H., & Sasaki, H. (2009).** The Hippo Signaling Pathway Components Lats and Yap Pattern Tead4 Activity to Distinguish Mouse Trophectoderm from Inner Cell Mass. *Developmental Cell*, 16(3), 398–410. <https://doi.org/10.1016/J.DEVCEL.2009.02.003>

**Niwa, H. (2018).** The principles that govern transcription factor network functions in stem cells. *Development*, 145(6), dev157420. <https://doi.org/10.1242/dev.157420>

- O'Malley, R. C., Huang, S. S. C., Song, L., Lewsey, M. G., Bartlett, A., Nery, J. R., Galli, M., Gallavotti, A., & Ecker, J. R. (2016). Cistrome and Epicistrome Features Shape the Regulatory DNA Landscape. *Cell*, 165(5), 1280–1292. <https://doi.org/10.1016/j.cell.2016.04.038>
- Oh, E., Zhu, J. Y., Bai, M. Y., Arenhart, R. A., Sun, Y., & Wang, Z. Y. (2014). Cell elongation is regulated through a central circuit of interacting transcription factors in the Arabidopsis hypocotyl. *ELife*, 3. <https://doi.org/10.7554/eLife.03031>
- Oh, E., Zhu, J. Y., & Wang, Z. Y. (2012). Interaction between BZR1 and PIF4 integrates brassinosteroid and environmental responses. *Nature Cell Biology*, 14(8), 802–809. <https://doi.org/10.1038/ncb2545>
- Ohashi-Ito, K., & Fukuda, H. (2010). Transcriptional regulation of vascular cell fates. *Current Opinion in Plant Biology*, 13(6), 670–676. <https://doi.org/10.1016/j.pbi.2010.08.011>
- Ohashi-Ito, K., Matsukawa, M., & Fukuda, H. (2013). An atypical bHLH transcription factor regulates early xylem development downstream of auxin. *Plant and Cell Physiology*, 54(3), 398–405. <https://doi.org/10.1093/pcp/pct013>
- Ohashi-Ito, K., Saegusa, M., Iwamoto, K., Oda, Y., Katayama, H., Kojima, M., Sakakibara, H., & Fukuda, H. (2014). A bHLH complex activates vascular cell division via cytokinin action in root apical meristem. *Current Biology*, 24(17), 2053–2058. <https://doi.org/10.1016/j.cub.2014.07.050>
- Okada, K., Ueda, J., Komaki, M. K., Bell, C. J., & Shimura, Y. (1991). Requirement of the Auxin Polar Transport System in Early Stages of Arabidopsis Floral Bud Formation. *Plant Cell*, 3(7), 677–684.
- Okushima, Y. (2005). Functional Genomic Analysis of the AUXIN RESPONSE FACTOR Gene Family Members in Arabidopsis thaliana: Unique and Overlapping Functions of ARF7 and ARF19. *Plant Cell*, 17(2), 444–463. <https://doi.org/10.1105/tpc.104.028316>
- Palovaara, J., de Zeeuw, T., & Weijers, D. (2016). Tissue and Organ Initiation in the Plant Embryo: A First Time for Everything. *Annual Review of Cell and Developmental Biology*, 32, 47–75. <https://doi.org/10.1146/annurev-cellbio-111315-124929>
- Palovaara, J., Saiga, S., Wendrich, J. R., Van 't Wout Hofland, N., Van Schayck, J. P., Hater, F., Mutte, S., Sjollem, J., Boekschoten, M., Hooiveld, G. J., & Weijers, D. (2017). Transcriptome dynamics revealed by a gene expression atlas of the early Arabidopsis embryo. *Nature Plants*, 3(11), 894–904. <https://doi.org/10.1038/s41477-017-0035-3>
- Palovaara, J., & Weijers, D. (2018). Adapting INTACT to analyse cell-type-specific transcriptomes and nucleocytoplasmic mRNA dynamics in the Arabidopsis embryo. *Plant Reproduction*, 1–9. <https://doi.org/10.1007/s00497-018-0347-0>
- Peer, W. A. (2013). From perception to attenuation: Auxin signalling and responses. *Current Opinion in Plant Biology*, 16(5), 561–568. <https://doi.org/10.1016/j.pbi.2013.08.003>
- Perrella, G., Carr, C., Asensi-Fabado, M. A., Donald, N. A., Páldi, K., Hannah, M. A., & Amtmann, A. (2016). The Histone Deacetylase Complex 1 Protein of Arabidopsis Has the Capacity to Interact with Multiple Proteins Including Histone 3-Binding Proteins and Histone 1 Variants. *Plant Physiology*, 171(1), 62–70. <https://doi.org/10.1104/pp.15.01760>
- Pina, A., Errea, P., & Martens, H. J. (2012). Graft union formation and cell-to-cell communication via plasmodesmata in compatible and incompatible stem unions of Prunus spp. *Scientia Horticulturae*, 143, 144–150. <https://doi.org/10.1016/j.scienta.2012.06.017>
- Popko, J., Fernandes, A., Brites, D., & Lanier, L. M. (2009). Automated analysis of neuronj tracing data. *Cytometry Part A*, 75(4), 371–376. <https://doi.org/10.1002/cyto.a.20660>
- R Core Team. (2013). R: A Language and Environment for Statistical Computing. *R Journal*, 3(1), 201. <https://doi.org/10.1007/978-3-540-74686-7>
- Rademacher, E. H., Möller, B., Lokerse, A. S., Llavata-Peris, C. I., Van Den Berg, W., & Weijers, D. (2011). A cellular expression map of the Arabidopsis AUXIN RESPONSE FACTOR gene family. *Plant Journal*, 68(4), 597–606. <https://doi.org/10.1111/j.1365-313X.2011.04710.x>

- Rademacher, E. H., Lokerse, A. S., Schlereth, A., Llavata-Peris, C. I., Bayer, M., Kientz, M., FreireRios, A., Borst, J. W., Lukowitz, W., Jürgens, G., & Weijers, D. (2012). Different Auxin Response Machineries Control Distinct Cell Fates in the Early Plant Embryo. *Developmental Cell*, 22(17), 211–222. <https://doi.org/10.1016/j.devcel.2011.10.026>
- Radoeva, T., Ten Hove, C. A., Saiga, S., & Weijers, D. (2016). Molecular Characterization of Arabidopsis GAL4/UAS Enhancer Trap Lines Identifies Novel Cell-Type-Specific Promoters. *Plant Physiology*, 171(2), 1169–1181. <https://doi.org/10.1104/pp.16.00213>
- Rappsilber, J., Mann, M., & Ishihama, Y. (2007). Protocol for micro-purification, enrichment, pre-fractionation and storage of peptides for proteomics using StageTips. *Nature Protocols*, (2), 1896–1906. <https://doi.org/10.1038/nprot.2007.261>
- Raven, P. H., Evert, R. F., & Eichhorn, S. E. (2005). *Raven Biology of Plants*. Biology of Plants. New York, W.H. Freeman and Co.
- Reece-Hoyes, J. S., Diallo, A., Lajoie, B., Kent, A., Shrestha, S., Kadreppa, S., Pesyna, C., Dekker, J., Myers, C. L., & Walhout, A. J. M. (2011). Enhanced yeast one-hybrid assays for high-throughput gene-centered regulatory network mapping. *Nature Methods*, 8(12), 1059–1064. <https://doi.org/10.1038/nmeth.1748>
- Robert, H. S., Grones, P., Stepanova, A. N., Robles, L. M., Lokerse, A. S., Alonso, J. M., Weijers, D., & Friml, J. (2013). Local auxin sources orient the apical-basal axis in arabidopsis embryos. *Current Biology*, 23(24), 2506–2512. <https://doi.org/10.1016/j.cub.2013.09.039>
- Robert, H. S., Grunewald, W., Sauer, M., Cannoot, B., Soriano, M., Swarup, R., Weijers, D., Bennett, M., Boutilier, K., & Friml, J. (2015). Plant embryogenesis requires AUX/LAX-mediated auxin influx. *Development*, 142(4), 702–711. <https://doi.org/10.1242/dev.115832>
- Rodriguez-Villalon, A., Gujas, B., Kang, Y. H., Breda, A. S., Cattaneo, P., Depuydt, S., & Hardtke, C. S. (2014). Molecular genetic framework for protophloem formation. *Proceedings of the National Academy of Sciences*, 111(31), 11551–11556. <https://doi.org/10.1073/pnas.1407337111>
- Rolland-Lagan, A. G., & Prusinkiewicz, P. (2005). Reviewing models of auxin canalization in the context of leaf vein pattern formation in Arabidopsis. *Plant Journal*, 44(5), 854–865. <https://doi.org/10.1111/j.1365-313X.2005.02581.x>
- Roodbarkelari, F., Du, F., Truernit, E., & Laux, T. (2015). ZLL/AGO10 maintains shoot meristem stem cells during Arabidopsis embryogenesis by down-regulating ARF2-mediated auxin response. *BMC Biology*, 13(1), 74. <https://doi.org/10.1186/s12915-015-0180-y>
- Roosjen, M., Paque, S., & Weijers, D. (2018). Auxin Response Factors: Output control in auxin biology. *Journal of Experimental Botany*, 69(2), 179–188. <https://doi.org/10.1093/jxb/erx237>
- Rossant, J., & Tam, P. P. L. (2009). Blastocyst lineage formation, early embryonic asymmetries and axis patterning in the mouse. *Development*, 136(5), 701–713. <https://doi.org/10.1242/dev.017178>
- Ryu, K. H., Huang, L., Kang, H. M., & Schiefelbein, J. (2019). Single-cell RNA sequencing resolves molecular relationships among individual plant cells. *Plant Physiology*, pp.01482.2018. <https://doi.org/10.1104/pp.18.01482>
- Sachs, T. (1969). Polarity and the induction of organized vascular tissues. *Annals of Botany*, 33(2), 263–275. <https://doi.org/10.1093/oxfordjournals.aob.a084281>
- Sachs, T. (1975). Plant tumors resulting from unregulated hormone synthesis. *Journal of Theoretical Biology*, 55(2), 445–453. [https://doi.org/10.1016/S0022-5193\(75\)80092-0](https://doi.org/10.1016/S0022-5193(75)80092-0)
- Sachs, T. (1981). The Control of the Patterned Differentiation of Vascular Tissues. *Advances in Botanical Research*, 9, 151–262. [https://doi.org/10.1016/S0065-2296\(08\)60351-1](https://doi.org/10.1016/S0065-2296(08)60351-1)
- Sachs, T. (1991). Cell polarity and tissue patterning in plants. *Development Supplement I*, 113, 83–93.
- Sachs, T. (2000). Integrating cellular and organismic aspects of vascular differentiation. *Plant and Cell Physiology*, 117(7), 1179–1190. <https://doi.org/10.1093/pcp/41.6.649>
- Sauer, M., Balla, J., Luschign, C., Wiśniewska, J., Reinöhl, V., Friml, J., & Benková, E. (2006). Canalization



- of auxin flow by Aux/IAA-ARF-dependent feedback regulation of PIN polarity. *Genes and Development*, 20(20), 2902–2911. <https://doi.org/10.1101/gad.390806>
- Scanlon, M. J. (2003).** The Polar Auxin Transport Inhibitor N-1-Naphthylphthalamic Acid Disrupts Leaf Initiation, KNOX Protein Regulation, and Formation of Leaf Margins in Maize. *Plant Physiology*, 133(2), 597–605. <https://doi.org/10.1104/pp.103.026880>
- Scarpella, E. (2017).** The logic of plant vascular patterning. Polarity, continuity and plasticity in the formation of the veins and of their networks. *Current Opinion in Genetics and Development*, 45, 34–43. <https://doi.org/10.1016/j.gde.2017.02.009>
- Scarpella, E., Barkoulas, M., & Tsiantis, M. (2010).** Control of leaf and vein development by auxin. *Cold Spring Harbor Perspectives in Biology*, 2(1).
- Scarpella, E., Marcos, D., Friml, J. J., & Berleth, T. (2006).** Control of leaf vascular patterning by polar auxin transport. *Genes and Development*, 20(8), 1015–1027. <https://doi.org/10.1101/gad.1402406>
- Scheres, B., Dilaurenzio, L., Willemsen, V., Hauser, M. T., Janmaat, K., Weisbeek, P., & Benfey, P. N. (1995).** Mutations affecting the radial organisation of the Arabidopsis root display specific defects throughout the embryonic axis. *Development*, 121(1), 53–62. <https://doi.org/10.1101/gad.1426606.rates>
- Scheres, B., Wolkenfelt, H., Willemsen, V., Terlouw, M., Lawson, E., Dean, C., & Weisbeek, P. (1994).** Embryonic origin of the Arabidopsis primary root and root meristem initials. *Development*, 120, 2475–2487. <https://doi.org/10.1038/36856>
- Schindler, U., Menkens, A. E., Beckmann, H., Ecker, J. R., & Cashmore, A. R. (1992).** Heterodimerization between light-regulated and ubiquitously expressed Arabidopsis GBF bZIP proteins. *The EMBO Journal*, 11(4), 1261–1273. Retrieved from <http://www.pubmedcentral.nih.gov/articlerender.fcgi?artid=556574&tool=pmcentrez&trendertype=abstract>
- Schlereth, A., Möller, B., Liu, W., Kientz, M., Flipse, J., Rademacher, E. H., Schmid, M., Jürgens, G., & Weijers, D. (2010).** MONOPTEROS controls embryonic root initiation by regulating a mobile transcription factor. *Nature*, 464(7290), 913–916. <https://doi.org/10.1038/nature08836>
- Schneider, C. A., Rasband, W. S., & Eliceiri, K. W. (2012).** NIH Image to ImageJ: 25 years of image analysis. *Nature Methods*, 9(7), 671–675. <https://doi.org/10.1038/nmeth.2089>
- Shaikhali, J., Norén, L., De Dios Barajas-López, J., Srivastava, V., König, J., Sauer, U. H., Wingsle, G., Dietz, K. J., & Strand, Å. (2012).** Redox-mediated mechanisms regulate DNA binding activity of the G-group of basic region leucine zipper (bZIP) transcription factors in Arabidopsis. *Journal of Biological Chemistry*, 287(33), 27510–27525. <https://doi.org/10.1074/jbc.M112.361394>
- Shannon, P., Markiel, A., Ozier, O., Baliga, N. S., Wang, J. T., Ramage, D., Amin, N., Schwikowski, B., & Ideker, T. (2003).** Cytoscape: A software Environment for integrated models of biomolecular interaction networks. *Genome Research*, 13(11), 2498–2504. <https://doi.org/10.1101/gr.1239303>
- Shin, R., Burch, A. Y., Huppert, K. A., Tiwari, S. B., Murphy, A. S., Guilfoyle, T. J., & Schachtman, D. P. (2007).** The Arabidopsis Transcription Factor MYB77 Modulates Auxin Signal Transduction. *Plant Cell*, 19(8), 2440–2453. <https://doi.org/10.1105/tpc.107.050963>
- Shulze, C. N., Cole, B. J., Turco, G. M., Zhu, Y., Brady, S. M., & Dickel, D. E. (2018).** High-throughput single-cell transcriptome profiling of plant cell types. *BioRxiv*, 402966. <https://doi.org/10.1101/402966>
- Smet, W., Seville, I., de Luis Balaguer, M. A., Wybouw, B., Mor, E., Miyashima, S., Blob, B., Roszak, P., Jacobs, T. B., Boekschoten, M., Hooiveld, G., Sozzani, R., Helariutta, Y., & De Rybel, B. (2019).** DOF2.1 Controls Cytokinin-Dependent Vascular Cell Proliferation Downstream of TMO5/LHW. *Current Biology*, 29(3), 520–529.e6. <https://doi.org/10.1016/J.CUB.2018.12.041>
- Smetana, O., Mäkilä, R., Lyu, M., Amiryousefi, A., Sánchez Rodríguez, F., Wu, M.-F., Solé-Gil, A., Leal Gavarrón, M., Siligato, R., Miyashima, S., Roszak, P., Blomster, T., Reed, J. W., Broholm, S., & Mähönen, A. P. (2019).** High levels of auxin signalling define the stem-cell organizer of the vascular cambium. *Nature*, 565(7740), 485–489. <https://doi.org/10.1038/s41586-018-0837-0>

- Smit, M. E., & Weijers, D. (2015). The role of auxin signaling in early embryo pattern formation. *Current Opinion in Plant Biology*, 28, 99–105. <https://doi.org/10.1016/j.pbi.2015.10.001>
- Soeno, K., Goda, H., Ishii, T., Ogura, T., Tachikawa, T., Sasaki, E., Yoshida, S., Fujioka, S., Asami, T., & Shimada, Y. (2010). Auxin Biosynthesis Inhibitors, Identified by a Genomics-Based Approach, Provide Insights into Auxin Biosynthesis. *Plant and Cell Physiology*, 51(4), 524–536. <https://doi.org/10.1093/pcp/pcq032>
- Sorefan, K., Girin, T., Liljegren, S. J., Ljung, K., Robles, P., Galván-Ampudia, C. S., Offringa, R., Friml, J., Yanofsky, M. F., & Østergaard, L. (2009). A regulated auxin minimum is required for seed dispersal in Arabidopsis. *Nature*, 459(7246), 583–586. <https://doi.org/10.1038/nature07875>
- Soyano, T., Thitamadee, S., Machida, Y., & Chua, N.-H. (2008). ASYMMETRIC LEAVES2-LIKE19/LATERAL ORGAN BOUNDARIES DOMAIN30 and ASL20/LBD18 Regulate Tracheary Element Differentiation in Arabidopsis. *Plant Cell*, 20(12), 3359–3373. <https://doi.org/10.1105/tpc.108.061796>
- Sparks, E. E., Drapek, C., Gaudinier, A., Li, S., Ansariola, M., Shen, N., Hennacy, J. H., Zhang, J., Turco, G., Petricka, J. J., Foret, J., Hartemink, A. J., Gordán, R., Megraw, M., Brady, S. M., & Benfey, P. N. (2016). Establishment of Expression in the SHORTROOT-SCARECROW Transcriptional Cascade through Opposing Activities of Both Activators and Repressors. *Developmental Cell*, 39(5), 585–596. <https://doi.org/10.1016/j.devcel.2016.09.031>
- Stathopoulos, A., & Levine, M. (2002). Dorsal gradient networks in the Drosophila embryo. *Developmental Biology*, 246(1), 57–67. <https://doi.org/10.1006/dbio.2002.0652>
- Stegle, O., Teichmann, S. A., & Marioni, J. C. (2015). Computational and analytical challenges in single-cell transcriptomics. *Nature Reviews Genetics*, 16(3), 133–145. <https://doi.org/10.1038/nrg3833>
- Stewart, C. N., Shrestha, S. K., Hewezi, T., Binder, B., & Piya, S. (2014). Protein-protein interaction and gene co-expression maps of ARFs and Aux/IAAs in Arabidopsis. *Frontiers in Plant Science*, 5, 744. <https://doi.org/10.3389/fpls.2014.00744>
- Taylor-Teeples, M., Lin, L., De Lucas, M., Turco, G., Toal, T. W., Gaudinier, A., Young, N. F., Trabucco, G. M., Veling, M. T., Lamothe, R., Handakumbura, P. P., Xiong, G., Wang, C., Corwin, J., Tsoukalas, A., Zhang, L., Ware, D., ... Brady, S. M. (2015). An Arabidopsis gene regulatory network for secondary cell wall synthesis. *Nature*, 517, 571–575. <https://doi.org/10.1038/nature14099>
- ten Hove, C. A., Lu, K.-J., & Weijers, D. (2015). Building a plant: cell fate specification in the early Arabidopsis embryo. *Development*, 142(3), 420–430. <https://doi.org/10.1242/dev.111500>
- ten Tusscher, K. H. W. J. (2013). Mechanisms and constraints shaping the evolution of body plan segmentation. *The European Physical Journal E*, 36(5), 54. <https://doi.org/10.1140/epje/i2013-13054-7>
- ten Tusscher, K., & Scheres, B. (2011). Joining forces: Feedback and integration in plant development. *Current Opinion in Genetics and Development*, 21(6), 799–805. <https://doi.org/10.1016/j.gde.2011.09.008>
- Terzaghi, W. B., Bertekap, R. L., & Cashmore, A. R. (1997). Intracellular localization of GBF proteins and blue light-induced import of GBF2 fusion proteins into the nucleus of cultured Arabidopsis and soybean cells. *Plant Journal*, 11(5), 967–982. <https://doi.org/10.1046/j.1365-3113X.1997.11050967.x>
- Tromas, A., Paque, S., Stierlé, V., Quettier, A.-L., Muller, P., Lechner, E., Genschik, P., & Perrot-Rechenmann, C. (2013). Auxin-Binding Protein 1 is a negative regulator of the SCFTIR1/AFB pathway. *Nature Communications*, 4, 2496. <https://doi.org/10.1038/ncomms3496>
- Turing, A. M. (1952). The Chemical Basis of Morphogenesis. *Philosophical Transactions of the Royal Society of London. Series B, Biological Sciences*, 237(641), 37–72. <https://doi.org/10.1098/rstb.1952.0012>
- Ulmasov, T., Liu, Z. B., Hagen, G., & Guilfoyle, T. J. (1995). Composite structure of auxin response elements. *The Plant Cell*, 7(10), 1611–1623. <https://doi.org/10.1105/tpc.7.10.1611>
- Ulmasov, T., Murfett, J., Hagen, G., & Guilfoyle, T. J. (1997). Aux/IAA Proteins Repress Expression of Reporter Genes Containing Natural and Highly Active Synthetic Auxin Response Elements. *Plant Cell*, 9(11), 1963–1971. <https://doi.org/10.2307/3870557>
- van den Berg, T., & ten Tusscher, K. H. (2017). Auxin information processing: partners and interactions



- beyond the usual suspects. *International Journal of Molecular Sciences*, 18(12), E2585. <https://doi.org/10.3390/ijms18122585>
- Van Leene, J., Stals, H., Eeckhout, D., Persiau, G., Van De Slijke, E., Van Isterdael, G., De Clercq, A., Bonnet, E., Laukens, K., Remmerie, N., Henderickx, K., De Vijlder, T., Abdelkrim, A., Pharazyn, A., Van Onckelen, H., Inze, D., Witters, E., & De Jaeger, G. (2007). A Tandem Affinity Purification-based Technology Platform to Study the Cell Cycle Interactome in *Arabidopsis thaliana*. *Molecular & Cellular Proteomics*, 6(7), 1226–1238. <https://doi.org/10.1074/mcp.M700078-MCP200>
- Varaud, E., Szecsi, J., Brioudes, F., Perrot-Rechenmann, C., Brown, S., Bendahmane, M., Leroux, J., Szecsi, J., Leroux, J., Brown, S., Perrot-Rechenmann, C., & Bendahmane, M. (2011). AUXIN RESPONSE FACTOR8 Regulates *Arabidopsis* Petal Growth by Interacting with the bHLH Transcription Factor BIGPETALp. *Plant Cell*, 23(3), 973–983. <https://doi.org/10.1105/tpc.110.081653>
- Vera-Sirera, F., De Rybel, B., Úrbez, C., Kouklas, E., Pesquera, M., Álvarez-Mahecha, J. C., Minguet, E. G., Tuominen, H., Carbonell, J., Borst, J. W., Weijers, D., & Blázquez, M. A. (2015). A bHLH-Based Feedback Loop Restricts Vascular Cell Proliferation in Plants. *Developmental Cell*, 35(4), 432–443. <https://doi.org/10.1016/j.devcel.2015.10.022>
- Wabnick, K., Robert, H. S., Smith, R. S., & Friml, J. (2013). Modeling framework for the establishment of the apical-basal embryonic axis in plants. *Current Biology*, 23(24), 2513–2518. <https://doi.org/10.1016/j.cub.2013.10.038>
- Weijers, D., Franke-van Dijk, M., Vencken, R. J., Quint, A., Hooykaas, P., & Offringa, R. (2001). An *Arabidopsis* Minute-like phenotype caused by a semi-dominant mutation in a RIBOSOMAL PROTEIN S5 gene. *Development (Cambridge, England)*, 128(21), 4289–4299. Retrieved from <http://www.ncbi.nlm.nih.gov/pubmed/11684664>
- Weijers, D., Schlereth, A., Ehrismann, J. S., Schwank, G., Kientz, M., & Jürgens, G. (2006). Auxin triggers transient local signaling for cell specification in *Arabidopsis* embryogenesis. *Developmental Cell*, 10(2), 265–270. <https://doi.org/10.1016/j.devcel.2005.12.001>
- Weijers, D., Van Hamburg, J.-P., Van Rijn, E., Hooykaas, P. J. J., & Offringa, R. (2003). Diphtheria toxin-mediated cell ablation reveals interregional communication during *Arabidopsis* seed development. *Plant Physiology*, 133(4), 1882–1892. <https://doi.org/10.1104/pp.103.030692>
- Weiste, C., & Dröge-Laser, W. (2014). The *Arabidopsis* transcription factor bZIP11 activates auxin-mediated transcription by recruiting the histone acetylation machinery. *Nature Communications*, 5(1), 3883. <https://doi.org/10.1038/ncomms4883>
- Wendrich, J. R. (2016). *Stem cell organization in Arabidopsis: from embryos to roots*. Wageningen University.
- Wendrich, J. R., Boeren, S., Möller, B. K., Weijers, D., & De Rybel, B. (2017). In Vivo Identification of Plant Protein Complexes Using IP-MS/MS. In *Methods in Molecular Biology* (pp. 147–158). Humana Press, New York, NY. [https://doi.org/10.1007/978-1-4939-6469-7\\_14](https://doi.org/10.1007/978-1-4939-6469-7_14)
- Wendrich, J. R., Liao, C.-Y., van den Berg, W. A. M., De Rybel, B., & Weijers, D. (2015). Ligation-Independent Cloning for Plant Research. In *Methods in Molecular Biology* (pp. 421–431). Humana Press, New York, NY. [https://doi.org/10.1007/978-1-4939-2444-8\\_21](https://doi.org/10.1007/978-1-4939-2444-8_21)
- Wendrich, J. R., & Weijers, D. (2013). The *Arabidopsis* embryo as a miniature morphogenesis model. *New Phytologist*, 199(1), 14–25. <https://doi.org/10.1111/nph.12267>
- Went, F. W., & Thimann, K. V. (1937). *Phytohormones*. New York: The Macmillan Company.
- Willemsen, V., Bauch, M., Bennett, T., Campilho, A., Wolkenfelt, H., Xu, J., Haseloff, J., & Scheres, B. (2008). The NAC Domain Transcription Factors FEZ and SOMBRERO Control the Orientation of Cell Division Plane in *Arabidopsis* Root Stem Cells. *Developmental Cell*, 15(6), 913–922. <https://doi.org/10.1016/j.devcel.2008.09.019>
- Wolpert, L. (2011). *Principles of development*. Oxford University Press.
- Xu, T., Dai, N., Chen, J., Nagawa, S., Cao, M., Li, H., Zhou, Z., Chen, X., De Rycke, R., Rakusová, H.,

- Wang, W., Jones, A. M., Friml, J., Patterson, S. E., Bleecker, A. B., & Yang, Z. (2014). Cell surface ABP1-TMK auxin-sensing complex activates ROP GTPase signaling. *Science*, 343(6174), 1025–1028. <https://doi.org/10.1126/science.1245125>
- Yamaguchi, M., Goue, N., Igarashi, H., Ohtani, M., Nakano, Y., Mortimer, J. C., Nishikubo, N., Kubo, M., Katayama, Y., Kakegawa, K., Dupree, P., & Demura, T. (2010). VASCULAR-RELATED NAC-DOMAIN6 and VASCULAR-RELATED NAC-DOMAIN7 Effectively Induce Transdifferentiation into Xylem Vessel Elements under Control of an Induction System. *PLANT PHYSIOLOGY*, 153(3), 906–914. <https://doi.org/10.1104/pp.110.154013>
- Yin, H., Yan, B., Sun, J., Jia, P., Zhang, Z., Yan, X., Chai, J., Ren, Z., Zheng, G., & Liu, H. (2012). Graft-union development: A delicate process that involves cell-cell communication between scion and stock for local auxin accumulation. *Journal of Experimental Botany*, 63(11), 4219–4232. <https://doi.org/10.1093/jxb/ers109>
- Yoshida, S., BarbierdeReuille, P., Lane, B., Bassel, G. W., Prusinkiewicz, P., Smith, R. S., & Weijers, D. (2014). Genetic control of plant development by overriding a geometric division rule. *Developmental Cell*, 29(1), 75–87. <https://doi.org/10.1016/j.devcel.2014.02.002>
- Yoshida, S., van der Schuren, A., van Dop, M., van Galen, L., Saiga, S., Adibi, M., Möller, B., ten Hove, C. A., Marhavy, P., Smith, R., Friml, J., & Weijers, D. (2019). A SOSEKI-based coordinate system interprets global polarity cues in Arabidopsis. *Nature Plants*, 5(2), 160–166. <https://doi.org/10.1038/s41477-019-0363-6>
- Yu, C.-P., Lin, J.-J., & Li, W.-H. (2016). Positional distribution of transcription factor binding sites in Arabidopsis thaliana. *Scientific Reports*, 6(1), 25164. <https://doi.org/10.1038/srep25164>
- Zhang, J.-Y., He, S.-B., Li, L., & Yang, H.-Q. (2014a). Auxin inhibits stomatal development through MONOPTEROS repression of a mobile peptide gene STOMAGEN in mesophyll. *Proceedings of the National Academy of Sciences of the United States of America*, 111(29), E3015–23. <https://doi.org/10.1073/pnas.1400542111>
- Zhang, Y., Werling, U., & Edlmann, W. (2014b). Seamless Ligation Cloning Extract (SLiCE) Cloning Method. In *Methods in Molecular Biology* (pp. 235–244). Humana Press, Totowa, NJ. [https://doi.org/10.1007/978-1-62703-764-8\\_16](https://doi.org/10.1007/978-1-62703-764-8_16)
- Zhao, Y. (2004). HANABA TARANU Is a GATA Transcription Factor That Regulates Shoot Apical Meristem and Flower Development in Arabidopsis. *Plant Cell*, 16(10), 2586–2600. <https://doi.org/10.1105/tpc.104.024869>
- Zhao, Y., Christensen, S. K., Fankhauser, C., Cashman, J. R., Cohen, J. D., Weigel, D., & Chory, J. (2001). A role for flavin monooxygenase-like enzymes in auxin biosynthesis. *Science*, 291(5502), 306–309. <https://doi.org/10.1126/science.291.5502.306>
- Zhou, Y., Honda, M., Zhu, H., Zhang, Z., Guo, X., Li, T., Li, Z., Peng, X., Nakajima, K., Duan, L., & Zhang, X. (2015). Spatiotemporal sequestration of miR165/166 by arabidopsis argonaute10 promotes shoot apical meristem maintenance. *Cell Reports*, 10(11), 1819–1827. <https://doi.org/10.1016/j.celrep.2015.02.047>
- Zhu, H., Hu, F., Wang, R., Zhou, X., Sze, S. H., Liou, L. W., Barefoot, A., Dickman, M., & Zhang, X. (2011). Arabidopsis argonaute10 specifically sequesters miR166/165 to regulate shoot apical meristem development. *Cell*, 145(2), 242–256. <https://doi.org/10.1016/j.cell.2011.03.024>

## Summary

During plant embryogenesis, a miniature plant is generated that contains the cells that form the basis for all future cell- and tissue types. Of the three major cell identities, the vascular cells will provide transport capabilities and structural support to the plant. In this thesis we have focused on the initiation of vascular identity during embryogenesis. **Chapter 1** provides an overview of the early steps in vascular development and discusses the correlation between auxin signaling and vascular development, followed by an outline on the scope of this thesis. In **Chapter 2**, we focused on the role of auxin in embryo patterning; describing the various roles auxin plays as well as the tools that can help us visualize and unravel the complex outputs of auxin signaling.

In **Chapter 3**, we have used transcriptional reporter lines of both previously described and newly identified vascular genes to trace the establishment of vascular tissue identity to the dermatogen stage embryo. For this we used a tissue-specific expression atlas of the *Arabidopsis* embryo to isolate genes that are enriched in vascular cells. Of the 36 selected genes, 6 were selected as markers of early vascular identity. Using this set of vascular markers, we explored tissue ontogeny in the embryo. After initiation of identity, vascular gene expression was not strictly contained to the vascular cells in the globular stage embryo, indicating that identity is a more diffuse trait than was previously assumed. The identity of the earliest vascular cells appeared unique in their co-expression of xylem and phloem markers, and the existence of inverse vascular markers, excluded from vascular cells. This distinguishes cell identity in the embryo from that in the root.

With the extensive set of vascular marker genes generated here, we next tested the influence of auxin signaling on vascular gene expression. Previous research had established firm links between auxin signaling and vascular tissue formation. In **Chapter 4**, treatment of roots from our collection of vascular reporters confirmed that auxin induces vascular gene expression but in addition revealed that expression remained confined to the original cell types within the vascular bundle. Thus, auxin was not able to induce vascular identity in any non-vascular cells in the root. As the embryo is less differentiated, we next attempted to ectopically induce vascular identity in the embryo. Misexpression of constitutively active MPΔPB1 across the embryo was not able to induce vascular gene expression. However, blocking auxin signaling in vascular cells did eliminate the expression of some vascular markers; indicating that auxin signaling is required for, but not sufficient in the initiation of vascular identity.

In **Chapter 5**, we used an enhanced Yeast One Hybrid screen on promoters of vascular

marker genes to identify candidate regulators of vascular identity. From a network containing 397 transcription factors that could bind to one or more vascular promoters, 23 candidate regulators of vascular identity were selected using a rational scoring approach. We showed that 10 of these proteins were present at the correct time and location to be involved in identity regulation. The broad expression pattern of these 10 candidates suggested that local protein modifications might play a role in differential transcription factor activity. An assay designed to screen candidate-promoter interactions in the root suffered from artefacts but did reveal that misexpression of SRDX-fused candidates induced developmental phenotypes for several candidates.

Regular misexpression of these candidate regulators in the meristem did not reveal strong developmental abnormalities in the early plant, suggesting a limited or conditional role of the 10 selected candidate regulators. In **Chapter 6**, we hypothesized that instead of acting alone, these candidate regulators might interact with auxin signaling. Indeed, misexpression of three separate candidates reduced auxin-responsive root growth and vascular gene expression. In addition, we found that G-BOX BINDING PROTEIN 1 and 2 (GBF1/2) could interact with a variety of AUXIN RESPONSE FACTORS (ARFs) via the ARF DNA-binding domain. Promoter sequences of several vascular marker genes contained G-boxes located close to Auxin Response Elements (AuxREs). Removal of both AuxRE and G-box led to a strong reduction of promoter activity in the vascular bundle while removal of only the G-box increased between-transformant variation in activity. These findings suggest that GBF proteins could play a role in modulating auxin response in vascular cells.

In **Chapter 7**, we focused on vascular initiation during graft formation. Vascular marker genes are induced early on in the rootstock half of Arabidopsis grafts indicating strong parallels between vascular initiation in the embryo and graft. Next, we performed an RNAseq experiment to compare gene expression induction between compatible and incompatible Cucumber grafts. We found that markers of Cucumber grafting success were generally induced in the rootstock and contained a large number of homologs of genes involved in auxin signaling and vascular development in Arabidopsis.

Finally, **Chapter 8** discusses the insights this work provides into vascular identity and its regulation. The results from this thesis indicate that vascular identity is a transitory state that is not maintained during further development and that the existence of a single master regulator of vascular identity is unlikely. We hypothesize that modulation of auxin signaling via GBF proteins could be contributing factor in the establishment of vascular identity.

## Acknowledgements

This PhD has been a journey, a puzzle and a Sisyphean task, and I have thoroughly enjoyed it. During these four years there were a lot of highs and a few lows. The people around me haven been there offering their laughter during the highs and their support during the lows. And made all the parts in between a great mix of fun, excitement and relaxation. I'd like to thank everyone who has helped me get to this point, both within and outside of the lab with several (groups of) people in particular.

Dolf, in 2013, when I started my MSc thesis I quickly realized that the 'Plant Development' group is special. The people you have gathered are motivated and ambitious but also friendly and open. This stew of diverse, fun and odd personalities results in an environment where everyone feels both challenged and at home. In addition, as my supervisor you were always able to put things into perspective, and you were the calm, motivating mentor that I needed whenever I was about to get lost in this sprawling project. Thanks for all your support, for helping me deal with all the disappoints, frustrations and discoveries. I know we'll keep seeing great things from both the Plant Development group and the Biochemistry department.

Thanks to my previous mentors: Bert, Peter, Siobhan, Rene and Vid. Each of you has motivated and taught me a lot during projects before I started my PhD. You helped me develop my lab skills, critical thinking and appreciation for good science. I am looking forward to running into you in the future.

During this project I had the chance to be a mentor for the first time and it was sometimes challenging but mostly very rewarding and enjoyable. Branimir, Koyan, Surabi, Henriette, Frederique and Caroline: thank you all for your work on this project. Being your supervisor taught me a lot and I enjoyed watching each of you grow during your projects. I wish you all the best in your future careers.

Thank you to the group of people that is the Department of Biochemistry. You weirdos are the best. I very much enjoyed the mix of focus and fun, of journal clubs and barbeques. Thanks to all of you who lent me your ear, expertise, cuvettes and patience over the years. Special thanks to my paranympths Nicole and Thijs for being helpful, fun, bouldering and board-game loving colleagues. Thanks also to Kuan-Ju, my lab neighbor who was always willing and able to respond to the question: 'Kuan-Ju, you're a postdoc, you know stuff, right?'. To the other members of the 'cool office': Maritza, Tanya, Mark and Prasad: thank you for the snacks, science feedback and long conversations, you are indeed very cool. To some of my fellow PhD-trip Barcelona survivors: Dasha, Heidi, Mattia, Wouter and

Sacco, it was a pleasure 'banging' all of you that week and hanging out during and after the trip. Willy, Cathy, Laura and Jan-Willem, thank you for all your advice and help, and for making sure this lab runs smoothly. To Jos, Seb, Colette, Joakim, Liao, Gudrun and all other previous lab members: thanks for being very welcoming and helpful. I wish everyone in the department the best within or outside of science and I am looking forward to future planned and impromptu Biochemistry reunions.

I'd also like to thank past and current members of the Brady lab at UC Davis in California where I had the pleasure of performing and analyzing Yeast One Hybrid screens. Anne-Maarit, Allie, Michelle, Gina and Joel, thanks for your help and for becoming an incredibly welcoming group! Clara, Kaisa, Lauri and Pawel, it has been great meeting up with you again in Europe. Thanks as well to my Club-I friends in Davis, it was always great fun to drink beers, taste wines and chill on Jay's couch. I'm looking forward to reconnecting when I move to California.

To my board game/climbing/escape room/nerd friends: it has been a blast and don't you dare lose touch! Ruben, Dorett, Wen, Paul, Thomas and assorted others: I very much enjoyed improving our strength, tactical skills and fun levels, but also the long conversations on the many car rides we shared over the years. You are amazing and I can't wait for my trips back and your trips to the Bay Area.

Thanks also to many of the friends I made attending 'school'. Evie en Jelle, thanks for all the fun and support, I very much enjoyed our board games and dinners over the years and I hope we keep in touch! Biotech chickies, you girls rock. Lucia, Savanne, Marcella and Sabine: I have enjoyed our many reunions and trips. It has been great watching your accomplishments both professional and personal, but also talking about being 'strong independent women'. I'm looking forward to our future meetups and 'excursions'. I'd also like to thank Aafke, Schevaa and my other friends from our Rietveld days, we've all gone in very different directions but I hope we keep reuniting often.

Finally I'd like to thank my family. Mam, pap, jullie zijn er altijd voor me en ik heb enorm veel geluk met zulke fantastische ouders. Ik ga het kleine paradijs dat jullie in Wehl hebben enorm missen de komende jaren. Leonie en Huub, vanaf jongs af aan mijn regelmatige partners-in-crime, samen opgroeien met jullie was en is geweldig. Jullie zijn allebei leuke, slimme, eerlijke en vooral gezellige mensen en ik kijk uit naar onze afzonderlijke en gezamenlijke avonturen. Ook wil ik graag de rest van mijn familie bedanken, in het bijzonder Katja, Tamar, Lotte en Inus, voor hun steun en gezelligheid.

## Curriculum Vitae

Margot Evelien Smit was born May 5<sup>th</sup> 1991 in Velp, the Netherlands, and grew up in Wehl. In 2009 she completed her secondary education at the Rietveld Lyceum in Doetinchem and moved to Wageningen. There she pursued a BSc degree in Biotechnology. During her studies she became interested in plant science, largely because of her BSc thesis in the group of prof. dr. Rene Geurts at the laboratory of Molecular Biology. She stayed in Wageningen studying Biotechnology and in 2015 completed her MSc degree, specializing in Molecular and Cellular Biotechnology. During her MSc she focused on plant science and completed two theses in the field of plant vascular development. In the first thesis project she worked with dr. Bert De Rybel in the group of prof. dr. Dolf Weijers at the laboratory of Biochemistry at Wageningen University, studying target genes of the TMO5-LHW dimer in Arabidopsis. During the second thesis project she worked with dr. Peter Etchells in the group of dr. Siobhan Brady at UC Davis in California, where she used Yeast One Hybrid to study regulation of genes involved in vascular proliferation in Arabidopsis. In the time between these projects she joined the EPS Graduate Program, where together with prof. dr. Dolf Weijers she wrote a PhD grant for a project studying the specification of vascular identity during plant embryogenesis. That grant was awarded and in March of 2015 Margo started the PhD project which resulted in this thesis. During her PhD project, an EMBO Short-Term Fellowship supported a 2,5-month return to the lab of dr. Siobhan Brady at UC Davis for further Yeast One Hybrid experiments, this time to find regulators of vascular identity. Next, Margo wants to pursue a career in academic research and will move to Stanford, California to join the lab of prof. dr. Dominique Bergman as a postdoctoral researcher, studying stomatal developmental.





## Publications

Truskina, J., Han, J., Galvan-Ampudia, C.S., Lainé, S., Brunoud, G., Porco, S., Bågman, A.M., **Smit, M.E.**, Bennett, M., Roudier, F., Brady, S.M., Bishopp, A., Vernoux, T. (in preparation) “A network of transcriptional repressors mediates auxin response specificity” doi: 10.1101/448860

**Smit, M.E.\***, McGregor, S.\*, Sun, H., Gough, C., Bågman, A.M., Soyars, C.L., Kroon, J.T., Gaudinier, A., Williams, C.J., Yang, X., Nimchuck, Z.L., Weijers, D., Turner, S.R., Brady, S.M. and Etchells, J.P. (submitted) “A transcriptional network integrates signalling mechanisms to control plant vascular development”

Möller, B.K.\*, Ten Hove, C.A.\*, Xiang, D., Williams, N., López, L.G., Yoshida, S., **Smit, M.**, Datla, R., Weijers, D. (2017) “Auxin response cell-autonomously controls ground tissue initiation in the early Arabidopsis embryo” *Proc Natl Acad Sci U S A*. doi: 10.1073/pnas.1616493114

Etchells, J.P., **Smit, M.E.**, Gaudinier, A., Williams, C.J., Brady, S.M. (2016) “A brief history of the TDIF-PXY signalling module: balancing meristem identity and differentiation during vascular development” *New Phytol.* doi: 10.1111/nph.13642

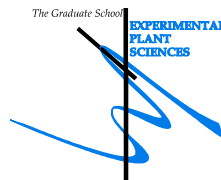
**Smit, M.E.**, Weijers, D. (2015) “The role of auxin signaling in early embryo pattern formation” *Curr Opin Plant Biol.* doi: 10.1016/j.pbi.2015.10.001

De Rybel, B.\*, Adibi, M.\*, Breda, A.S., Wendrich, J.R., **Smit, M.E.**, Novák, O., Yamaguchi, N., Yoshida, S., Van Isterdael, G., Palovaara, J., Nijse, B., Boekschoten, M.V., Hooiveld, G., Beeckman, T., Wagner, D., Ljung, K., Fleck, C., Weijers, D. (2014) “Plant development. Integration of growth and patterning during vascular tissue formation in Arabidopsis” *Science*. doi: 10.1126/science.1255215

\* These authors contributed equally

## Education Statement of the Graduate School

### Experimental Plant Sciences



**Issued to:** Margot Evelien Smit  
**Date:** 19 June 2019  
**Group:** Laboratory of Biochemistry  
**University:** Wageningen University & Research

1) Start-Up Phase	<u>date</u>	<u>cp</u>
► <b>First presentation of your project</b> At the Haigerloch embryo meeting, title 'On the origin of vascular species: finding developmental switches that control vascular identity'	12 May 2015	1.5
► <b>Writing or rewriting a project proposal</b>		
► <b>Writing a review or book chapter</b> Smit & Weijers, <i>The role of auxin signaling in early embryo pattern formation</i> , <i>Current Opinion in Plant Biology</i> 2015, 28:99-105. doi.org/10.1016/j.pbi.2015.10.001	Dec 2015	2.0
► <b>MSc courses</b>		
<i>Subtotal Start-Up Phase</i>		3.5

2) Scientific Exposure	<u>date</u>	<u>cp</u>
► <b>EPS PhD student days</b> EPS PhD student day, Get2Gether, Soest, the Netherlands	28-29 Jan 2016	0.6
EPS PhD student day, Get2Gether, Soest, the Netherlands	15-16 Feb 2018	0.6
► <b>EPS theme symposia</b> EPS theme 1 'Developmental Biology of Plants', Wageningen University	21 Jan 2016	0.3
EPS theme 1 'Developmental Biology of Plants', Wageningen University	30 Jan 2018	0.3
► <b>Lunteren Days and other national platforms</b> Annual Meeting 'Experimental Plant Sciences', Lunteren	13-14 Apr 2015	0.6
Annual Meeting 'Experimental Plant Sciences', Lunteren	11-12 Apr 2016	0.6
Annual Meeting 'Experimental Plant Sciences', Lunteren	10-11 Apr 2017	0.6
Annual Meeting 'Experimental Plant Sciences', Lunteren	9-10 Apr 2018	0.6
► <b>Seminars (series), workshops and symposia</b> Invited Speaker Biochemistry: prof. Tony Bacic (University of Melbourne, Australia)	27 Mar 2015	0.1
Invited Speaker Biochemistry: prof. Alain Goossens (VIB Ghent, Belgium)	8 Dec 2015	0.1
EPS Flying Seminar: prof. Siobhan Brady (UC Davis, USA)	8 Sep 2015	0.1
Invited Speaker Biochemistry: dr. Francois Parcy (CEA Sciences, France)	15 Oct 2015	0.1
Invited Speaker Biochemistry: prof. Mark Estelle (UC San Diego, USA)	7 Apr 2016	0.1
Invited Speaker Biochemistry: dr. Helene Robert-Boisivon (CEITEC, Czech Republic)	3 Jun 2016	0.1
Invited Speaker Biochemistry: prof. Chun-Ming Liu (Institute of Crop Science, CAAS, China)	20 Jun 2016	0.1
Invited Speaker Biochemistry: prof. Lars Østergaard (John Innes Centre, UK)	21 Dec 2016	0.1
Farewell Symposium EPS Ton Bisseling	2 Feb 2017	0.2
Invited Speaker Biochemistry: prof. Gerd Jürgens (Max Planck Tübingen Germany)	11 May 2017	0.1
Invited Speaker Biochemistry: dr Katharina Bärstenbinder (Leibniz Institute for Plant Biochemistry, Germany)	01 Jun 2017	0.1
Invited Speaker Biochemistry: dr. Arnold Boersma (RUG, NL)	19 Jul 2017	0.1
Seminar on Integrative Bioinformatics	12 Sep 2017	0.1
Symposium Plant Developmental Systems Biology	4 Oct 2017	0.3
Symposium Future of Biochemistry	26 Oct 2017	0.2
Invited Speaker Biochemistry: prof. Richard Notebaart (WUR, NL)	2 Nov 2017	0.1
Invited Speaker Biochemistry: prof. Charles Delwiche (University of Maryland, USA)	18 Jun 2018	0.1
Invited Speaker Biochemistry: prof. Victoria Mironova (Novosibirsk State University, Russia)	27 Jun 2018	0.1
Invited Speaker Biochemistry: prof. Lucia Strader (Washington University, USA)	10 Sep 2018	0.1
Molecular Life Sciences Seminar: prof. Ludwik Leibler (ESPCI ParisTech, France)	22 Nov 2018	0.1
Invited Speaker Biochemistry: prof. Alexis Maizel (COS Heidelberg, Germany)	17 Dec 2018	0.1
Invited Speaker Biochemistry: prof. Jifi Friml (IST Austria)	18 Dec 2018	0.1
Molecular Life Sciences Seminar: prof. Wolf Frommer (Universität Düsseldorf, Germany)	17 Jan 2019	0.1
► <b>Seminar plus</b>		
► <b>International symposia and congresses</b> Embryo development meeting, Haigerloch 2015	11-13 May 2015	0.6
International Conference on Arabidopsis Research (ICAR) Paris 2015	5-9 Jul 2015	1.2
European Plant Science Retreat (EPSR) Paris 2015	10-13 Jul 2015	1.0
Vascular Get Together, Corsendonk 2015	24-25 Nov 2015	0.6
Vascular Get Together, Corsendonk 2016	14-16 Nov 2016	0.6
Plant Vascular Biology (PVB) Conference Shenzhen 2016	19-23 Jul 2017	1.2
Vascular Get Together, Corsendonk 2017	13-15 Nov 2017	0.5
Embryo development meeting, Haigerloch 2018	7-9 May 2018	0.6
International Plant Molecular Biology (IPMB) Montpellier 2018	5-10 Aug 2018	1.2
► <b>Presentations</b> Vascular Get Together, Corsendonk 2015 (Talk)	24 Nov 2015	1.0
International Conference on Arabidopsis Research (ICAR) Paris 2015 (Poster)	5-9 Jul 2015	1.0
Vascular Get Together, Corsendonk 2016 (Talk)	15 Nov 2016	0.0

Plant Vascular Biology Conference Shenzhen 2016 (Poster)	19-23 Jul 2017	1.0
Vascular Get Together, Corsendonk 2017 (Talk)	14 Nov 2017	1.0
Annual Meeting 'Experimental Plant Sciences', Lunteren 2018 (Talk)	10 April 2018	1.0
Embryo development meeting, Haigerloch 2018 (Talk)	8 May 2018	1.0
International Plant Molecular Biology (IPMB) Montpellier 2018 (Talk)	8 Aug 2018	1.0
► <b>IAB interview</b>		
► <b>Excursions</b>		
PhD Trip Biochemistry to Barcelona	15-21 May 2017	1.0
<i>Subtotal Scientific Exposure</i>		22.4
<b>3) In-Depth Studies</b>	<u><i>date</i></u>	<u><i>CP</i></u>
► <b>Advanced scientific courses &amp; workshops</b>		
Course: Transcription Factors and Transcriptional Regulation	12-14 Dec 2016	1.0
Course: Microscopy and Spectroscopy in Food and Plant Sciences	14-16 May 2018	1.0
► <b>Journal club</b>		
Journal club Weijers lab		3.0
► <b>Individual research training</b>		
<i>Subtotal In-Depth Studies</i>		5.0
<b>4) Personal Development</b>	<u><i>date</i></u>	<u><i>CP</i></u>
► <b>General skill training courses</b>		
WSG Workshop Carousel	17 Apr 2015	0.3
EPS Introduction Course	22 Sep 2015	0.2
Course: Project and Time Management	Sep-Oct 2015	1.5
Course: Teaching and Supervising Thesis Students	22-23 Feb 2016	0.6
Course: Scientific Artwork with Photoshop and Illustrator	28-29 Mar 2017	0.6
Course: Adobe InDesign Essential Training	4-5 Jun 2018	0.6
Course: Scientific Writing	Sep-Oct 2018	1.8
► <b>Organisation of meetings, PhD courses or outreach activities</b>		
► <b>Membership of EPS PhD Council</b>		
<i>Subtotal Personal Development</i>		5.6
<b>TOTAL NUMBER OF CREDIT POINTS*</b>		<b>36.5</b>
Herewith the Graduate School declares that the PhD candidate has complied with the educational requirements set by the Educational Committee of EPS with a minimum total of 30 ECTS credits.		
* A credit represents a normative study load of 28 hours of study.		

---

The research presented in this thesis was performed at the Laboratory of Biochemistry, Wageningen University & Research, and was financially supported by a grant from the Netherlands Organization for Scientific Research (NWO; ALW-Topsector grant 831.14.003).

Financial support from the Laboratory of Biochemistry for printing this thesis is gratefully acknowledged.

Cover design by Margot Smit

*Cover contains an exhibition with models featuring LEGO® bricks and figures. LEGO is a trademark of the LEGO Group which did not sponsor or support this exhibition.*

Layout design by Tatyana Radoeva and Margot Smit

Printed by GVO drukkers & vormgevers, Ede